At the Crossroads of Genetics and Environment: Circadian Rhythms and Metabolism in the APOE-/- Mouse Model of Atherosclerosis



Philippa Louise Harris Gleave

Somerville College

University of Oxford

A thesis submitted for the degree of Doctor of Philosophy

Department of Pharmacology, University of Oxford

Michaelmas 2023

Abstract

The complexities of life are fundamentally governed by 24-hour biological cycles known as circadian rhythms. Notably, disturbances in these rhythms have been identified as a crucial risk factor in the development of cardiovascular disease (CVD). Despite this, the interaction between biological clocks and this widespread disease is still poorly understood. In my research, I explored the effects of circadian rhythm disruption in relation to CVD. Specifically, I examined the response of APOE knockout (APOE-/-) mice, which are prone to atherosclerosis, to a compounded challenge by exposing them to constant light (L:L). This approach is based on the "double hit" hypothesis in CVD, suggesting that its development and progression often involve multiple contributing factors, often with an interaction between genetic predisposition and environmental stressors.

The study measured circadian rhythms and sleep patterns in these mice, along with home cage behaviour, exploratory tendencies, anxiety-like behaviours, and anhedonia. These observations were correlated with gene expression profiles and the analysis of downstream metabolite profiles using ^{1}H nuclear magnetic resonance (NMR). Markers of microglial and astrocyte activation were also assessed.

Results showed that APOE-/- mice were hyperactive, displaying significant increases in the amplitude of their behavioural circadian rhythms, changes in sleep patterns, and home cage behaviour. They exhibited heightened exploratory instincts, paradoxically paired with increased anxiety-like behaviour, and an increase in appetite without corresponding body mass changes. These mice also showed an upregulation of activated microglia in the brain, disturbances in the rhythmic expression of hepatic core clock genes, and altered expression of genes involved in lipid and cholesterol synthesis in the liver. These changes likely contribute to the observed suppression of carbohydrate metabolism and the pro-atherogenic lipid state as revealed by ^{1}H NMR.

Exposure to L:L further modified the circadian rhythms in APOE-/- mice by extending the period, delaying the phase, and diminishing the amplitude. Sleep amount and body mass increased, alongside a decrease in hepatic gene expression related to lipogenesis. Notably, L:L markedly affected astrocyte morphology in APOE-/- mice, suppressed carbohydrate metabolism and reverse cholesterol transport.

While L:L normalized general locomotor activity, it exacerbated anxiety-like and hedonic behaviours. Astrocyte morphology was altered, and the hepatic expression of genes regulating lipid metabolism and oxidative stress were suppressed. This was coupled with shifts towards a pro-atherogenic state in lipid metabolism, reduced choline metabolism, increased oxidative stress, and a compensatory upregulation of glutathione production.

In conclusion, this study vividly demonstrates how circadian disruption in a CVD model intensifies the disease's pathology. It orchestrates a series of events including the downregulation of carbohydrate and lipid metabolic pathways, induction of oxidative stress, lipid accumulation, mitochondrial overload, glial cell activation, altered circadian rhythms, locomotor activity, and increased sleep. Central to these events is mitochondrial dysfunction, highlighting a need for further research to confirm the role of mitochondria in the interaction between CVD and circadian disruption, and to identify biomarkers and potential therapies.

Acknowledgements

I have been incredibly fortunate to be able to complete my DPhil and be part of such a historic and world-class institution. I have been able to work with some remarkable people, who have given me a lot of support. Additionally, this DPhil would not have been possible without receiving funding from UKHSA and receiving Covid-19 relief funding from Somerville College.

Firstly, to my supervisors. Kerry, thank you so much for your unwavering support, kindness, encouragement and endless patience, from my initial project start to our regular teams catch ups over lockdown, through to reading my thesis chapters – some several times over. Daniel, thank you for your non-stop flow of ideas, your advice and your infectious *joie de vivre*.

Thank you to current and former members of the Anthony Lab. I would like to say particular thank yous to Fay Probert, for teaching me 1H NMR and multivariate analysis and for reading my methods chapter, Abi Yates for setting me up in the lab, and to Jaezah Zainal Azman, Wenzheng Xiong (Victor) and Daniel Radford-Smith for helping me with experiments and analysis. Additionally, I would like to thank Isobel Dunstan, Ross McLeod, Tien Ho and Carolina Costa for their support and entertainment as well as keeping me sane whilst I wrote my thesis.

At UKHSA I would like to thank Chris Whiteman for being a wonderful and generous friend, and for helping me with experiments. I would also like to thank the animal technicians Kevin Whitehill, Mandy Stanton, Liz Marshall, and Raymond Shek for taking such good care of my mice and helping facilitate my experiments. Additionally, I would like to thank Liz Ainsbury, Marina Khazova, Luke Price and Gareth Banks (MRC) for helping me with experimental design, statistical analyses, light measurements and other technical and scientific advice.

To all of my Oxford friends, thank you so much for making Oxford my favourite place to live. Thank you to my parents and brother, for your support, encouragement and listening ears. Thank you to Joe for supporting me along on this journey, for always trying to cheer me up, for making sure I ate and slept, and for staying up with me whilst I submitted this thesis (many many months later than when I assured you I would be finished).

Finally, I would like to mention my darling Grandma and Grandpa, Deborah and Harold Harris, and my wonderful Granny, Sheila Gleave, who all sadly passed away during the latter part of my DPhil. I will never forget how proud you were of me.

Table of Contents

Abstract 2

Acknowledgements 4

List of Abbreviations 11

List of Figures 17

List of Tables 19

1 Introduction 20

1.1 Atherosclerosis 21

1.2 Cholesterol and lipoproteins 22

1.3 Lipoprotein metabolism 24

1.3.1 Exogenous lipoprotein metabolism 24
1.3.2 Endogenous lipoprotein metabolism 24
1.3.3 HDL metabolism and reverse cholesterol transport 25
1.4 Apolipoprotein E 25

1.4.1 APOE in humans 26
1.4.2 The APOE-/- mouse model 27
1.5 Gene-environment interaction 28

1.6 An overview of circadian rhythms 29

1.6.1 Molecular circadian clock 30
1.6.2 Entrainment and the central clock 32
1.6.3 Clock communication and peripheral oscillators 34
1.7 An overview of sleep 35

1.7.1 The two-process model of sleep regulation 36
1.8 The importance of light conditions 37

1.8.1 The relevance of light conditions for humans 38
1.8.2 Light and Oxidative stress 38
1.9 Circadian disruption, sleep and the cardiovascular system 39

1.10 Hypotheses and aims of work 40

2 Materials and Methods 42

2.1 Animals 42

2.1.1 APOE-/- mouse model 42
2.2 Circadian manipulation 42

2.2.1 Entrainment and L:D cycle shifts 42
2.2.2 Constant Darkness 43
2.2.3 Instrumented observation cage and constant light exposure 44
2.3 Behaviour 45

2.3.1 Free running behaviour 46
2.3.2 Immobility-defined sleep 47
2.3.3 Home Cage and Hatbox Cage behaviour 47
2.3.4 Behavioural Tests 47
2.4 Tissue collection 50

2.5 Histology 50

2.5.1 Sectioning 50
2.5.2 Immunohistochemistry 50
2.5.3 Quantification and analysis of immunohistochemistry 51
2.6 Molecular Biology 52

2.6.1 mRNA extraction and cDNA conversion 52
2.6.2 Quantitative real-time polymerase chain reaction (qRT-PCR) 53
2.6.2.1 Primer Design ..... **Error! Bookmark not defined.**
2.6.2.2 Primer Testing 56
2.7 ^{1}H Nuclear Magnetic Resonance (NMR) Metabolomics 56

2.7.1 Sample processing 57
2.7.1.1 Plasma 57
2.7.1.2 Liver and Brain 57
2.7.2 ^{1}H NMR Spectroscopy 57
2.7.3 Spectra pre-processing 58
2.8 Statistical Analysis 59

2.8.1 Univariate Analyses 59
2.8.2 Cosinor analysis 59
2.8.3 Multivariate Analyses 59
3 Phenotyping the APOE-/- mouse model 61
3.1 Introduction 61
3.1.1 The APOE-/- mouse model 61
3.1.2 Behavioural investigations 61
3.1.3 Molecular investigations 62
3.1.4 Aims of chapter 62
3.2 Materials and Methods 64
3.2.1 Behaviour in normal L:D conditions 64
3.2.2 Behaviour in constant D:D conditions 64
3.3 Results 65
3.3.1 Behavioural rhythms in L:D 65
3.3.2 Immobility-defined sleep in L:D 68
3.3.3 Home cage behaviour in L:D 69
3.3.4 Appetitive behaviour and body mass in L:D 70
3.3.5 Behavioural rhythms in D:D 73
3.3.6 Immobility-defined sleep in D:D 74
3.3.7 Body mass in D:D 75
3.3.8 Behaviour in the OFT 76
3.3.9 Behaviour in the LDB 77
3.3.10 Behaviour in the SPT 78
3.3.11 Hepatic expression of genes involved in circadian control in D:D 78
3.3.12 Hepatic expression of genes involved in lipid metabolism in D:D 80
3.4 Discussion 81
3.5 Conclusions 91
4 The effect of constant light exposure on behaviour, gene expression and the glial cell response in the APOE-/- mouse model 92
4.1 Introduction 92
4.1.1 CVD and circadian disruption 92

4.1.2 Circadian disruption and behavioural alterations in mice 92
4.1.3 The APOE-/- mouse model and constant light exposure (L:L) 93
4.1.4 APOE and the Brain 93
4.1.5 Aims of chapter 94
4.2 Experimental Design 95
4.3 Results 97
4.3.1 Behavioural rhythms in L:L 97
4.3.2 Immobility-defined sleep in L:L 99
4.3.3 Home cage behaviour in L:L 102
4.3.4 Appetitive behaviour and body mass in L:L 103
4.3.5 Behaviour in the OFT in L:L 104
4.3.6 Behaviour in the LDB in L:L 105
4.3.7 Sucrose preference in L:L 106
4.3.8 The expression of genes involved in energy metabolism and oxidative stress in the brain in L:L 107
4.3.9 The expression of hepatic genes involved in FA β-oxidation in L:L 109
4.3.10 The expression of hepatic genes involved in lipid metabolism in L:L 110
4.3.11 The expression of hepatic genes involved in circadian regulation and antioxidant activity in L:L 111
4.3.12 The glial cell response in the brain in L:L 112
4.4 Discussion 115
4.4.1 Conclusions 126
5 Effect of the APOE-/- genotype and 3 weeks of constant light exposure on the metabolome 128
5.1 Introduction 128
5.1.1 Atherosclerosis and the metabolome 128
5.1.2 L:L and the metabolome 129
5.1.3 Aims of Chapter 129
5.2 Results 130
5.2.1 Plasma metabolite levels 132
5.2.2 Brain metabolite levels 137
5.2.3 Liver metabolites levels 140

5.2.4 Correlations of metabolites with behavioural outcomes 143
5.3 Discussion 150
5.4 Conclusions 166
6 General Discussion 168
Future work and limitations 170
Final remarks 171
References 173
Supplementary 198

List of Abbreviations

ABC	ATP-binding cassette
ABCA1	Atp binding cassette subfamily a member 1
ACD	Advanced chemistry development
ACS	Acute coronary syndrome
AD	Alzheimer's disease
ALAN	Artificial light at night
ALT	Alanine aminotransferase
ANOVA	Analysis of variance
APOA	Apolipoprotein A
APOB	Apolipoprotein B
APOE	Apolipoprotein E
ATP	Adenosine triphosphate
BBB	Blood-brain barrier
BH	Benjamini-hochberg
BMAL	Basic helix-loop-helix ARNT-like protein
CAC	Coronary artery calcium
CAD	Coronary artery disease
CCD	Charge-coupled device
CETP	Cholesteryl ester transfer protein
CHD	Coronary heart disease
CLOCK	Circadian locomotor output cycles kaput
CNS	Central nervous system
CPMG	Carr-purcell-meiboom-gill
CRY	Cryptochrome
CSF	Cerebrospinal fluid
CT	Cycle threshold

CVD	Cardiovascular disease
DAB	3,3’-diaminobenzidine
D:D	Constant darkness
DG	Dentate gyrus
Dgat1	Diacylglycerol O-acyltransferase 1
DNA	Deoxyribonucleic acid
DNL	De novo lipogenesis
DPX	Dibutylphthalate polystyrene xylene
DR	Dorsal raphe
DRP1	Dynamin-related protein 1
EEG	Electroencephalogram
ER	Endoplasmic reticulum
FA	Fatty acid
FABP7	Fatty acid binding protein 7
FASN	Fatty acid synthase
FEO	Food-entrainable oscillator
FFA	Free fatty acid
FIJI	Fiji is just imagej
GABA	Γ-Aminobutyric acid
GAD	Glutamate decarboxylase
GC-MS	Gas chromatography mass spectrometry
GCL	Glutamate–cysteine ligase
GDH	Glutamate dehydrogenase
GFAP	Glial fibrillary acidic protein
GHT	Geniculohypothalamic tract
GLUT1	Glucose transporter protein type 1
GPX4	Glutathione peroxidase 4

GS	Glutamine synthetase
HAB	High anxiety-related behaviour
HCB	Home cage behaviour
HDAC	Histone deacetylase
HDL	High-density lipoprotein
HFD	High fat diet
HFHC	High fat and high cholesterol
HMDB	Human metabolome database
HMG-CoA	3-hydroxy-3-methylglutaryl-Coenzyme A reductase
HMGCR	3-hydroxy-3-methylglutaryl-Coenzyme A reductase
HSPG	Heparan sulphate proteoglycan
5-HT	5-Hydroxytryptophan, serotonin
Iba-1	Ionized calcium binding adaptor molecule 1
ICAC	Internal carotid artery calcification
IDL	Intermediate density lipoprotein
IGL	Intergeniculate leaflet
IMT	Carotid intima-media thickness
JNK	C-Jun N-terminal kinase
KO	Knockout
LCAT	Lecithin-cholesterol acyltransferase
L:D	Light:dark
LDB	Light-dark box
LDH	Lactate dehydrogenase
LDL	Low-density lipoprotein
LDLR	Low-density lipoprotein receptor
L:L	Constant light
LOLIPOP	Life sciences prospective population study

LPL	Lipoprotein lipase
LPS	Lipopolysaccharide
LRP1	Low-density lipoprotein receptor-related protein 1
LXR	Liver X receptor
MESA	Multi-Ethnic Study of Atherosclerosis
MESOR	Midline-estimating statistic of rhythm
MI	Myocardial infarction
MMP	Matrix metalloproteinase
MR	Median raphe
NAD	Nicotinamide adenine dinucleotide
NHS	National health service
NMDA	N-methyl-D-aspartate
NMR	Nuclear magnetic resonance
NOESY	Nuclear overhauser effect spectroscopy
NPY	Neuropeptide Y
OFT	Open field test
OH	Hydroxyl
OPLS-DA	Orthogonal partial-least squares discriminant analysis
OXPHOS	Oxidative phosphorylation
PAG	Phosphate-activated glutaminase
PBS	Phosphate buffered saline
PCA	Principle component analysis
PCR	Polymerase chain reaction
PER	Period
PFA	Paraformaldehyde
Pfkfb3	6-phosphofructo-2-kinase/fructose-2,6-bisphosphate 3

PGC-1α	Peroxisome proliferator-activated receptor gamma coactivator 1-alpha
PLS-DA	Partial least-squares discriminant analysis
PPAR-α	Peroxisome Proliferator-Activated Receptor-α
PPRE	PPAR response elements
PRC	Phase-response curve
PRR	Pattern recognition receptor
PUFA	Polyunsaturated fatty acid
PVN	Paraventricular nucleus
REM	Rapid eye movement
ipRCG	Intrinsically photosensitive retinal ganglion cell
RHT	Retinohypothalamaic tract
RNA	Ribonucleic acid
ROR-α	Receptor-related orphan receptor alpha
ROS	Reactive oxygen species
RXR-α	Retinoid X receptor
SCFA	Short-chain fatty acid
SCN	Suprachiasmatic nucleus
SD	Standard deviation
SIRT1	Sirtuin 1
SOD	Superoxide dismutase
SPT	Sucrose preference test
SR-B1	Scavenger receptor B1
SREBP	Sterol regulatory element-binding protein
SWS	Slow wave sleep
TCA	Tricyclic acid
TG	Triglyceride

TMAO	Trimethylamine N-oxide
TOCSY	2D total correlation spectroscopy
TTFL	Transcriptional-translational feedback loop
VIP	Variable importance in projection
VLDL	Very low-density lipoproteins
WT	Wildtype
WTD	Western-type diet
ZT	Zeitgeber time

List of Figures

Figure 1.1: Schematic showing the properties of a circadian oscillation. 30
Figure 1.2: The mammalian molecular clock. 31
Figure 1.3: Example of the photic phase response in mice..... 33
Figure 1.4. The two-process model of sleep regulation. 36
Figure 2.5. “Hatbox” cage dimensions..... 43
Figure 2.6. “Arena” set up in the instrumented observation cages (PhenoTypers). 45
Figure 2.7. “Arena” set up in the “hatbox” cages. 46
Figure 2.8. Arena set up for behavioural test analysis. 49
Figure 2.9. Example of a skeletonized tracing of a GFAP+ astrocyte. 51
Figure 3.1: L:D Experimental design 64
Figure 3.2: D:D Experimental design for Chapter 1 and 2 65
Figure 3.3: Locomotor activity in wildtype and ApoE−/− mice, in normal L:D conditions. 66
Figure 3.4: APOE-/- mice have a significantly higher amplitude of behavioural rhythms, but they have the same period and acrophase as the wildtype mice in normal L:D conditions. . 67
Figure 3.5: APOE-/- mice have longer Activity Bouts but show no difference in total number of Activity Bouts in normal L:D conditions..... 68
Figure 3.6: There is a significant time-genotype interaction for immobility-defined sleep over time, but APOE-/- mice display the same total amount of immobility-defined sleep and have the same sleep distribution in the light phase as the wildtype mice in normal L:D conditions. 69
Figure 3.7: APOE-/- mice display increased locomotor behaviour in normal L:D conditions. 70
Figure 3.8: APOE-/- mice have differences in appetitive behaviour compared to the wildtypes, but don’t differ in body mass in normal L:D conditions. 71
Figure 3.9: Locomotor activity in wildtype and ApoE−/− mice, in D:D conditions. 72
Figure 3.10: APOE-/- mice have a longer free running period, or Tau, and have a higher amplitude of behavioural rhythms compared to wildtype mice in D:D conditions. 72
Figure 3.11: APOE-/- mice have more activity in D:D but have no difference in Activity Bouts compared to wildtype mice..... 73
Figure 3.12: APOE-/- mice display less immobility-defined sleep and have a reduced sleep distribution in the light phase than wildtype mice in free running conditions, and there is a significant time-genotype interaction when looking at Hourly immobility-defined sleep in D:D conditions..... 74
Figure 3.13: APOE-/- mice have no difference in body mass in D:D conditions..... 75
Figure 3.14: APOE-/- mice had increased locomotor behaviour and time spent at the edges of the arena compared to wildtypes in the Open Field Test. 76
Figure 3.15: APOE-/- mice spend longer in the Light Zone of the Light Dark box and make more visits to the Light Zone than wildtypes. 77
Figure 3.16: Sucrose Preference in APOE-/- mice and wildtype mice. 78
Figure 3.17: The expression of genes involved in circadian rhythm control in APOE-/- and wildtype mice. 79
Figure 3.18: Rhythmical expression of genes involved in lipid metabolism in APOE-/- mice and controls. 80
Figure 4.1: Experimental design for Chapters 4 and 5..... 96
Figure 4.2: Locomotor activity in C57BL/6J and APOE−/− mice, in L:D conditions and L:L conditions..... 97

Figure 4.3: Constant light exposure strongly impacts behavioural rhythms and has a stronger impact on APOE-/- period compared to controls. 98
Figure 4.4: APOE-/- mice have fewer activity bouts and longer activity bouts compared to the control group, and constant light exposure reduces the length of activity bouts..... 99
Figure 4.5: Constant light exposure increases total immobility-defined sleep, interacts with genotype to affect sleep distribution in the light phase. There is a significant impact of the interaction of light, genotype and time on hourly immobility-defined sleep..... 101
Figure 4.6: APOE-/- mice display increased locomotor behaviour, and constant light exposure reduces locomotor behaviour. 102
Figure 4.7: APOE-/- mice have differences in appetitive behaviour to the control group and the interaction between constant light exposure and genotype impacts the change in body mass over the experiment. 103
Figure 4.8: APOE-/- mice showed increased locomotor behaviour compared to controls, and constant light exposure increased the time spent around the edges of the arena in the Open Field Test. 105
Figure 4.9: APOE-/- mice spend longer in the light zone and visit it more, but constant light exposure has no impact on behaviour in the Light Dark Box. 106
Figure 4.10: L:L increases sucrose preference..... 107
Figure 4.11: Neither genotype nor light have significant effects on gene expression in the brain..... 108
Figure 4.12: The expression of genes involved in energy metabolism in the liver were impacted by L:L and genotype. 109
Figure 4.13: The expression of genes involved in lipid metabolism in the liver were impacted by the interaction between L:L and genotype, as well as genotype and light. 110
Figure 4.14: The expression of genes involved in energy metabolism, circadian regulation and antioxidant activity in the liver was decreased by L:L. 111
Figure 4.15: The expression of markers involved in neuroinflammation were affected by the interaction between L:L and genotype, as well as genotype and L:L. 114
Figure 5.1: Principal component analysis (PCA) of the effect of the APOE-/- genotype and L:L exposure on the plasma, brain and liver metabolomes. 131
Figure 5.2: PLS-DA scores plot of the effect of the APOE-/- genotype and L:L exposure on the plasma, brain and liver metabolomes. 132
Figure 5.3: Plasma metabolites involved in energy metabolism are significantly altered by genotype, light or the interaction between the two. 135
Figure 5.4: Brain metabolites involved in energy metabolism are significantly altered by genotype, light or the interaction between the two. 139
Figure 5.5: Brain metabolites involved in antioxidant decreased by light exposure..... 139
Figure 5.6: Liver metabolites involved in antioxidant activity are significantly altered by 3 weeks of constant light exposure. 143
Figure 5.7.: Liver levels of essential nutrient choline reduced by L:L exposure..... 143
Figure 5.8: Plasma metabolites correlate with circadian and locomotor parameters..... 144
Figure 5.9: Behavioural outcomes correlate with gene expression but not metabolites. 145
Figure 5.10: Locomotor and circadian behaviour correlate with liver metabolites and genes 146
Figure 5.11: Correlations of brain, liver and plasma metabolites with gene expression in the brain and liver. 147
Figure 5.12: Multi-organ metabolomics reveals changes in carbohydrate and lipid metabolism, and alterations in redox homeostasis. 148

List of Tables

Table 2.1: Antibodies for immunohistochemistry 52
Table 2.2: Components of the High-Capacity cDNA Reverse Transcription Kit 53
Table 2.3: Temperature cycles for qRT-PCR reactions 54
Table 2.4: qRT-PCR primer sequences..... 55
Table S1: Plasma metabolite statistics..... 199
Table S2: Brain metabolite statistics 200
Table S3: Liver Metabolite Statistics 201
Table S4: Correlations between plasma metabolites and behavioural results 202
Table S5: Correlations between brain metabolites and behavioural results..... 205
Table S6: Correlations between brain gene expression and behavioural results..... 207
Table S7: Correlations between liver metabolites and behavioural results 208
Table S8: Correlations between liver gene expression and behavioural results 210
Table S9: Correlations between gene expression and metabolites across tissues..... 212
Table S10: Correlations between all metabolites..... 217
Table S11: Correlations between gene expression in the brain and liver 222
Table S12: Correlations between behavioural results 225

1 Introduction

Cardiovascular disease (CVD) is the leading cause of death worldwide [4]. In the UK, 460 people a day die from heart and circulatory disease, and 28% of those daily deaths are in people under 75 years old [5]. Hospital admissions for heart attacks are as frequent as one every five minutes [5]. This is a significant burden on the NHS, costing £9 billion in healthcare costs each year, and costing the economy around £19 billion each year [5]. Atherosclerosis is a major cause of CVD [6]. Dysregulated cholesterol levels and proportionally high low-density lipoprotein (LDL) cholesterol are the biggest risk factors for atherosclerosis. Lowering LDL levels is a major focus for CVD prevention [7]. Around half the adult population of the UK have total cholesterol levels above the national guidelines, and lipid lowering drugs such as statins are currently being taken by between 7 and 8 million adults [5].

The incidence of adverse cardiovascular events exhibit a circadian rhythm, for example the onset of myocardial infarctions (MI) are 1.6 times more likely to happen between 06:00 and 12:00 than at other times throughout the day [8]. The demands on the cardiovascular systems change with time of day, and the close interaction of the circadian system with the cardiovascular system allow these demands to be met. Circadian rhythms underlie many processes in the cardiovascular system, such as autonomic input, blood pressure, heart rate and platelet activity [9-11]. However, this tight association means that the disruption of circadian rhythms is a risk factor for CVD. For example, changing the clocks to enter and exit daylight saving time significantly increased the incidence of acute MI in humans in the week following the clock change [12]. Shift work and social jetlag, where activity and sleep on workdays differs significantly to free days, are both common forms of circadian disruption, and are associated with an increase in triglycerides (TGs) and a decrease in high-density lipoprotein (HDL) cholesterol, obesity, atherosclerosis, type 2 diabetes, and other risk factors for CVD [13-15].

However, whilst circadian factors have been identified as playing an important role in cardiovascular health, the mechanism linking circadian disruption and CVD is not well characterised. No clear biological pathways have been identified, which means that there has been no development of targeted mitigation strategies or ways to identify those more at risk of circadian disruption-associated CVD.

This introduction aims to provide an overview on atherosclerotic CVD, cholesterol and lipoprotein metabolism, the APOE-/- mouse model of atherosclerosis, circadian rhythms and sleep function and dysfunction and the connection to CVD.

1.1 Atherosclerosis

Atherosclerosis is a chronic inflammatory disease of the arterial wall that is the biggest contributor to CVD. Characterised by progressive accumulation of lipids and inflammatory cells, cell death and fibrosis in the arterial walls, it can lead to thrombosis or stenosis and can cause MI and ischaemic stroke.

Lesion-prone areas of the arterial vasculature exhibit dysfunctional endothelial cells, leading to hyperpermeability [16]. This allows LDL to cross the endothelium into the subintimal space, where it is oxidised to Ox-LDL through the process of lipid peroxidation [17]. The presence of Ox-LDL within the subintimal space results in a damage signal being recognised by pattern recognition receptors (PRRs) on monocytes, leading to their emigration into the subintimal space and eventual differentiation into macrophages [17, 18]. T-cells are also recruited [16, 19]. The macrophages internalise Ox-LDL and hydrolyse and re-esterize the cholesterol esters contained within the Ox-LDL particles into cholesterol-FA esters [17, 19]. They remove excess cholesterol using enzymatic modification to transform the cholesterol esters into soluble forms, and by using membrane transporters to efflux cholesterol to HDL particles for reverse cholesterol transport [19]. However, the macrophages become unable to remove cholesterol quickly enough and it accumulates, inducing the morphological change of macrophages into foam

cells [17]. Lipid-laden foam cells accumulate, forming a fatty streak. This is driven by oxidative stress-induced changes in the lipid and APOB components of LDL. The fatty streak progresses into a lesion through infiltration of smooth muscle cells into the subintimal space [20]. The smooth muscle cells take up Ox-LDL, inducing PRR expression, and leading to more foam cell formation [19, 21]. They also synthesise extracellular matrix proteins that begin forming the fibrous cap of the atherosclerotic plaque [19]. Macrophages and T-cells interact within the lesion, leading to chronic inflammation [19]. As the content of the atherosclerotic plaque grows, stenosis of the artery occurs, impacting vascular flow and putting more pressure on the heart. The vessel may become so narrow that blood flow is completely obstructed, leading to ischaemia, which, depending on location, can cause MI or stroke. Additionally, the atherosclerotic plaque can rupture if it becomes unstable. The increase in the size of the necrotic core of the plaque, and reactive oxygen species (ROS) -mediated activation of matrix metalloproteinases (MMPs), which digest the extracellular matrix components of the plaque, both lead to plaque instability and rupture [19, 21, 22]. Rupture can lead to thrombosis, through activation of the coagulation cascade and platelet adherence, and is a major cause of acute cardiac events [19].

1.2 Cholesterol and lipoproteins

Abnormal cholesterol levels are a risk factor for CVD. However, cholesterol is also an important structural component of cell membranes and is a precursor in the synthesis of steroid and sex hormones, and vitamin D [23]. Therefore, maintaining cholesterol homeostasis is important. Cholesterol is lipophilic and so it is transported through the circulatory system inside lipoprotein particles. Lipoproteins are water-soluble macromolecular structures that allow transport of hydrophobic lipids in the plasma and the central nervous system (CNS) [24-27]. They transport TGs between tissues and mediate cholesterol homeostasis [28]. They consist of a hydrophobic core, containing cholesterol

esters and TGs, surrounded by free cholesterol, phospholipids and apolipoproteins [29, 30]. Clinically, lipoprotein levels are used as a marker for cholesterol levels.

Lipoproteins can be separated into classes according to density and apolipoprotein content [28]. The major classes, in order of size, are chylomicrons, very low-density lipoproteins (VLDL) and high-density lipoproteins (HDL) [24, 31]. Chylomicrons are >100 nm in diameter and are synthesised by the intestine to transport dietary TGs and cholesterol from the site of absorption in the intestinal epithelium to various cells of the body [24]. They contain apolipoprotein (APO) A-I, -II, -IV and IV, APOB-48, APOC-II and -III and APOE [30]. VLDL are 30- to 90-nm in diameter and transport triglycerides and cholesterol from the liver for redistribution to various tissues [24]. They contain APOB-100, APOC-I, II and -III, and APOE [30]. The triglycerides of VLDL are hydrolysed to free fatty acids (FFA) by lipoprotein lipase (LPL), generating a series of smaller, cholesterol-enriched lipoproteins including intermediate density lipoproteins (IDL) and low-density lipoproteins (LDL) [24]. IDL are ~27-35nm in diameter and are an intermediate product VLDL hydrolysis [32]. They contain APOB-100 and APOE [30]. LDL are ~20 nm in diameter and represent the end product of VLDL catabolism and are the major cholesterol-transporting lipoproteins in the plasma [24]. They contain APOB-100 [30]. High density lipoproteins (HDL) are ~8-12 nm in diameter and transport cholesterol from peripheral tissues to the liver for excretion [24]. They are synthesised from the liver, intestine and lipolysis of chylomicrons in the plasma, and contain APOA-I, -II and -IV, APOC-I, -II, III and APOE [24, 30].

Apolipoproteins are important structural components of lipoproteins that are essential for lipid transport as they mediate lipoprotein metabolism and cholesterol homeostasis by binding to specific cell surface receptors [24, 33]. They also act as cofactors for enzymes involved in lipid metabolism; and soluble apolipoproteins, such as APOA, APOC and APOE, can transfer between different lipoprotein classes [24, 28, 34, 35].

1.3 Lipoprotein metabolism

1.3.1 Exogenous lipoprotein metabolism

Dietary fats are absorbed into the mucosal cells of the small intestine as FFAs and cholesterol. They are re-esterized into TGs and cholesterol esters and packaged into the core of chylomicrons in the endoplasmic reticulum (ER) [29, 30, 36]. Chylomicrons are secreted into the lymphatic system using APOB-48 [29, 30]. Chylomicrons interact with LPL on capillary endothelial cell surfaces in fat and muscle tissue via APOC-II and are hydrolysed into chylomicron remnants and FFA, which are used as an energy source by fat and muscle cells [29, 30, 36-38]. The rate of hydrolysis is modified by APOC-III, which inhibits LPL activity [29, 30, 37]. After hydrolysis, other chylomicron components, such as phospholipids, APOA and APOC, are recycled to HDL [29, 30]. LPL activity ceases with the absence of APOC, and chylomicron remnants bind to hepatic LDL receptor (LDLR), LDLR-related protein and Heparan Sulphate Proteoglycan (HSPG) using APOE, clearing them from circulation via the liver [29, 38].

1.3.2 Endogenous lipoprotein metabolism

VLDL is assembled and secreted by hepatocytes [36, 38]. Structurally, VLDL consists of triglycerides, either newly synthesised or taken up from the plasma; cholesterol, either synthesised from acetate or taken up by hepatocytes as part of chylomicron remnants; APOB and phospholipids [29]. The VLDL particles are transported to peripheral tissues and hydrolysed by LPL. This process is similar to chylomicron hydrolysis: using APOC-II as a cofactor and releasing fatty acids (FA), resulting in IDL [29, 38]. Excess VLDL components are also released into the HDL pool [29, 38]. APOE is acquired by IDL from HDL and binds to LDLR, LDLR-related protein and HSPG on hepatocytes, clearing some (~50%) IDL particles [30, 38]. Remaining IDL particles are lipolyzed by hepatic lipase to LDL [36, 38]. LDL particles contain APOB-100, which binds to LDLRs and clears LDL from the plasma [29, 30, 38]. APOE is divided between the VLDL and HDL pools, to ensure optimal rates of lipolysis, VLDL clearance and HDL formation [38].

1.3.3 HDL metabolism and reverse cholesterol transport

There are multiple subtypes of HDL, but generally, HDL is synthesised by the liver and intestine [24, 29, 30, 36]. APOA-I is the crucial structural component of HDL and acquires cholesterol and phospholipids from hepatocytes and enterocytes using ATP Binding Cassette Subfamily A Member 1 (ABCA1), and acquires lipids from other tissues and lipoproteins, including from chylomicron and VLDL hydrolysis [24, 29, 30, 36]. HDL is the initial acceptor of free cholesterol [29, 30]. This free cholesterol sits on the surface of HDL particles, until it is converted into cholesteryl esters by lecithin-cholesterol acyltransferase (LCAT) and moves into the core of the HDL particles [29, 30]. HDL particles increase in size as they collect cholestryl esters, allowing other apoprotein incorporation [29]. The cholesteryl esters can be transferred to triglyceride rich APOB-containing lipoproteins (chylomicrons and VLDL) using Cholesteryl Ester Transfer Protein (CETP), and are taken up by the liver as described above, leaving triglyceride-enriched HDL particles which are metabolised by lipases [29, 30]. The cholesteryl esters can also be transferred directly to tissues, primarily the liver, from HDL. HDL “docks” using hepatic Scavenger Receptor B1 (SR-B1) and cholesterol is transported from the HDL particle to the liver [29, 30]. Additionally, HDL particles or components containing APOE can be taken up by the hepatic LDLRs, and the APOA-I component is catabolized by the kidneys and liver [29, 30]. As HDL accepts free cholesterol, it is used to remove cholesterol from peripheral cells which cannot catabolise it. These cells efflux cholesterol to mature HDL particles, in a process called reverse cholesterol transport [24, 29, 30]. HDL delivers the cholesterol to the liver using the mechanisms described above, and the cholesterol is then converted to bile acid and secreted in bile, or excess cholesterol is directly secreted into bile [24, 30].

1.4 Apolipoprotein E

APOE is a mediator of lipid transport and has been implicated in CVD. It is a structural constituent of VLDL, HDL and chylomicrons, and regulates cellular uptake of these

particles by binding to members of the LDLR family [25, 39-41]. Therefore, a change in *ApoE* expression can affect APOE, and therefore lipoprotein, structure, and may prevent lipoprotein uptake by receptors, increasing cholesterol levels and the risk of atherosclerotic CVD [25, 40].

In the periphery, the liver synthesises the majority (~75%) of plasma APOE, whilst macrophages and adipocytes are the other main sites of peripheral APOE synthesis [42, 43]. The brain is the secondary site of APOE production [44]. APOE is the most abundant apolipoprotein in the central nervous system (CNS), playing a central role in CNS lipid transport, as APOB is absent [45]. APOE doesn't cross the blood-brain-barrier (BBB) and so is synthesised locally [46-48]. Astrocytes are the primary site of APOE synthesis in the brain, and APOE is also produced by oligodendrocytes, microglia and, when stressed, neurons [49, 50]. In the CNS APOE is found within HDL-like particles, and APOE secretion and lipidation is regulated by ABCA1 [45, 51, 52]. These HDL-like lipoproteins transport phospholipids and cholesterol to neurons for repair, growth and synaptogenesis, processes which are essential for neuronal plasticity [53-56]. Cholesterol in the CNS is synthesised de novo, as the BBB restricts the crossing of plasma lipids from the periphery [45]. However, cholesterol synthesis is supressed in neurones, and so they rely on astrocytic cholesterol production and APOE-mediated cholesterol transport [57, 58].

The APOE protein has two independent domains – the N-terminal domain and the C-terminal domain, linked with a central hinge region. The N-terminal contains the receptor binding domain and binds to the LDLR family. The C-terminal contains the lipid binding domain [59, 60].

1.4.1 APOE in humans

In humans, the *ApoE* gene is located on chromosome 19 and is polymorphic, with different isoforms of *ApoE* affecting the binding affinity of APOE to LDL-Rs [25]. There are three common isoforms of the gene: *ApoE-ε2*, *ApoE-ε3* and *ApoE-ε4*. The distribution of these isoforms is uneven, with most of the general population carrying the ε3 isoform,

which is considered the physiological isoform [61]. Each isoform differs by a single amino acid substitution. In the *ApoE-ε2* isoform, the substitution of arginine to cysteine at position 158 leads to significantly reduced affinity to the LDLR, and so impaired lipid clearance [59, 60]. In the *ApoE-ε4* isoform, substitution of cysteine to arginine at position 112 changes the conformation of the N-terminal domain, charged residues from the protein core move to the surface and establish interactions that modify the protein structure, and results in a change in lipid preference of the C-terminal from HDL to VLDL [59, 60]. Due to their differences in structures, the different *ApoE* isoforms impact LDL levels, and LDL cholesterol levels increase with isoform status from homozygous *ApoE-ε2* to homozygous *ApoE-ε4* [62, 63]. The *Apoe-ε2* isoform is the primary underlying cause of type III hyperlipoproteinemia, due to impaired clearance of APOE-rich lipoproteins [64, 65]. There is an accumulation of VLDL and TGs, with reduced VLDL hydrolysis and therefore LDL formation [64]. Individuals with type III hyperlipoproteinemia prematurely develop coronary heart disease (CHD), peripheral vascular disease and atherosclerosis [64-66]. Atherosclerosis in those with type III hyperlipoproteinemia seems to be driven by lipoprotein remnants rather than LDL [67]. The *ApoE-ε4* allele is best known for being a risk factor in developing late-onset and sporadic Alzheimer's disease (AD), showing the importance of functional APOE in the CNS, whilst the *ApoE-ε2* isoform can be protective against AD [25, 26, 60, 68-72].

1.4.2 The APOE-/- mouse model

The APOE knockout (KO; APOE-/-) mouse model was developed to study the role of APOE in lipid metabolism and atherosclerosis development. The mice show delayed clearance of lipoproteins and accumulate high plasma cholesterol levels, which are 5-fold higher than wildtype controls [73, 74]. They also show altered plasma lipoprotein content, with a reduction in HDL and increased VLDL, TG, LDL and IDL, showing what would be considered a "pro-atherogenic" profile in humans [73, 74]. This occurs independently of diet, age, or sex. The mice spontaneously develop atherosclerotic plaques at vascular

sites commonly affected in human atherosclerosis [75, 76]. Fatty streaks in the aorta are seen from 3 months of age and aortic lesions have been reported as early as 5-6 weeks of age [76]. Lesions increase with age and progress to pre-atherosclerotic lesions: less lipid and increased elongated cells. Aged APOE-/- mice can develop xanthomatous lesions, which contain lipid-laden foam cells, in the brain. They also develop progressive eruptive xanthomas, severe enough that the mice aren't allowed to be kept alive longer than 18 months [39]. The model also experiences premature death, 35% of a cohort died before 18 months due to advanced atherosclerotic lesions [39]. A high-fat diet accelerates this pathology and results in mice having to be euthanised by 7 months of age [25].

1.5 Gene-environment interaction

The risk of CVD is recognized as a combination of genetic and environmental factors. Individuals with a genetic predisposition are more likely to develop CVD when leading a particular lifestyle [77]. This combination of these two distinct factors can be termed a "double-hit hypothesis", where the "hits" interact and contribute to the development and progression of the disease. The most well-known risk factors are smoking, diet and exercise, yet despite this knowledge, the prevalence of CVD remains high [78]. Interventions aimed at preventing and treating CVD may face challenges in effectiveness due to a limited understanding of how interactions between genetics and environmental factors can impact the risk of developing CVD or its progression.

Gene-environment interactions are defined as interactions where the combined effect of genotype and environmental exposure is significantly different to the additive effects of genotype and environmental exposure [79]. Studying gene-environmental interactions allows identification of biological pathways that are key for disease pathogenesis, and so improves understanding of disease aetiology.

As circadian rhythms are known to be an environmental factor which affects the risk of CVD, studying the interaction between a genetic model of atherosclerotic CVD and environmental circadian disruption may shed light on the underlying mechanisms.

1.6 An overview of circadian rhythms

Circadian rhythms are oscillations with a period of ~ 24 hours that are found at a molecular, physiological, and behavioural level in most organisms; named from the Latin "*circa diem".* These rhythms developed in response to the light/dark environment imposed by the Earth's rotation. This pattern of light and dark allows anticipation of temperature changes, food and light availability as well as alignment of biological functions to the external environment [80]. The sleep-wake cycle is the most well-known circadian rhythm, but there are other cycles, including feeding-fasting, body temperature, metabolism, T-cell immune response and hormone secretion [81-86]. Circadian rhythms persist in the absence of environmental factors; a master clock generates these endogenous oscillations which can be synchronised to the external environment [87, 88]. See Figure 1.1 for the properties of circadian oscillations.

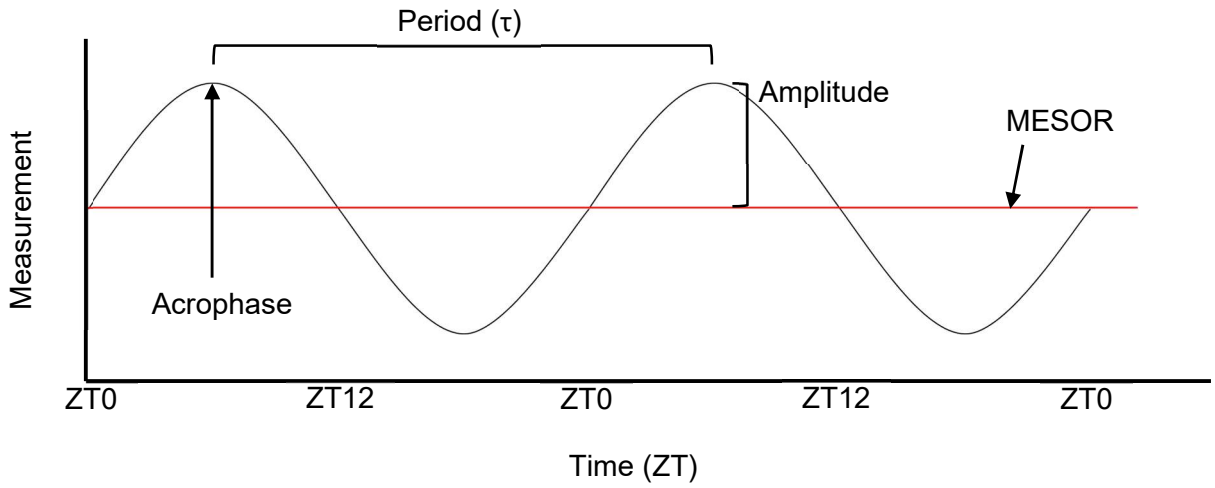


Figure 1.1: Schematic showing the properties of a circadian oscillation.
Amplitude: Strength of the rhythm, the difference between the peak and the midline-estimating statistic of rhythm (MESOR) of the oscillation. Period: time it takes for the rhythm to complete one full oscillation. Tau, or free running period, is the period in the absence of entraining factors. Acrophase: The time at which the peak of a rhythm occurs. MESOR: the average around which the rhythm oscillates.

1.6.1 Molecular circadian clock

Virtually every mammalian cell, tissue and organ system has their own circadian clock [89]. Cellular circadian rhythms are driven at a molecular level, with an autoregulatory transcriptional-translational feedback loop of highly conserved proteins, Circadian locomotor output cycles kaput (CLOCK), Basic helix-loop-helix ARNT-like protein (BMAL1), Period (PER) and Cryptochrome (CRY) (Figure 1.2). CLOCK and BMAL1 are in the positive limb of the loop, and PER and CRY are in the negative limb [90, 91]. This molecular feedback activates a rhythmic cascade of transcriptional and posttranscriptional events involving thousands of target genes, and ~5-10% of genetic transcripts exhibit circadian periodicity, and an even larger number of proteins undergo oscillations at the post-transcriptional and post-translational levels [92, 93]. The molecular clockwork is sensitive to perturbation, and changes in clock gene expression and desynchrony between the central and peripheral oscillators have an impact on genes and physiological processes [94]. This is associated with chronic illnesses, and an increased risk of adverse

health conditions, including CVD [94-96]

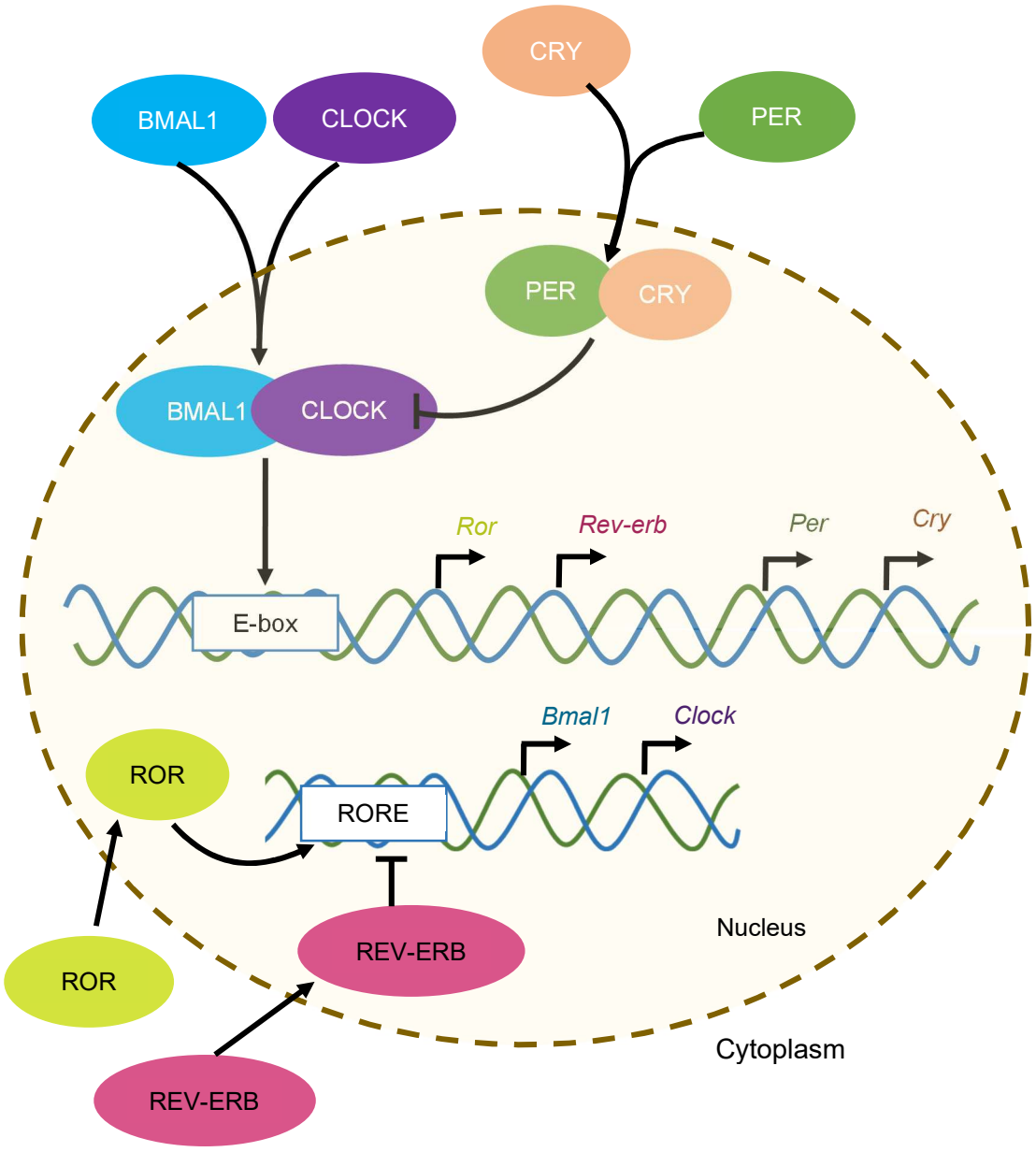


Figure 1.2: The mammalian molecular clock.
The CLOCK:BMAL1 heterodimer binds to E-box DNA motifs, initiating transcription of PER and CRY, which dimerize and inhibit CLOCK:BMAL1 activity. This inhibits their own transcription and once degraded the inhibition of CLOCK and BMAL1 is removed, allowing the cycle to start again [1,2]. Another feedback loop is activated by CLOCK and BMAL1, involving the retinoid-related orphan receptor (RORs) and REV-ERB proteins binding to the Retinoic acid-related Orphan receptor Response Element (RORE) binding sites in the Bmal1 promotor. ROR activates transcription of Bmal1 and REV-ERB represses it, regulating the timing of Bmal1 expression.

1.6.2 Entrainment and the central clock

Cues from the external environmental, or Zeitgebers, synchronize an organism's circadian rhythms to the environment. The most common zeitgebers are light, food availability, temperature, social activity, and exercise [97, 98]. Light is the dominant zeitgeber for most organisms, as there is a high contrast between "day" and "night", which is the most reliable environmental indicator of "time". From day to night the change in light intensity is around 130,000-fold, and depending on species, organisms display diurnal, nocturnal or crepuscular behaviour [97, 99, 100].

The hierarchical organisation and coordination of these clocks and rhythms is essential for biological function and health [101]. The master clock, or the central clock, is in the suprachiasmatic nucleus (SCN) of the hypothalamus. SCN neurones, like other cells, can autonomously generate circadian rhythms. However, the SCN is the only clock to receive direct photic input. Rods and cones in the retina detect photic information and transmit to the SCN via the retinohypothalamic tract (RHT) [102]. A third type of photoreceptor, the intrinsically photosensitive retinal ganglion cell (ipRGC) is non-image forming and is key for detecting and transmitting photic information. ipRGCs contain melanopsin, which is essential for photosensitivity [103, 104]. They measure environmental irradiance and spectral qualities of light, and modulate the physiological responses to light [105]. ipRGCs combine rod- and cone- outputs with melanopsin-driven activities and transduce them into the excitatory glutamatergic signal that affects the SCN molecular clockwork predominantly via NMDA receptors [106]. SCN neurones are activated and synchronise to the external light pattern. The SCN coordinates the individual cellular oscillations and drives rhythms of peripheral oscillators downstream using neuropeptide signalling to maintain and synchronise physiological and behavioural rhythms [107].

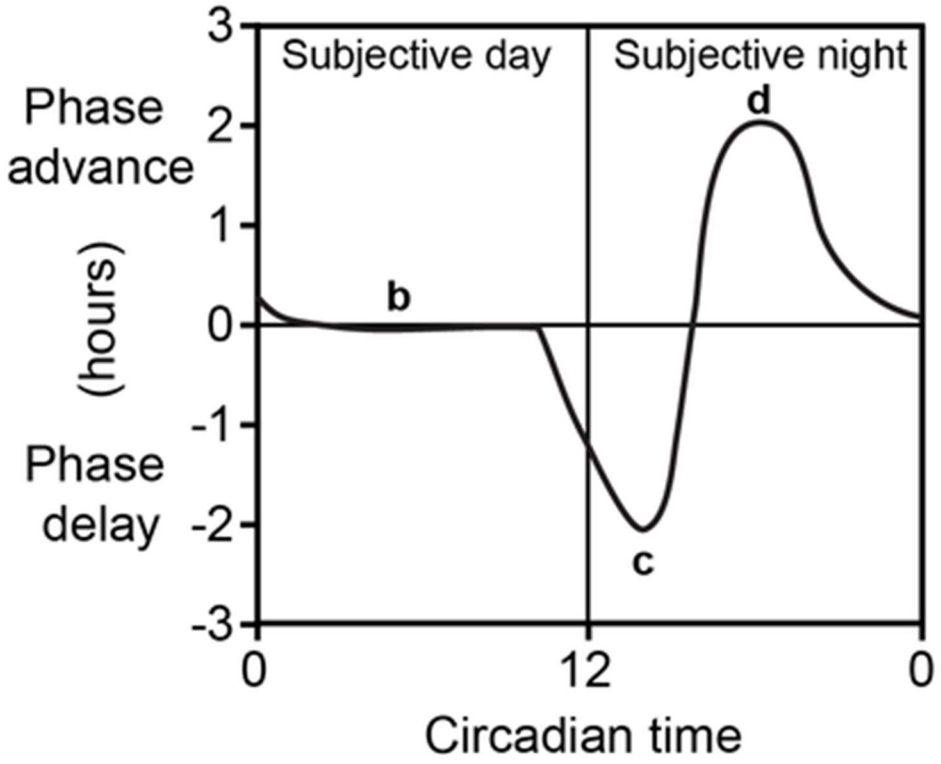


Figure 1.3: Example of the photic phase response in mice.
Photic stimulation is relatively ineffective throughout the middle of the subjective day (b). Photic stimulation during late subjective day or early subjective night /i.e., at around subjective dusk) results in phase delays (c). Photic stimulation during late subjective night or early subjective day/i.e., at around subjective dawn results in phase advances (d). Adapted from Grippo and Guler [3]

Light can also directly reset the clock, as shown by changes in locomotor wheel running rhythms, but the impact of the light pulse depends on the time [108, 109]. The relationship between the time of the light pulse and the response is called the photic phase-response curve (PRC; Figure 1.3)[110]. Phase refers to when the peaks and troughs of the oscillations of the organism occur. In mammals, re-setting of the clock by light depends on retinal input [111]. In other vertebrates, deep brain structures are involved, and invertebrates have light-sensitive cells and tissues [112]. Therefore, the visual system is important for entrainment.

As well as receiving direct light input, the SCN also receives information from other brain areas which allows non-photic cues to entrain and reset the circadian system. Non-photic cues can be cyclic cues, e.g., time restricted feeding, conditioned stimuli and temperature variation; or non-cyclic, e.g., a novel environment or sleep deprivation [82, 113-115]. The

SCN receives non-photic information through multiple pathways. The intergeniculate leaflet (IGL), a nucleus in the lateral geniculate of the visual thalamus, receives retinal input via the primary optic tract, and projects to the SCN through the geniculohypothalamic tract (GHT) using inhibitory γ-Aminobutyric acid (GABA) and Neuropeptide Y (NPY) [116]. The median raphe (MR) projects to the SCN using serotonin (5-Hydroxytryptophan or 5-HT), which has an inhibitory effect on SCN neurones, regulating the rhythm of neuronal firing [117]. Additionally, the dorsal raphe (DR) projects to the IGL using 5-HT, which also inhibits the firing of SCN neurones [117].

The SCN integrates both photic and non-photic cues to align with the external environment and to control the resetting of the clock to ensure the organism is functioning on a 24-hour rhythm. If the photic and non-photic cues are not in sync, this could lead to conflicting signals reaching the SCN. The clock may continually reset, leading to a loss of its ability to predict the environment and increased predation in animals, whilst humans experience decreased cognitive performance, insulin insensitivity, hypertension, and blunted cortisol rhythms amongst other adverse metabolic changes [118].

1.6.3 Clock communication and peripheral oscillators

The SCN clock projects to various brain centres, some contain local circadian clocks that direct behavioural (for example, feeding–fasting and sleep–wakefulness), autonomic and neuroendocrine circadian rhythms [119, 120]. These systemic cues synchronize local molecular clocks of peripheral tissues, and these local clocks direct local programs of circadian gene expression regulating critical physiological rhythms [101, 121]. For example, sympathetic projections from the SCN to the paraventricular nucleus (PVN) and then the liver control the circadian rhythm of plasma glucose [122].

Rhythms are generated even in the absence of the SCN; for example, in cultured fibroblasts, showing that endogenous circadian oscillators are ubiquitous [89, 101, 123]. Peripheral oscillators integrate signals from the SCN with environmental and behavioural cues and their own autonomous rhythms to regulate metabolism [101, 124]. Additionally,

they can entrain to some zeitgebers independently from the SCN. Animals show anticipatory behaviour to regular meals, and this is independent of the light:dark (L:D) cycle [125]. There is also evidence this food anticipatory behaviour is independent of SCN as it persists in rodents with abated SCN [125]. The concept of the food-entrainable oscillator (FEO) was developed to explain these SCN-independent rhythms associated with food, and it was shown that the FEO could generate rhythms autonomously and integrate SCN signals [126, 127]. Peripheral oscillators can entrain to the FEO, but the SCN cannot [127, 128]. If the SCN and peripheral oscillators are entrained to different zeitgebers, they can fall out of sync, termed “internal desynchrony” [128, 129].

Jet lag is a common example of internal desynchrony in humans [130]. Air travel often involves crossing time zones, resulting in changes in the input to the circadian system. The central clock adapts quickly, but peripheral oscillators adapt at different rates, leading to different rhythmic phases between organs, and a common experience of “malaise” [130].

1.7 An overview of sleep

The sleep-wake cycle is the most widely known circadian rhythm. However, whilst it is under the “circadian umbrella”, it is not solely under the control of the circadian system. Sleep can be defined as a normal loss of consciousness with reduced response to external stimuli that is rapidly reversible [131]. It has a distinct electrophysiological profile with complex alternating patterns of specific neurological activity [131, 132]. It is highly conserved throughout evolution, occurring in all multicellular organisms and duration appears to increase with organism size [133]. For example, although mice are nocturnal, they display sleep and activity in both the light and dark phases. However, sleep bouts are more frequent in the light phase and active bouts are more frequent in the dark phase [134].

Sleep is a basic need and occurs in regular intervals. Functions of sleep have been hypothesised to include clearance of metabolic waste, conservation of metabolic energy, neural maturation, cognition, and memory consolidation [131, 135]. It has three underlying regulatory processes – homeostatic, circadian and ultradian [131]. The relationship between homeostasis and circadian rhythms in regulating sleep is described in the two-process model of sleep regulation.

1.7.1 The two-process model of sleep regulation

There is a homeostatic drive for sleep which is determined by the quality of previous periods of sleep and time spent awake. The drive for wake, and so sleep duration, is regulated by the circadian system. When the circadian drive for arousal is low, and the homeostatic drive for sleep is high, the “sleep gate” opens (Figure 1.4).

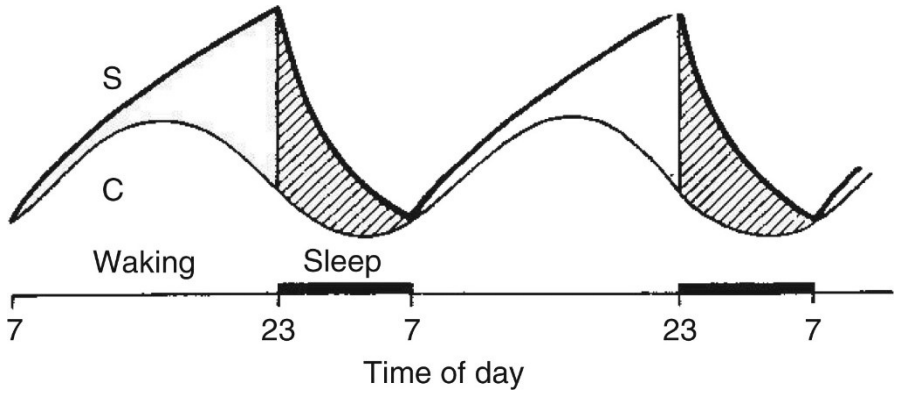


Figure 1.4. The two-process model of sleep regulation.
S is the homeostatic drive for sleep. C is the circadian regulation of wake and sleep. Adapted from Ong and Park [2].

These two processes balance, to prevent a sleep debt or multiple short bouts of sleep, neither of which are biologically advantageous. Homeostatic sleep regulation allows compensation for sleep loss and can adjust duration and depth to match the need for sleep. Homeostatic drive increases with time spent awake and decreases with time spent asleep. Circadian regulation maintains the sleep-wake cycle on the 24-hour cycle that the organism is entrained to, and maintains wakefulness once the organism is awake,

opposing the homeostatic drive [136, 137]. The interaction of homeostatic and circadian processes determines sleep duration.

1.8 The importance of light conditions

One of the defining characteristics of a circadian rhythm is its ability to persist in the absence of zeitgebers. In constant conditions, the period (τ) is generated by an organism's endogenous oscillators. T usually has a different length to the 24 hours that is maintained by the L:D cycle, and this difference is known as free running. Free running τ is species specific, and depends on the type of constant environment, the individual organism and its physiological state [138-140]. Since light is the primary zeitgeber for most organisms, its impact is well characterised. Constant darkness and constant light have different effects on τ, and τ has been shown to change with light intensity and is impacted by temperature [141].

Constant darkness (D:D) allows the endogenous circadian rhythm of the organism to be dominant, without the masking effects of light. Conversely, continuous exposure to light (L:L) sends conflicting time signals to biological clock. It desynchronises SCN neurons, disrupting SCN organisation; and subsequently peripheral clocks, leading to internal desynchrony [142]. Internal desynchrony has biological consequences, for example the amplitudes of glucocorticoid rhythms and body temperature rhythms are significantly dampened in L:L [143, 144]. During L:L exposure, rodents have been shown to lose behavioural rhythmicity, show an abnormally lengthened period which subsequently can become arrhythmic, and some rodents show split locomotor activity rhythms, where active behaviours start occurring twice within each 24-hour period [145]. Additionally, L:L impacts multiple aspects of sleep in rodents, including altering the proportion of rapid-eye-movement (REM) and non-REM sleep, and increases depressive-like behaviour, whilst having an anxiolytic effect [146, 147].

1.8.1 The relevance of light conditions for humans

For humans, artificial light is ubiquitous in modern society, enabling society to function around the clock. Exposure to artificial light at night (ALAN) has been estimated to have increased annually by 6% [148]. Even a few hours of bright light or blue light in the “dark” period of humans impacts circadian rhythms and sleep. For example, light-emitting eReader use before sleep decreased delta/theta activity, increased latency to sleep, and reduced the amount of REM sleep as measured by electroencephalogram (EEG) compared to printed book use using reflected light [149]. Additionally, a decrease in subjective sleepiness and impaired morning alertness was reported; and the phase of melatonin secretion was delayed [149].

Shift workers, who are crucial in maintaining our 24-hour society, are the most impacted by ALAN. Shift work leads to workers being misaligned to the external environment; their endogenous circadian system will entrain to the natural light-dark cycle, but their behavioural rhythms (including fasting-feeding cycle) and sleep-wake cycle occur in the rhythm of the shift pattern. This circadian misalignment is known to lead to internal desynchrony, abnormal glucose metabolism, increased blood pressure, sleep changes and abnormal cortisol rhythms [150]. Both shift work and chronic jet lag are associated with adverse health outcomes, such as type 2 diabetes, CVD, and cancer [150-153].

1.8.2 Light and Oxidative stress

In addition to the disruption of circadian rhythms and sleep, light can also induce oxidative stress [154]. Oxidative stress is defined as an imbalance between prooxidants and antioxidants resulting in macromolecular damage and disruption of redox signalling and control [155].

Photons of light are absorbed by photosensitisers, endogenous pigments which can transfer light energy. Photon absorption results in the photosensitiser reaching an excited singlet state forming an excited triplet state. Interactions with other molecules result in

ROS generation through type I photosensitization (electron transfer) or type 2 photosensitization (energy transfer forming singlet oxygen) [156, 157].

Oxidative stress has been shown to be a key process in atherosclerosis development and is implicated in the pathogenesis of multiple health conditions, such as cardiovascular disease, heart failure, cancer, and neurodegenerative diseases [158-161]. It is also associated with the circadian system, as the antioxidant defence system has circadian rhythm of expression, and induction of oxidative stress using ROS has a different effect depending on time of day [162].

1.9 Circadian disruption, sleep and the cardiovascular system

Circadian rhythms underlie many processes in the cardiovascular system, such as autonomic input, blood pressure, heart rate and platelet activity [9-11]. Cyclic expression of ion channels and metabolic enzymes enables diurnal variations in cardiac electrical properties and metabolism, which match daily fluctuations in energy demand and nutrient availability [121]. However, if demands on the cardiovascular system of an organism are not met there is a risk of an adverse cardiac event occurring.

Atherosclerosis is the underlying pathology for most CVDs [163]. The lipid transport system is under circadian control, likely to maintain energy balance; and circadian variations in lipids can be seen in rodents and humans [163, 164]. Circadian disruption has an effect on lipid transport, models of abnormal lipid metabolism show increased atherosclerosis with a mutation of a core clock gene [165]. The circadian system also controls daily variations in the immune and vascular systems, both of which are dysregulated in atherosclerosis [163].

Generally, time spent asleep has decreased across the world over the past few decades, as the pressure of working and living in “24/7” world has increased [166]. Both short and long sleep durations (≤6, ≥10 hours a night) are associated with an increased risk of hypertension [166]. Short sleep length has shown to be an independent marker of incident

hypertension; and is associated with a higher risk of atherosclerosis [166, 167]. It has been suggested that sleep loss has a sympathoexcitatory effect, and enhanced cardiac sympathetic drive has been documented after sleep loss and short sleep length [168]. Additionally, short sleep length impairs glucose homeostasis and insulin sensitivity, as well as being associated with a stimulation of pro-inflammatory immune pathways, which are all risk factors for CVD [168, 169].

Disrupted circadian rhythms, whether by internal desynchrony, circadian misalignment or another mechanism, and disrupted sleep are key risk factors in atherosclerosis development and cardiovascular disease. The mechanisms underpinning the relationship between disrupted circadian rhythms and cardiovascular disease development are not well understood and more research is needed to improve our understanding in order to be able to mitigate CVD risk and develop targeted prevention and treatment strategies.

1.10 Hypotheses and aims of work

The aim of this thesis was to investigate the gene-environment interaction between genetic susceptibility to CVD and environmental circadian disruption using the APOE-/- mouse model and L:L exposure in a “double hit” approach.

Specifically, this thesis aimed:

1. To characterise the circadian rhythms of behaviour and gene expression in the APOE-/- mouse model, as well as investigating differences in sleep, home cage behaviour and anxiety-like behaviour and hedonic behaviour.

It was hypothesised that the absence of APOE in the CNS would cause alterations in sleep and behaviour in the APOE-/- model. In addition, it was hypothesised that APOE mice would show abnormal peripheral rhythms of core clock genes and genes regulating lipid metabolism, as the absence of APOE disrupts lipid transport.

2. To examine how circadian disruption with L:L exposure interacts with the APOE-/- mouse model to affect behaviour, sleep, lipid homeostasis, oxidative stress and the glial cell response.

It was hypothesised that L:L exposure in the APOE-/- model would further exacerbate abnormalities in behaviour and sleep already present in the model, as well as dampen behavioural rhythms and induce anhedonia. Additionally, it was hypothesised that APOE-/- mice would show a significant glial cell response, as glia are the site of production for APOE in the CNS, and they would show altered lipid homeostasis which is further exacerbated by L:L.

3. To investigate the effect of the gene-environment interaction between L:L and the APOE-/- model on the metabolome of the plasma, brain and liver.

It was hypothesised that the gene-environment interaction between the APOE-/- model and L:L would cause changes in lipid and carbohydrate metabolism across the three tissue. Additionally, it was hypothesised that L:L would cause alterations in lipid metabolism and oxidative stress pathways.

2 Materials and Methods

2.1 Animals

All experiments were performed consistent with the UK Animals (Scientific Procedures) Act, 1986 and were approved by the local Animal Welfare Ethical Review Body (UK Health Security Agency, formerly Public Health England, Chilton). Male C57BL/6J mice, supplied by Envigo (Bicester, UK) and homozygous ApoE^{tm1Unc} (APOE-/-), supplied by Charles River (Charles River, USA) were used. Mice were group housed unless otherwise stated, with food and water available *ad libitum*. They were maintained on a regular 12-hour L:D cycle (06:00-18:00) at an average of 57 lux unless otherwise stated, with temperature at 21°C and humidity at 65%.

2.1.1 APOE-/- mouse model

The apolipoprotein E (APOE) knockout mouse model (B6.129P2-ApoE$^{tm1Unc/J}$) was developed as a model for atherosclerosis by Dr Nobuyo Maeda at The University of North Carolina at Chapel Hill through gene targeting in murine embryonic stem cells (129P2/OlaHsd-derived E14Tg2a ES cell line) [40]. The ApoE locus was inactivated by homologous recombination, using the pNMC109 plasmid [40]. The ApoE^{tm1Unc} strain was produced by backcrossing at least 10 generations to C57BL/6J inbred mice [40]. The C57BL/6J mice were used as controls. They are a well characterised strain, and the C57BL/6J line is the genetic background upon which the APOE$^{-/-}$ model was developed.

2.2 Circadian manipulation

2.2.1 Entrainment and L:D cycle shifts

Entraining to shifted L:D cycles took place in a ventilated cabinet (ScanTainer) fitted with a light adjustment kit (Scanbur, Karlslunde, Denmark). The lights reached a maximum of 80 lux, and the dark period was measured as less than 0.5 lux. The “dusk” and “dawn” period lasted 30 minutes, with 50% of the max lux changing gradually within the first 15

minutes, and the remaining 50% changing gradually within the next 15 minutes. Mice had a minimum of 2 weeks to adjust to the new L:D cycle to ensure full entrainment at a rate of one hour per day.

2.2.2 Constant Darkness

Exposure to constant darkness were performed using black, light-tight, cylindrical "hatbox" cages, made from polymethyl methacrylate material (diameter 45 cm, height 38 cm; Figure 2.5). Each hatbox cage had two separate compartments which contained up to 3 mice. The walls of the compartments were covered in white tape to provide contrast to the black mice for video tracking. Food and water were available *ad libitum* and airflow in the cages was 2L/min.

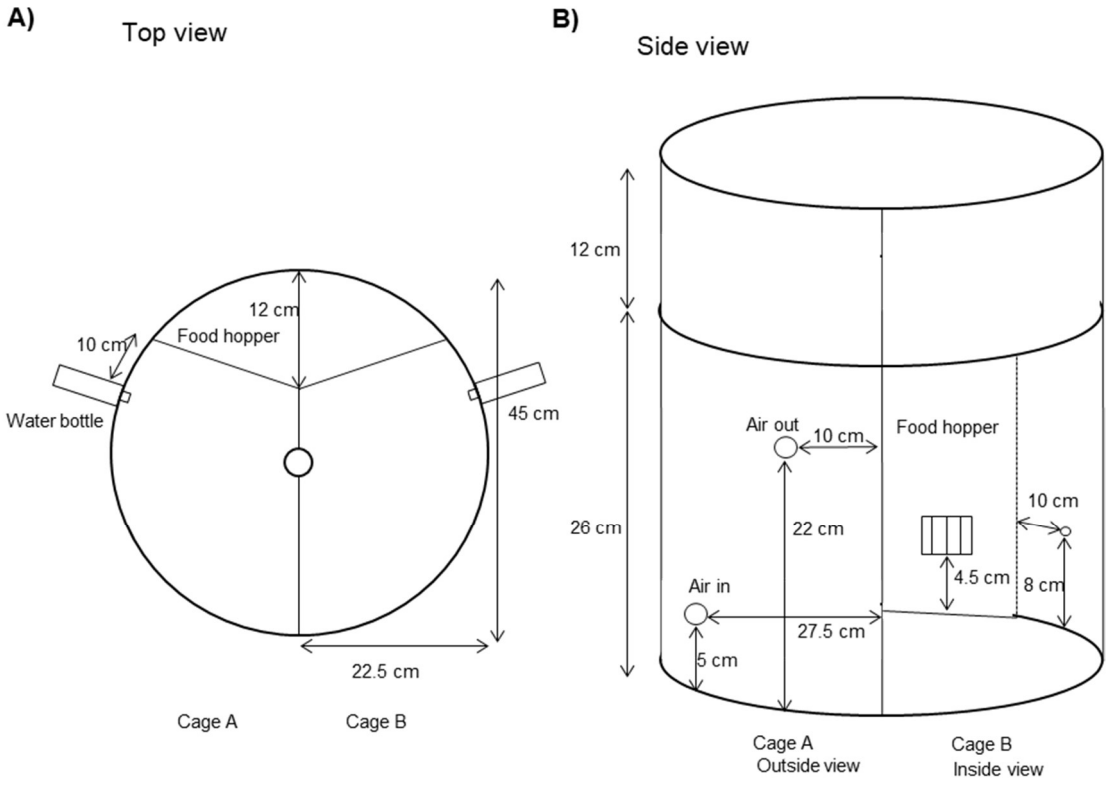


Figure 2.5. "Hatbox" cage dimensions.
Schematic showing the measurements of the light tight hatbox cages where **A)** gives the top-down view, and **B)** gives a side on view. Each cage was 38 cm high and had a diameter of 45 cm. A divider went down the midline of each cage, dividing them into two compartments. Adapted from Lundberg et al [1].

2.2.3 Instrumented observation cage and constant light exposure

PhenoTyper 4500 home cages (45 x 45 x 56 cm; Noldus, NL), with USB-IO boxes (Noldus, NL) were used to track, measure and assess behaviour as well as control experiment conditions, together with EthoVision XT 14 (Noldus, NL) software. Each cage had a top unit, (30 x 30 x 9 cm) with an integrated infrared sensitive camera with three arrays of infrared LED lights. The yellow “house” light had a wavelength of 590nm and a maximum lux of 40 lux. The white spotlight had a maximum lux of 1000 lux. For exposure to constant light, both the yellow house light and the white spotlight were used, to ensure complete illumination of the cage. Each cage also had a PhenoWheel – a running wheel magnetically attached to the side of the cage where the number of rotations is counted by the magnet and magnetic sensor. Mice were individually housed, and food and water were available *ad libitum*. A lickometer (Noldus, NL) was used to detect contact made with the water bottle by the mice and the food hoppers uses the Mouse Feeding Monitor (Noldus, NL) – a beam break mechanism utilised to track feeding duration and frequency. EthoVision XT 14 (Noldus, NL) software was used to track the mice individually, using centre-point tracking, and analyse behaviour, integrating data collected from the camera, PhenoWheel, Lickometer and Mouse Feeding Monitor (Figure 2.6). Recording was paused whilst data was backed up weekly, and mice were weighed during this time.

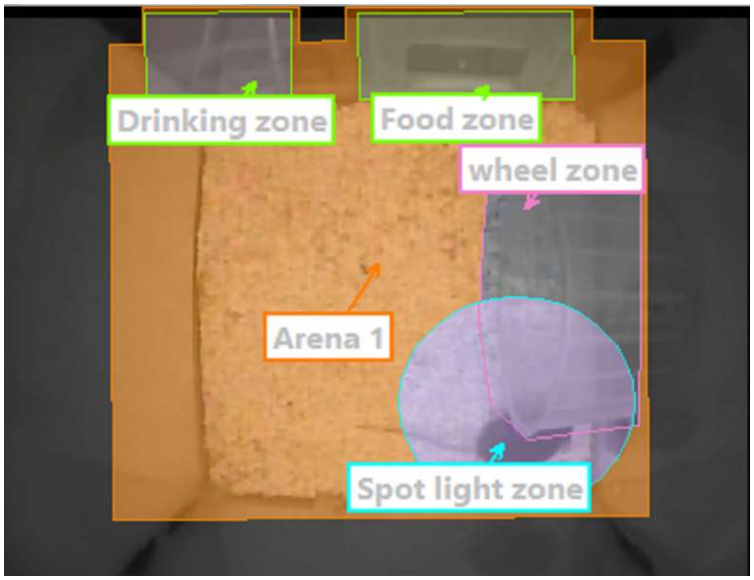


Figure 2.6. "Arena" set up in the instrumented observation cages (PhenoTypers). Schematic showing the analysis zones set up in EthoVision XT 14. Mice were in the PhenoTyper cages for 2 weeks in L:D conditions and then 3 weeks in either L:L or L:D conditions.

2.3 Behaviour

Standard tests were used to assess behavioural changes in the mice induced by different environmental conditions or to phenotype the mouse model. Mice were previously habituated to individual housing prior to all forms of behavioural assessment.

Behaviour in the hatbox cages was recorded using digital infra-red charge-coupled device (CCD) cameras (Sony, NC1358WA) in the lid of each cage compartment, connected to a digital video recorder (Samsung, SRD-476D). EthoVision XT 14 (Noldus, NL) was used to track the individual mice from the recorded videos, using centre point detection (Figure 2.7). The Lowess track smoothing profile was applied, which is based on 10 samples before and after every sample point.

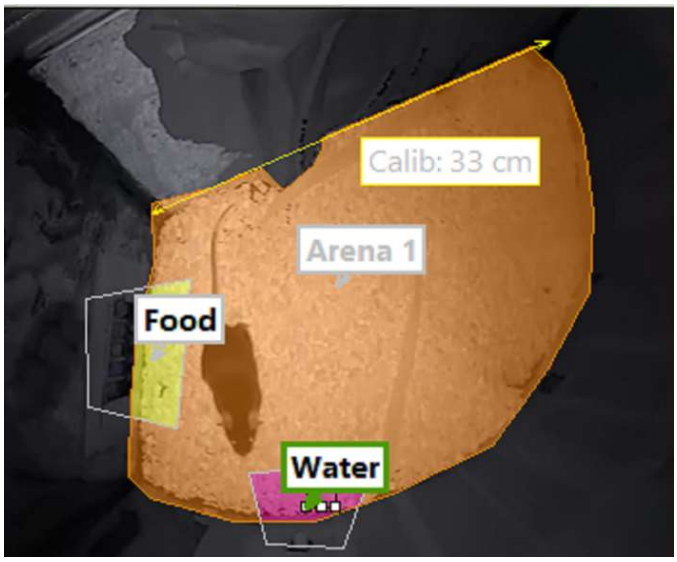


Figure 2.7. "Arena" set up in the "hatbox" cages.
Schematic showing the analysis zones set up in EthoVision XT 14. Mice were in the "hatbox" cages for 10 days in D:D conditions.

2.3.1 Free running behaviour

Free running is used to identify reoccurring features in behaviour in constant conditions, such as the underlying period of the rhythms. With environmental circadian disruption, changes are usually observed in activity bouts of the mice, where the number of bouts increase, and the duration of these bouts decrease. Additionally, the amplitude of the underlying rhythms decreases as activity becomes fragmented across the active and rest periods. Period is usually unaffected unless light is involved [170]. The total distance travelled (cm) calculated in EthoVision (Noldus, NL) was split into 1-minute time bins, exported as a Microsoft Excel file, formatted, and changed to an .AWD file extension and opened in ClockLab (ClockLab Analysis V6.1.01, Actimetrics) to generate actograms. Free-running period was calculated using a chi-squared periodogram (significance set at 0.001) using data from the final 7 days of exposure. Amplitude of the rhythms were also calculated using the chi-squared periodogram. Activity bouts are defined by ClockLab as, "periods during which the activity (counts/min) does not fall below a threshold for more than a specified gap length". Activity bouts were measured using the threshold of 20 counts per minute and the maximum gap length of 5 minutes.

2.3.2 Immobility-defined sleep

Immobility-defined sleep has been defined as ≥40 seconds of immobility, with a threshold set at 95% [171-173]. This is a much less invasive method to assess sleep. This method has previously been validated using EEG recordings [171-173]. Cumulative duration immobile (with a mobility threshold of 5%) was split into 10-second time bins in Ethovision XT 14 (Noldus, NL). This was exported into Microsoft Excel and a rolling sum was set up over 4 bins, using the IF function, based on the method described in Brown et al. [171].

2.3.3 Home Cage and Hatbox Cage behaviour

Tracking behaviour in the hatbox cages and instrumented observation cages allows assessment of behaviour that is spontaneous and has reduced external influences. Tracked data from the recorded hatbox cage videos was also analysed in EthoVision XT for distance travelled (cm), mean velocity (cm/s), cumulative duration in different zones (s) and cumulative duration in different mobility states (s). Using the instrumented observation cages, behaviour was tracked real time in addition to video being recorded, using EthoVision XT, for the same parameters as in the hatbox cages.

2.3.4 Behavioural Tests

Well characterised behavioural tests were used to assess the impact of genotype and light exposure on behaviour. Mice were taken from the instrumented observation cages and placed in individual cages in the same room with food and water available *ad libitum*. The mice were assigned different identifications to allow their exposure and genotype status to be blinded. They were weighed prior to beginning any of the tests. The open field test (OFT) performed first, and then light-dark box (LDB). The order in which the mice did the OFT and the order in which they did the LDB was randomised, using a random list generator at random.org [174]. The sucrose preference test (SPT) was performed last to avoid increased blood glucose level impacting behaviour. The tests were run on the same day due to the limited timescale of the study.

The OFT is a popular test used in rodent behavioural assessments. It allows assessment of locomotor and exploratory behaviour in a “novel” contained environment [175]. The length of the OFT tends to be between 2 and 10 minutes, as any longer may result in the animal habituating to the environment and assessment of baseline activity rather than the response to novelty. The OFT is also useful to assess whether the animal has normal or impaired locomotor behaviour before undergoing other behavioural tests that require movement. Aspects of behaviour can also be analysed, such as thigmotaxis – where mice move around the edge of the arena close to the walls and avoid going in the central area, grooming, and rearing. Mice were placed in the centre of a 45 x 45cm open field arena for 5 minutes, and locomotor activity was tracked using a camera mounted in the ceiling and EthoVision XT 14 (Noldus, NL; Figure 2.8A). Total distance travelled (cm), average velocity (cm/s), time spent immobile, and time spent in different “zones” were measured. The arena was cleaned with 70% ethanol between mice.

The LDB is a commonly used assessment of anxiety in rodents, who have a natural aversion to brightly illuminated spaces. It allows measurement of the spontaneous reaction to mild stress, and the juxtaposition between aversion and the innate drive to explore the novel area [176]. Mice were placed into the LDB, which was a box with two compartments connected by a small opening (L3 x W2.7 cm^2). One compartment was small (L21 x W16 x H16 cm^3) and black with a lid, known as the “dark” zone; and the other compartment was open and white (L 46.5 x W21 x H21 cm^3) and known as the “light” zone (Figure 2.8B). The camera was in the ceiling of the room and faced the top of the LDB. Mice were placed into the dark zone and the lid was immediately closed. The test was run for 5 minutes, and latency to fully enter the light zone (s), cumulative duration spent in the light zone (s) and frequency of visits into the light zone were measured. The LDB was cleaned with 70% ethanol between mice to eliminate any olfactory cues.

A) **B)**

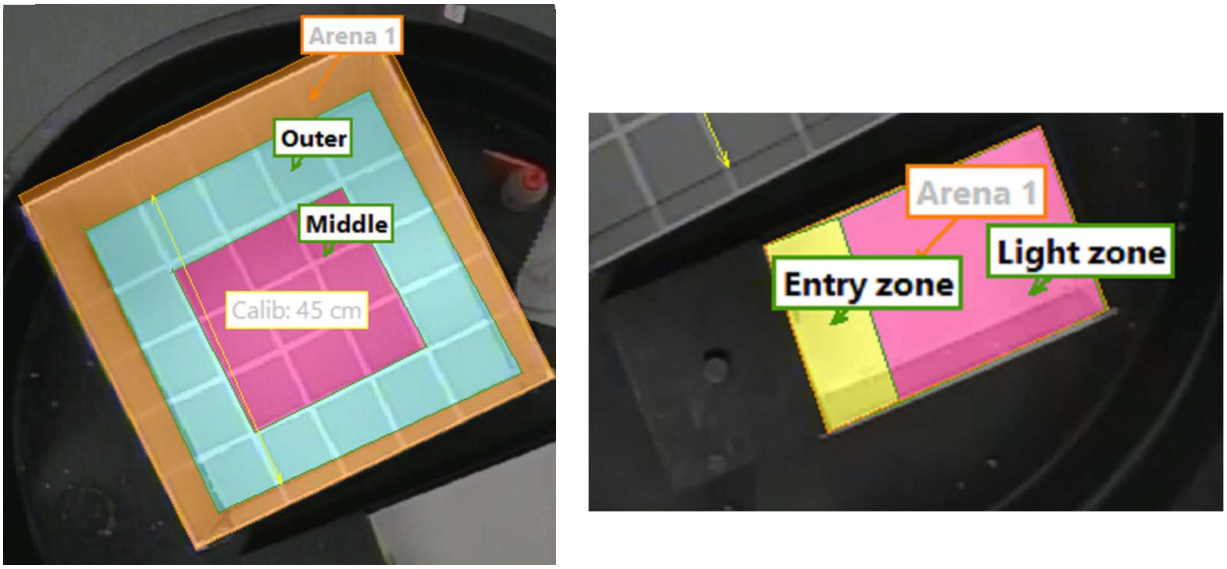


Figure 2.8. Arena set up for behavioural test analysis.
Schematic showing the analysis zones set up for **A)** The Open Field Test and **B)** The Light-Dark box in EthoVision XT 14. Mice were in each arena for 5 minutes at a time.

The SPT is commonly used to measure a deficit in hedonic behaviour in the paradigm of depression. A hedonic deficit results in a reduced sensitivity to reward stimuli and in rodents this is shown with reduced preference for, and intake of, palatable solutions [177]. Previous studies have used this test to assess the impact of chronic mild stress [178]. Prior to undertaking the SPT, mice were habituated to the sucrose solution over 3-5 days, starting at least week before beginning any type of behavioural assessment or behavioural tests. The protocol for the SPT was carried out in accordance with Yates et al. [179]. The mice were given free access to two bottles, one containing normal water and the other containing 1% sucrose solution. The test lasted 6 hours, with bottles being switched over 3 hours after the start to prevent location bias. Percentage sucrose preference was calculated using the following formula: (volume [sucrose solution] / volume [total fluid intake of water + sucrose solution]) x 100.

2.4 Tissue collection

Mice were terminally anesthetised with CO_2 overdose, or heavily anaesthetised with isoflurane, and blood was collected via cardiac puncture into heparin coated vacutainers. Plasma was collected after vacutainers stood for 30-60 mins at room temperature and were spun for 10 mins at 1000 x g. Plasma was stored at -80°C. Mice were transcardially perfused with cold heparinised saline (0.9%) through the left ventricle with the right atrium pierced to remove remaining blood. The liver and whole brain were removed, the brain was sectioned into right and left hemispheres, and all tissue was snap frozen on dry ice and were stored at -80°C.

2.5 Histology

2.5.1 Sectioning

The left hemisphere of fresh frozen brains was sectioned on the sagittal plane at -15°C at a thickness of 10µm using a Leica Cryostat (CM1850) and stored at -20°C until immunohistochemical analysis.

2.5.2 Immunohistochemistry

Fresh frozen brain sections were post-fixed in 4% paraformaldehyde (PFA) for 1 hour at 4°C. They were briefly washed in phosphate buffered saline (PBS), and sections being stained for glial fibrillary acidic protein (GFAP) were incubated in boiling citrate buffer for 3 minutes for antigen retrieval. The sections were quenched to block for endogenous peroxidase activity with 1% H_2O_2 in methanol for 10 minutes. The sections were briefly washed in PBS, before being washed in PBS for 2x5 minutes. The sections were blocked for non-specific binding with 10% normal goat serum in PBS for 1 hour at room temperature. They were then incubated with the primary antibody (see Table 2.*1* for dilutions) diluted in 1% normal goat serum overnight at 4°C. The following day the sections were washed in PBS 3x5 mins before being incubated with the secondary

antibody, biotinylated IgG (Vector Laboratories, CA, USA) diluted 1:200 in 1% serum PBS for 2 hours at room temperature. The sections were washed in PBS for 3x5 minutes before being incubated in Avidin-Biotin Complex (1:100; Vector Laboratories, CA, USA) for 1 hour at room temperature. The sections were then washed in PBS for 2x5 minutes prior to being incubated in 3,3'-Diaminobenzidine (DAB) in order to visualise reactivity, until a suitable level of staining developed. Next, the sections were counterstained in cresyl violet for 1 minute and then dehydrated through graded alcohols (80%, 90%, 2 x 100%) for 10 seconds each, cleared in xylene (2x5 minutes) and mounted with dibutylphthalate polystyrene xylene (DPX).

2.5.3 Quantification and analysis of immunohistochemistry

Ionized calcium binding adaptor molecule 1 (Iba-1)+ cells were counted in 2-3 sections per 2-4 animals in each group at 63X magnification in the dentate gyrus (DG) of the hippocampus and expressed as cells per mm^2. Cell counting was performed blinded.

The morphology of reactive astrocytes was assessed by tracing 10 GFAP+ astrocytes per section, of 3 sections per 3-4 animals in each group at 40X magnification using a Camera Lucida. The traced images were scanned and imported into ImageJ (FIJI), converted to 8-bit greyscale, converted to binary and skeletonized using the Skeleton Plugin (Figure 2.9). The resulting skeletons were analysed with the "Analyze Skeleton" analysis. The number of branches and average branch length were measured.

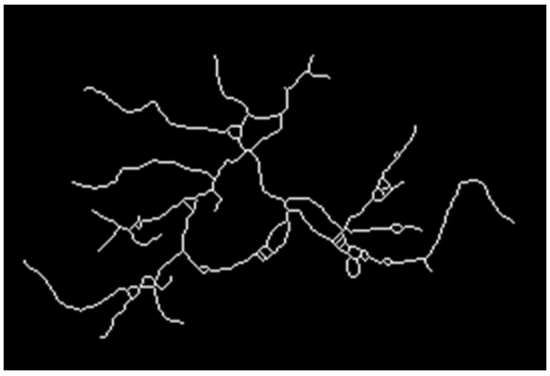


Figure 2.9. Example of a skeletonized tracing of a GFAP+ astrocyte.

Table 2.1: Antibodies for immunohistochemistry

	Antibody	Target	Dilution	Company
Primary antibodies	Anti-Iba-1, Rabbit anti-mouse	Microglia, macrophages	1:2000	AbCam
	Anti-GFAP, Rabbit anti-mouse	Astrocytes	1:1000	Dako
Secondary antibodies	Goat anti-rabbit IgG, Biotinylated	N/A	1:200	Vector Labs

2.6 Molecular Biology

2.6.1 mRNA extraction and cDNA conversion

RNA was extracted from the liver using the RNeasy minikit (Qiagen, 74106). 10mg of liver was homogenised in 600µl buffer RLT and 1% β-Mercaptoethanol (Sigma-Aldrich, M3148) with a pestle homogeniser (Kimble, 749540-0000). The lysate was then centrifuged through QIAshredder homogenisers (Quiagen, 79656). RNA extraction was completed following manufacturer's protocol and RNA was eluted in a volume of 50µl of nuclease free water. RNA was extracted from the brain using the RNeasy minikit (Qiagen, 74106). The remaining left hemisphere of the brain after sectioning was homogenised in 600µl buffer RLT and 1% β-Mercaptoethanol (Sigma-Aldrich, M3148) with a pestle homogeniser (Kimble, 749540-0000). The lysate was then centrifuged through QIAshredder homogenisers (Quiagen, 79656). RNA extraction was completed following manufacturer's protocol and RNA was eluted in a volume of 30µl of nuclease free water. RNA concentration was measured using a NanoDrop 2000 Spectrophotometer (Thermo

Fisher, MA, USA). RNA purity was checked by evaluating the 260/280 ratio, where ratios between 1.8 and 2.2 were considered pure.

RNA was converted to cDNA using the High-Capacity cDNA Reverse Transcription Kit (Applied Biosystems, CA, USA). 1000ng of liver RNA and 400ng of brain RNA were used. 10ul of RNA was mixed with 10ul of master mix (see Table 2.*2* for master mix components). Conversion was performed on a BIORAD T100 Thermal Cycler using the following cycle: 25°C x 10 minutes, 37°C x 120 minutes, 85°C x 5 minutes and held at 4°C. cDNA was stored at -20°C.

Table 2.2: Components of the High-Capacity cDNA Reverse Transcription Kit

	Volume per sample (µl)
10x RT buffer	2
25x dNTP mix (100mM)	0.8
10x RT random primers	2
Multiscribe Reverse Transcriptase	1
Nuclease free water	4.2

2.6.2 Quantitative real-time polymerase chain reaction (qRT-PCR)

qRT-PCR was performed using SsoAdvanced™ Universal SYBR® Green Supermix (1725271, Bio-Rad Laboratories Ltd, UK) on a LightCycler 480 machine (Roche Life Science, CA, USA), see Primer Design

Primers were designed using Primer-BLAST [180]. RefSeq accession numbers were inputted into the program and primer sequences were generated [181]. The sequences were checked for specificity by inputting the newly generated primer sequences back into Primer-BLAST and making sure only genes of interest would be amplified. OligoCalc was used to check the sequences for hairpin structures and self-dimers [182].

Table 2.3 for cycle program. 10ng of brain cDNA and 25ng of liver cDNA was used per well. Samples were run in duplicate, and water was used as non-transcript control. The resulting CT values were normalised to the housekeeping genes and relative expression was calculated using the 2-ΔΔCT method. Primers for genes were purchased from Integrated DNA Technologies (IA, USA) and Sigma (Sigma-Aldrich, USA) and used at a working concentration of. Primer sequences are listed in Table 2.4

2.6.2.1 Primer Design

Primers were designed using Primer-BLAST [180]. RefSeq accession numbers were inputted into the program and primer sequences were generated [181]. The sequences were checked for specificity by inputting the newly generated primer sequences back into Primer-BLAST and making sure only genes of interest would be amplified. OligoCalc was used to check the sequences for hairpin structures and self-dimers [182].

Table 2.3: Temperature cycles for qRT-PCR reactions

Step	Temperature (°C)	Duration	Cycles
Enzyme Activation	95	2 minutes	1
Amplification	95	10 seconds	40
	60	1 minute	
Melting curve	95	5 seconds	1
	65	1 minute	
Cooling	40	30 seconds	1

Table 2.4: qRT-PCR primer sequences.

Gene	Forward sequence (5'-3')	Reverse sequence (5'-3')	Literature/Accession number/Purchased from
β actin	CGTTGACATCCGTAAAGACC	AACAGTCCGCCTAGAAGCAC	Ji et al., 2013 [183]
Clock	TTCCTTCCTTAGAGACGAGACT	CTAAATGCTACCCTGAGGATAGAG	Primerdesign
Arntl1 (Bmal1)	CCACCTCAGAGCCATTGATACA	GAGCAGGTTTAGTTCCACTTTGTCT	NM_007489.4
Per1	TCCTCCTCCTACACTGCCTCT	TGGCTGACGACGGATCTTT	Loh et al.,2008 [184]
Per2	CTCAGCCTCCCACTCTATATGT	AGGACCAGCAGCACAGATAG	Primerdesign
Cry1	GATCCACCATTTAGCCAGACAC	ACAGCCACATCCAACTTCCA	Primerdesign
Cry2	CAAGCACTTGGAACGGAAGG	GAAGAGGCGGCAGGAGAG	Primerdesign
Ppar-α	TCGGCGAACTATTCGGCTG	GCACTTGTGAAAACGGCAGT	Zhu et al., 2016 [185]
Ror-α	TCTCCCGCCCCATAAAACAC	GTAAGCAGTGGCCCTGTGAT	NM_001289916.1
Sirt1	GACGCTGTGGCAGATTGTTA	GGAATCCCACAGGAGACAGA	Long et al., 2019 [186]
Sod1	GTCGGCTTCTCGTCTTGCTC	GCTTTCATCGCCATGCTTCC	NM_011434.2
Dgat1	TGGGTTCCCTGTTTGCTCTGGC	GCTTTGGCCTTGACCCTTCGCT	Dettlaff-Pokora et al., 2015[187]
Rxr-α	ACATGCAGATGGACAAGACG	GGGTTTGAGAGCCCCTTAGA	Garay-Lugo et al., 2016 [188]
Hmgcr	CTTGTGGAATGCCTTGTGATTG	AGCCGAAGCAGCACATGAT	Seo et al., 2019 [189]
Fasn	GGAGGTGGTGATAGCCGGTAT	TGGGTAATCCATAGAGCCCAG	Nasiri-Ansari et al., 2021 [190]
Pfkfb3	AGAGGTCAGAGAACATGAAGAGC	TGCTGCTCTACACAGGAAGC	NM_001177752.1
Slc2a1	GTGACGATCTGAGCTACGGG	TGCATTGCCCATGATGGAGT	NM_011400.3
Gpx4	CGCCAAAGTCCTAGGAAACG	TATCGGGCATGCAGATCGAC	NM_001037741.4
Fabp7	TGGGAAACGTGACCAAACCA	AGCTTGTCTCCATCCAACCG	NM_021272.3
Gcl	GGCACAAGGACGTGCTCAAGT	TTTGTCCTCTCCCCCTTCTC	Vicente-Gutierrez et al., 2019[191]

2.6.2.2 Primer Testing

All primers were tested to ensure efficient amplification of the intended target by generating a standard curve. cDNA was pooled from multiple samples of liver cDNA, and separately, brain cDNA. The pooled liver and brain cDNA was serial diluted and underwent qRT-PCR. The resulting CT values were plotted against the log of the cDNA concentrations to form a standard curve. The gradient and the R^2 value of the standard curve were calculated, and efficiency was calculated:

$$^0/_0\, Efficiency = \left(\left(10^{\frac{-1}{gradient}}\right) - 1\right) \times 100$$

Primers with R^2 values above 0.7, and efficiency of 100±40% were selected. Primers with an efficiency of >140% were considered if the R^2 value was above 0.8.

2.7 ^{1}H Nuclear Magnetic Resonance (NMR) Metabolomics

Metabolomics is the study of low molecular weight molecules present as metabolic intermediates, or metabolites, in biological samples. It uses analytical chemistry techniques to identify a metabolic “fingerprint” of any given sample. This allows an untargeted approach, which is proving to be a powerful method for identifying previously unknown metabolic changes involved in disease pathology [192].

Hydrogen nuclei possess a property known as “spin”. This allows them to generate a directional magnetic field. When an external magnetic field is applied, the proton spins can take up either a parallel, or antiparallel orientation in alignment with this field. These orientations are associated with a specific energy level: parallel with a low energy level, and antiparallel with a high energy level. As the strength of the applied magnetic field increases, so does the difference in energy between the two orientations. If a specific frequency of an electromagnetic radiation is applied, the proton in the lower energy level will flip to the orientation of the higher energy level to be in resonance with the field, absorbing energy at the resonance frequency that corresponds to the difference in energy

between the proton's two spin states, as well as the chemical configuration of the molecules the protons are part of. ^{1}H NMR measures the resonance frequencies and produces peaks in an NMR spectrum measured by chemical shift in ppm, that reflect the chemical structure of the molecules. One-dimensional (1D) ^{1}H NMR is the most common technique to use for metabolomic analysis. However, metabolite signals overlap, so two-dimensional (2D) ^{1}H NMR can be used to identify coupled proton spins between the different signals on the spectra, and so allows identification of unclear signals.

2.7.1 Sample processing

2.7.1.1 Plasma

100 µL plasma was added to 500µl 75 mM NMR buffer (5:1 disodium phosphate [Na_2HPO_4] and monosodium phosphate [NaH_2PO_4] in 100% D_2O, pH = 7.4) and vortexed, before being transferred to 5 mm Borosilicate NMR tubes (Norell, USA) with a glass pipette dropper.

2.7.1.2 Liver and Brain

100 mg ± 15mg of fresh snap-frozen liver or brain (right hemisphere excluding cerebellum and brainstem) was homogenised on dry ice with a mortar and pestle. A proportional volume of 50% Acetonitrile was added: 800 uL per 100 mg of tissue. The samples were spun for 5 minutes at 5000 x g and 4°C before the supernatant was drawn off and frozen on dry ice. The samples were lyophilised overnight. The lyophilised samples were then resuspended in 600 uL of 75 mM NMR buffer, vortexed and centrifuged at 3000 x g for 5 minutes at 4°C to remove remaining particulate matter. They were then transferred to 5 mm Borosilicate NMR tubes (Norell, USA) with a glass pipette dropper.

2.7.2 ^{1}H NMR Spectroscopy

^{1}H NMR spectra were acquired at 298K using a 700-MHz Bruker AVII NMR Spectrometer operating at 16.4 T equipped with a ^{1}H (^{13}C/^{15}N) TCI cryoprobe (Department of Chemistry, University of Oxford). ^{1}H NMR spectra were acquired on all samples using a one-

dimensional (1D) Nuclear Overhauser Effect Spectroscopy (NOESY) pre-saturation scheme for attenuation of the water resonance with a 2 s pre-saturation.

For brain, the 1D NOESY water suppression sequence was used with 32 data collections and 1.5 s acquisition time. For liver the Painless sequence [193] was also used, with 32 data collections and 1.5 acquisition time. For the plasma, the spin-echo Carr-Purcell-Meiboom-Gill (CPMG) sequence was used with a τ interval of 400 μs, 80 loops, 32 data collections, an acquisition time of 1.5 s, a relaxation delay of 2 s, and a fixed receiver gain. The NMR buffer was also run as a control to check that there was no contamination.

2.7.3 Spectra pre-processing

NMR spectra were processed in in Topspin (version 4.1.1, Bruker, Germany). They were manually phased, referenced to the lactate doublet at 1.33ppm, and baselines were corrected. The spectra underwent visual inspection, to check for distortion or contamination, before being exported to ACD/Labs Spectrus Processor Academic Edition 12.01 (Advanced Chemistry Development, Inc.). Regions of the NMR spectra (Liver: 0.65-9.35; Brain: 0.45-9.35; Plasma: 0.04-8.47) were automatically split into bins with a width of 0.02 ppm. The water resonance region was removed from the brain and plasma spectra. The integral of each spectral bin was calculated for statistical analysis and normalised to the sum of the total spectral integrals. Spectra were visually inspected to exclude bins with absent spectral resonances to remove noise. The sum normalised integral values of the spectral bins were labelled according to sample ID and experimental group and imported into R Studio (2021.9.0.351) for multivariate analyses [194]. Metabolites were assigned to peaks in the NMR spectra using literature, 2D total correlation spectroscopy (TOCSY) and to the Human Metabolome Database (HMDB) [195]. Automatic binning sometimes separated chemical peaks, and so VIPs were reported by bin rather than metabolite.

2.8 Statistical Analysis

2.8.1 Univariate Analyses

GraphPad Prism 8 software (CA, USA) and R was used to perform statistical analyses [194]. Normality was assessed using the D'Agostino-Pearson test. Data were analysed using the unpaired t-test, the Mann-Whitney U test, the 2-way ANOVA and the 3-way ANOVA. The post hoc Tukey-Kramer multiple comparison test was used when appropriate. Differences were considered significant when $p<0.05$. In all figures, data are presented as mean ± SD. Correlations analyses were carried out using the R package corrplot [196]. Results were adjusted to control for multiple comparisons using the Benjamini-Hochberg (BH) method. P values of <0.05 and R values of >±0.4 were considered significant.

2.8.2 Cosinor analysis

The Nitecap web application was used to perform cosinor analysis on qPCR data to analyse and visualise the rhythmic expression of genes over 24 hours [197]. The Rhythmicity Analysis Incorporating Nonparametric methods (RAIN) statistical test was used to assess rhythmicity, and in-built cosinor-based statistical tests assessed differences in MESOR, phase and amplitude [197, 198]. P values of <0.05 were considered significant.

2.8.3 Multivariate Analyses

R was used for multivariate analyses, using scripts developed in-house [194]. Principal component analysis (PCA) was performed using the ropls package to visualise the data [199]. PCA is an unsupervised analysis, where it ignores the data class and looks for greatest variation, making a vector to explain it. Orthogonal partial-least squares discriminant analysis OPLS-DA was used to investigate differences between two classes, using the ropls package [199]. OPLS-DA discriminates between two data classes using multivariate data. It constructs a regression model between the multivariate data and a

response variable that contains only class information. The model gives information about what metabolites are driving differences between the classes.

To ensure OPLS-DA models were not a result of overfitting, 10-fold cross validation with 100 repetitions was used to build 1000 models. In each iteration of the external cross-validation scheme, samples are randomly selected to match class sizes before splitting the data in to 10 folds, each fold is used as an independent test to predict the classification of sample (using data only trained on the remaining 9 folds) and determine the accuracy, sensitivity, and specificity of the models. These are assessed against "random" models, which were built with randomly classified data (a permutation test). For each model, the parameters R^2X, R^2Y and Q^2 were generated, which assess the ability of the model to describe/predict the training data. Only if model performed significantly better than the random models was the model considered robust and the variables driving the model interrogated.

The partial least-squares discriminant analysis (PLS-DA) was performed using the ropls package [199]. The PLS-DA was used to investigate group differences, it reduces dimensionality but has awareness of class

The metabolites driving differences between the classes were identified using average variable importance in projection (VIP) scores. A graph of VIP scores was inspected visually to identify the inflection point (the point at which the delta VIP score decreases). The spectral bins with the top-ranking VIP scores (those with VIP scores higher than the identified inflection point) then underwent univariate analyses and metabolite assignment.

3 Phenotyping the APOE-/- mouse model

3.1 Introduction

3.1.1 The APOE-/- mouse model

The APOE-/- model is used as a model of atherosclerosis, as the mice exhibit hyperlipidaemia and develop vascular atherosclerotic plaques in a way similar to humans [75, 76]. The model allows investigation into the development of atherosclerosis, and exploration of interventions that may ameliorate or exacerbate dyslipidaemia and plaque development. There are many studies on the peripheral characteristics of this model, but few that extensively examine the brain, despite APOE being the principal apolipoprotein in the CNS [45]. However, this is an important area of research, as CVD has an impact on the brain. In humans, subclinical atherosclerosis is associated with reduced brain metabolic activity [200]. Severe Circle of Willis atherosclerosis is associated with sporadic Alzheimer's disease (AD) [201], and a high cardiovascular risk factor has shown to be associated with a reduction of energy-dependent long axonal projections and a lower verbal IQ [202].

3.1.2 Behavioural investigations

Behaviour is the final output of the nervous system [203]. Assessing the behaviour of genetically modified mice allows insight into what changes may have occurred in the brain and the CNS, and can lead to new functions and pathways being discovered with downstream investigation and analysis [203].

In terms of behavioural differences, there is a vast amount of literature on behaviour in humans possessing the ApoE-ε4 isoform, and in animal models of the ApoE-ε4 isoform. In humans, the ApoE-ε4 isoform is associated with reduced visual recall, verbal memory and memory retention [204]. In mice, addition of human ApoE-ε4 is associated with

deficits in spatial memory and learning [204]. However, there is a much smaller pool of literature on behaviour in APOE-/- mice.

Altered circadian rhythms and CVD are tightly associated, therefore assessing the circadian rhythmicity of behaviours in the APOE-/- model will give an indication of whether the generation of circadian rhythms has been altered by the absence of the *ApoE* gene [205]. Assessment of circadian behaviour by looking at rest-activity patterns is simple and non-invasive and can assess multiple parameters [206]. Additionally, investigating sleep is informative, as it is under both circadian and homeostatic control, and can give indications about changes in excitatory and inhibitory neural networks [132].

3.1.3 Molecular investigations

Circadian rhythms are generated at a cellular level by the transcriptional-translational feedback loop (TTFL) of the core clock genes [90]. Alterations to the rhythmical expression of the genes involved in the TTFL have a significant effect on the circadian rhythms of an organism. The liver is a key peripheral oscillator, and is a site of crosstalk between the circadian clock and metabolism [207]. It can entrain to time-restricted feeding and can synchronise other peripheral oscillators to a rhythm different to the SCN [127]. Additionally, the liver is the primary site of clearance of APOE-containing lipoproteins, and so is a site of interest for investigating molecular changes in the APOE-/- mouse model [24].

3.1.4 Aims of chapter

The aims of this chapter are to establish the effect of the absence of the *ApoE* gene by assessing changes in behavioural rhythms and sleep in the APOE-/- mice in normal L:D conditions and D:D conditions, investigating differences in behaviour in the APOE-/- model using home cage behavioural assessments in L:D and D:D and behavioural tests and examining changes in 24-hour rhythmical expression of genes involved in circadian rhythm generation and energy metabolism in D:D. It was hypothesised that the absence

of APOE in the CNS would cause alterations in sleep and behaviour in the APOE-/- model. In addition, it was hypothesised that APOE mice would show abnormal peripheral rhythms of core clock genes and genes regulating lipid metabolism, as the absence of APOE disrupts lipid transport.

3.2 Materials and Methods

3.2.1 Behaviour in normal L:D conditions

5-6-month-old male APOE-/- mice and C57BL/6J control mice (n=16-18 per group) were habituated to individual housing and 1% sucrose for 5 days prior to the start of the study. They were then put into individual PhenoTyper cages, in the normal L:D conditions of the animal facility, for 14 days. Behaviour was tracked and recorded with EthoVision XT 14 (Noldus, NL). On day 14, mice were removed from the PhenoTyper cages and underwent the OFT, the LDB and the SPT. See Figure 3.1 for experimental timeline.

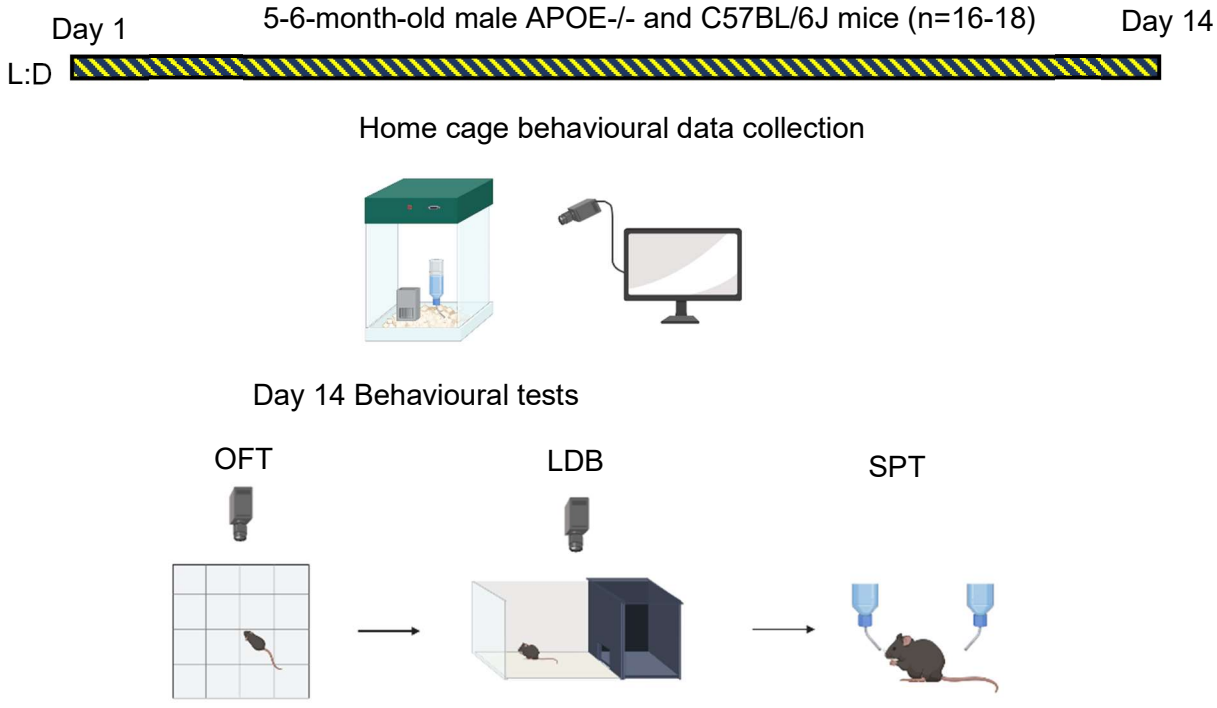


Figure 3.1: L:D Experimental design

3.2.2 Behaviour in constant D:D conditions

6-week-old male APOE-/- and C57BL/6J mice were chosen to assess behaviour prior to any CVD development and were group housed in scantainers on a specific L:D cycle for 2

weeks to allow full entrainment. This was done to control the time points of this kills at the end of the study.

At the start of the study, beginning at ZT12 – the beginning of the dark phase, the mice were individually housed in light tight “hatbox” cages for 10 days in D:D. Food and water were available *ad libitum*, and behaviour was recorded using cameras in the lid of the hatbox cages, and later tracked in EthoVision XT 14 (Noldus, NL). After 10 days, the mice were culled at 4 time points over 24 hours. See Figure 3.2 for experimental timeline.

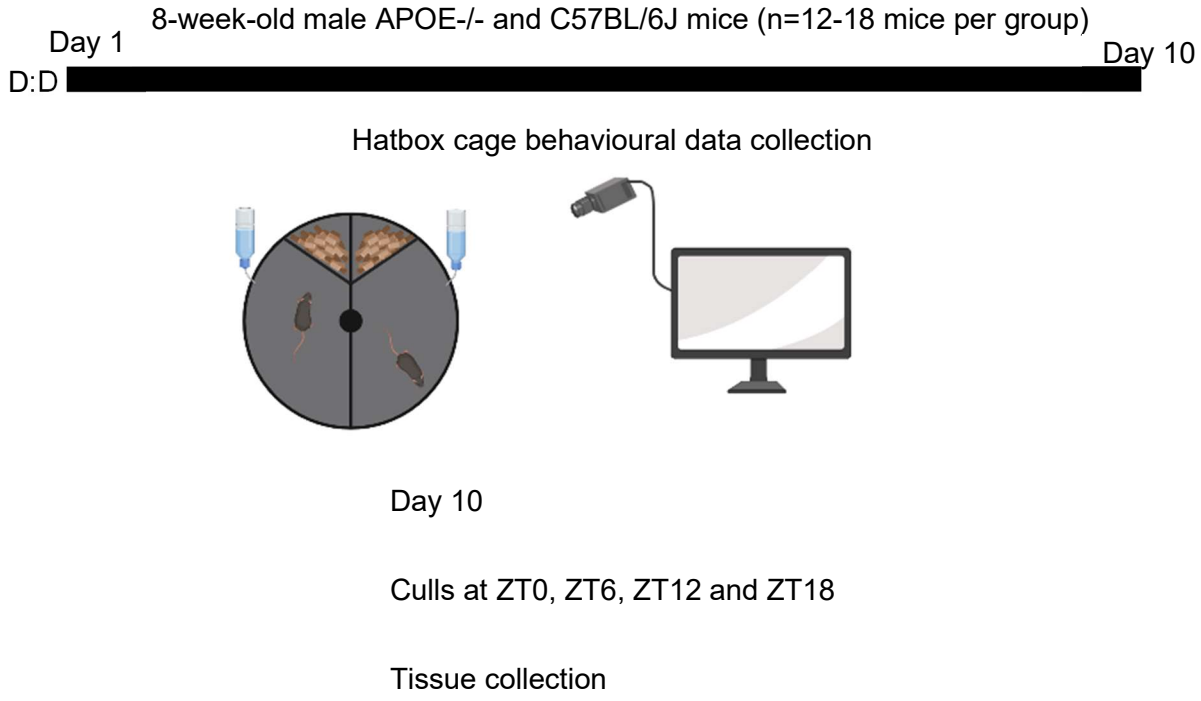


Figure 3.2: D:D Experimental design for Chapter 1 and 2

C57BL/6J mice will be referred to as wildtype mice for the rest of this chapter.

3.3 Results

3.3.1 Behavioural rhythms in L:D

The rhythmical behaviour of 6-month-old APOE-/- mice was assessed using ClockLab over 2 weeks in normal L:D conditions (**Error! Reference source not found.**).

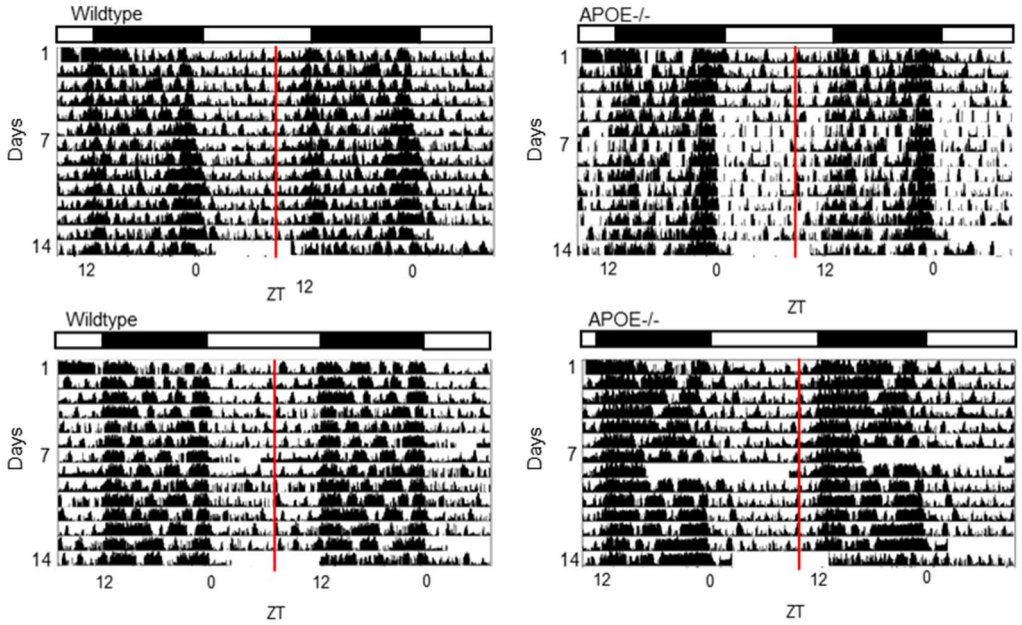


Figure 3.3: Locomotor activity in wildtype and ApoE−/− mice, in normal L:D conditions.

Representative double-plotted actograms of wildtype mice (left) and ApoE−/− mice (right) in normal L:D conditions. Bin size is 5 min. Missing data due to pausing recording to back up data.

No difference was found in the period of the behavioural rhythms of the APOE-/- mice compared to wildtype mice (t=0.3392, p=0.7366; Figure 3.4A). The amplitude of behavioural rhythms in APOE-/- mice was 38% higher than the amplitude of behavioural rhythms in wildtype mice (t=2.377, p=0.0236; Figure 3.4B). No difference was found in the acrophase of the behavioural rhythms of the APOE-/- mice compared to wildtype mice (t=1.624, p=0.1142; Figure 3.4C). No difference was found in the total number of activity bouts of the APOE-/- mice compared to wildtype mice (t=0.2897, p=0.7739; Figure 3.5A). The average length of activity bouts in APOE-/- mice was 44% higher than the average length of activity bouts in wildtype mice (t=2.845, p=0.0077; Figure 3.5B).

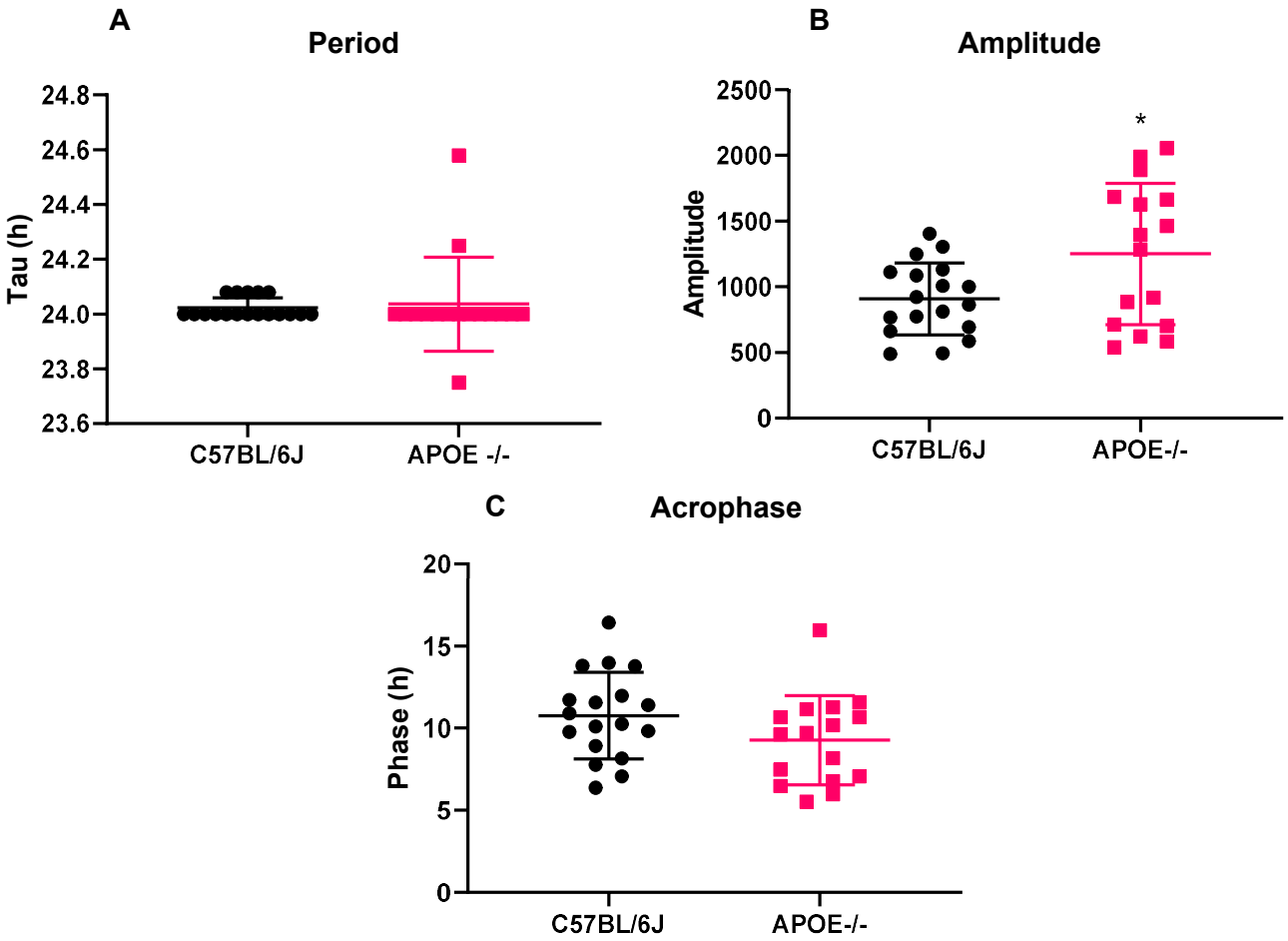


Figure 3.4: APOE-/- mice have a significantly higher amplitude of behavioural rhythms, but they have the same period and acrophase as the wildtype mice in normal L:D conditions.

A) There are no differences in the period of behavioural rhythms in APOE-/- and wildtype mice. **B)** APOE-/- mice have a significantly higher amplitude of behavioural rhythms compared to wildtypes. C) There is no difference in the acrophase of behavioural rhythms between APOE-/- mice and wildtypes. Unpaired t-test; data presented as mean ± SD of 16-18 mice per group. Statistically significant differences between wildtype and APOE-/- mice are shown as *, $P \leq 0.05$.

A

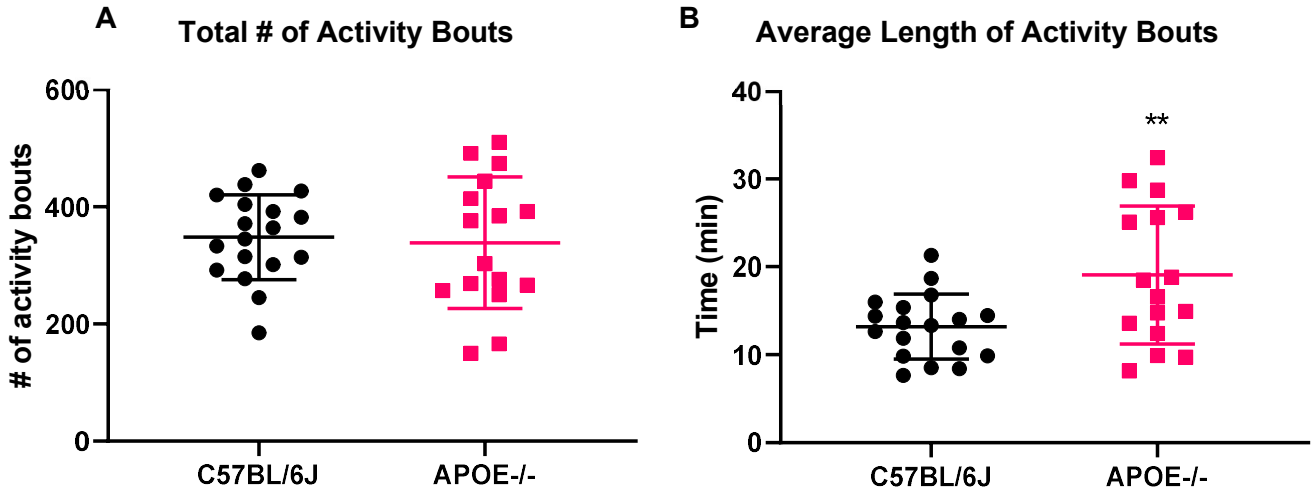


Figure 3.5: APOE-/- mice have longer Activity Bouts but show no difference in total number of Activity Bouts in normal L:D conditions.
A) There was no significant effect of genotype on the total number of Activity Bouts, but there was a significant genotypic effect on **B)** the average length of Activity Bouts. Unpaired t-test; data presented as mean ± SD of 16-18 mice per group. Statistically significant differences between wildtype and APOE-/- mice are shown as **, P ≤ 0.01.

3.3.2 Immobility-defined sleep in L:D

Immobility-defined sleep was investigated in APOE-/- mice in normal L:D conditions using the method described in Chapter 2.3.2. No difference was found in total immobility-defined sleep in APOE-/- mice compared to wildtype mice ($t=0.0525$, $p=0.9585$; Figure 3.6A). The percentage of total immobility-defined sleep taking place in the light phase was calculated. No difference was found in the distribution of immobility-defined sleep in the light phase in APOE-/- mice compared to wildtype mice ($t=0.7396$, $p=0.4653$; Figure 3.6B). As time is a known confounding variable of sleep, total immobility-defined sleep was divided into hourly time points over the 2 weeks of the study. There was a significant interaction between genotype and time ($F(330, 9373)=1.451$, $p<0.0001$). There was also a significant effect of time, as expected, ($F(330, 9373)=8.287$, $p<0.0001$). However, there was no effect of genotype ($F(1, 29)=0.01257$, $p=0.9115$; Figure 3.6C).

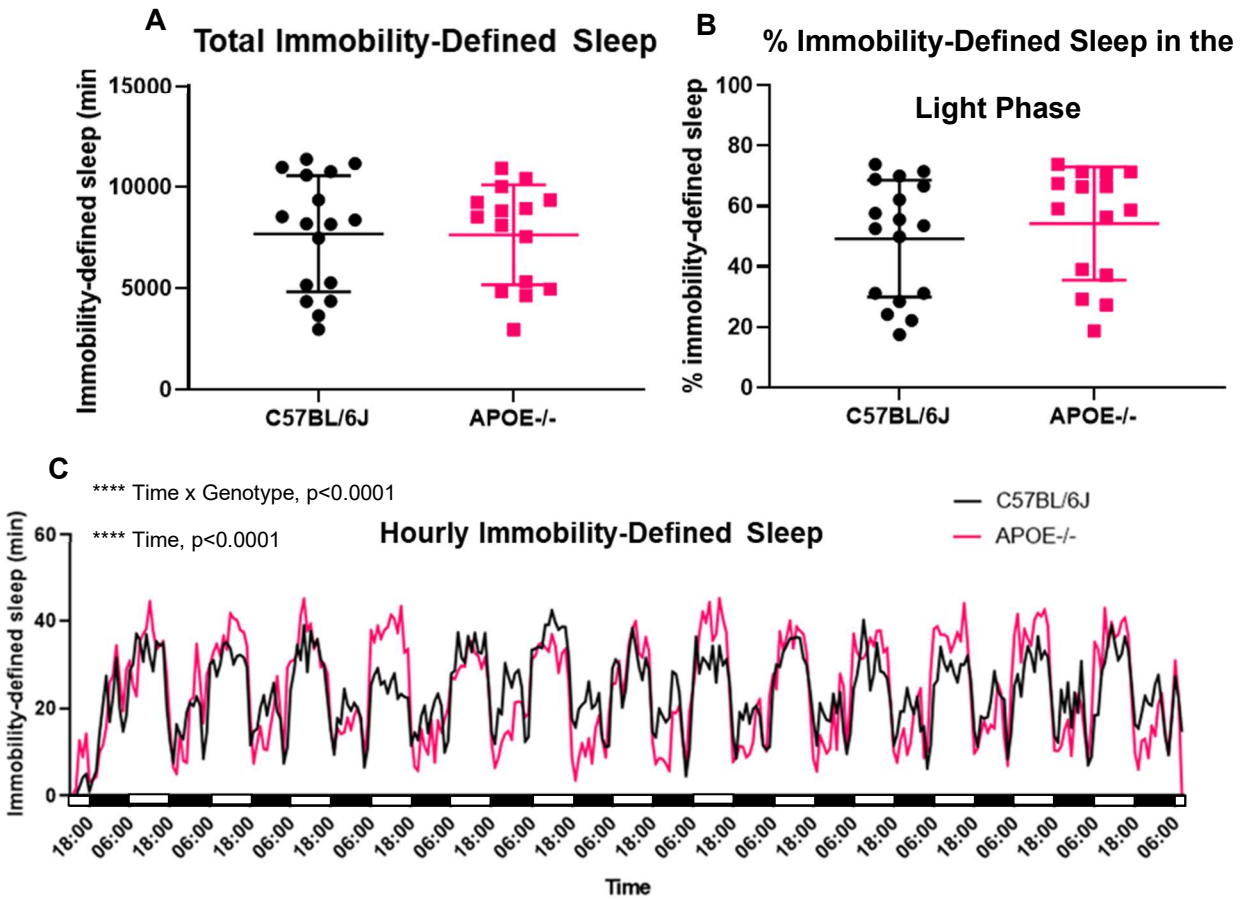


Figure 3.6: There is a significant time-genotype interaction for immobility-defined sleep over time, but APOE-/- mice display the same total amount of immobility-defined sleep and have the same sleep distribution in the light phase as the wildtype mice in normal L:D conditions.
A) There are no differences in the total amount of immobility-defined sleep in APOE-/- and wildtype mice. **B)** There is no difference the percentage of immobility-defined sleep occurring in the light phase in APOE-/- mice compared to wildtype mice. **C)** There is a significant effect of time on immobility-defined sleep in both APOE-/- and wildtype mice; and there is a significant effect of the interaction between time and genotype on immobility-defined sleep. Unpaired t-test; data presented as mean ± SD of 15-17 mice per group. 2-way ANOVA; data presented as mean of 15-17 mice per group. Statistically significant differences between wildtype and APOE-/- mice are shown as ****, P ≤ 0.0001.

3.3.3 Home cage behaviour in L:D

Home cage behaviour was assessed to investigate baseline behaviours in the mice without the potential stress induced by handling during behavioural tests. The total distance travelled of APOE-/- mice was 82% higher than wildtype mice over 2 weeks in normal L:D conditions, ($t=4.936$, $p<0.0001$; Figure 3.7A). The total mean velocity of APOE-/- mice was 66% higher than wildtype mice over 2 weeks in normal L:D conditions, ($t=4.602$, $p<0.0001$; Figure 3.7B).

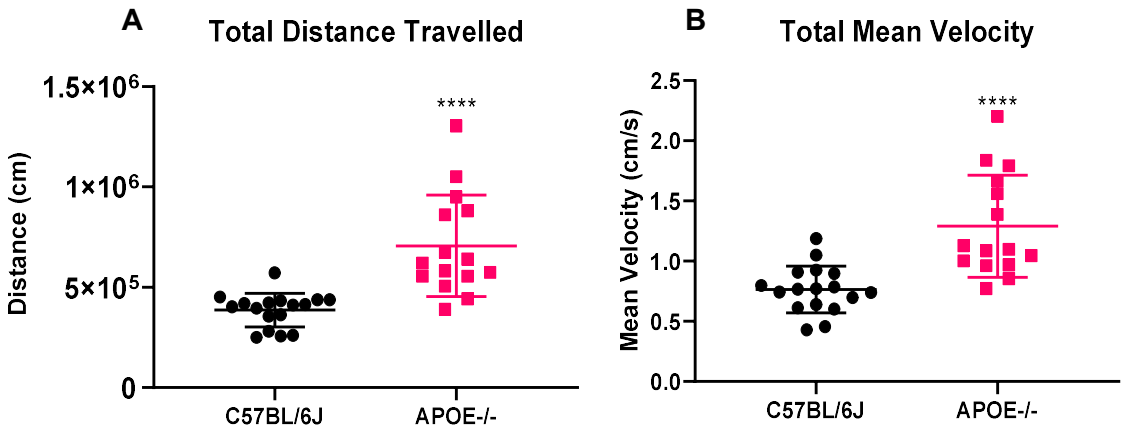


Figure 3.7: APOE-/- mice display increased locomotor behaviour in normal L:D conditions.
A) There was a significant effect of genotype on the total distance travelled in L:D conditions**. B)** There was also a significant effect of genotype on the total mean velocity in L:D conditions. Unpaired t-test; data presented as mean ± SD of 15-17 mice per group. Statistically significant differences between wildtype and APOE-/- mice are shown as ****, P ≤ 0.0001.

3.3.4 Appetitive behaviour and body mass in L:D

Using the lickometer to assess drinking behaviour, the total number of licks on the water bottle in each PhenoTyper cage was recorded. APOE-/- mice had 66% higher number of recorded licks than wildtype mice (t=2.53, p=0.0177; Figure 3.8A). Food hopper visits were measured using an infrared beam across the front of the hopper. There were no differences in the total number of hopper beam breaks between the genotypes (t=1.166, p=0.2547; Figure 3.8B). Prior to the start of the study, APOE-/- mice had a slightly lower body mass than wildtype mice by 6%, but the difference was not significant (t=1.852, p=0.0733; Figure 3.8C). Genotype had no effect on the change in body mass throughout the study (t=0.01861, p=0.9853; Figure 3.8D). The final body mass was also slightly lower in APOE-/- mice, by 6.49%, but again, not quite significant (t=1.999, p=0.054; Figure 3.8E). An indication of food intake was assessed by weighing all food added to the food hoppers during the study and weighing the food remaining at the end of the study. There was a significant effect of genotype on food intake, where APOE-/- mice ate 29% more than wildtypes (t=4.25, p=0.0002; Figure 3.8F).

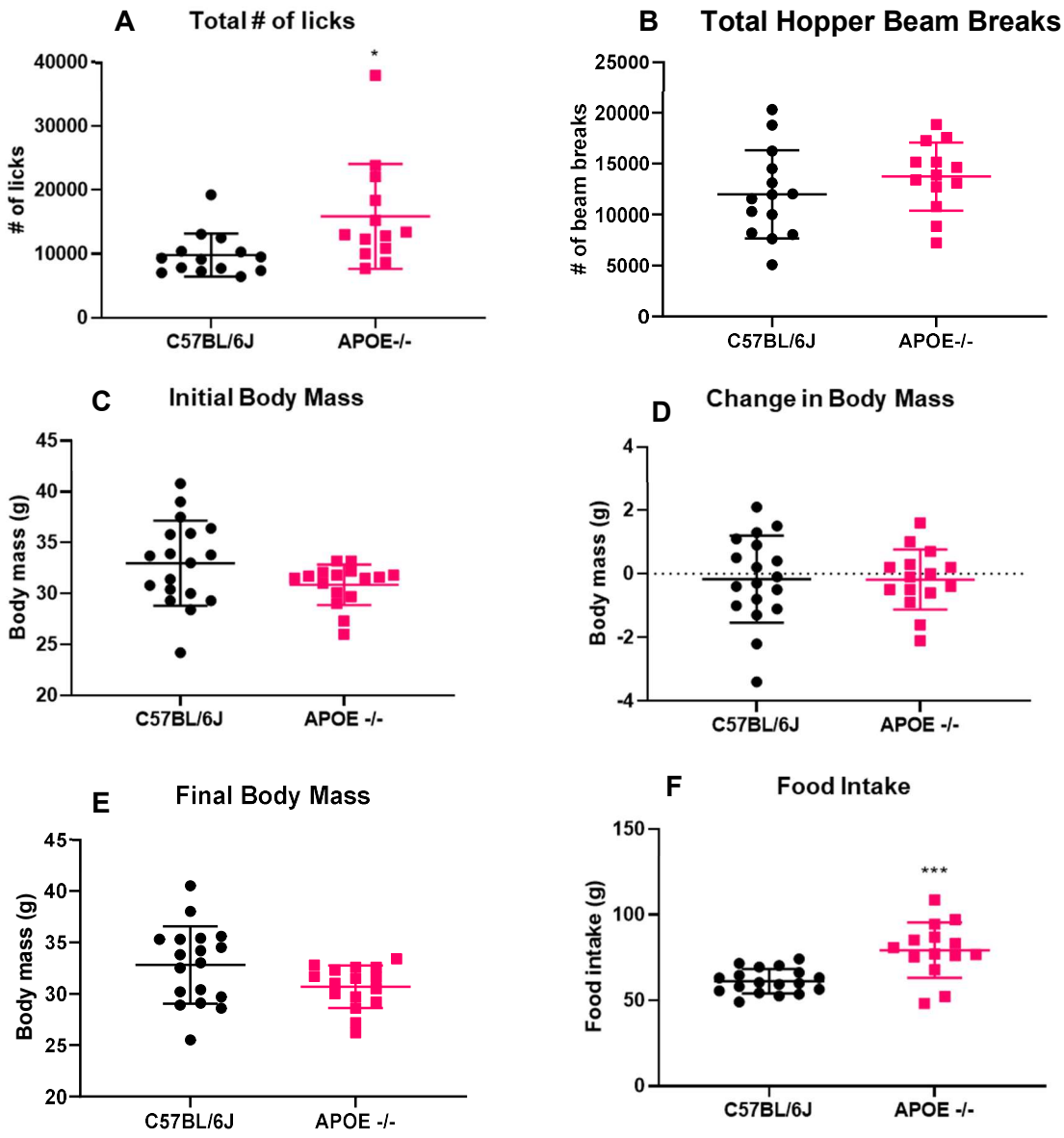


Figure 3.8: APOE-/- mice have differences in appetitive behaviour compared to the wildtypes, but don't differ in body mass in normal L:D conditions.
A) There was a significant effect of genotype on the total number of licks on the water bottles, but there was no significant genotypic effect on B) the breaks of the infrared beam across the food hopper. C) There was no significant difference in initial body mass, although there was almost a significant difference. D) There was no difference in the change in body mass between APOE-/- mice and wildtype mice. E) There was no difference in final body mass. F) APOE-/- mice had a significantly higher food intake than wildtype mice. Unpaired t-test; data presented as mean ± SD of 13-18 mice per group. Statistically significant differences between wildtype and APOE-/- mice are shown as *, $P \leq 0.05$ and ***, $P \leq 0.001$.

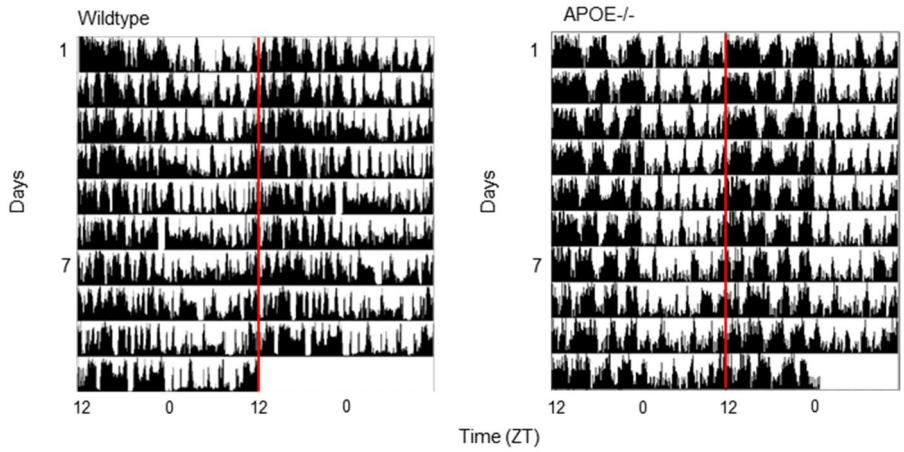


Figure 3.9: Locomotor activity in wildtype and ApoE−/− mice, in D:D conditions.
Representative double-plotted actograms of wildtype mice (left) and ApoE−/− mice (right) in D:D conditions. Bin size is 5 min.

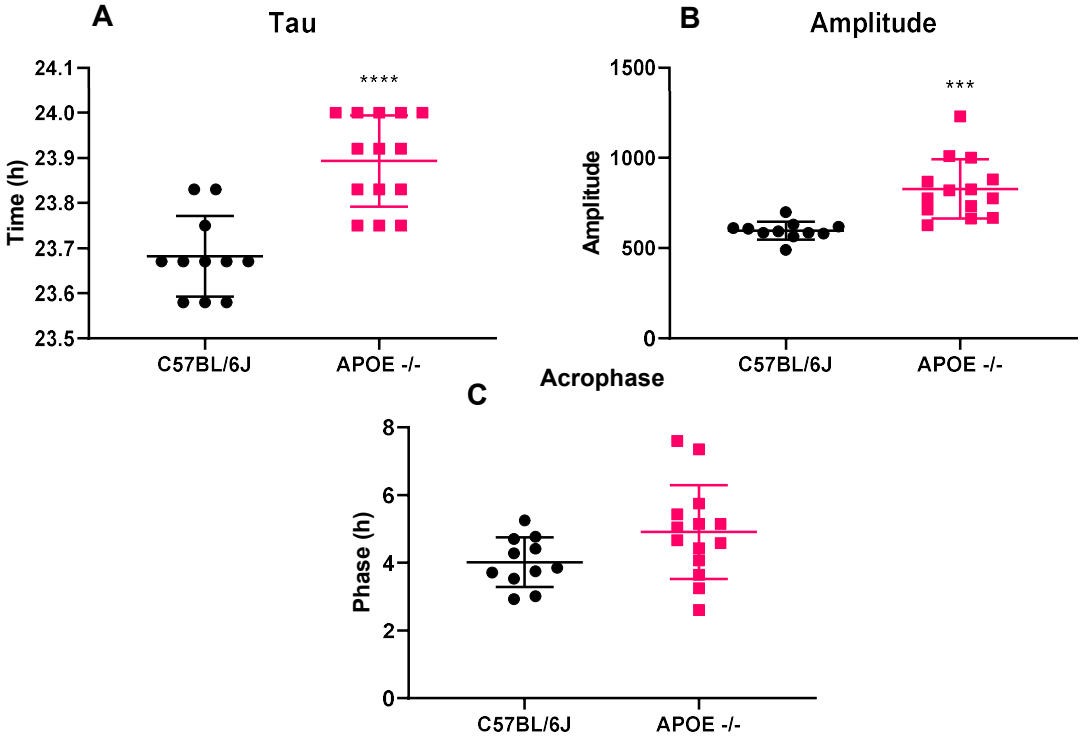


Figure 3.10: APOE-/- mice have a longer free running period, or Tau, and have a higher amplitude of behavioural rhythms compared to wildtype mice in D:D conditions.
A) There was a significant effect of genotype on Tau B) There was a significant effect of genotype on Amplitude. C) There was no difference in acrophase between genotypes, but there was a nearly significant difference. Unpaired t-test; data presented as mean ± SD of 11-14 mice per group. Statistically significant differences between wildtype and APOE-/- mice are shown as ***, P ≤ 0.001 and ****, P ≤ 0.0001.

3.3.5 Behavioural rhythms in D:D

The rhythmical behaviour of 2-month-old APOE-/- mice was assessed using ClockLab over 10 days in D:D conditions (Figure 3.9). APOE-/- mice were found to have a longer free-running period than wildtype mice over 10 days in D:D ($t=5.442$, $p<0.0001$; Figure 3.10A). APOE-/- mice also had a significantly higher amplitude of behavioural rhythms in D:D than wildtypes, amplitude was increased by 39% ($t=4.498$, $p=0.0002$; Figure 3.10B). No significant difference in the acrophase of the behavioural rhythms was found between the APOE-/- mice and wildtype mice, however there is a trend towards there being a significant difference ($t=1.919$, $p=0.0675$; Figure 3.10C). APOE-/- mice had 20% more activity bouts than wildtypes over the course of the study ($t=2.608$, $p=0.0157$; Figure 3.11A). There were no differences found between APOE-/- mice and wildtype mice when looking at the average length of the activity bouts ($t=1.49$, $p=0.1499$; Figure 3.11B).

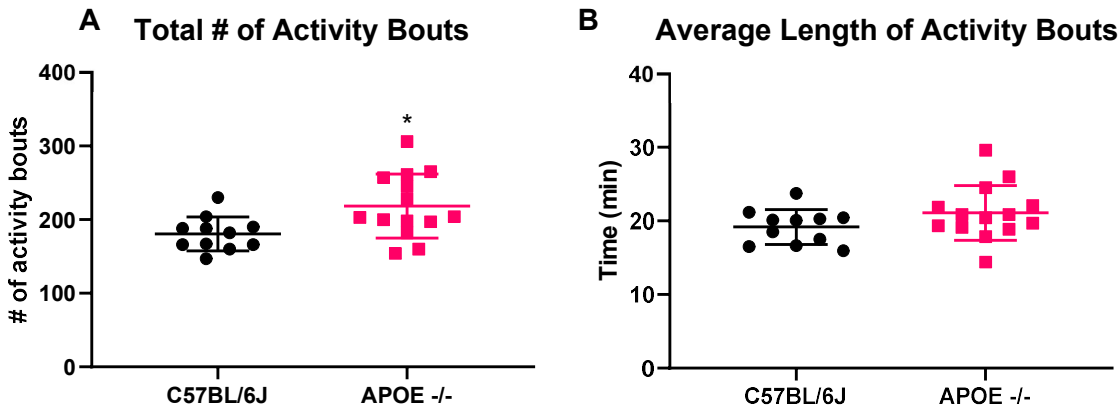


Figure 3.11: APOE-/- mice have more activity in D:D but have no difference in Activity Bouts compared to wildtype mice.
A) There was a significant effect of genotype on the total number of Activity Bouts, but there was no significant genotypic effect on **B)** the average length of Activity Bouts. Unpaired t-test; data presented as mean ± SD of 11-14mice per group. Statistically significant differences between wildtype and APOE-/- mice are shown as *, $P \leq 0.05$.

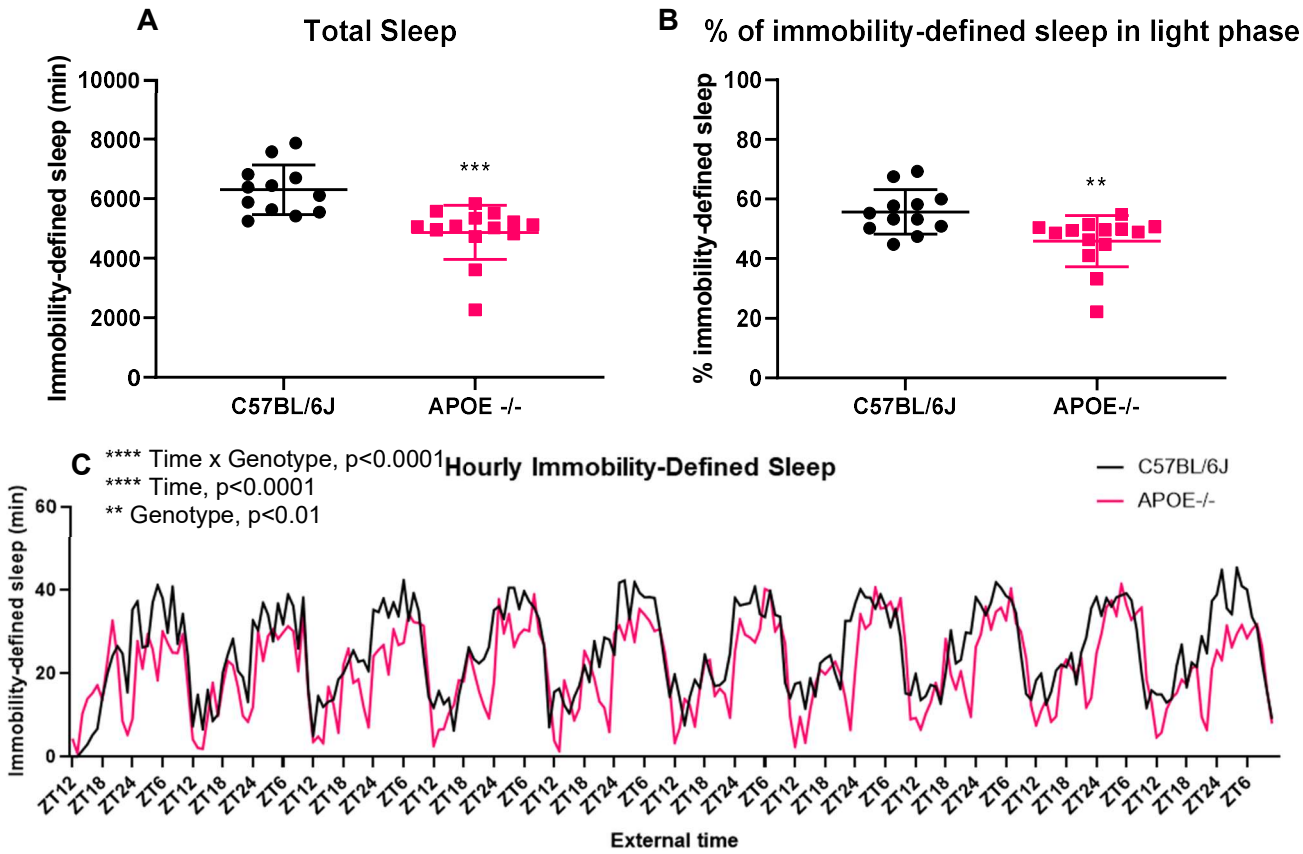


Figure 3.12: APOE-/- mice display less immobility-defined sleep and have a reduced sleep distribution in the light phase than wildtype mice in free running conditions, and there is a significant time-genotype interaction when looking at Hourly immobility-defined sleep in D:D conditions.
A) There is less total immobility-defined sleep in APOE-/- mice compared to wildtype mice. **B)** There is a reduction in the percentage of immobility-defined sleep occurring in the light phase in APOE-/- mice compared to wildtype mice. **C)** There is a significant effect of time, genotype and a significant interaction between time and genotype on hourly immobility-defined sleep. Unpaired t-test; data presented as mean ± SD of 12-14 mice per group. 2-way ANOVA; data presented as mean of 12-14 mice per group. Statistically significant differences between wildtype and APOE-/- mice are shown as **, P ≤ 0.01; ***, P ≤ 0.001 and ****, P ≤ 0.0001.

3.3.6 Immobility-defined sleep in D:D

Immobility-defined sleep was assessed in APOE-/- mice in constant D:D conditions. APOE-/- mice slept a significantly shorter total duration, 22.67% less than wildtype mice ($t=4.153$, $p=0.0004$; Figure 3.12A). APOE-/- mice also showed an altered distribution of sleep, with significantly less, 17.62%, sleep occurring in the “light” phase compared to wildtype mice ($t=3.086$, $p=0.0051$; Figure 3.12B). Analysis of the hourly variation in sleep over the time spent in D:D to avoid the masking effect of time, showed that there was a significant interaction between genotype and time ($F(239, 4541)=1.992$, $p<0.0001$). As

expected, there was also a significant effect of time, ($F(239, 4541)=13.06$, $p<0.0001$). There was also a significant effect of genotype ($F(1, 19)=14.91$, $p=0.0011$; Figure 3.12C).

3.3.7 Body mass in D:D

There were no differences in body mass between APOE-/- mice and wildtype mice at the beginning at the study ($t=1.278$, $p=0.2117$; Figure 3.13A) or the end of the study ($t=1.7171$, $p=0.097$; Figure 3.13C), and there were no differences in the change in body mass over the course of the study ($t=0.5027$, $p=0.6191$; Figure 3.13B).

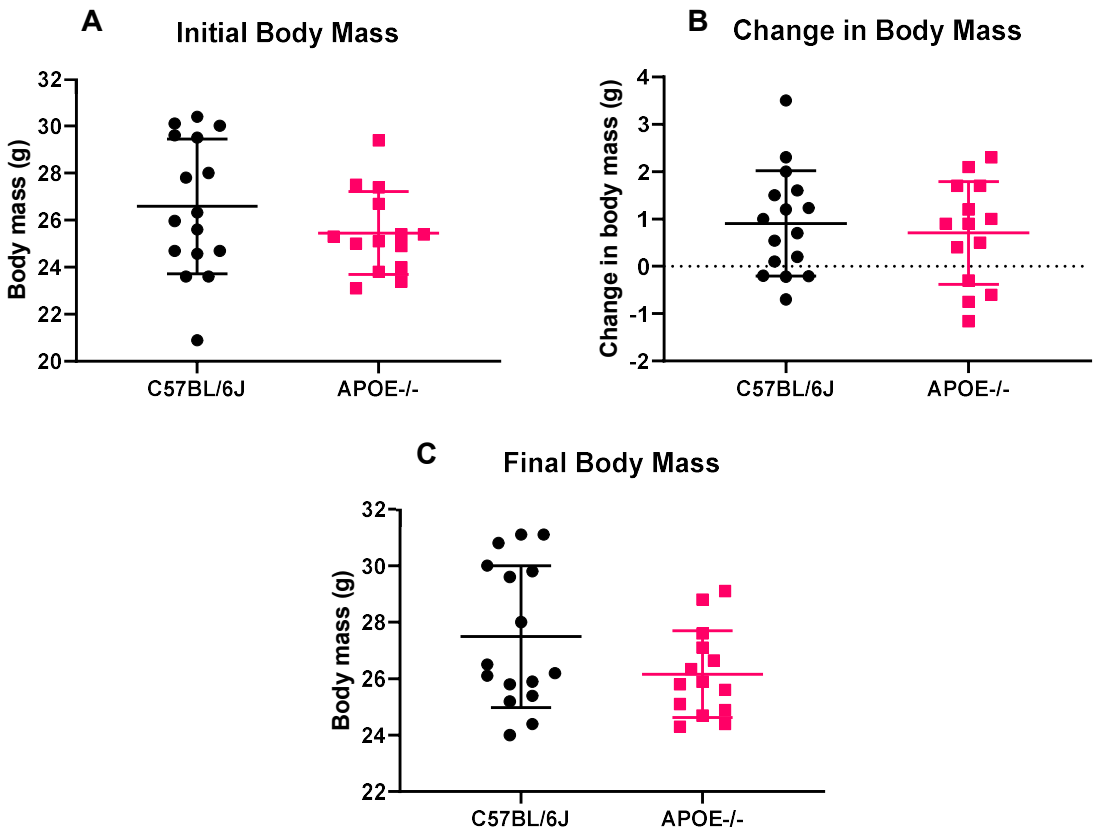


Figure 3.13: APOE-/- mice have no difference in body mass in D:D conditions. There was no significant effect of genotype on **A)** Initial body mass. **B)** Change in body mass, or **C)**. Final body mass. Unpaired t-test; data presented as mean ± SD of 14-16 mice per group.

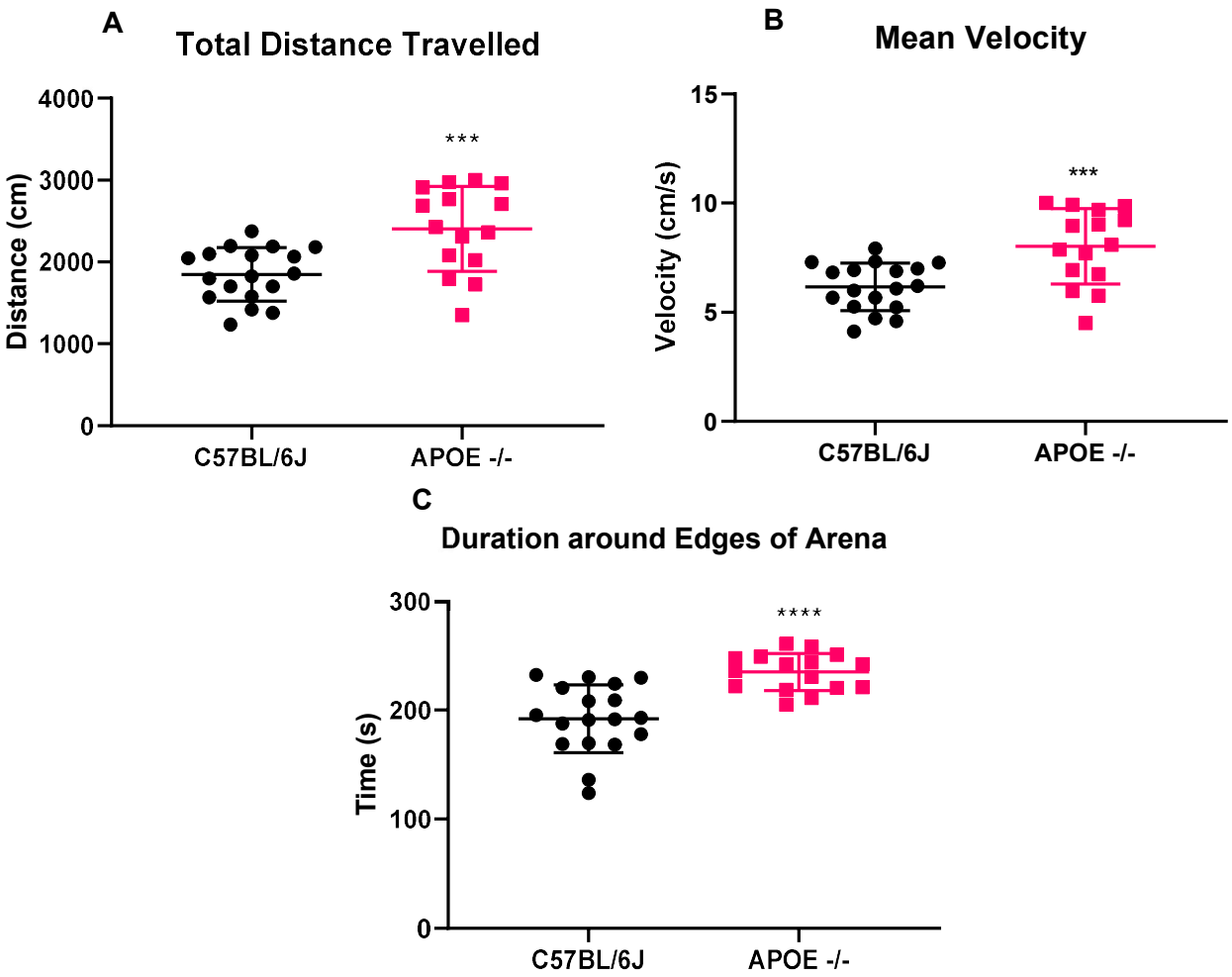


Figure 3.14: APOE-/- mice had increased locomotor behaviour and time spent at the edges of the arena compared to wildtypes in the Open Field Test.
APOE-/- mice had a higher **A)** Total Distance Travelled **B)** Total Mean Velocity and **C)** Cumulative Duration spent around the edges of the Open Field Arena compared to wildtypes. Unpaired t-test; data presented as mean ± SD of 15-18 mice per group. Statistically significant differences between wildtype and APOE-/- mice are shown as ***, P ≤ 0.001 and ****, P ≤ 0.0001.

3.3.8 Behaviour in the OFT

Behavioural tests were carried out on 6-month-old APOE-/- and wildtype mice housed in normal L:D conditions. The OFT was used as an assessment of locomotor and exploratory behaviour. In the OFT, APOE-/- mice had a significantly higher level of activity than wildtype mice, measured by a 30% increase in the total distance travelled (t=3.745, p=0.0007; Figure 3.14A), and a 30% increase in the mean velocity of the mice (t=3.746, p=0.0007; Figure 3.14B). Looking at thigmotaxis, the time spent around the edges of the Open Field arena was 21.51% higher in

APOE-/- mice (t=4.614, p<0.0001; Figure 3.14C).

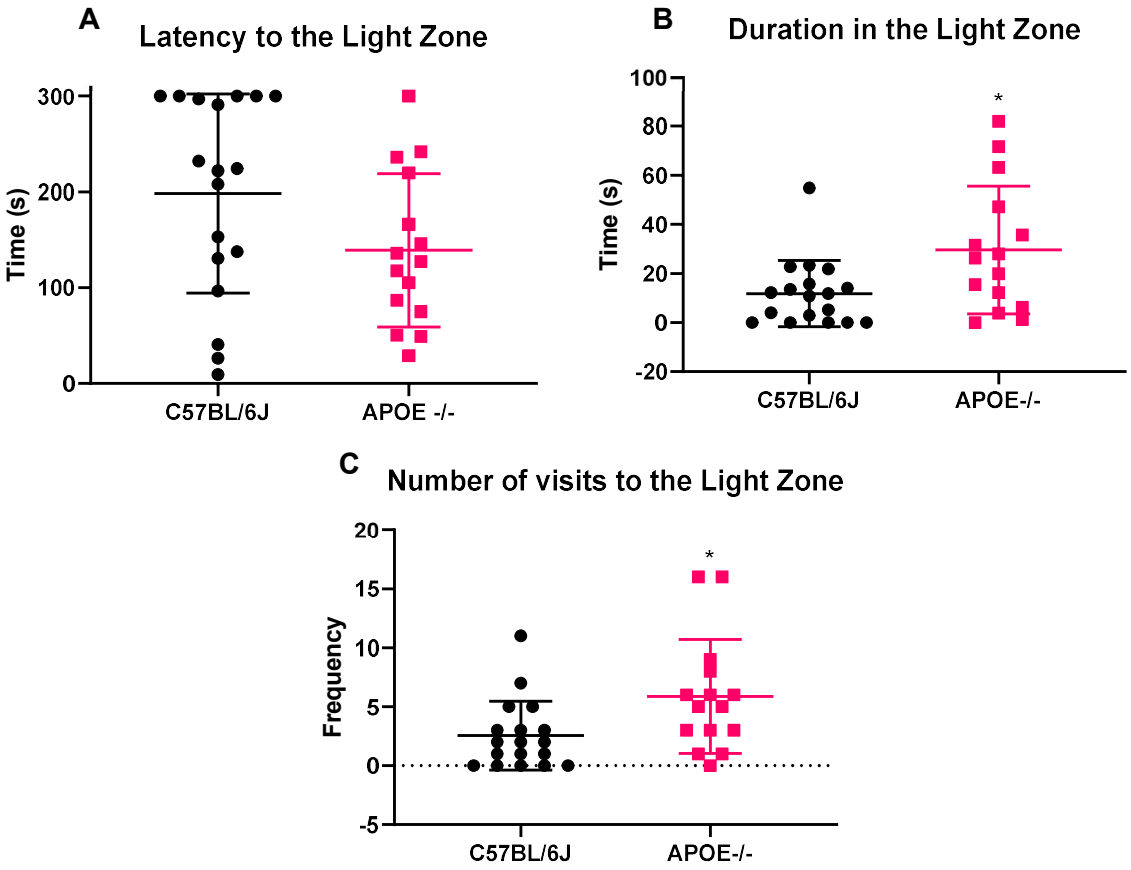


Figure 3.15: APOE-/- mice spend longer in the Light Zone of the Light Dark box and make more visits to the Light Zone than wildtypes.
In the Light Dark Box, APOE-/- mice had no difference compared to wildtype mice in **A)** Latency to Light Zone, but they did have an increased **B**) Duration spent in the Light Zone compared to wildtype mice**. C)** There were also significantly more visits into the light zone compared to wildtypes. Unpaired t-test and Mann-Whitney U test; data presented as mean ± SD of 15-18 mice per group. Statistically significant differences between wildtype and APOE-/- mice are shown as *, $P \leq 0.05$.

3.3.9 Behaviour in the LDB

The LDB was carried out to assess anxiety-like behaviour of APOE-/- and wildtype mice housed in L:D conditions. In the LDB, there were no significant differences in the time taken to enter the light zone, although there was a trend towards genotype being significant (t=1.801, p=0.0.0815; Figure 3.15A). However, APOE-/- mice made 150% more visits into the light zone compared to wildtype mice (p=0.0149; Figure 3.15B) and they also spent significantly 150.42% longer in the light zone compared to wildtype mice (t=2.256, p=0.0169; Figure 3.15C).

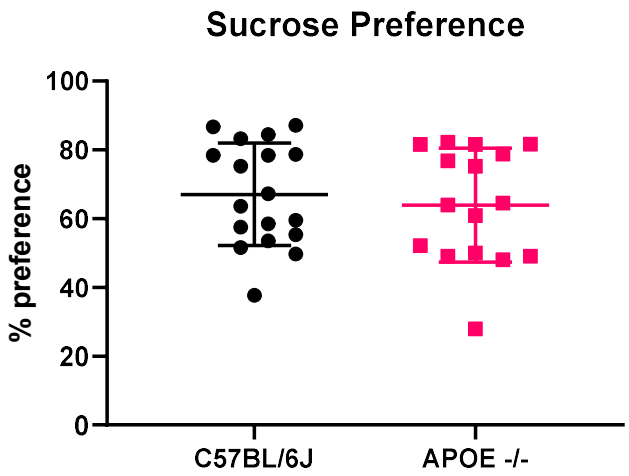


Figure 3.16: Sucrose Preference in APOE-/- mice and wildtype mice.
There was no difference in sucrose preference between APOE-/- mice and wildtype mice. Unpaired t-test; data presented as mean ± SD of 16-18 mice per group.

3.3.10 Behaviour in the SPT

The SPT was undertaken to assess anhedonia in APOE-/- and wildtype mice housed in L:D conditions. There was no difference in sucrose preference in the SPT due to genotype (t=0.5732, p=0.5705; Figure 3.16).

3.3.11 Hepatic expression of genes involved in circadian control in D:D

The rhythmical expression of core clock genes at 4 time points over 24-hours was investigated (Figure 3.17) [208]. *Clock* expression was significantly rhythmic in both APOE-/- (p=0.025) and wildtype mice (p=0.001; Figure 3.17A). The MESOR was significantly reduced in APOE-/- mice by 32.11% compared to wildtypes (p=0.0020). *Bmal1* expression was also significantly rhythmic in both APOE -/- (p<0.0001) and wildtype mice (p=0.00022; Figure 3.17B). Additionally, the phase of *Bmal1* expression was delayed by ~5 hours in APOE-/- mice, from ~ZT14 in wildtypes to ~ZT19 (p=0.024). *Cry1* expression was significant rhythmic in APOE-/- (p<0.0001) and wildtype mice (p<0.0001; Figure 3.17C), but no differences in the rhythm or level of expression were seen. However, *Cry2* expression showed a significant phase delay in APOE-/- mice, from ~ZT8 to ~ZT13 (p=0.007; Figure 3.17D).

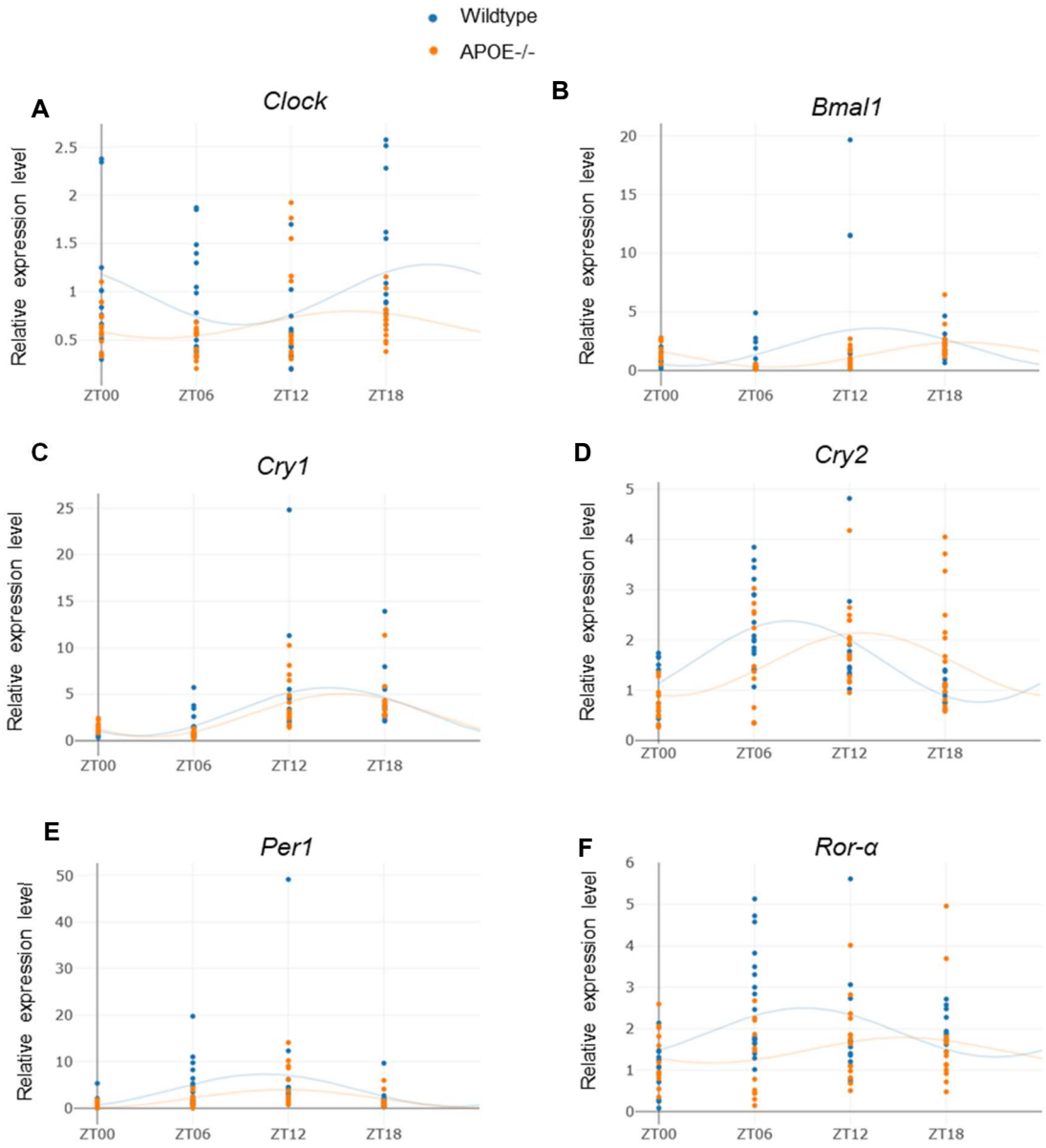


Figure 3.17: The expression of genes involved in circadian rhythm control in APOE-/- and wildtype mice.
A) *Clock* expression has a reduced MESOR and an increased phase in APOE-/- mice. **B**) *Bmal1* expression has a phase delay in APOE-/- mice. **C)** *Cry1* expression is unchanged in APOE-/- mice. **D)** The phase of *Cry2* expression is advanced in APOE-/- mice. **E)** *Per1* expression has a reduced MESOR in APOE-/- mice. **F)** *Ror-α* expression is arrhythmic in APOE-/- mice, but rhythmic in wildtypes. Cosinor analysis, n=12-18 mice

Significant rhythmicity was present in APOE-/- ($p<0.0001$) and wildtype mice ($p<0.0001$). Expression of *Per1* was significantly rhythmic in both APOE-/- ($p<0.0001$) and wildtype mice ($p<0.0001$; Figure 3.17E). However, there were no significant differences in MESOR, amplitude or phase. When investigating *Ror-α* expression, APOE-/- mice did not

show rhythmical expression (p>0.05) whilst the wildtype mice did (p=0.002), and the MESOR (or average expression) was significantly lower in APOE-/- mice (Figure 3.17F).

3.3.12 Hepatic expression of genes involved in lipid metabolism in D:D

The rhythmical expression of genes involved in lipid metabolism was investigated (Figure 3.18). *Sirt1* expression was not rhythmic in APOE-/- or wildtype mice (p>0.05), and no differences were found between the groups (Figure 3.18A). *Rxr-α* expression was significantly rhythmic in APOE-/- mice (p=0.007) but arrhythmic in wildtype mice (p>0.05; Figure 3.18B). There were no differences between the genotypes for MESOR, amplitude or phase. *Hmgcr* expression was significantly rhythmic in the APOE-/- mice (p<0.0001) but was arrhythmic in wildtype mice (p>0.05; Figure 3.18C). The amplitude of expression was significantly different between groups (p=0.040).

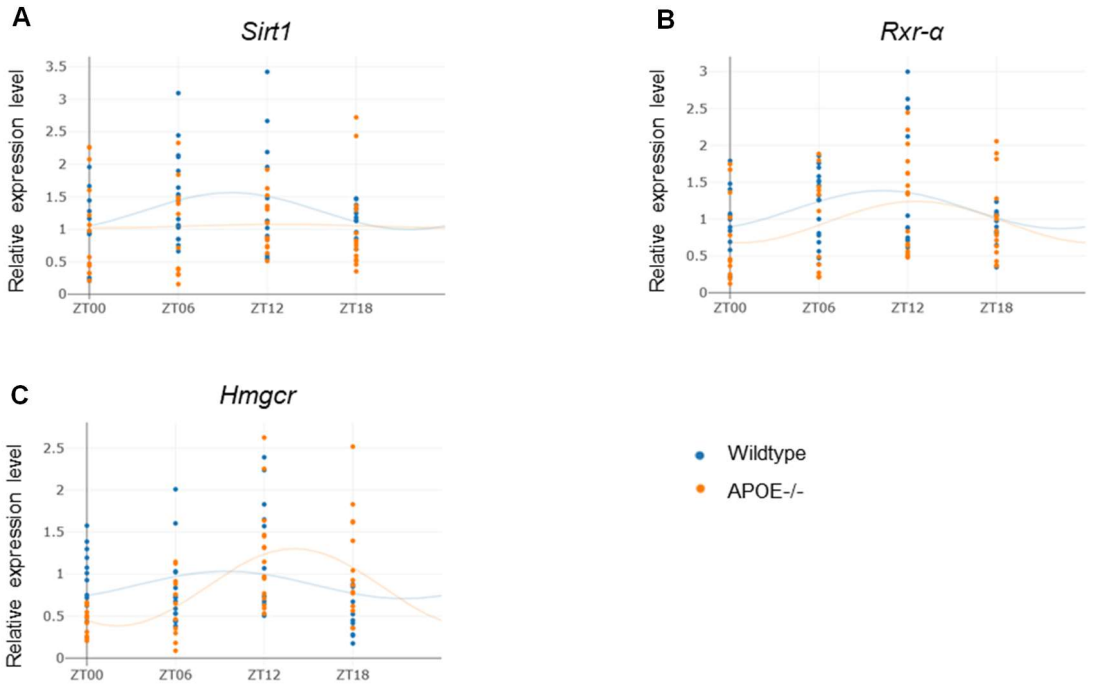


Figure 3.18: Rhythmical expression of genes involved in lipid metabolism in APOE-/- mice and controls.
A) *Sirt1* expression is unchanged in APOE-/- mice, **B)** *Rxr-α* expression is unchanged in APOE-/- mice. **C**) *Hmgcr* expression is arrhythmic in control mice, but significantly rhythmic in APOE-/- mice. Cosinor analysis and 2-way ANOVA, n=12-18 mice per group.

3.4 Discussion

It has been shown for the first time that APOE-/- mice display significantly increased locomotor activity, which is evident in the amplitude of behavioural rhythms, immobility-defined sleep, home cage behaviour monitoring and the OFT. Additionally, this is the first time that sleep has been investigated in the APOE-/- mouse model.

To summarize, in this chapter, it was discovered that that APOE-/- mice have stronger behavioural rhythms as seen with a higher amplitude, longer activity bouts, stronger sleep rhythms and increased locomotor activity in the home cage environment in L:D conditions. They also show alterations in appetitive behaviour but not body mass in L:D conditions. In D:D conditions, it was discovered that APOE-/- had a longer free-running rhythm, stronger behavioural rhythms, and reduced sleep. The behavioural tests revealed that APOE-/- mice had increased exploratory behaviour in the OFT and LDB but showed no difference in sucrose preference. Finally, APOE-/- mice showed alterations in hepatic expression of the core clock genes and genes involved in energy metabolism in D:D conditions.

The APOE-/- genotype showed differences in rhythmical circadian-controlled behaviour, but these differences were more evident in D:D conditions. In normal L:D conditions there was no difference in circadian period. However, in D:D conditions, the circadian period was lengthened in APOE-/- mice, yet it was still shorter than the circadian period in L:D. Normal circadian period in L:D is expected in APOE-/- mice [26, 209]. Light is a strong zeitgeber, and also has a strong masking effect on locomotor behavioural rhythms, so abnormal circadian behavioural period is very rare in L:D conditions [210]. However, when light is removed, endogenous rhythms can be observed without masking. In a previous study assessing the behaviour of APOE-/- mice of the same age in D:D, there were no differences in tau compared to the controls [26, 209]. This could be explained by genetic background - Zhou et al., studied APOE-/- mice from Laboratory Animal Center of Peking University and the Experimental Animal Center of Chinese Academy of Medical Sciences (Beijing, China) [26]. However, Chalfant et al., studied APOE-/- mice from the Jackson

Laboratory [209], which is the same background as the mice used in this study. However, Chalfant et al., bred the APOE-/- mice with C57BL/6J mice to generate APOE-/+ mice which were then used to generate APOE-/- mice and APOE+/+ controls, so this extended breeding programme may have resulted in genetic drift [209]. A lengthened free running period is associated with ageing in C57BL/6J mice, and it is seen in mouse models of mood disorders [211-213]. Here, a lengthened period may indicate some disturbance in endogenous circadian rhythm generation because of the lack of APOE.

The amplitude of behavioural rhythms was increased in APOE-/- mice in both L:D and D:D, by a similar amount. This is contrast to a previous study, where APOE-/- mice showed no difference in amplitude to controls in L:D conditions, and showed a reduced amplitude compared to controls in D:D conditions [209]. Again, the genetics and breeding background may have an effect [209]. The increased amplitude, and therefore stronger rhythms of the APOE-/- mice in D:D, may contribute to the lengthened free running period.

There were no significant differences in the acrophase of the activity of the mice between genotype in either L:D or D:D. Phase changes only usually happen after a light pulse in the dark phase [109]. APOE-/- mice were trending towards a slightly delayed phase compared to wildtypes in D:D, which connects with the lengthened period, meaning that their activity peak may occur slightly later than the wildtypes every day.

In normal L:D conditions, APOE-/- mice have longer bouts of activity than wildtype mice, but they have the same number of total activity bouts. In D:D conditions, the opposite is seen; APOE-/- mice have the same length of activity bouts as the wildtype mice but they have a higher number of activity bouts compared to wildtypes. In normal L:D, the longer activity bouts are likely to be connected to the increased amplitude of the APOE-/- mice compared to wildtypes. In D:D a higher number of activity bouts per day is likely to be associated with the lengthened period in APOE-/- mice compared to wildtypes. Additionally, models of AD, including the APOE-ε4 model show an increased number of

bouts per day in normal L:D conditions, and older C57BL/6J mice show more bouts of wheel running activity compared to adult C57BL/67J mice [211, 214]. A mouse model of anxiety shows more activity bouts per day in L:D and D:D and also shows sleep differences in the form of sleep fragmentation [212].

For total immobility-defined sleep, there was no difference between APOE-/- mice and C57BL/6J mice in L:D. This is not surprising, as the APOE-/- model is not a known sleep disorder model and light has a very strong masking effect on the circadian mechanisms of sleep [210]. In D:D, APOE-/- mice show a reduced amount of total immobility-defined sleep. This is likely connected with the increased number of activity bouts and the increased free running period, and could indicate sleep fragmentation [212].

With the percentage of immobility-defined sleep in the light phase, there was no difference between APOE-/- mice and wildtype mice in L:D conditions. Again, light likely masks any intrinsic differences in sleep. In D:D however, APOE-/- has a lower percentage of immobility-defined sleep in the “light” phase compared to wildtypes. The “light” phase is subjective here, as the mice are in D:D. However, when free running, there are clear active and inactive periods that follow the L:D conditions that the mice were previously housed in. In the literature, Zhou et al also reported an abnormal activity distribution in D:D, with more activity in the “light” phase in the APOE-/- mice [26]. This supports the results reported here. An altered distribution of sleep between active and inactive phases could also indicate sleep fragmentation.

For total immobility-defined sleep per hour over time, there was an interaction between genotype and time in both L:D and D:D. The APOE-/- mice showed a stronger circadian amplitude of their behavioural rhythms in both L:D and D:D which also seems evident in their immobility-defined sleep. Additionally, there was an effect of genotype, which associates with reduced total sleep and increased number of activity bouts seen in APOE-/- mice in D:D.

In humans, irregularities in sleep and reduced sleep are associated with higher levels of atherosclerotic markers [167, 215]. APOE-/- mice subjected to chronic sleep fragmentation developed larger atherosclerotic lesions and showed aortic immune cell infiltration compared to control APOE-/- mice without sleep fragmentation [216, 217]. An alteration in sleep is associated with changes in the neural network, and the excitatory/inhibitory circuit balance [218]. To my knowledge there are no published sleep studies or electrophysiological studies in the APOE-/- model. When investigating hippocampal CA1 neurones in the APOE-ε4 model, enhanced CA3 - CA1 basal synaptic transmission was found, as well as enhanced paired-pulse facilitation, and reduced long-term potentiation [219]. As an altered form of APOE has an effect on the neural network, this indicates that a lack of APOE could also have an effect. Any alterations on the neural network are likely through impaired synaptogenesis and neuronal plasticity, which require cholesterol transported by APOE [53-56].

In this study, the APOE-/- model showed altered sleep both in L:D and D:D, although alterations are more evident in D:D. Reduced total sleep, interactions between genotype and time, and abnormal sleep distribution all indicate that the absence of APOE may affect sleep through alterations in neural networks, alterations in the circadian system, or alterations in APOE-mediated transport in the CNS.

In L:D conditions, home-cage behaviour analysis revealed that APOE-/- mice have increased locomotor behaviour, as indicated by distance travelled and velocity. Increased locomotor activity, or hyperactivity, in the “home cage” environment has not been reported in APOE-/- mice before. Hyperactivity in APOE-/- mice is likely to be associated with the increased behavioural amplitude and reduced sleep in D:D, and aberrant cholesterol transport in the CNS because of the absence of APOE is likely to be the cause. Hyperactivity may also be due to metabolic abnormalities in the APOE-/- model, as hyperactivity is seen in the PGC-1α knockout mouse, a model with abnormal energy metabolism and mitochondrial function [220].

When assessing the food intake and body mass changes over the 2 weeks in L:D, APOE-/- mice appeared to eat more food than wildtype mice, but had no differences in body mass, and no differences in the change in body mass over the course of the study compared to wildtypes. Additionally, APOE-/- mice were shown to activate the lickometer more than wildtypes, indicating that they drank more water than wildtypes. No differences were seen in body mass in D:D conditions.

APOE has been shown to regulate food intake in rats, administration of APOE reduces food intake, whilst inhibition of APOE stimulated feeding, thought to be through a mechanism enhancing melanocortin signalling [221]. Therefore, the regulation of food intake may be impaired when APOE is absent, leading to increased intake.

The dichotomy between food intake and body mass has not been shown before, although one study showed that APOE-/- mice on a high fat diet (HFD) did not increase in body mass, whilst the wildtype mice did [222]. Increased food intake without an increase in body mass indicates a metabolic difference in the APOE-/- mice. The increased activity level displayed by the APOE-/- mice may explain why the body mass does not increase with increased food intake, as the mice are doing more exercise.

This study found that the APOE-/- genotype displayed increased locomotor activity, as seen in the OFT, and reduced anxiety-like behaviour, as seen in the LDB. There was no effect of genotype on depressive-like behaviour as measured by the SPT.

The OFT is a common, first pass behavioural assessment. It allows assessment of locomotor ability, activity and some anxiety-like behaviours. In the OFT, APOE-/- mice showed increased activity levels than wildtype mice, as seen by total distance travelled and mean velocity, and they also spent more time in the corners of the arena, (and less time in the middle of the arena) than the wildtype controls. Jansen et al., showed that there were no differences between 8-10-month-old APOE-/- mice and wildtype controls in activity levels in the OFT, [223]. Additionally, no differences were found in the distance

travelled and mean velocity in the open field between 4-5-month-old male APOE-/- mice and APOE+/+ control mice by Grootendorst et al, and no differences were found in the OFT between 6-month-old female APOE-/- and C57BL/6J mice by Raber et al., [224, 225]. Additionally, Hu et al., showed no differences in the OFT between 8-week-old male wildtype mice and APOE-/- mice [226]. However, reduced OFT locomotor activity was reported in 5-6-month-old male APOE-/- mice on a HFD compared to wildtype mice on a normal diet, and reduced general locomotor activity has been reported in 7-8-month-old APOE-/- mice compared to wildtypes [227, 228].

These reported locomotor activity results contrast with the results found in this study, which show an increase in activity. APOE-/- mice also displayed increased locomotor activity compared to wildtypes in other parameters, e.g., the stronger amplitude of behavioural rhythms in both L:D and D:D, and the increased distance travelled in the home cage behavioural assessment in L:D. This indicates that the increased activity seen in the OFT is not attributed only to exploration of a novel environment, but also to the increased activity of the APOE-/- mice. Interestingly, the LDLR-/- model also showed increased locomotor activity in the open field [229]. The LDLR binds to APOE to transport cholesterol to the liver, and so the LDLR-/- mouse has a similar phenotype of hypercholesterolaemia to the APOE-/- model [230]. This suggests that APOE-mediated cholesterol transport may have a role in regulating locomotor activity.

Jansen et al., reported that the APOE-/- mice spent less time in the centre of the open field and more time in the corners compared to wildtype mice, which is in accordance with the results reported here [222, 223]. Avoiding the centre of the OFT and staying close to the edges of the arena (thigmotaxis) is associated with anxiety-like behaviour [231]. This suggests that the APOE-/- mice may be more anxious than the wildtype mice.

The LDB results show that APOE-/- mice make more visits to the light zone and have a longer duration in the light zone, indicating reduced anxiety-like behaviour, increased exploratory activity and potentially increased impulsivity. APOE-/- mice were almost

quicker to visit the light zone, although this was not statistically significant compared to wildtypes. Looking at previous studies, in a light/dark preference test similar to the LDB, 4-5-month-old APOE-/- mice showed no difference in preference to stay in the dark zone compared to control APOE+/+ mice [224]. 22-week-old male APOE-/- mice on a HFD for 16 weeks spent significantly less total time in the light zone compared to wildtypes [227]. It has been shown that a HFD leads to increased depressive and anxiety-like behaviours in wildtype mice, so the difference in behaviour compared to what is shown in this chapter could be due to the HFD, rather than the APOE-/- genotype [232]. There are no other studies using the LDB to assess behaviour in APOE-/- mice. However, as the LDB is used as measure of anxiety-like behaviour, other studies have assessed anxiety-like behaviour in APOE-/- mice using the elevated plus maze. 12-14-week-old male and female APOE-/- mice showed reduced anxiety-like behaviour in the elevated plus maze [233]. However, Robertson et al., reported increased anxiety-like behaviour in 6-8-month-old male APOE-/- mice in the elevated plus maze compared to wildtypes [234]. However, these differences were not seen in 2-4-month-old mice [234]. Additionally, 20-week-old APOE−/− mice showed no difference to wildtypes [235]. Given the wide range of results in the literature, it is difficult to know what the typical anxiety-like behavioural profile is for APOE-/- mice, but from the investigations in this study, it seems that APOE-/- mice are less anxious, more impulsive, and more explorative than wildtype mice.

The SPT is used as a measure of depressive-like behaviour. In this work, an overall preference for 1% sucrose solution over water is seen by both groups, but there was no difference in sucrose preference between the APOE-/- mice and the wildtype mice. In concordance with this result, Hu et al., showed no difference in sucrose preference between male wildtype mice and APOE-/- mice on a HFD at the start of experiment (week 0), or at 4 weeks [226]. Like the experiment in this study, mice were acclimatized to the sucrose prior to the SPT, and the water and sucrose bottles were swapped halfway through the study to eliminate place preference. However, the SPT duration was 24 hours

rather than 6 hours like in this study. In contrast, it has been shown that 22-week-old male APOE-/- mice on a HFD had significantly lower sucrose preference than the wildtype group [227]. However, this could be due to place preference rather than sucrose preference, as the position of the sucrose and water bottles were not swapped halfway. Additionally, the time frame of the SPT was different – mice were fasted for 24 hours prior and had 24 hours to do the test [236, 237]. Additionally, the APOE-/- mice had been on a HFD for 16 weeks, which has been shown to cause rodents to lose preference for sucrose at 15-17 weeks [227, 237]. Dere et al., showed that 3-month-old female APOE-/- mice showed a higher sucrose preference compared to wildtypes [238]. This could be due to place preference, as the bottles were not swapped during the SPT, or due to timeframe, as Dere carried out the SPT for 24-hours. This also may be due to a sex difference. Sex differences have been shown to impact SPT results, and they were shown to be strain-dependent [239]. The APOE-/- genotype, with no additional effect of diet, seems to have no effect on sucrose preference, and therefore anhedonia in male mice. Comparing sucrose preference in male and female APOE-/- mice would be an interesting follow-up experiment to explore the differences seen by Dere et al., that were not seen in this study.

The differences between the behavioural results in this study and results found in the literature could, again, be explained by a different genetic background affecting behaviour in the APOE-/- mice. [223, 225-228, 240]. Furthermore, there were variations in testing conditions that may have affected behavioural results. The OFT and LDB used for this study were 5 minutes each in duration, but the other tests discussed here ranged from 250 seconds to 30 minutes in length, which will affect exploratory behaviour due to habituation [223-226, 240, 241].

The rhythmical expression of core clock genes in the liver, a robust peripheral oscillator, was investigated, revealing that *Clock* had a reduced MESOR and that *Bmal1* and *Cry2* had phase delays in APOE-/- mice, whilst *Per1* and *Cry1* expression was unchanged in

APOE-/- mice. In the literature, there are only two studies assessing the rhythmic expression of core clock genes in the liver in APOE-/- mice. Hou *et a*l., showed that hepatic *Bmal1* expression exhibited a phase delay in APOE-/- mice in D:D, which is in accordance with the results shown here. Additionally, it was shown that the MESORs of hepatic *Clock* and *Cry1* expression were reduced in APOE-/- mice in D:D [242]. The reduced MESOR for *Clock* expression agrees with the results of this study, but the reduced MESOR for *Cry1* is not seen in this study. Zhu *et al*., also investigated the circadian expression pattern of hepatic core clock genes and found that the rhythmical expression of *Cry1* had a reduced amplitude in APOE-/- mice in L:D compared to wildtypes [185]. This result is similar to the findings by Hou *et al.,* but again is not seen in this study. *Ror-α* expression was not rhythmic in APOE-/- mice, and APOE-/- mice had a lower average level of expression. Zhu et al., also found that the amplitude of hepatic *Ror-α* expression was attenuated in APOE-/- mice compared with wildtype mice, which supports what is shown here [185]. ROR-α is involved in regulating metabolism and circadian rhythms, where it is induces expression of *Bmal1* among other functions. The result here implies that the absence of APOE may exert an effect on the circadian system through the abolishment of the rhythmical expression of *Ror-α*.

These results indicate that the absence of the APOE gene effects the expression of the core clock genes in peripheral oscillators, which could mean that the APOE gene directly interacts with the core clock machinery in the liver, or that the hyperlipidaemia and hypercholesterolaemia that occurs as a result of the APOE gene knockout effects the expression of the core clock genes. Additionally, these results are different from what is observed in behaviour, where the amplitudes of behavioural rhythms were much stronger in the APOE-/- mice. This could indicate that the absence of APOE has a different effect on circadian rhythms in the brain compared to in the periphery, or that there is internal desynchrony, resulting in dampened and altered peripheral gene expression.

The rhythmical gene expression of genes involved in lipid metabolism were assessed in the liver. SIRT1 is a member of the sirtuin (SIRT) family and is a class III histone deacetylase (HDAC) which is nicotinamide adenine dinucleotide (NAD)-dependant. It is involved in broad range of physiological functions including cellular senescence, apoptosis, glucose and lipid metabolism, oxidative stress and inflammation [243]. It also plays a role in the circadian clock machinery as it binds to the CLOCK-BMAL1 complex in the transcriptional-translational feedback loop (TTFL) [244]. Here it was shown that hepatic *Sirt1* expression is not rhythmical and does not differ between APOE-/- and wildtype mice. This is different to previously reported results, where rhythmic *Sirt1* expression is seen in the liver. However, Zhu et al., found that the oscillation of hepatic *Sirt1* expression was not in a 24-hour rhythm in APOE-/- mice [185]. Additionally, Zhou et al., found that in the SCN, the amplitude of *Sirt1* expression was reduced, and showed an 8-hour phase advance [26]. SIRT1 should have a circadian oscillation, so it is unexpected that the wildtype group did not show circadian rhythmicity, and it is unexpected that there are no differences in expression between wildtypes and APOE-/- mice.

Retinoid X receptor (RXR) is a member of the superfamily of nuclear hormone receptors, which are transcription factors that regulate the expression of genes involved in a diverse range of physiological processes [245]. RXR-α has been shown to form heterodimers with multiple nuclear receptors, including receptors for FAs, and so plays a role in lipid homeostasis [246, 247]. RXR-α interacts with CLOCK and inhibits the transcriptional activity of the CLOCK-BMAL1 heterodimer, and so inhibiting *Per* transcription [248]. *Rxr-α* expression levels were not significantly different in APOE-/- mice, despite APOE-/- mice showing significant rhythmicity in *Rxr-α* expression when wildtypes were arrhythmic. APOE-/- mice have been shown to have rhythmic *Rxr-α* expression, but arrythmicity in wildtypes is not expected [185].

3-hydroxy-3-methylglutaryl-Coenzyme A reductase (HMGCR), commonly known as HMG-CoA reductase, is a protein present in the ER membrane. It is a rate-limiting enzyme in

mevalonate production, a precursor to cholesterol, and is involved in a cellular feedback mechanism to balance internally synthesised and externally sourced cholesterol [249, 250]. *Hmgcr* expression had no overall difference between APOE-/- and wildtype mice, despite having rhythmical expression in APOE-/- but not wildtype mice. As the APOE-/- mice are young (~9-weeks-old), it could be that the differences in cholesterol metabolism have not yet had time to affect overall mRNA transcript levels. *Hmgcr* levels tend to peak in the “dark” phase, as that is when most feeding activity is taking place [251]. As APOE-/- mice had stronger behavioural rhythms, it may be that these behavioural rhythms induce this strong oscillation in *Hmcgr* levels compared to wildtype.

3.5 Conclusions

In this chapter it has been shown for the first time that APOE-/- mice display increased locomotor activity, and this was shown across multiple behavioural parameters. This seems to be associated with an increased amplitude of behavioural rhythms in both L:D and D:D, as well as alterations to circadian period in D:D, and alterations to sleep in both L:D and D:D. They also display alterations in energy metabolism, with increased food intake but no change in weight, and it is likely that the increased activity plays a role in this. They may show less anxiety-like behaviour, or they may be more impulsive in the LDB, whilst they do show increased anxiety-like behaviour in the OFT. APOE is required for cholesterol transport in the CNS, and cholesterol is essential for neuronal plasticity and synaptogenesis [53-56]. It is likely that impaired CNS cholesterol transport underlies the hyperactivity seen in the APOE-/- model. The APOE-/- mice also show changes in the expression of genes involved in circadian rhythm generation and energy metabolism that indicate that the absence of the APOE-/- gene affects peripheral circadian rhythms in a different way compared to behavioural rhythms.

4 The effect of constant light exposure on behaviour, gene expression and the glial cell response in the APOE-/- mouse model

4.1 Introduction

4.1.1 CVD and circadian disruption

Disruption of circadian rhythms is known to impact CVD, and light is known to be a potent circadian disruptor [252]. Shift work, in particular night shifts, is the most common example of circadian disruption with abnormal light exposure. It has been associated with incidence of microvascular obstruction and increased infarction site after reperfusion therapy for MIs in a study population that was matched and adjusted for covariates [253]. Regular night shifts have also been shown to increase the risk of coronary heart disease (CHD) independently of genetic factors [254]. However, the mechanisms linking shift work and CVD are not well characterised. Shift workers tend to be in occupations that are considered essential, and so, increasing understanding the links between abnormal lighting conditions and CVD would have benefit both to the individuals and wider society.

4.1.2 Circadian disruption and behavioural alterations in mice

The early experiments in circadian biology resulted in characterisation of free-running using running wheels, and also the observation of how these free-running behavioural rhythms changed in altered light conditions, including constant light (L:L) [145]. As mentioned in Chapter 1.8, nocturnal rodents such as mice show a lengthened period in L:L, which can, depending on light intensity and time in L:L, result in split behavioural rhythms or complete behavioural arrhythmicity [143, 145, 255, 256]. Additionally, L:L has been shown to affect sleep in rodents by altering the distribution between sleep stages [147, 257]. L:L has also been shown to increase depressive-like behaviours and alter anxiety-like behaviours, as assessed by standard batteries of behavioural tests [146, 255, 258]. Chronic exposure to L:L has also been shown to alter immune parameters and

cause metabolic disturbances and in mice [259-262].

4.1.3 The APOE-/- mouse model and constant light exposure (L:L)

The APOE-/- mouse model, as a model of dyslipidaemia and spontaneous atherosclerosis, can be used to investigate the gene-environment interaction between circadian disruption and CVD by exposing APOE-/- mice to L:L, or other forms of chronic circadian disruption, and assessing any changes. Previously, Chalfant *et al.*, demonstrated that L:L exposure exacerbated atherosclerosis in male, but not female APOE-/- mice, where the male APOE-/- mice exhibited increased atherosclerotic lesions and a higher VLDL/LDL level [209]. However, only wheel running behaviour was investigated, and changes in the brain and liver, which are key circadian oscillators and sites of APOE synthesis, weren't investigated [209].

4.1.4 APOE and the Brain

APOE is a primary apolipoprotein in the CNS [51]. Secreted by astrocytes and microglia, it is involved in CNS lipid transport and metabolism, and therefore has a key role in maintaining brain lipid homeostasis [49]. Cholesterol is abundant in the brain, where it is a crucial component of myelin, present in neuronal and glial membranes, and has key roles in neuronal plasticity, synaptic vesicle transport and neurotransmitter release [263]. APOE, and therefore cholesterol, is independently regulated in the CNS from the periphery due to the BBB [263]. Cerebrospinal fluid (CSF) lipoproteins have been shown to be involved in lipid removal from regions of degeneration and delivery of lipids to regions of neuritic remodelling; and APOE specifically has been shown to be required to clear axonal degeneration products [264, 265].

Glia are the non-neuronal component of the CNS and make up around 50% of cells in the CNS in a 1:1 ratio with neurones [266]. They are heterogeneous and can be categorised into four broad groups, including microglia and astrocytes. Microglia are the resident immune cells of the CNS and are similar in function and morphology to macrophages

[267]. Among their functions, they protect and support neurons, maintain homeostasis and activate astrocytes. They exhibit a small soma with dynamic processes that monitor the CNS environment for changes [268, 269]. In response to challenges, microglial morphology changes to become “amoeba-like”, with a larger soma and shortened processes [270]. When activated, the expression of Iba-1 is upregulated and they produce inflammatory mediators, which in succession activate astrocytes [271-275]. Astrocytes are also involved in maintaining neuronal homeostasis. In physiological conditions they have a range of functions, including providing trophic support to neurones, regulating energy metabolism in the brain, and regulating neuronal activity through uptake and metabolism of neurotransmitters [276-278]. In response to a challenge, they become reactive, undergoing morphological changes and upregulating the expression of GFAP [279, 280].

4.1.5 Aims of chapter

Previously, in chapter 3, it was demonstrated that APOE-/- mice showed significant hyperactivity and an increased amplitude of circadian rhythms. They also showed a metabolic deficit, with disparities between food intake and body mass.

The aims of this study are to investigate behavioural changes induced by L:L exposure in the APOE-/- model. Additionally this study aims to investigate how the interaction between L:L and the APOE-/- genotype affects the expression of genes involved in energy metabolism and circadian regulation, and the glial cell response in the brain.

It was hypothesised that L:L exposure in the APOE-/- model would further exacerbate abnormalities in behaviour and sleep already present in the model, as well as dampen behavioural rhythms and induce anhedonia. Additionally, it was hypothesised that APOE-/- mice would show a significant glial cell response, as glia are the site of production for APOE in the CNS, and they would show altered lipid homeostasis which is further exacerbated by L:L.

4.2 Experimental Design

Male APOE-/- and C57BL/6J mice aged 23-30 weeks were individually housed in PhenoTyper 4500 home cages (already habituated). All mice received regular chow and water *ad libitum*. The mice were exposed to 3 weeks of L:L, or continued on the normal L:D cycle as controls (n=8-9 per group). The home cage activity of the mice was tracked using EthoVision XT 14 (Noldus, NL) for behavioural assessment. After the three weeks of L:L was complete, the mice underwent the OFT, the LDB and the SPT. Then they were culled between ZT11-13 and tissue was taken for qPCR (left cerebrum and liver), immunohistochemistry (left cerebrum) and metabolomics (plasma, right cerebrum and liver), n=7-9 per group. qPCR, histology and metabolomics were carried out as described in Chapter 2, the metabolomics is discussed in Chapter 5. Figure 4. summarises the experimental design.

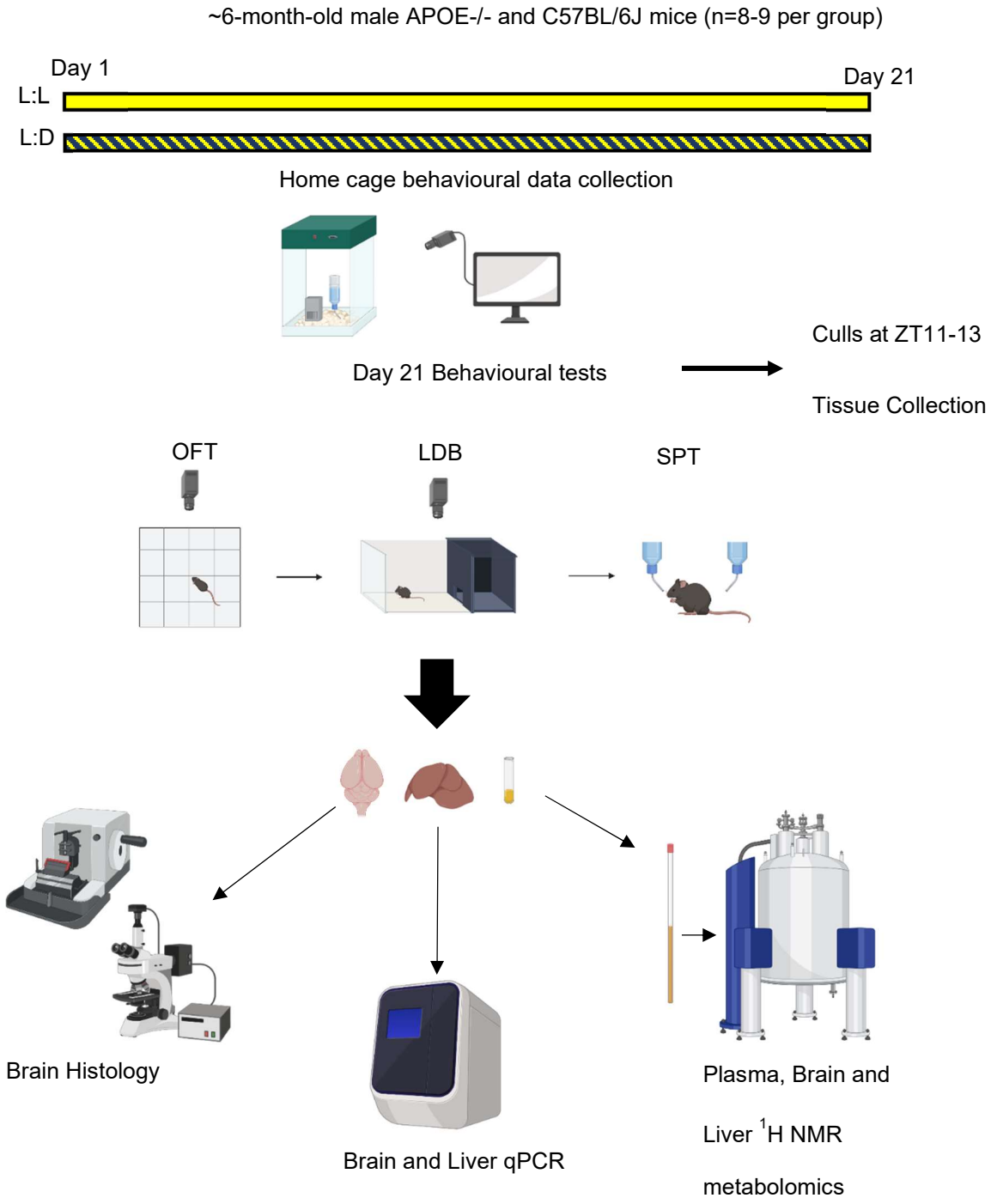


Figure 4.1: Experimental design for Chapters 4 and 5

From here, the C57BL/6J:LD group will be referred to as controls

4.3 Results

4.3.1 Behavioural rhythms in L:L

The rhythmical behaviour of 6-month-old APOE-/- mice was assessed using ClockLab over 3 weeks in L:L conditions (Figure 4.2**Error! Reference source not found.**).

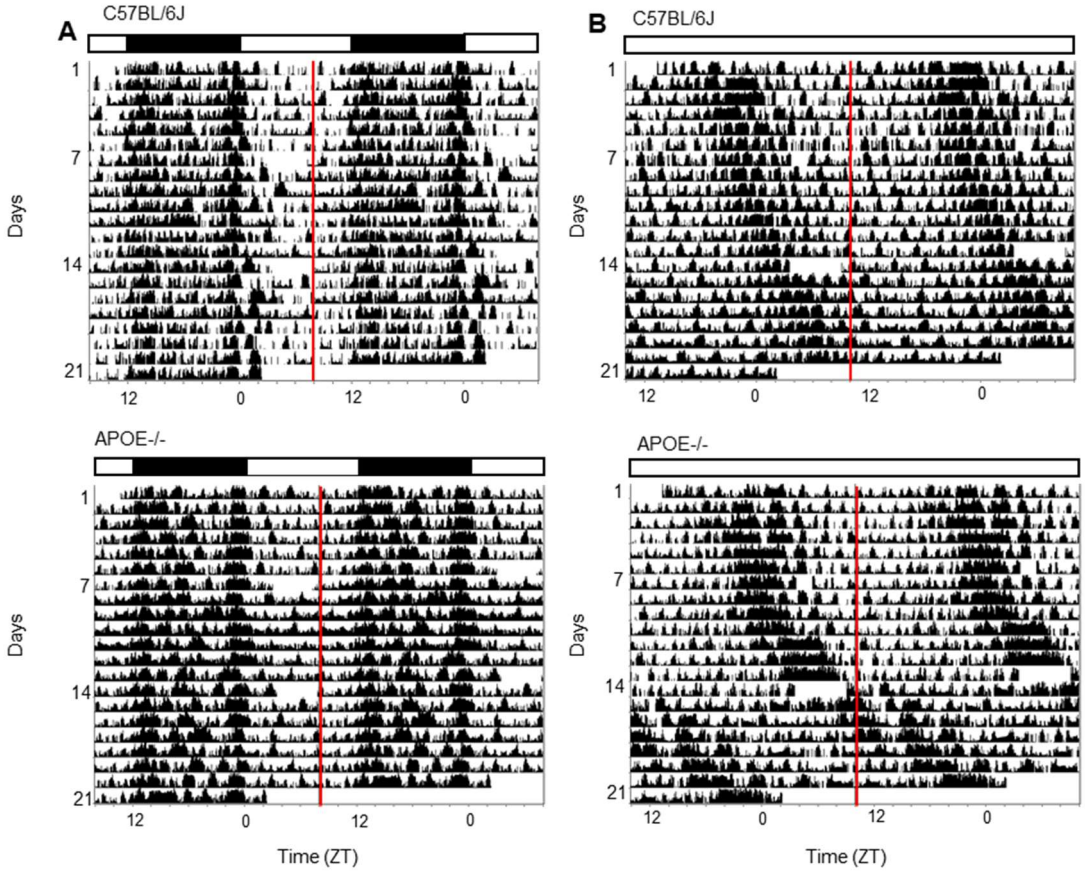


Figure 4.2: Locomotor activity in C57BL/6J and APOE−/− mice, in L:D conditions and L:L conditions.
A) Representative double-plotted actograms of a C57BL/6J mouse (top) and an APOE−/− mouse (bottom) in normal L:D conditions. B) Representative double-plotted actograms of a C57BL/6J mouse (top) and an APOE−/− mouse (bottom) in L:L conditions. Bin size is 5 min. Missing data due to pausing recording to back up data.

The period of the behavioural rhythms was significantly altered by the interaction between L:L and the APOE-/- genotype ($F(1,30)=10.05$, $p=0.0035$), and the APOE-/- genotype significantly increased period length by 4.2% ($F(1,30)=10.87$, $p=0.0025$). L:L also increased period length by 3.4% ($F(1,30)=86.07$, $p<0.0001$; Figure 4.3A). Post hoc testing revealed that the C57BL/6J:LL group and the APOE-/-:LL group had a significantly longer

period than the control group (p=0.0006 and p<0.0001 respectively). Additionally the APOE-/-:LL group had a significantly longer period than the APOE-/-:LD group (p<0.0001).

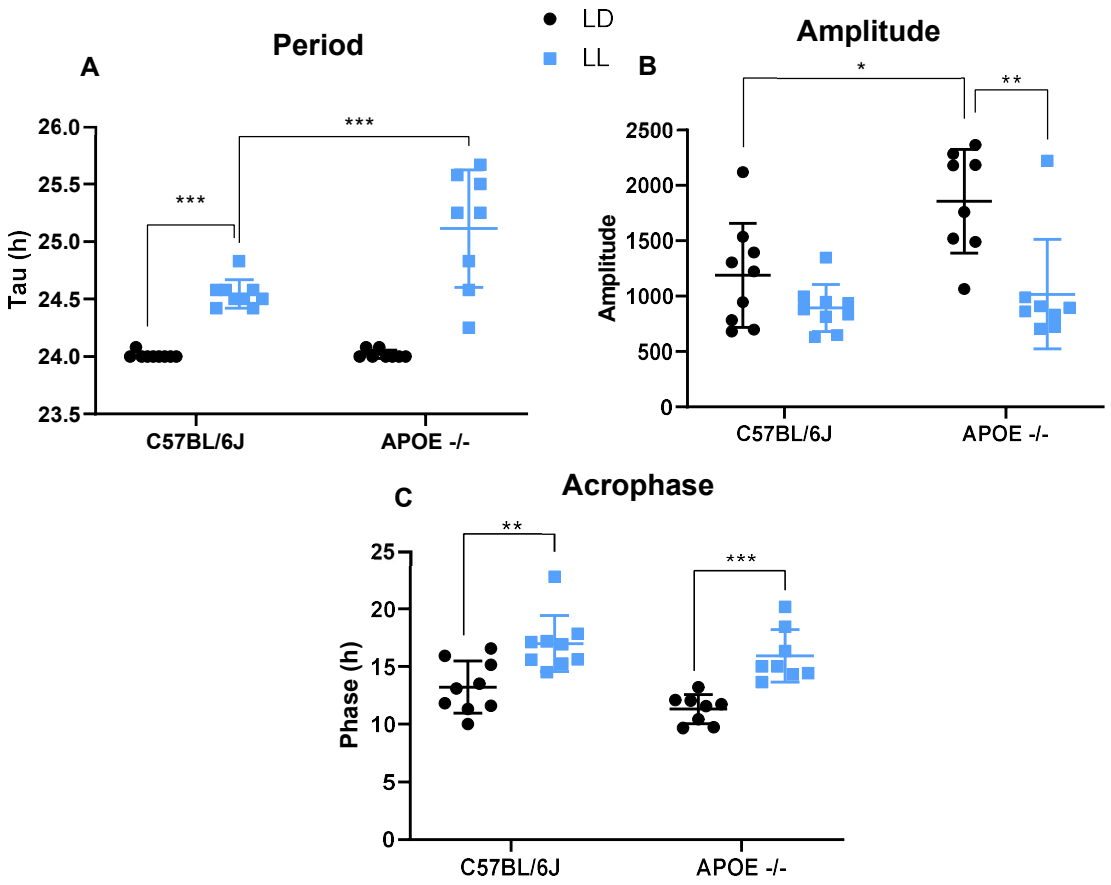


Figure 4.3: Constant light exposure strongly impacts behavioural rhythms and has a stronger impact on APOE-/- period compared to controls.
A) Light, genotype and the interaction between light and genotype have an impact on the period of the behavioural rhythms. **B**) APOE-/- mice have a higher amplitude of behavioural rhythms compared to controls, and light exposure reduces amplitude in both APOE-/- mice and controls. **C**) There is no effect of genotype on the phase of behavioural rhythms, but light increases the phase of rhythms in both APOE-/- mice and controls. 2-way ANOVA; data presented as mean ± SD of 8-9 mice per group. Statistically significant differences between control and APOE-/- mice are shown as *, P ≤ 0.05; **, P ≤ 0.01; ***, and P ≤ 0.001.

The amplitude of the behavioural rhythms was significantly increased by 38% by the APOE-/- genotype (F(1,30)=7.424, p=0.011; Figure 4.3B). L:L exposure significantly decreased amplitude by 37% (F(1,30)=15.12, p=0.0005). Post hoc analysis revealed that the APOE-/-:LD group was significantly higher than all other groups (p=0.014, p=0.0003, p=0.0023 respectively). The acrophase was significantly delayed by 34% by light (F(1,30)=33.07, p<0.0001; Figure 4.3C). Post hoc testing showed that the C57BL/6J:LL

group had a significantly later acrophase than the control group (p=0.0038), and the APOE-/-:LL group had a significantly later acrophase than the than APOE-/-:LD group (p=0.0008). The total number of activity bouts was decreased in the APOE-/- mice compared to the C57BL/6J mice (F(1,30)=4.355, p=0.046; Figure 4.4A). Post hoc analysis showed that the APOE-/-:LD group had fewer activity bouts than the control group (p=0.036). The average length of activity bouts was significantly lengthened by genotype by 53.83% (F(1,30)=13.5, p=0.0009; Figure 4.4B) and was significantly decreased by L:L by 30.51% (F(1,30)=9.72, p=0.004). Post hoc testing showed that the APOE-/-:LD group had significantly longer bouts than the control group (p=0.0034), and that the APOE-/-:LL had significantly shorter bouts compared to APOE-/-:LD (p=0.012).

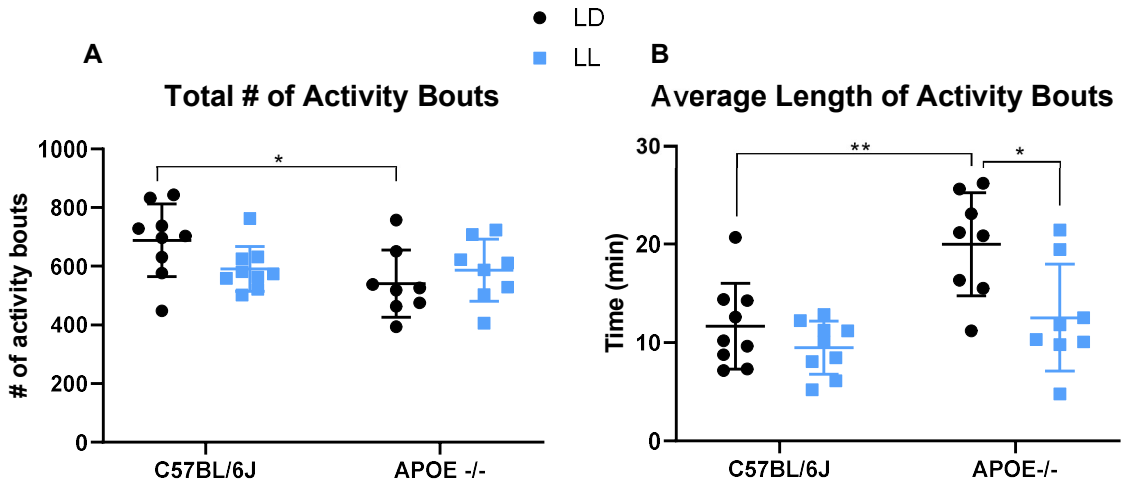


Figure 4.4: APOE-/- mice have fewer activity bouts and longer activity bouts compared to the control group, and constant light exposure reduces the length of activity bouts. **A)** There was a significant effect of genotype on the total number of Activity Bouts**. B)** There was a significant effect of both light and genotype on the average length of Activity Bouts. 2-way ANOVA; data presented as mean ± SD of 8-9 mice per group. Statistically significant differences between control and APOE-/- mice are shown as *, P ≤ 0.05; and **, P ≤ 0.01.

4.3.2 Immobility-defined sleep in L:L

Total immobility-defined sleep across the 3 weeks of the study was significantly increased by L:L by 46.57% (F(1,30)=18.78, p=0.0002; Figure 4.5A). Post hoc testing showed that the C57BL/6J:LL group had a significantly longer total immobility-defined sleep than the control group (p=0.0004). The distribution of immobility-defined sleep between the light phase and the dark phase was significantly affected by the interaction between L:L and

genotype ($F(1,30)=4.637$, $p=0.0394$; Figure 4.5B). Post hoc testing did not reveal any further differences. To be able to prevent time being a confounding variable, and to look at the circadian properties of sleep, immobility-defined sleep was assessed in hourly time points over the three-week study using the method detailed in Chapter 2.3.2 (Figure 4.5C). There was a significant three-way interaction between L:L exposure, genotype and time ($F(495,15264) = 1.589$, $p<0.0001$). There were also significant interactions between

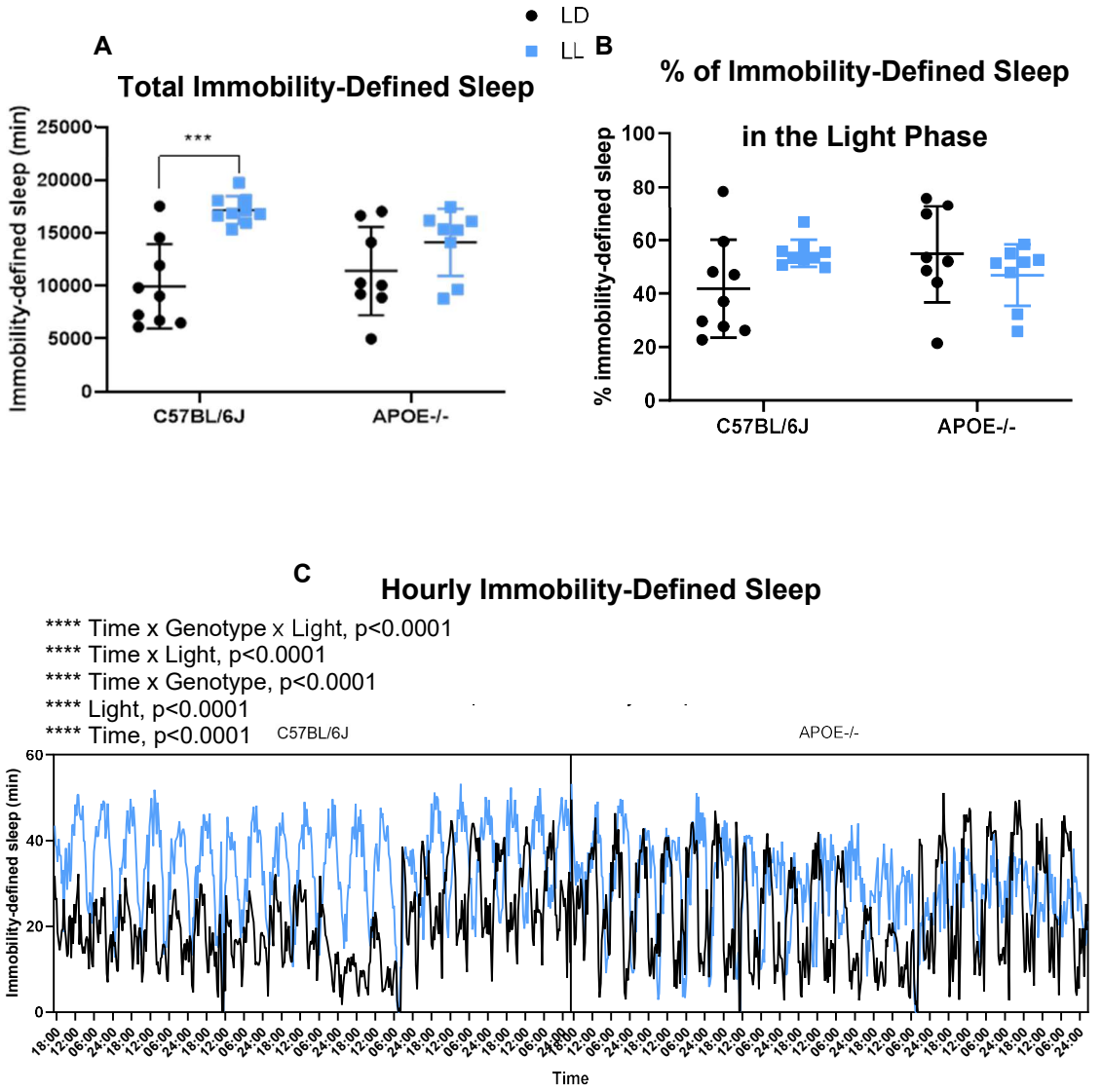


Figure 4.5: Constant light exposure increases total immobility-defined sleep, interacts with genotype to affect sleep distribution in the light phase. There is a significant impact of the interaction of light, genotype and time on hourly immobility-defined sleep.
A) Constant light exposure significantly increases immobility-defined sleep in both APOE-/- and control mice. **B)** There a significant interaction between light and the APOE-/- genotype impacting the percentage of immobility-defined sleep occurring in the light phase. **C)** There is a significant effect of time, light, a significant interaction between time and genotype, a significant interaction between time and light, and a significant interaction between time, genotype and light on hourly immobility-defined 2-way ANOVA; data presented as mean ± SD of 8-9 mice per group. 3-way ANOVA; data presented as mean of n=8-9 mice per group. Statistically significant differences between control and APOE-/- mice are shown as **, P ≤ 0.01; ***, P ≤ 0.001 and ****, P ≤ 0.0001.

L:L and time ($F(495,15264)=7.012$, $p<0.0001$), and genotype and time ($F(495,15264)=2.002$, $p<0.0001$). Additionally, L:L had a significant effect on hourly immobility-defined sleep ($F(1,31)=20.79$, $p<0.0001$), and as expected there was a significant effect of time ($F(19.72,608.0)=7.601$, $p<0.0001$).

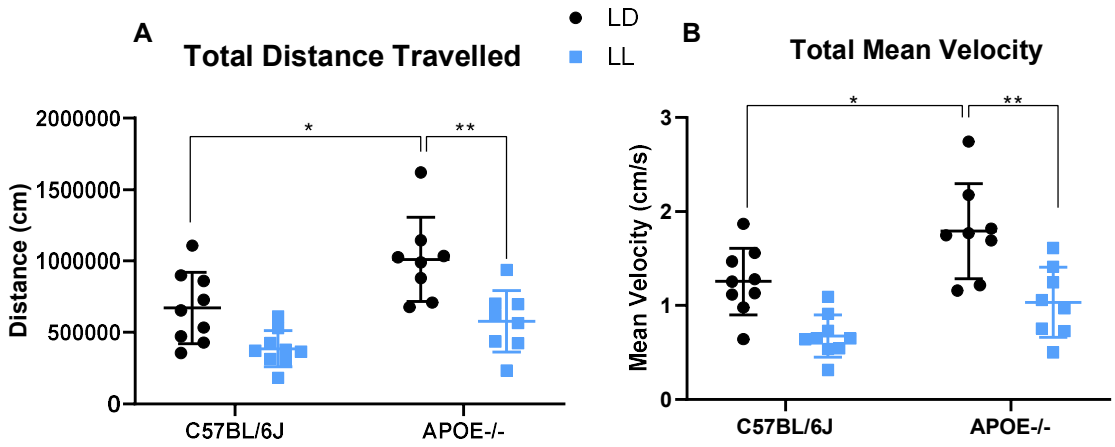


Figure 4.6: APOE-/- mice display increased locomotor behaviour, and constant light exposure reduces locomotor behaviour.
A) APOE-/- mice had a significantly higher total distance travelled, and constant light exposure reduced total distance travelled in both APOE-/- mice and C57BL/6J mice. **B)** APOE-/- mice had a significantly higher total mean velocity, and constant light exposure reduced total mean velocity in both APOE-/- mice and C57BL/6J mice. 2-way ANOVA; data presented as mean ± SD of 8-9 mice per group. Statistically significant differences between control and APOE-/- mice are shown as *, P ≤ 0.05 and **, P ≤ 0.01.

4.3.3 Home cage behaviour in L:L

Home cage behaviour was evaluated to non-invasively measure changes in stereotypical behaviours. The total distance travelled was significantly decreased by 42% with L:L exposure ($F(1,30)=21.03$, $p<0.0001$; Figure 4.6A) and it was significantly increased by 50.14% in the APOE-/- genotype ($F(1,30)=11.45$, $p=0.002$). Post hoc testing showed that the APOE-/-:LD group had a significantly further distance travelled compared to the control and APOE-/-:LL groups ($p=0.023$ and $p=0.0035$). Mean velocity was significantly decreased by L:L by 43.89% ($F(1,30)=27.1$, $p<0.0001$; Figure 4.6B), and significantly increased by genotype by 31.68% ($F(1,30)=12.18$, $p=0.0015$). After post hoc testing, it was found that the APOE-/-:LD group had a significantly higher mean velocity than the control and APOE-/-:L:L groups, ($p=0.030$ and $p=0.0018$), and that the control group was significantly higher than the C57BL/6J:LL group ($p=0.012$).

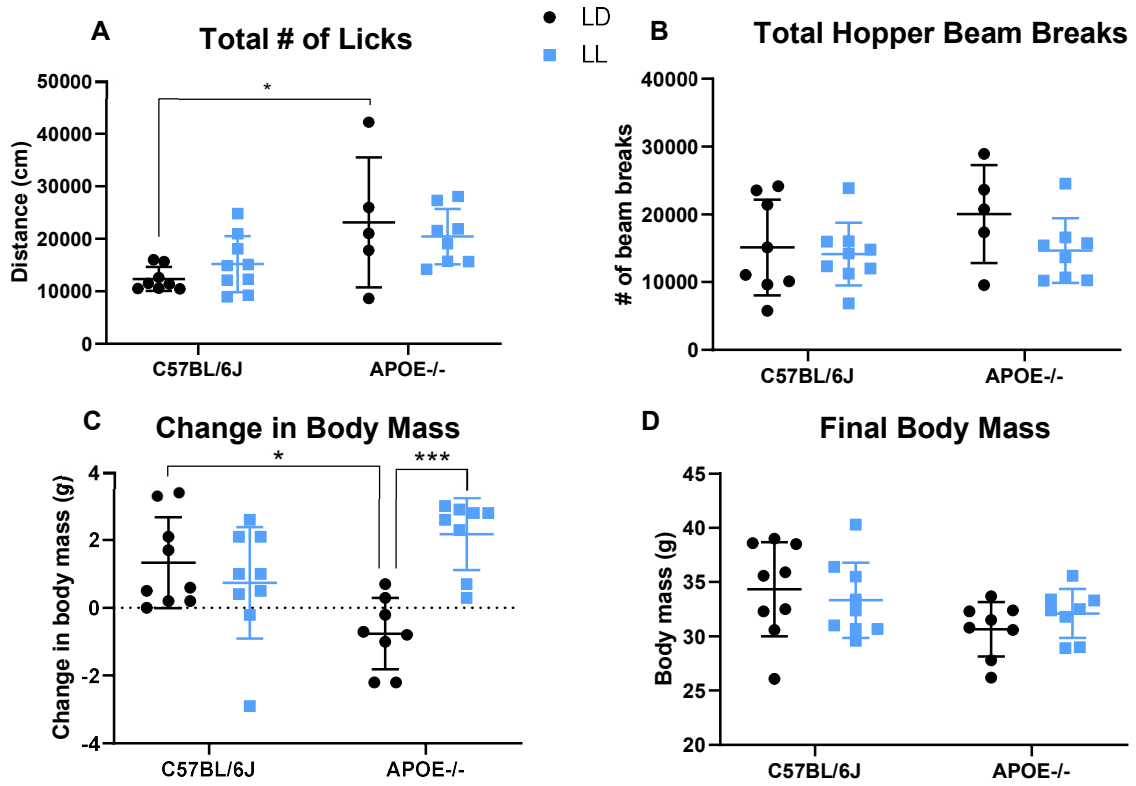


Figure 4.7: APOE-/- mice have differences in appetitive behaviour to the control group and the interaction between constant light exposure and genotype impacts the change in body mass over the experiment.
A) There was a significant effect of genotype on the total number of licks on the water bottles, but there was no significant genotypic effect on **B)** the breaks of the infrared beam across the food hopper. **C)** The interaction between the APOE-/- genotype and light had a significant impact on the change in body mass over the experiment, and light also significantly affected the change in body mass. **D**) APOE-/- mice had a significantly lower final body mass than controls. 2-way ANOVA; data presented as mean ± SD of 8-9 mice per group, and unpaired t-test; data presented as mean ± SD of 15-18 mice per group. Statistically significant differences between control and APOE-/- mice are shown as *, P ≤ 0.05; **, P ≤ 0.01 and ***, P ≤ 0.001.

4.3.4 Appetitive behaviour and body mass in L:L

The total number of licks on the water bottles recorded by the lickometer was significantly increased in the APOE-/- genotype by 36.81% ($F(1,26)=11.13$, $p=0.0026$; Figure 4.7A). Post hoc testing revealed that the APOE-/-:LD group had significantly more licks than the control group ($p=0.0319$). There were no significant differences in the number of food hopper infrared beam breaks (Figure 4.7B). The change in body mass over the three weeks in L:L or L:D was significantly altered by the interaction between L:L and genotype ($F(1,30)=15.38$, $p=0.0005$; Figure 4.7C), and the change in body mass was increased in L:L by 409% ($F(1,30)=6.715$, $p=0.0146$). Post hoc tests showed that the APOE -/-:LD

group had a decrease in body mass compared to control (p=0.013), and the APOE -/-:LL group had an increase in body mass compared to the APOE -/-:LD group (p=0.0006). Final body mass was significantly reduced by 7.24% in the APOE-/- mice (F(1,30)=4.674, p=0.0387 Figure 4.7D).

4.3.5 Behaviour in the OFT in L:L

Behavioural tests were carried out to assess the effect of L:L conditions. In the OFT, the total distance travelled was significantly increased by 57.35% by the APOE-/- genotype (F(1,30)=25.99, p<0.0001; Figure 4.8A). Post hoc testing showed that the APOE-/-:LD group travelled a further distance than the control group (p=0.0006) and the C57BL/6J:LL group (p=0.0005). Additionally, the APOE-/-:LL travelled a further distance compared to the C57BL/6J:LL group (p=0.0492). The mean velocity of the mice showed the same pattern, with genotype significantly increasing the mean velocity of the mice by 57.28% (F(1,30)=25.98, p<0.0001; Figure 4.8B). With post hoc testing it was again found that the APOE-/-:LD group had a higher mean velocity than the control group (p=0.0006) and the C57BL/6J:LL group (p=0.0005), and that the APOE-/-:LL group had a higher mean velocity than the C57BL/6J:LL group (p=0.0492). When investigating thigmotaxis, it was found that L:L exposure increased the duration of time spent around edges of the open field arena by 37.43% (F(1,30)=7.954, p=0.0084; Figure 4.8C). The APOE-/-:LL group was shown to be significantly higher than the control group in post hoc testing (p=0.0392).

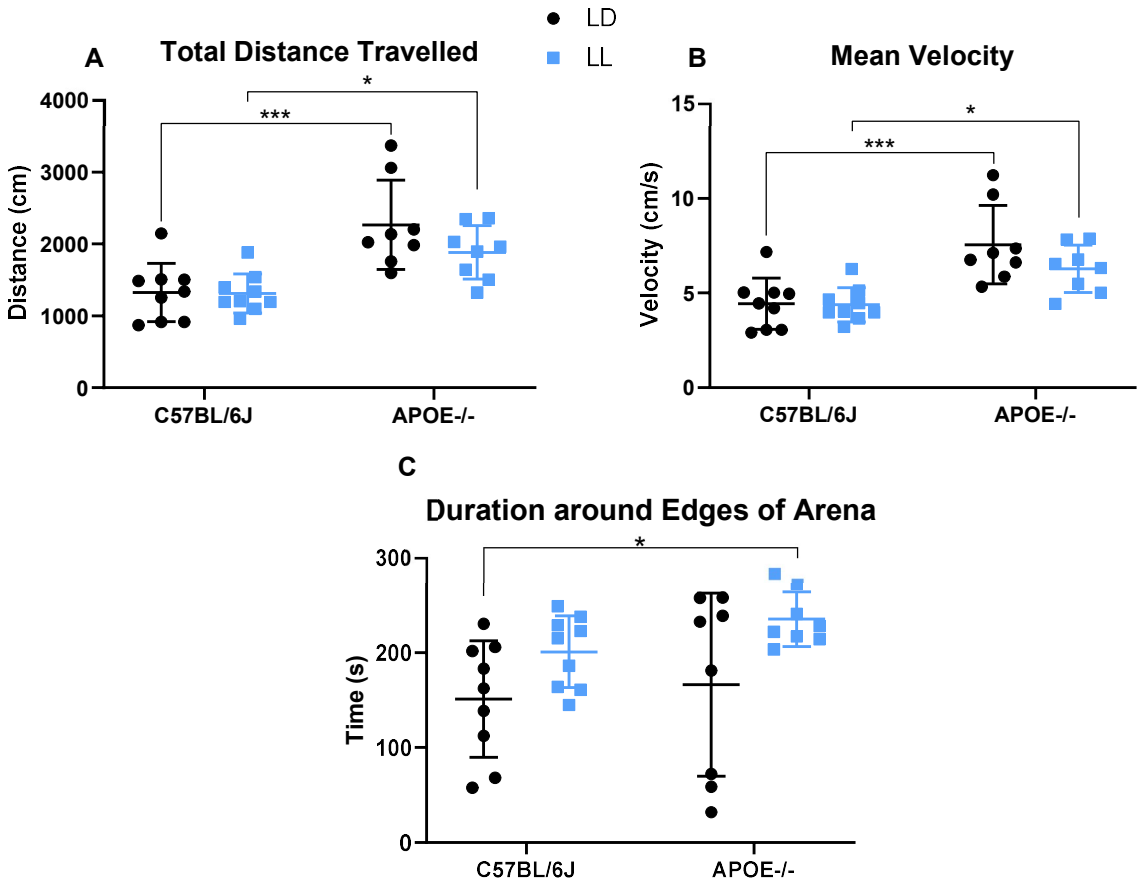


Figure 4.8: APOE-/- mice showed increased locomotor behaviour compared to controls, and constant light exposure increased the time spent around the edges of the arena in the Open Field Test.
A) APOE-/- mice had a higher Total Distance Travelled compared to controls **B)** APOE-/- mice had a higher Total Mean Velocity compared to controls **C)** Constant light exposure significantly increased the cumulative duration spent around the edges of the Open Field Arena compared to controls. 2-way ANOVA; data presented as mean ± SD of 8-9 mice per group. Statistically significant differences between control and APOE-/- mice are shown as *, $p \leq 0.05$ and ***, $p \leq 0.001$.

4.3.6 Behaviour in the LDB in L:L

In the LDB, there was no significant difference in the latency to enter the light zone caused by light or genotype (Figure 4.9A), but the APOE-/- genotype significantly increased the duration in the light zone by 115.74% ($F(1,30)=9.354$, $p=0.0047$; Figure 4.9B). Post hoc testing showed that the APOE-/-:LD group spent significantly longer in the light zone compared to the control group ($p=0.0476$). The APOE-/- genotype also significantly increased the number of visits to the light zone by 122.13% ($F(1,30)=13.04$, $p=0.0011$; Figure 4.9C). Post hoc testing showed that the APOE-/-:LD group made

significantly more visits into the light zone than the control group (p=0.013).

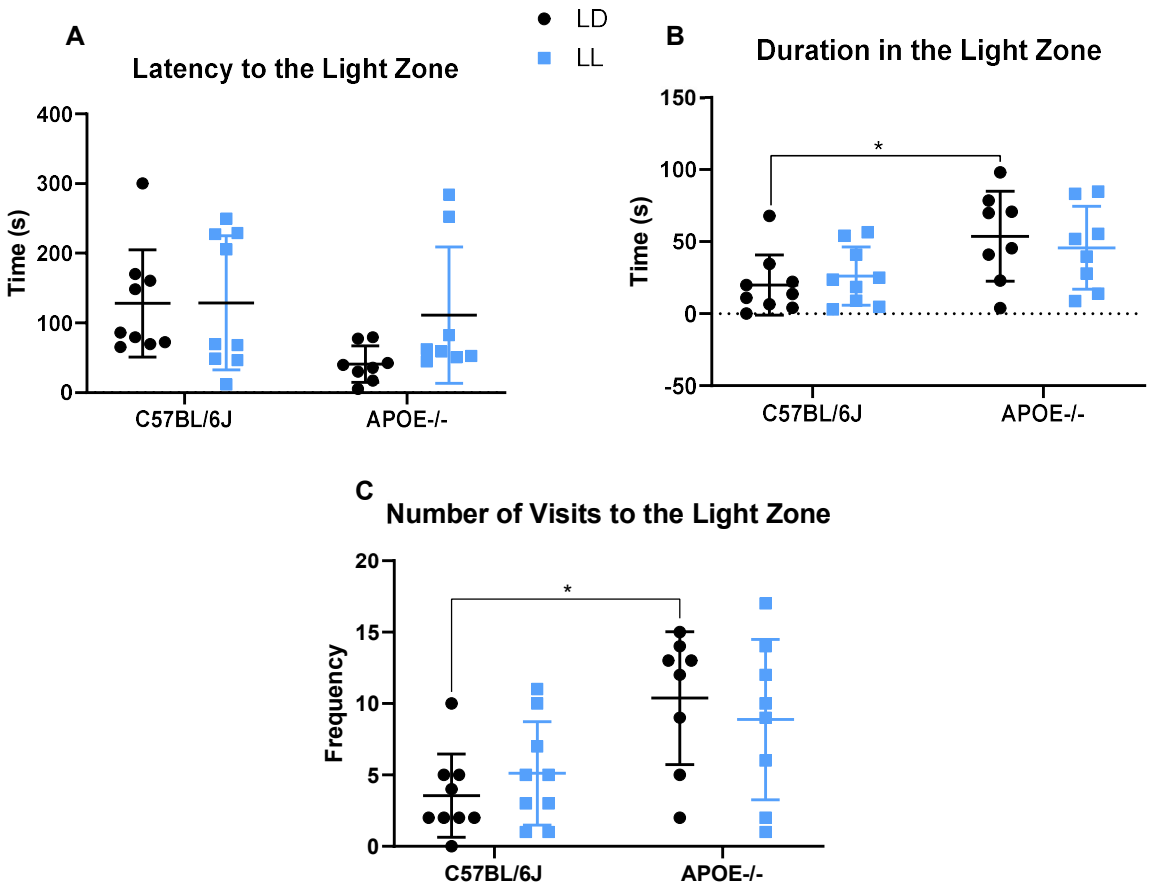


Figure 4.9: APOE-/- mice spend longer in the light zone and visit it more, but constant light exposure has no impact on behaviour in the Light Dark Box. **A)** There were no differences due to genotype or due to constant light exposure in Latency to Light Zone **B)** APOE-/- mice had a significantly higher duration spent in the Light Zone, but light had no impact. **C)** APOE-/- mice had significantly more visits into the light zone, but constant light exposure had no effect. 2-way ANOVA; data presented as mean ± SD of 8-9 mice per group. Statistically significant differences between groups are shown as *, $p \leq 0.05$.

4.3.7 Sucrose preference in L:L

The sucrose preference test (SPT) revealed that sucrose preference was increased by

12.83% by L:L ($F(1,29)=7.746$, $p=0.0094$; Figure 4.10).

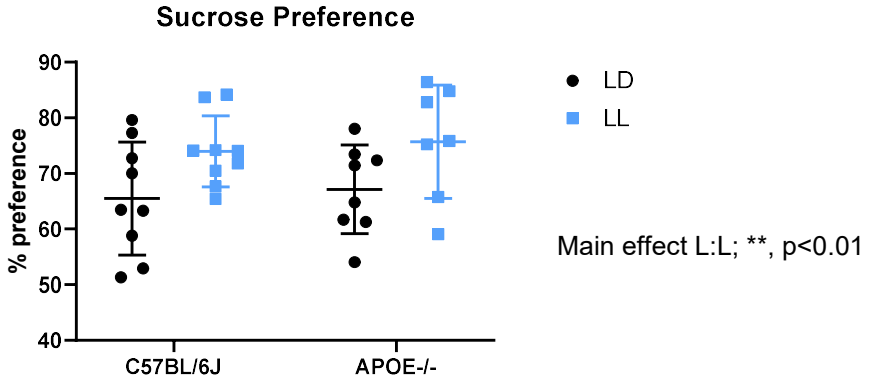


Figure 4.10: L:L increases sucrose preference.
Constant light exposure significantly increases sucrose preference in APOE-/- and control mice. 2-way ANOVA; data presented as mean ± SD of 8-9 mice per group.

4.3.8 The expression of genes involved in energy metabolism and oxidative stress in the brain in L:L

Expression of genes involved in energy metabolism and antioxidant activity were examined in the brain, and genes involved in energy and lipid metabolism, circadian regulation and antioxidant activity were examined in the liver of APOE-/- mice after 21 days in L:L.

In the brain, *Pfkfb3* expression was not significantly altered by L:L or genotype, although genotype did trend towards decreasing expression by 33% ($F(1,17)=3.345$, $p=0.085$; Figure 4.11A). *Slc2a1* expression was also unaltered by L:L or genotype, although again there was a trend towards the APOE-/- genotype decreasing expression by 63.93% ($F(1,17)=4.467$, $p=0.0517$; Figure 4.11B). *Gpx4* expression was not significantly affected by L:L or genotype, although there was a trend towards light decreasing expression by 67.26% ($F(1,15)=3.380$, $p=0.0859$; Figure 4.11C). *Gcl* expression was unaffected by L:L or genotype (Figure 4.11D). Expression of *Fabp7* was unaffected by L:L or genotype, but there was a trend towards the interaction between L:L and genotype having an effect ($F(1,17)$, $p=0.0603$; Figure 4.11E).

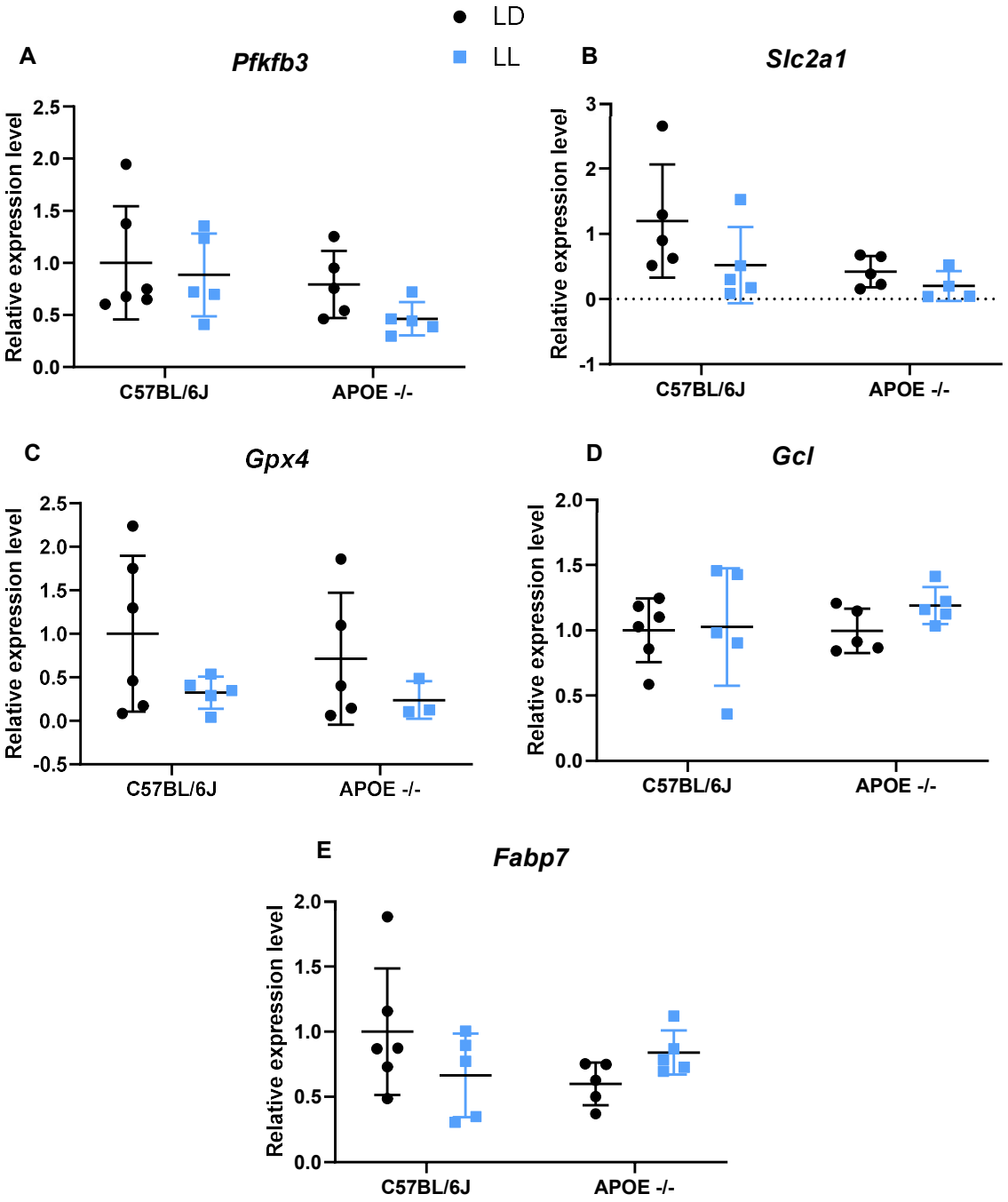


Figure 4.11: Neither genotype nor light have significant effects on gene expression in the brain.
A) *Pfkfb3*, **B)** *Slc2a1*, **C)** *Gpx4*, **D)** *Gcl* and **E)** *Fabp7* expression was unaffected by genotype or constant light exposure. 2-way ANOVA; data presented as mean ± SD of 3-6 mice per group.

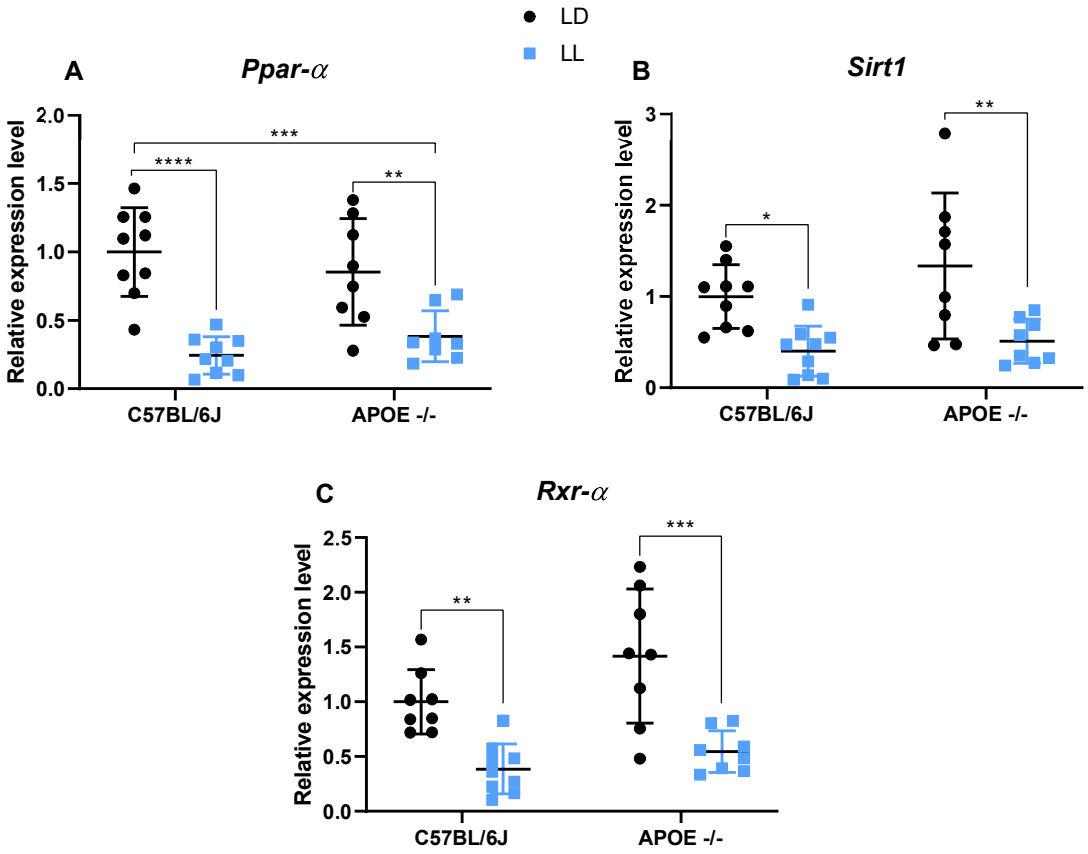


Figure 4.12: The expression of genes involved in energy metabolism in the liver were impacted by L:L and genotype.
A) *Ppar-α* expression was reduced by L:L exposure **B)** *Sirt1* expression reduced by L:L **C)** *Rxr-α* expression was reduced by L:L and increased by genotype. 2-way ANOVA; data presented as mean ± SD of 8-9 mice per group. Statistically significant differences between groups are shown as *, p ≤ 0.05; **, P ≤ 0.01 and ***, P ≤ 0.001.

4.3.9 The expression of hepatic genes involved in FA β-oxidation in L:L

In the liver, *Ppar-α* expression was significantly decreased by L:L by 66% ($F(1,30)=41.92$, $p<0.0001$; Figure 4.12A). Post hoc testing found relevant differences; where the C57BL/6J:LL group had lower expression than the control group ($p<0.0001$), and the APOE-/-:LL group had lower expression than the control group ($p=0.0004$) and the APOE -/-:LD group ($p=0.0096$). *Sirt1* expression was significantly decreased by L:L by 60.88% ($F(1.30)=19.86$, $p=0.0001$; Figure 4.12B). Post hoc testing showed that the C57BL/6J:LL group had significantly reduced *Sirt1* expression compared to the control ($p=0.0485$), as did the APOE -/-:LL group compared to the APOE -/-:LD ($p=0.0068$). Hepatic *Rxr-α* expression was both significantly decreased by L:L by 61.41% ($F(1,30)=33.81$, $p<0.0001$; Figure 4.12C), and significantly increased by genotype by 41.51% ($F(1,30)=5.091$,

p=0.0318). Post hoc testing showed that the C57BL/6J:LL group had significantly lower *Rxr-α* expression than the control group (p=0.009), and that the APOE -/-:LL group had significantly lower expression than the APOE -/-:LD group (p=0.0003).

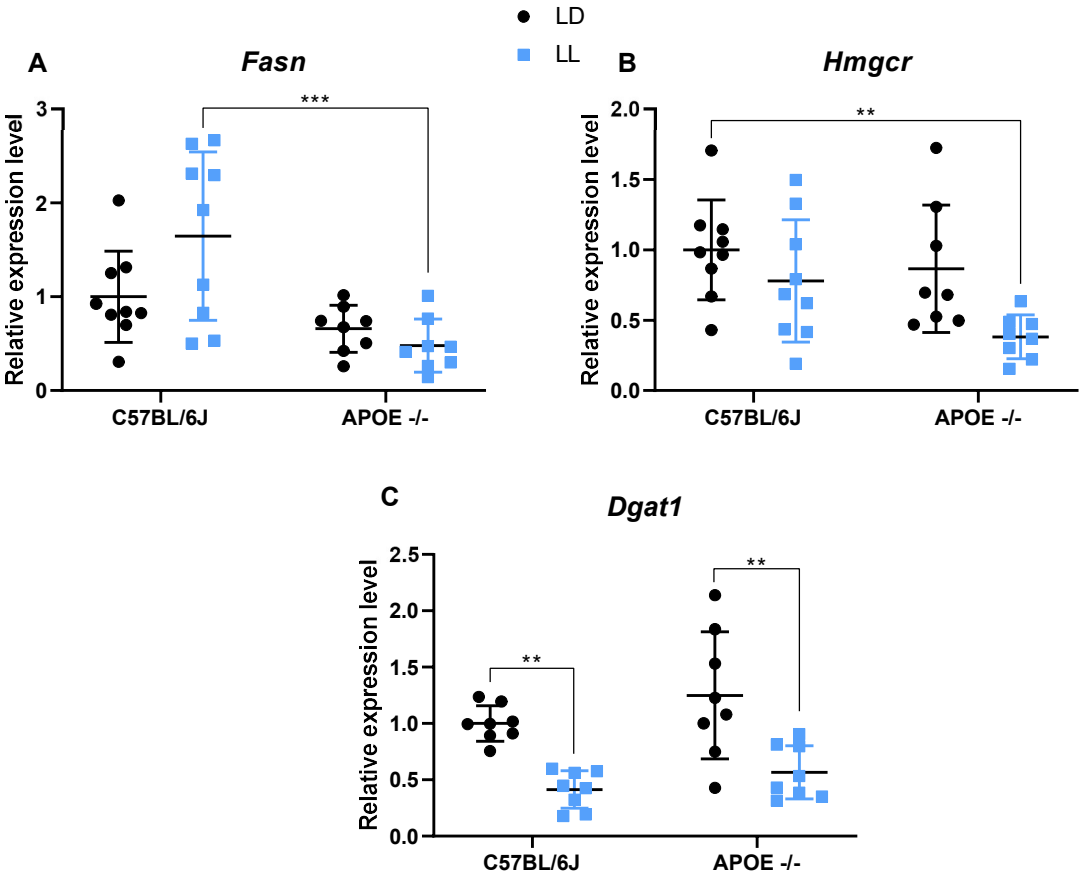


Figure 4.13: The expression of genes involved in lipid metabolism in the liver were impacted by the interaction between L:L and genotype, as well as genotype and light. **A)** *Fasn* expression was impacted by the interaction between L:L and genotype, and reduced by the APOE-/- genotype **B)** *Hmgcr* expression was reduced by both L:L exposure and genotype, **C)** *Dgat1* expression was reduced by L:L. 2-way ANOVA; data presented as mean ± SD of 8-9 mice per group. Statistically significant differences between groups are shown as **, P ≤ 0.01 and ***, P ≤ 0.001.

4.3.10 The expression of hepatic genes involved in lipid metabolism in L:L

The interaction between L:L and genotype had a significant effect on *Fasn* expression (F(1,30)=4.632, p=0.0395; Figure 4.13A), and genotype significantly decreased expression by 56.99% (F(1,30)=15.5, p=0.0005). Post hoc testing showed that the APOE-/-:LL group had significantly reduced expression compared to the C57BL/6J:LL group (p=0.0009). Expression of *Hmgcr* was significantly reduced by 37.796% by L:L (F(1,30)=7.682, p=0.0095; Figure 4.13B), and significantly reduced by 29% by the APOE-

/- genotype (F(1,30)=4.350, p=0.0456). Post hoc testing showed that the APOE -/-:LL group had significantly reduced *Hmgcr* expression compared to the control group (p=0.0090). *Dgat1* expression was decreased by L:L by 56.41% (F(1,30)=30.18, p<0.0001; Figure 4.13C). Post hoc testing revealed that the C57BL/6J:LL group had significantly lower expression than the control group (p=0.0064), and that the APOE -/-:LL group had significantly lower expression than the APOE -/-:LD group (p=0.0014).

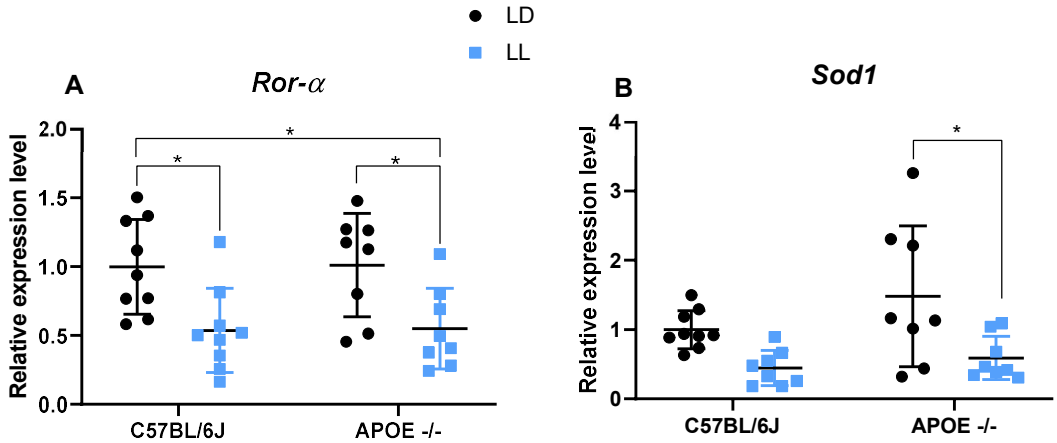


Figure 4.14: The expression of genes involved in energy metabolism, circadian regulation and antioxidant activity in the liver was decreased by L:L.
A) *Ror-α* expression was reduced by L:L. **B)** *Sod1* expression was decreased by light. 2-way ANOVA; data presented as mean ± SD of 8-9 mice per group. Statistically significant differences between groups are shown as *, p ≤ 0.05.

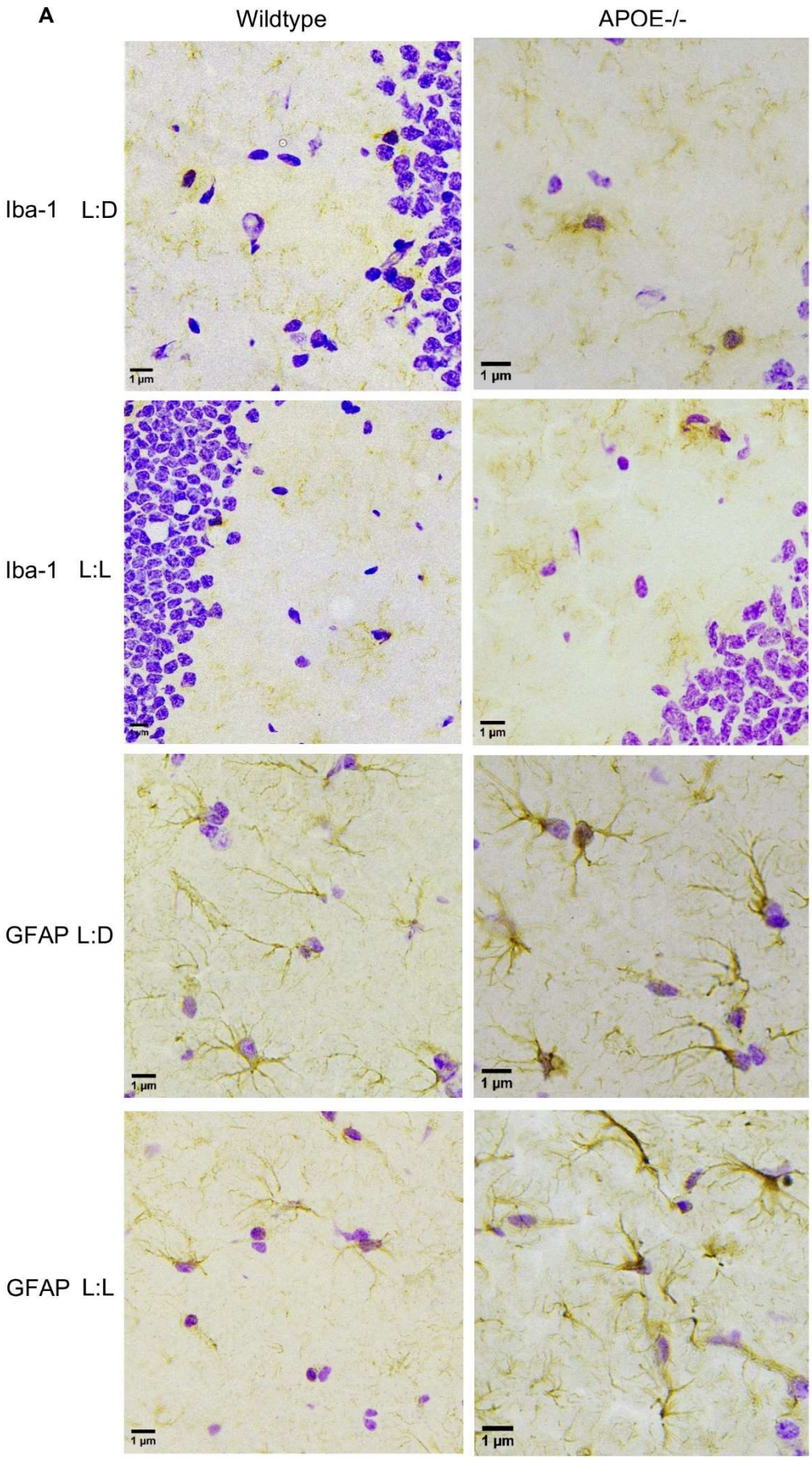
4.3.11 The expression of hepatic genes involved in circadian regulation and antioxidant activity in L:L

A significant decrease in *Ror-α* expression by 45.95% was induced by L:L (F(1,30)=16.54, p=0.0003; Figure 4.14A). It was shown through post hoc testing that the C57BL/6J:LL group had significantly lower expression than the control group (p=0.0282), and that the APOE -/-:LL had significantly lower *Ror-α* expression than the control group (p=0.0416) and the APOE -/-:LD group (p=0.0425). L:L significantly decreased *Sod1* expression by 58% F(1,30)=13.85, p=0.0008; Figure 4.14B). Post hoc testing showed that the APOE -/-:LL group had significantly reduced expression compared to the APOE -/-:LD group (p=0.0169).

4.3.12 The glial cell response in the brain in L:L

To assess glial cell behaviour in APOE-/- mice after 21 days in L:L, activated microglia and astrocytes in the dentate gyrus (DG) of the hippocampus were assessed through immunohistochemistry using the markers Iba-1 and GFAP . Representative images of Iba-1 and GFAP reactivity are shown in Figure 4.15A. The number of Iba-1-positive cells per mm^2 was significantly increased in the APOE-/- mice by 74.03% ($F(1,10)=5.134$, $p=0.047$; Figure 4.15B), however, there was no effect of L:L on the Iba-1-positive cell count ($p=0.77$).

GFAP-positive astrocytes underwent analysis of their branched structures using the skeleton analysis in FIJI (as described in Chapter 2.5.3). The number of branches per astrocyte was significantly affected by the interaction between L:L and the APOE-/- genotype ($F(1,11)=5.239$, $p=0.043$), and also significantly decreased by L:L by 24.74% ($F(1,11)=5.008$, $p=0.047$; Figure 4.15C). There was also a nearly significant effect of genotype, increasing the number of astrocytic processes by 31.15% ($F(1,11)=4.564$, $p=0.056$). Post hoc testing revealed that the APOE-/-:LD group had a significantly higher number of branches compared to the control group ($p=0.0495$) and the APOE-/-:LL group ($p=0.029$). The average length of astrocytic branches was significantly affected by the interaction between L:L and the APOE-/- genotype ($F(1,11)=9.998$, $p=0.009$), and also significantly increased by L:L by 20.71% ($F(1,11)=31.78$, $p=0.0002$; Figure 4.15D). Post hoc testing revealed that the APOE-/-:LD group had significantly shorter branches compared to the control group ($p=0.0094$) and the APOE-/-:LL group ($p=0.0002$).


A
Wildtype
APOE-/-
Iba-1 L:D
Iba-1 L:L
GFAP L:D
GFAP L:L
1 µm

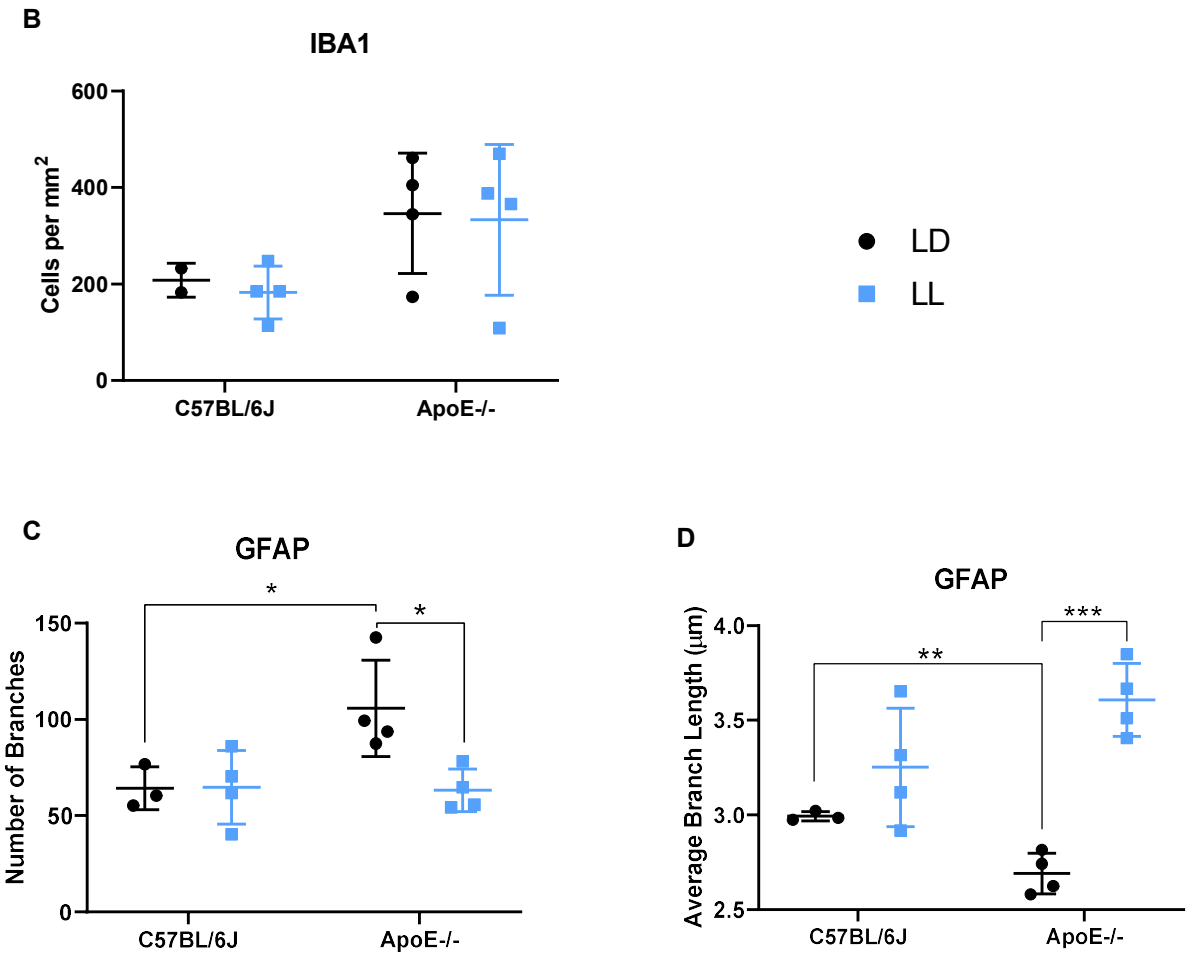


Figure 4.15: The expression of markers involved in neuroinflammation were affected by the interaction between L:L and genotype, as well as genotype and L:L.
A) Representative images of Iba-1 and GFAP staining **B)** The number of Iba-1+ cells was significantly increased in the APOE-/- genotype **C**) The number of astrocytic branches was affected by the interaction between L:L and genotype, and L:L decreased the number of branches. **D)** The average length of astrocytic branches was affected by the interaction between L:L and genotype and increased by L:L. 2-way ANOVA; Iba-1 data presented as mean ± SD of 1-3 sections per animal, n of 2-4 animals per group. GFAP data presented as mean ± SD of 10 astrocytes per section, n of 3 sections per animal, n of 3-4 animals per group. Statistically significant differences between groups are shown as *, $p \leq 0.05$; **, $P \leq 0.01$ and ***, $P \leq 0.001$.

4.4 Discussion

Circadian disruption is a risk factor for cardiovascular disease, but the mechanism is not fully known. To gain insight, APOE-/- mice were exposed to circadian disruption through L:L exposure and investigated changes in behaviour, the glial response in the brain and genes involved in energy metabolism, circadian regulation and oxidative stress. It was found that L:L interacts with APOE-/- to change circadian behaviour, sleep, glial cell behaviour and the expression of a gene involved in lipid synthesis

The period of behavioural circadian rhythms was altered by the interaction between L:L and genotype, and was lengthened by both genotype and L:L. This is the first time the interaction between the APOE-/- genotype and L:L exposure on circadian period has been shown, and it shows a synergistic effect on circadian period. This indicates that the mechanism underlying the timing of behavioural rhythms is a point of gene-environment interaction and it needs further exploration to understand how it could increase the risk of CVD. In Chapter 3.3, APOE-/- mice displayed a lengthened period in D:D, away from the masking of a regular L:D cycle, and so that is consistent with the effect of genotype seen here. Chronic L:L exposure is known to disrupt behavioural rhythms and lengthens circadian period until rhythmicity is lost in mice with food available *ad libitum* [145, 256, 262, 281-283]. This could be through L:L-induced desynchronisation of SCN neurons, which effects subsequent circadian rhythm generation and timing, leading to an altered period [142]. The amplitude of the behavioural rhythms was increased in the APOE-/- mice, as shown in Chapter 3.3, and was decreased in L:L. Decreased amplitude of behavioural rhythms has been shown in mice exposed to L:L [261, 283]. Work by Coomans *et al*., carrying out *in vivo* recordings from the suprachiasmatic nucleus (SCN) of mice which were freely moving, found that L:L decreased the peak firing rate in the SCN whilst increasing the trough firing rate, resulting in a diminished amplitude of the rhythm [262]. It is likely that these changes in SCN firing rate in L:L alter the rhythmical behavioural output, therefore reducing the amplitude of the behavioural rhythms as seen

here. Interestingly, the amplitude in the APOE-/- mice is reduced by L:L to a point where it is not different to the control group. The acrophase, the time at which the mice displayed the most activity, was delayed in L:L. A delay in acrophase of rhythmical expression of multiple genes has been observed in mice exposed to dim light in the evening [284]. This delayed acrophase is because of the lengthened period in L:L, which will push the peak of activity later and later as the number of days spent in L:L increase. The total number of bouts of activity over the 21 days of the study was decreased in APOE-/- mice. This differs to what was seen in Chapter 3.3, where there were no differences due to genotype in normal L:D conditions, and the number of activity bouts was increased in D:D. The average length of the activity bouts was increased by genotype, as seen in L:D in Chapter 3.3.1, and they were decreased by L:L. The increased bout length in APOE-/- mice is likely the reason that they have fewer total bouts of activity. Ketelauri *et al.,* found that mice had a lower total activity in L:L compared to mice in L:D [261]. This is likely associated with the reduced amplitude of the behavioural rhythms induced by L:L.

This is the first time sleep was measured in APOE-/- mice exposed to L:L. Total immobility-defined sleep was increased by L:L, and L:L had a bigger effect within the control mice compared to the APOE-/- group. There only seem to be two studies assessing sleep in L:L. They showed, using electrophysiology, that latency to sleep was shortened and total rapid eye movement (REM) sleep episodes and total amount of sleep were increased by L:L [147, 257]. Additionally, slow wave sleep (SWS) duration and wake duration were reduced by L:L, wake reduction being concurrent with the increased sleep seen here [147]. Immobility-defined sleep, as used in this chapter, is a first pass assessment for assessing sleep differences. It is defined as 40 seconds or more of immobility [171-173]. Therefore, it is difficult to compare immobility-defined sleep results to electrophysiological results looking at REM and non-REM sleep states. Increased total sleep in L:L is likely associated with the reduced amplitude of behavioural rhythms and the decreased activity bout length seen in L:L. Additionally, L:L is likely to reduce sleep

quality, and mice may increase their sleep duration to compensate for this [283]. The proportion of immobility-defined sleep taking place in the subjective “dark” and “light” phases were investigated, and this proportion was significantly altered by the interaction between L:L and genotype. This indicates that the mechanisms controlling the timing of sleep behaviour are a point of gene-environment interaction and could be involved in modulating the risk of CVD. Whilst mice in L:L had no clear indicator of “dark” and “light” phases, prior to being in L:L, they were on a regular L:D cycle, and so their previous L:D cycle was used to assign “dark” and “light” phases. In the C57BL/6J group, L:L increased the amount of immobility-defined sleep in the subjective light phase, but in APOE-/- mice L:L decreased the amount of sleep in the light phase. Lobo et al., found that L:L altered the proportion sleep in the light phase so that there was an increased proportion of REM sleep and a reduced proportion of SWS taking place during the light phase [257]. Again, immobility-defined sleep cannot differentiate between REM and non-REM sleep, but concurs that L:L is alter distribution of sleep, and given that the distribution of immobility-defined sleep is effected by the interaction between L:L and genotype rather than just L:L, further investigation is warranted to follow up on the changes in immobility-defined sleep seen in this chapter. However, this would only be achieved using electrophysiology where an in-depth assessment of sleep architecture can be made. Hourly immobility-defined sleep was significantly increased by L:L, affected by the interaction between L:L and genotype, and affected by the 3-way interaction between time, L:L and genotype. The sleep-wake cycle shows a circadian rhythm, which is evident here in the ~12/12 hour periods of sleep and wake. The interaction between L:L and genotype indicates that L:L leads to a smaller increase in sleep in APOE-/- mice compared to control mice. This may be because APOE-/- mice already had a significantly higher amount of immobility-defined sleep. These results show that sleep is a key process regarding the gene-environment interaction in CVD.

In the home cage environment, assessing total distance travelled and total mean velocity

for spontaneous locomotor activity showed that they were both increased in the APOE-/- genotype, as seen and discussed in Chapter 3, and that they were also both decreased by L:L. In the literature, L:L is reported to reduce general activity [147, 209, 261]. This is likely connected to the increased sleep in L:L, and the reduced activity bout lengths in L:L. Interestingly, L:L exposure in the APOE-/- mice seemed to suppress, or normalise, locomotor activity to be indistinguishable from the control group. This may be an evolutionary instinct, where moving about in the light phase, and therefore light, is associated with increased predation. This seems to be associated with the reduction in amplitude of the behavioural rhythms and the reduced number of activity bouts in APOE-/- mice in L:L.

The amount drunk by the mice was increased in the APOE-/- genotype, and the number of visits to the food hopper was the same regardless of light exposure or genotype, which was seen and discussed in Chapter 3. The APOE-/- genotype showed lower final body mass measurements, which differs from Chapter 3.3. The change in body mass over the 21 days of the study, was impacted by the interaction between L:L and genotype, and L:L exposure led to an increase in body mass, driven by the difference between the APOE groups in L:D and L:L, and by the difference between the control and APOE-/- groups in L:D. This is the first time this interaction has been reported to the best of my knowledge. These differences revealed that L:L increases weight gain only in the APOE-/- mice, and that in L:D, APOE-/- mice lose weight compared to the control C57BL/6J group. This result is partially explained by the difference in activity in APOE-/- mice between L:D and L:L conditions, where APOE-/- mice are hyperactive in L:D but their activity is suppressed to control levels by L:L. There are varying results in the literature for L:L and body mass. Chalfant *et al.,* and Wei *et al.,* found no difference in food intake or body weight in rats and APOE-/- mice in L:L compared to control rats and APOE-/- mice in L:D, similar to what is seen in this chapter [209, 285]. Additionally, Coomans et al., also found that mice in L:L gained more weight than mice in L:D, regardless of diet [262]. However, Yue et al.,

found that L:L rats had a reduced food intake but no difference in body weight compared to L:D rats, whereas Yamamuro et al., found that the food intake of mice was unaffected by L:L, but body weight was increased in L:L [286, 287]. Additionally, Ketelauri et al., found that L:L did not affect weight gain [261]. Here, the change in body mass was affected by the interaction between L:L and genotype rather than just L:L. L:L only seemed to increase weight gain in the APOE-/- mice, indicating a metabolic difference, which is an area to further investigate the connection between circadian disruption and CVD, especially when final body mass was unaffected by L:L.

Both distance travelled and mean velocity in the OFT were increased by the APOE-/- genotype, as seen and discussed in Chapter 3, but were unaffected by L:L. This is unexpected, as L:L has a profound effect on other locomotor measurements. This could be because of a dichotomy between general activity levels and the drive to explore novel environments. Thigmotaxis, where mice avoid the open centre of the arena and stay close to the arena edge and in the corners, was increased by L:L, where previously in Chapter 3.3.8 it was increased in the APOE-/- genotype. However, here the APOE-/-:LD group had a very big data spread for this measurement, which may have affected the results. Increased thigmotaxis is associated with increased anxiety, as mentioned earlier [231]. Previous studies have shown that L:L has no effect on the motor activity of rodents in the OFT, and time in the centre of the arena was found to increase or stay the same in L:L, not decrease, indicating reduced anxiety-like behaviour [146, 255, 288]. It is surprising that results shown here differ.

The LDB did not show any differences due to L:L, and, as seen and discussed in Chapter 3, the APOE-/- genotype increased the duration spent in the light zone and the number of visits to the light zone. As the LDB is a common behavioural assessment of anxiety-like behaviour, and did not show any effect of L:L, the increased thigmotaxis seen in the OFT is unexpected.

Whilst there was an overall preference for sucrose over water in the SPT, sucrose

preference was increased in L:L. Reduced consumption of sucrose is associated with anhedonia and a depressive phenotype, whilst increased sucrose preference is associated with hedonistic behaviour. However the results of the test can be affected by multiple variables [289]. Sucrose consumption and preference follows a circadian rhythm [290]. L:L is a potent circadian disruptor and likely disrupts these rhythms of sucrose intake and preference, which could account for the increased preference in L:L compared to L:D. In a *Clock* mutant model of circadian disruption, sucrose preference is increased compared to controls. Other reward seeking behaviour was also increased, revealing an important role for Clock and an intact circadian system in regulating the dopaminergic system [291]. However, existing literature shows that L:L decreased sucrose consumption or had no effect on sucrose consumption [146, 255]. The results here, taken together with the changes in circadian behaviour, sleep and changes in body mass, indicate that an altered metabolic state is induced by L:L which makes the mice want to consume palatable substances.

In the liver, genes involved in in FA β-oxidation were affected by the APOE-/- genotype and L:L. FA β-oxidation is a metabolic process where energy is generated by breaking down FAs. Ultimately, FAs are metabolised into Acetyl-CoA (acetyl coenzyme-a), which enters the tricyclic acid (TCA) cycle and produces ATP [292]. *Ppar-α*, *Sirt1* and *Rxr-α* expression was reduced by L:L whilst *Rxr-α* expression was also increased in APOE-/- mice. Peroxisome Proliferator-Activated Receptor-α (PPAR-α) is a nuclear hormone receptor which regulates lipid and glucose metabolism and is regulated by the circadian clock [293]. The circadian expression of *Ppar-α* is directly regulated by CLOCK via E-box elements and BMAL1 has been shown to have a reciprocal regulatory relationship with PPAR-α in peripheral clocks [294, 295]. *Ppar-α* expression is activated by SIRT1 in conditions of energy deprivation, promoting uptake, utilization, and catabolism of FAs. SIRT1 activates PPAR-α signalling through deacetylation of its co-activator PGC-1α [296]. When activated, PPAR-α forms a heterodimer with RXR and this heterodimer binds to

PPAR response elements (PPREs) present in promotor regions of PPAR-α-regulated genes, which are involved in FA β-oxidation and FA uptake [296-299].

The results in this chapter indicate that FA β-oxidation is inhibited by L: L. There don't seem to be any studies investigating how L:L affects β-oxidation. However, the effect of L:L on expression of individual genes involved in FA β-oxidation is documented. L:L exposure has been shown to abolish the rhythmical expression of *Ppar-α*, and also decreased the average expression levels [40]. Additionally, L:L has been shown to eradicate rhythmical Sirt1 expression in the liver and adipose tissue, and hypothalamic Sirt1 expression was decreased with L:L [58, 90]. Abnormal lighting conditions have also been shown to delay the phase of the hepatic rhythm of *Rxr-α* expression in APOE-/- mice compared to APOE-/- and C57BL/6J mice in L:D, however a decrease in expression has not been reported in L:L [185]. Inhibition of FA β-oxidation by L:L may be through increased oxidative stress. Light is known to cause oxidative stress, as discussed in Chapter 1.8.2, and exposure to L:L has been shown to induce oxidative stress in the brain of rats [156, 157, 300, 301]. Oxidative stress has been shown to suppress *Rxr-α* expression and the action of the RXR-α protein [302, 303]. Furthermore, the expression of *Sod1* was decreased by L:L. Copper and zinc-dependent superoxide dismutase (SOD1) is an antioxidant enzyme, which catalyses the dismutation of superoxide radicals produced by mitochondria into hydrogen peroxide and oxygen [304, 305]. SOD1 deficiency results in oxidative stress [306].

Interestingly, expression of *Rxr-α* was increased in APOE-/- mice. This is contrary to the literature, where RXR shows an anti-atherogenic effect. Decreased activity of the RXR-liver X receptor (LXR) pathway was strongly associated with late progression of atherosclerosis in APOE-/- mice, and upregulation of RXR activity reduced atherosclerotic lesions and alleviated the progression of atherosclerotic plaques in APOE-/- mice [307-309]. This result is also contrary to Chapter 3.3, where there was no difference in expression between APOE-/- and control mice. This could be a change in expression over

time, as atherosclerosis in this model is reported to worsen over time, *Rxr-α* may be upregulated to try and compensate for the increasing atherosclerotic burden.

Hepatic expression of genes involved in lipid homeostasis was affected by the genotype-L:L interaction, as well as L:L and the APOE-/- genotype. Fatty acid synthase (FASN) is an enzyme involved in de novo lipogenesis (DNL). It uses Acetyl-CoA to initiate a new acyl chain, which is subsequently elongated into long chain FAs by malonyl-CoA [310-312]. In the liver, FAs can be converted to triglycerides (TG) and stored in lipid droplets, packaged into very low-density lipoprotein (VLDL) particles and enter the circulation, used to synthesize complex lipids and can provide energy via β-oxidation [313]. The interaction between L:L and genotype affected the expression of *Fasn*, where L:L increased expression in control mice and slightly decreased expression in APOE-/- mice. Additionally, *Fasn* expression was reduced in the APOE-/- mice.

The interaction between genotype and L:L indicates that *Fasn* expression is a point of gene-environment interaction and could modify CVD risk. This is the first time this interaction has been reported. In the literature, L:L (~3000 lux) abolished the rhythmic expression of *Fasn*, and decreased the average expression, [287]. However, no difference was seen in rhythmical expression of *Fasn* between rats in L:D and rats exposed to artificial light at night (ALAN) [293]. However, the ALAN was a very low lux (2-3.5 lux), and there was a considerable difference in lux between “day” (150 lux) and “night”, which is likely why the rhythm of *Fasn* expression persisted. With regards to the effect of genotype, there are no published studies, as far as I am aware, investigating *Fasn* expression in the APOE-/- model, and so this has been shown for the first time. DNL is likely downregulated in the APOE-/- model due to impaired lipid transport resulting in lipid accumulation. In a human hepatic cell line, application of both native and oxidised LDL reduced *Fasn* expression, likely as negative feedback against lipid accumulation [314]. L:L inhibited genes in FA β-oxidation, the suppression of FA β-oxidation will also result in an accumulation of FAs in cells, which would reduce DNL and so *Fasn*

expression. Therefore, *Fasn* expression is likely reduced in APOE-/- mice due to negative feedback from increased cellular FA content, and L:L in the APOE-/- model increases cellular FA content through suppression of FA β-oxidation, leading to a further reduction in *Fasn* expression.

Hmgcr codes for HMG-CoA reductase, the enzyme that catalyses the rate-limiting step in cholesterol biosynthesis [315]. Both L:L and genotype reduced the expression of *Hmgcr*. L:L has been shown to eliminate the rhythmical expression of *Hmgcr* and also reduce the average expression [287]. However, previous studies show that the expression of *Hmgcr* and protein levels of HMGCR is unchanged in APOE-/- mice, which is not seen here [316, 317]. APOE-/- mice exhibit hypercholesterolaemia, and high levels of cholesterol inhibit the transcription of the *Hmgcr* gene, and trigger HMGCR degradation [74, 318, 319]. Here, it is likely that the expression of *Hmgcr* is inhibited as a mechanism to compensate for the accumulation of cholesterol seen in the APOE-/- model due to impaired cholesterol transport.

Diacylglycerol O-acyltransferase 1 (*Dgat1*) encodes an ER membrane-bound metabolic enzyme which is a catalyst in the conversion of diacylglycerol and fatty acyl CoA to triacylglycerols, more commonly referred to as triglycerides (TGs) [320]. It regulates the supply of FA to mitochondria, and also has a regulatory role in the expression of *Ppar* genes [321, 322]. L:L reduced the expression of *Dgat1*. L:L has previously been shown to significantly decrease the average expression of *Dgat1* and abolish its rhythm of expression, as well as suppress the rhythm of hepatic levels of TGs [287]. The suppression of *Dgat1* expression may be linked to the suppression of *Ppar-α* expression. It may also be due to a loss of rhythmicity of the mice, as seen with increased behavioural period and suppressed amplitude, where feeding rhythms and therefore the dietary supply of TGs may be altered. The suppression of *Dgat1* expression may contribute to the change in *Fasn* expression, due to its regulation of FAs.

Receptor-related orphan receptor alpha (ROR-α) is a transcription factor and is a member

of the nuclear hormone receptor superfamily. It has roles in regulating metabolism, circadian rhythms, neural function, immune function and cellular differentiation [323, 324]. L:L has previously been shown to decrease the amplitude of rhythm of *Ror-α* expression [287]. ROR is involved in the molecular core clock loop as a positive regulator of *Bmal1*. Light interacts with the core clock loop by inducing the expression of the *Period* genes [325]. Therefore L:L likely disrupts the negative feedback by consistently increasing *Period* expression, leading to aberrant cellular rhythm generation, and altered *ROR-α* expression.

Sod1 levels were decreased by L:L, as briefly mentioned above. ALAN was shown to decrease SOD activity in the brain [326]. This is most likely in association with L:L-induced oxidative stress. Decreased FA β-oxidation and inhibition of DGAT1 protein activity are associated with oxidative stress, and an accumulation of FAs in mitochondria, as both gene products regulate cellular FA levels, resulting in significant levels of reactive oxygen species (ROS) [321, 327, 328].

In the brain, a non-significant trend towards downregulation of genes involved in glucose metabolism was observed in the APOE-/- mice. 6-phosphofructo-2-kinase/fructose-2,6-bisphosphate 3 (*Pfkfb3*) is expressed highly in astrocytes, and produces fructose-2,6-bisphosphate, which is an enzyme involved in a rate limiting step in glycolysis [329, 330]. Solute carrier family 2 (facilitated glucose transporter), member 1 (*Slc2a1*) produces protein Glucose transporter protein type 1 (GLUT1). It is key for brain glucose homeostasis, as it is the principal glucose transporter in the brain and transports glucose across the BBB [331, 332]. It is expressed in endothelial cells, neurones and less in glial cells [331]. Given that there were no significant changes in expression level, it is unlikely that glucose metabolism in the brain is affected at the level of transcription.

There was a trend towards downregulation of a gene coding for an antioxidant enzyme in L:L. Glutathione peroxidase 4 (*Gpx4*) codes for an antioxidant enzyme which uses reduced glutathione as a cofactor to reduce peroxides to their corresponding alcohols,

limiting free radical production and protecting cells against oxidative stress [333, 334]. GPX4 acts in cell membranes to prevent lipid peroxidation, and so is essential to maintain cellular lipid homeostasis [333, 334]. However, the expression of glutamate–cysteine ligase (GCL) - an enzyme which catalyses the first step of glutathione synthesis, the formation of γ-glutamylcysteine from glutamate and cysteine in an ATP-dependent reaction – was unchanged [335]. The lack of significant changes indicates that transcription associated with glutathione-related genes is not affected by L:L or genotype.

There was a trend towards an interaction between the APOE-/- genotype and L:L on the expression of a gene involved in FA transport. Fatty acid binding protein 7 (FABP7), also known as brain-type FABP or brain lipid binding protein, is a protein involved in FA uptake and transport and thought to play roles in cell growth and differentiation and behavioural processes [336-338]. Again, the lack of significant changes indicates that transcription levels were unaffected by L:L and genotype.

Changes to glial cells in the brain were assessed using immunohistochemistry, which showed that the APOE-/- genotype leads to an increase in activated microglia. Additionally, the interaction between the APOE-/- genotype and L:L led to an increased number of visible astrocytic processes in the APOE-/- mice in L:D as well as a shorter length of visible processes, but not in the APOE-/- mice in L:L. L:L decreased the number and increased the length of visible astrocytic branches.

Previous studies have shown an increase in activated microglia in the brains of APOE-/- mice using CD-68 as a marker [222]. Additionally, Iba-1+ cells are significantly higher in APOE-/- deficient mice after an immune challenge [339]. It has been proposed that APOE has an anti-inflammatory effect, cultured cells lacking APOE, and APOE-/- mice show a significant inflammatory response compared to controls when presented with immune challenges [340-342]. It is thought that this anti-inflammatory effect is mediated, at least partially, through inhibition of c-Jun N-terminal kinase (JNK). Application of an APOE

mimetic peptide to cultured microglial cells attenuated the inflammatory response to LPS by inhibition of JNK through binding to low-density lipoprotein receptor-related protein 1 (LRP1), and APOE-/- mice show increased activation of JNK and increased expression of downstream inflammatory cytokines of JNK in microglia [339, 343, 344].

In this chapter, the morphology of reactive GFAP+ astrocytes was assessed, rather than the amount of reactive astrocytes. When reactive, astrocyte processes become thicker, which makes it easier to see further along the length of the processes, making them appear longer [280]. They also have more main processes extending from the soma [280]. There seems to be a disconnect between the length and number of astrocytic processes seen in this chapter. This is likely due to all visible branches being included in the data, rather than just the primary processes. APOE-/-:LD mice showed a shorter average process length. APOE-/- mice show no difference in astrocyte reactivity in normal conditions, although there are indications that astrocyte reactivity increases with age [342, 345, 346]. However, when presented with an immune challenge, APOE-/- mice had a significantly elevated level of GFAP+ astrocytes in the hippocampus [342, 345]. So in this instance, L:L may be acting as a challenge and significantly increases astrocyte process length in APOE-/- mice. Previous studies on the effect of L:L on astrocyte reactivity show that rats and mice exposed to L:L had an increased number of GFAP+ cells in the hippocampus; including the DG, the retina and the intergeniculate leaflet (IGL), but had a reduction in the SCN, indicating region specific changes [347-349]. Rats exposed to L:L had a significant increase in the level of GFAP protein in the hippocampus, and also had a significant increase in levels of a lipid peroxidation product, indicating the presence of oxidative stress [350]. L:L seems to give the astrocytes a “more reactive” morphology, likely through oxidative stress.

4.4.1 Conclusions

It has been shown for the first time that the interaction between L:L and the APOE-/- genotype significantly lengthened the period of behavioural rhythms, altered sleep

distribution, increased body mass, decreased *Fasn* expression, and altered the length and number of astrocytic branches in reactive astrocytes. L:L exposure induced an altered metabolic state, through suppression of FA β-oxidation, and the suppression of cholesterol and TG synthesis. Additionally L:L altered circadian behaviour, sleep, home cage activity, thigmotaxis/anxiety-like behaviour in the OFT and sucrose preference; as well as the expression of genes involved in lipid metabolism and homeostasis, redox balance and circadian regulation, and astrocyte morphology. Furthermore, the APOE-/- genotype altered final body mass, the expression of genes involved in FA β-oxidation and lipid homeostasis and increased microglial activation. These effects are likely mediated through lipid accumulation and oxidative stress, as well as the loss of the anti-inflammatory actions of APOE. Lipid accumulation indicates an imbalance between FA usage and supply, which points to metabolic dysregulation. Downregulation of genes involved in FA β-oxidation means that there will be more ATP demand on glucose metabolic pathways. These alterations in energy metabolism likely underlie the behavioural changes seen in activity, sleep and hedonistic behaviour.

5 Effect of the APOE-/- genotype and 3 weeks of constant light exposure on the metabolome

5.1 Introduction

Previous chapters revealed that APOE-/- mice possibly have a metabolic deficit, as they are hyperactive, display increased food intake without an increase in body mass, and display alterations in the rhythmic expression of genes involved in circadian rhythm generation and energy metabolism. Exposing APOE-/- mice to an environmental stressor in the form of L:L led to profound changes in behavioural rhythms, sleep, glial cell morphology and changes in expression of genes involved in lipid metabolism. However, the downstream effects and underlying pathways have not been confirmed.

^{1}H NMR Metabolomics is proving to be a powerful tool in the characterisation and diagnosis of diseases, identifying biomarkers and providing a cheaper and less invasive method for clinical investigations [351-353]. Using an untargeted approach, it provides a metabolic fingerprint for any given sample and can identify key metabolites that are involved in disease, or that are induced by experimental conditions. Linking these metabolites to metabolic pathways can provide mechanistic insights and can reveal new areas of investigation for disease prevention and treatment.

5.1.1 Atherosclerosis and the metabolome

Atherosclerosis has been shown to alter the peripheral metabolome. In humans, alterations in carbohydrate, cholesterol and amino acid metabolism, oxidative stress and inflammatory pathways are associated with atherosclerosis [354, 355]. Similar changes are seen in animal models of atherosclerosis, including the APOE-/- model [356, 357]. Although these changes in peripheral metabolites are relatively well characterised in atherosclerosis and atherosclerosis models, there are no studies to date, which have explored the changes in the brain metabolome in association with atherosclerosis, including in the APOE-/- model. Changes in the brain metabolome may shed insight into

the mechanisms underlying the behavioural changes in the APOE-/- mice reported in this thesis.

5.1.2 L:L and the metabolome

There are several studies investigating the effect of circadian and sleep disruption on the metabolome. They highlight changes in several metabolic pathways including glutathione, carbohydrate, amino acid, and lipid metabolism [358-362]. However, these studies were done using liquid chromatography-mass spectrometry (LC-MS). LC-MS differs from NMR in that it is significantly more sensitive, but NMR is significantly more reproducible, and is quicker and cheaper, making it the choice for diagnostic research [363]. Only one study exists that investigates the effect of constant light on the metabolome [364]. Kim et al., assessed the effect of 12 weeks of L:L on the plasma metabolome of male C57BL/6J mice using gas chromatography mass spectrometry (GC-MS) [364]. They showed decreases in pyruvate and erythritol, and increases in glycolic acid and ribitol, indicating alterations in carbohydrate metabolism [364]. However, they did not assign most plasma metabolites and used $p<0.1$ as their significance threshold, and so this study is not a reliable characterisation of the plasma metabolome in L:L. The effect of L:L on the mammalian brain and liver metabolome has not been characterised at all. However, the downstream metabolic effects of L:L have been well documented, and comprise of reduced insulin sensitivity, oxidative damage and changes of markers involved in glucose and lipid metabolism [144, 262, 287, 288]. This suggests that L:L exposure will have a significant downstream effect on the liver and brain metabolome.

5.1.3 Aims of Chapter

Metabolomics provides downstream information that is the sum of the gene-environment interaction between L:L and the APOE-/- knockout model, and can provide information on biomarkers and physiological mechanisms that underlie the changes in behaviour.

The aim of this chapter is to perform a multi-organ metabolomic analysis, using plasma, brain and liver tissue from APOE-/- mice and wildtypes exposed to L:L and controls in L:D using ^{1}H NMR to investigate the gene-environment interaction between APOE-/- and L:L.

The APOE-/- model has altered lipid transport in the CNS and the periphery due to the role of APOE as a transport medium, and so it was expected that there would be changes in lipid and energy metabolism across the three tissues. L:L has been shown to induce oxidative stress and dysregulate glucose and lipid metabolism, as mentioned above, and so it was expected that changes in these pathways would be seen across tissues.
It was expected that the interaction between L:L and the APOE-/- genotype would be reflected in changes in glucose metabolism in the brain, due to changes in astrocyte morphology as astrocytes are site of glucose metabolism [277], and in changes in lipid metabolism in the brain, plasma, and liver due to previous changes in behaviour and hepatic *Fasn* expression. It was also hypothesised that changes in lipid transport would be correlated with behavioural changes, as APOE is required for functional cholesterol transport in the CNS.

5.2 Results

The experimental design for this chapter can be seen in Chapter 4.2. The metabolite composition of plasma, brain and liver samples from APOE-/- and wildtype mice exposed to L:L were assessed using ^{1}H NMR metabolomics. PCA scores plots revealed a clear separation between genotypes in the plasma (Figure 5.1). To further investigate the differences in the metabolome, OPLS-DA was performed, but as it was limited to two groups and had the same top VIPs as PLS-DA, PLS-DA was used to investigate the differences due to genotype, L:L and their interaction (**Error! Reference source not found.**). The key metabolites driving the differences were identified by variable importance in projection (VIP) scores.

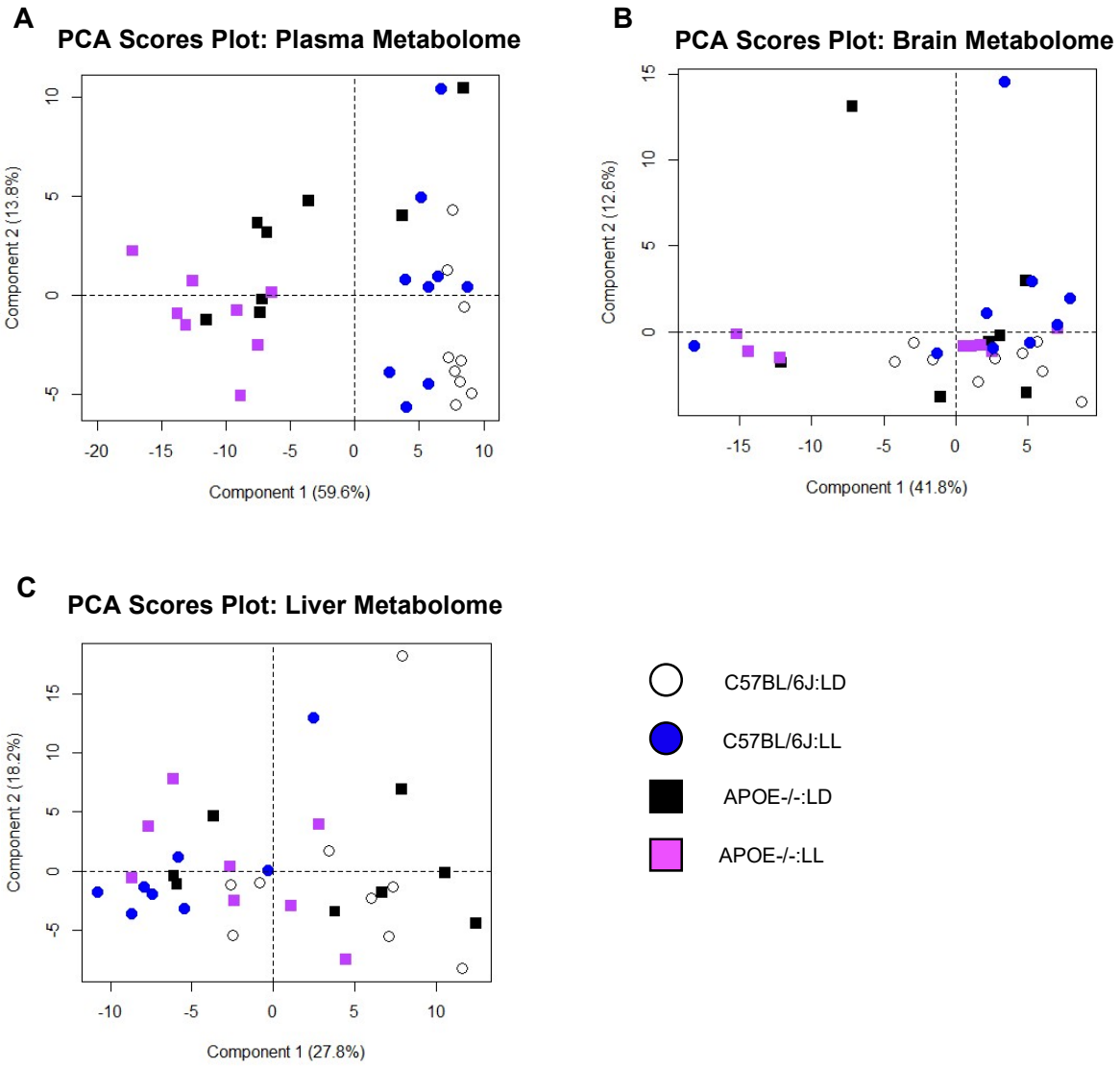


Figure 5.1: Principal component analysis (PCA) of the effect of the APOE-/- genotype and L:L exposure on the plasma, brain and liver metabolomes.
A) PCA scores plot of the plasma metabolome, principal component 1 vs principal component 2, n=8-9 per group. **B)** PCA scores plot of the brain metabolome, principal component 1 vs principal component 2, n=7-9 per group. **C)** PCA scores plot of the liver metabolome, principal component 1 vs principal component 2, n=7-9 per group.

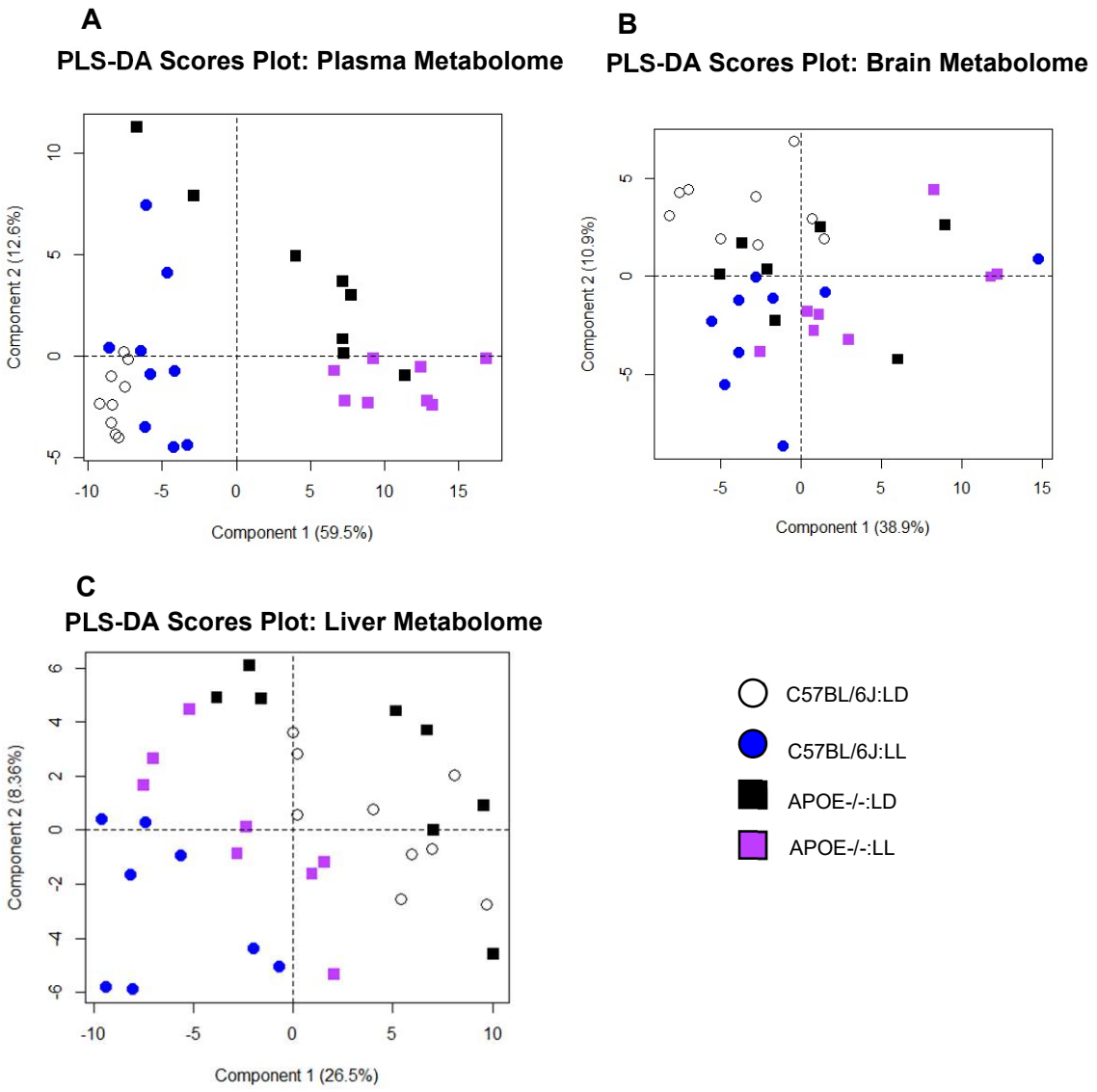
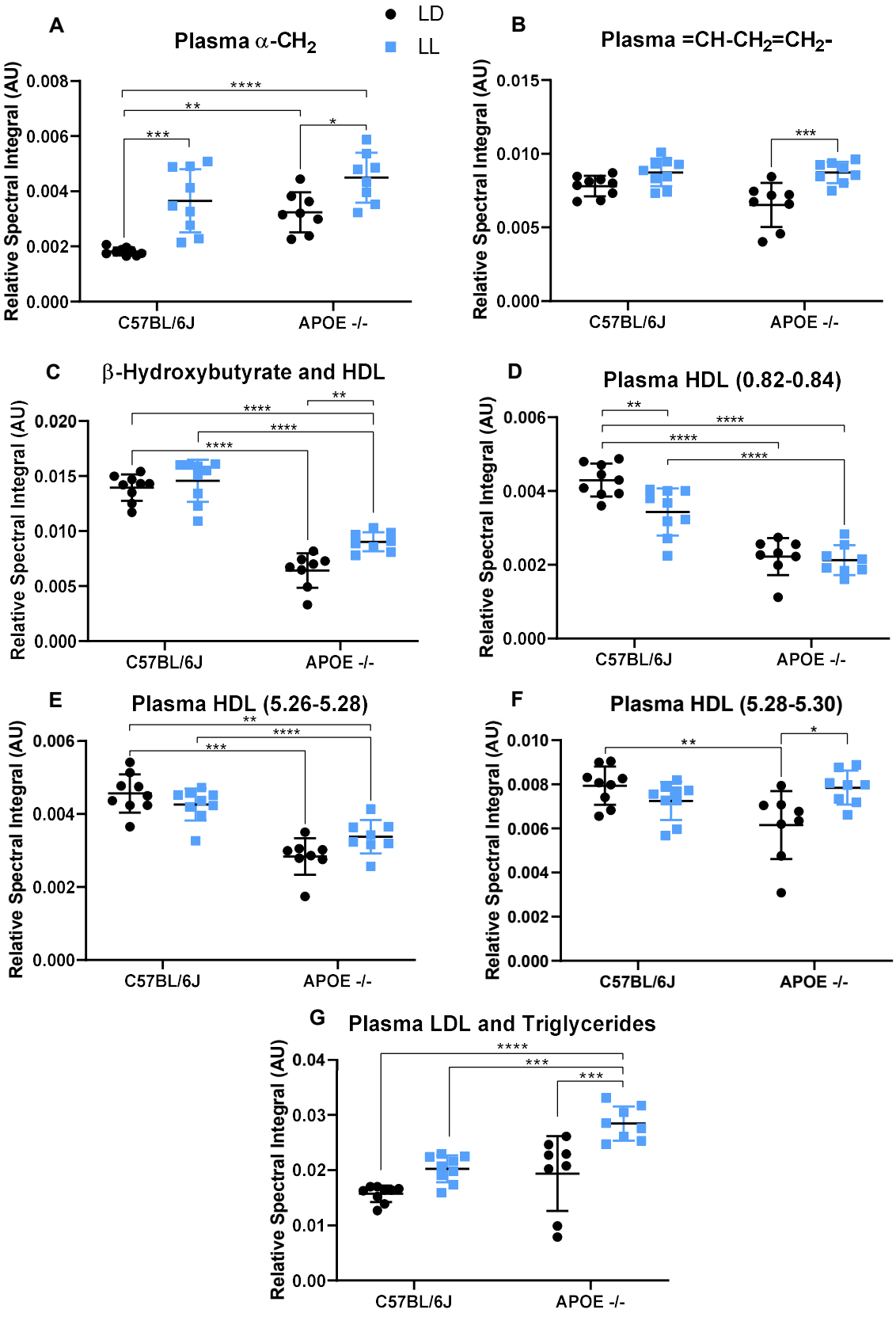


Figure 5.2: PLS-DA scores plot of the effect of the APOE-/- genotype and L:L exposure on the plasma, brain and liver metabolomes.
A) The plasma metabolome, cumulative R^2X=0.819, cumulative R^2Y=0.696, and cumulative Q^2=0.501, n=8-9 per group. **B)** The brain metabolome, cumulative R^2X=0.498, cumulative R^2Y was 0.253, and cumulative Q^2=0.00649, n=7-9 per group. **C)** The liver metabolome, cumulative R^2X=0.349, cumulative R^2Y=0.3, and cumulative Q^2=0.041, n=7-9 per group.

5.2.1 Plasma metabolite levels

In the plasma, PLS-DA showed a clear separation between the genotypes, and separation due to L:L exposure (Figure 5.2A). Cumulative R2X was 0.819, cumulative R2Y was 0.696, and cumulative Q2 was 0.501. Two-way ANOVA was used to investigate differences between groups for each metabolite. Results are summarised in Table S1.

α-CH2 lipoprotein was significantly increased by both genotype (p=0.0004, F(1,30)=16.12) and L:L exposure (p<0.0001, F(1,30)=30.48; Figure 5.3A). Genotype increased α-CH2 levels by 41%, and L:L exposure increased α-CH2 levels by 61%. Post hoc testing revealed that the control group had significantly lower α-CH2 lipoprotein levels than all other experimental groups (p=0.0002, p=0.0064, p<0.0001), and the APOE-/-:LL group had significantly higher levels than the APOE-/-:LD group (p=0.0213). =CH-CH2=CH2- lipoprotein was significantly increased by L:L exposure (p<0.0001, F(1,30)=20.52; Figure 5.3B). There were also trends towards the interaction between genotype and L:L affecting =CH-CH2=CH2- levels (p=0.0713, F(1,30)=3.496) and genotype decreasing =CH-CH2=CH2- levels (p=0.0717, F(1,30)=3.485), but these did not reach significance. L:L increased =CH-CH2=CH2- levels by 22%, genotype decreased =CH-CH2=CH2- levels by 8%. Post hoc testing revealed that the APOE-/-:LD group had significantly lower =CH-CH2=CH2- levels than the APOE-/-:LL group (p=0.0007). β-hydroxybutyrate and HDL levels significantly decreased by genotype (p<0.0001, F(1,30)=171.8; Figure 5.3C) and significantly increased by L:L exposure (p=0.0029, F(1,30)=10.50). There was a trend towards a significant interaction between genotype and L:L (p=0.0554, F(1,30)=3.974). Genotype decreased β-hydroxybutyrate and HDL levels by 95%, L:L exposure increased β-hydroxybutyrate and HDL levels by 16%. Post hoc testing revealed that the control group had higher β-hydroxybutyrate and HDL levels than the APOE-/-:LD group (p<0.0001) and the APOE-/-:LL group (p<0.0001). The C57BL/6J:LL group also had higher levels than the APOE-/-:LL group (p<0.0001). The APOE-/-:LL group had higher β-hydroxybutyrate and HDL levels than the APOE-/-:LD


A
Plasma α-CH2
LD
LL
Relative Spectral Integral (AU)
0.008
0.006
0.004
0.002
0.000
****
**
*
***
C57BL/6J
APOE -/-
B
Plasma =CH-CH2=CH2-
Relative Spectral Integral (AU)
0.015
0.010
0.005
0.000
***
C57BL/6J
APOE -/-
C
β-Hydroxybutyrate and HDL
Relative Spectral Integral (AU)
0.020
0.015
0.010
0.005
0.000
**
****
****
****
C57BL/6J
APOE -/-
D
Plasma HDL (0.82-0.84)
Relative Spectral Integral (AU)
0.006
0.004
0.002
0.000
**
****
****
****
C57BL/6J
APOE -/-
E
Plasma HDL (5.26-5.28)
Relative Spectral Integral (AU)
0.006
0.004
0.002
0.000
**
****
***
C57BL/6J
APOE -/-
F
Plasma HDL (5.28-5.30)
Relative Spectral Integral (AU)
0.010
0.008
0.006
0.004
0.002
0.000
**
*
C57BL/6J
APOE -/-
G
Plasma LDL and Triglycerides
Relative Spectral Integral (AU)
0.04
0.03
0.02
0.01
0.00
****
***
***
C57BL/6J
APOE -/-

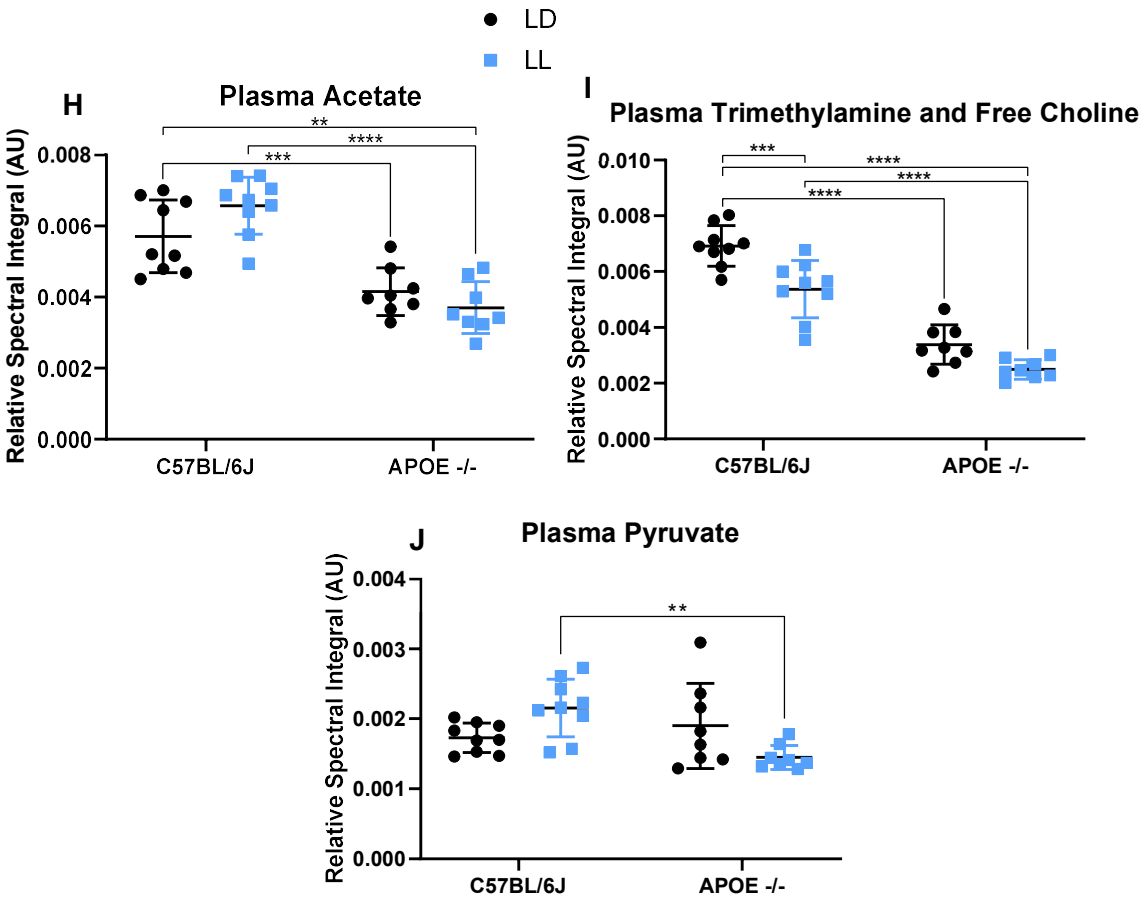


Figure 5.3: Plasma metabolites involved in energy metabolism are significantly altered by genotype, light or the interaction between the two.
A) α-CH_2 levels were significantly higher due to light and genotype. **B)** =CH_2-CH_2=CH_2- levels were increased by L:L exposure. **C)** β-hydroxybutyrate and HDL levels were significantly reduced by the APOE-/- genotype and increased by L:L exposure. HDL levels were all impacted by the interaction between genotype and light **F)**, and also **D)** reduced by genotype and L:L exposure, and **E)** reduced by genotype. **G)** LDL and triglycerides were increased by both the APOE-/- genotype and L:L exposure**. H)** The interaction between light and genotype had an effect on Acetate levels, and genotype also significantly decreased Acetate levels**. I)** Trimethylamine and free choline levels were reduced by both genotype and light. **J)** Pyruvate levels were affected by the interaction between genotype and light. 2-way ANOVA; data presented as mean ± SD of 8-9 mice per group. Statistically significant differences between groups are shown as *, p ≤ 0.05, **, p ≤ 0.01; ***, p ≤ 0.001 and ****, p ≤ 0.0001

group (p=0.006). Multiple bins on the plasma spectra were assigned as components of HDL. HDL at 5.28-5.30ppm had a significant interaction between genotype and L:L exposure (p=0.0023, F(1,30)=11.11; Figure 5.3F). Post hoc testing revealed that the APOE-/-:LD group had significantly lower HDL levels than the controls (p=0.0072) and the APOE-/-:LL group (p=0.0144). HDL at 5.26-5.28ppm had a significant interaction between genotype and L:L exposure (p=0.0166, F(1,30)=6.434), and genotype significantly lowers

HDL levels by 13% ($p<0.0001$, $F(1,30)=61.89$; Figure 5.3E). Post hoc testing revealed that the control group had significantly higher HDL levels than the APOE-/-:LD group ($p<0.0001$) and the APOE-/-:LL group ($p=0.0001$). Additionally, the C57BL/6J:LL group had significantly higher HDL levels than the APOE-/-:LL group ($p=0.0038$). Looking at HDL at 0.82-0.84ppm, the interaction between the APOE-/- genotype and L:L exposure had a significant effect on the levels of HDL ($p=0.0366$, $F(1,30)=4.786$;Figure 5.3D). Genotype significantly decreased HDL levels by 44% ($p<0.0001$, $F(1,30)=93.62$) and L:L exposure also significantly decreased HDL levels by 15% ($p=0.0099$, $F(1,30)=7.577$). Post hoc testing revealed that that the control group had significantly higher HDL levels than the C57BL/6J:LL group ($p=0.0059$), the APOE-/-:LD group ($p<0.0001$) and the APOE-/-:LL group ($p<0.0001$). Additionally, the C57BL/6J:LL group had significantly higher HDL levels than the APOE-/-:LL group ($p<0.0001$). Genotype significantly increased LDL and triglyceride levels by 33% ($p=0.0001$, $F(1,30)=19.64$) and L:L exposure increased LDL and triglycerides by 39% ($p<0.0001$, $F(1,30)=25.88$; Figure 5.3G). Post hoc testing showed that the APOE-/-:LL group had significantly higher LDL and triglyceride levels than the controls ($p<0.0001$), the C57BL/6J:LL group ($p=0.0008$) and the APOE-/-:LD group ($p=0.0003$). Acetate levels were found to be significantly affected by the interaction between L:L and genotype ($p=0.0272$, $F(1,30)=5.392$), and genotype also significantly decreased acetate levels ($p<0.0001$, $F(1,30)=60.86$; Figure 5.3H). Genotype decreased acetate levels by 36%. Post hoc testing revealed that the control group had higher levels of acetate than the APOE-/-:LD group ($p=0.0029$) and the APOE-/-:LL group ($p=0.0001$). Also, the C57BL/6J:LL group had significantly higher acetate levels than the APOE-/-:LL group ($p<0.0001$). Trimethylamine and free choline levels were significantly decreased by the APOE-/- genotype by 52% ($p<0.0001$, $F(1,30)=154.2$) and L:L exposure decreased levels by 23.7% ($p<0.0001$, $F(1,30)=22.31$; Figure 5.3I). Post hoc tests showed that the control group had significantly higher levels of trimethylamine and free choline than the C57BL/6J:LL group ($p=0.0007$), the APOE-/-:LD group ($p<0.0001$) and the APOE-/-:LL group ($p=<0.0001$). Additionally, the C57BL/6J:LL

group had significantly higher levels of trimethylamine and free choline than the APOE-/-:LL group ($p<0.0001$). The interaction between genotype and L:L exposure had a significant effect on plasma pyruvate levels ($p=0.0025$, $F(1,30)=10.88$; Figure 5.3J). There was also a trend towards the APOE-/- genotype reducing pyruvate levels but this did not reach significance ($p=0.0548$, $F(1,30)=3.993$). Post hoc testing revealed that the C57BL/6J:LL group had higher levels of pyruvate than the APOE-/-:LL group ($p=0.004$).

5.2.2 Brain metabolite levels

In the brain, the PLS-DA scores plot revealed some separation between classes due to L:L exposure (Figure 5.2B). Cumulative R^2X was 0.498, cumulative R^2Y was 0.253, and cumulative Q^2 was -0.00649. Group differences were then examined by two-way ANOVA. Results are summarised in Table S2.

Levels of the ATP adenosine moiety were decreased by 7% in the APOE-/- genotype ($p=0.0093$, $F(1,29)=7.762$) and L:L exposure decreased ATP adenosine levels by 9.7% ($p=0.0006$, $F(1,29)=14.66$; Figure 5.4A). Post hoc testing revealed that the control group had higher ATP levels than the C57BL/6J:LL group ($p=0.0408$) and the APOE-/-:LL group ($p=0.0003$). L:L exposure significantly reduced the levels of ATP ribose moiety by 11.4% ($p=0.0009$, $F(1,29)=13.67$), and genotype significantly reduced the levels of ATP ribose moiety by 7.4% ($p=0.0257$, $F(1,29)=5.531$; Figure 5.4B). Post hoc testing showed that the control group had significantly higher levels of ATP than the C57BL/6J:LL group ($p=0.047$) and the APOE-/-:LL group ($p=0.0008$). The interaction between genotype and :LL had a significant effect on lactate levels ($p=0.0361$, $F(1,29)=4.829$), and genotype also significantly reduced lactate levels by 5.6% ($p=0.016$, $F(1,29)=6.549$; Figure 5.4C). Post hoc testing showed that the C57BL/6J:LL group had significantly lower lactate levels than the APOE-/-:LL group ($p=0.0095$). The interaction between the APOE-/- genotype and L:L exposure had a significant effect on alanine levels ($p=0.0381$, $F(1,29)=4.723$; Figure 5.4D). L:L exposure also significantly increased

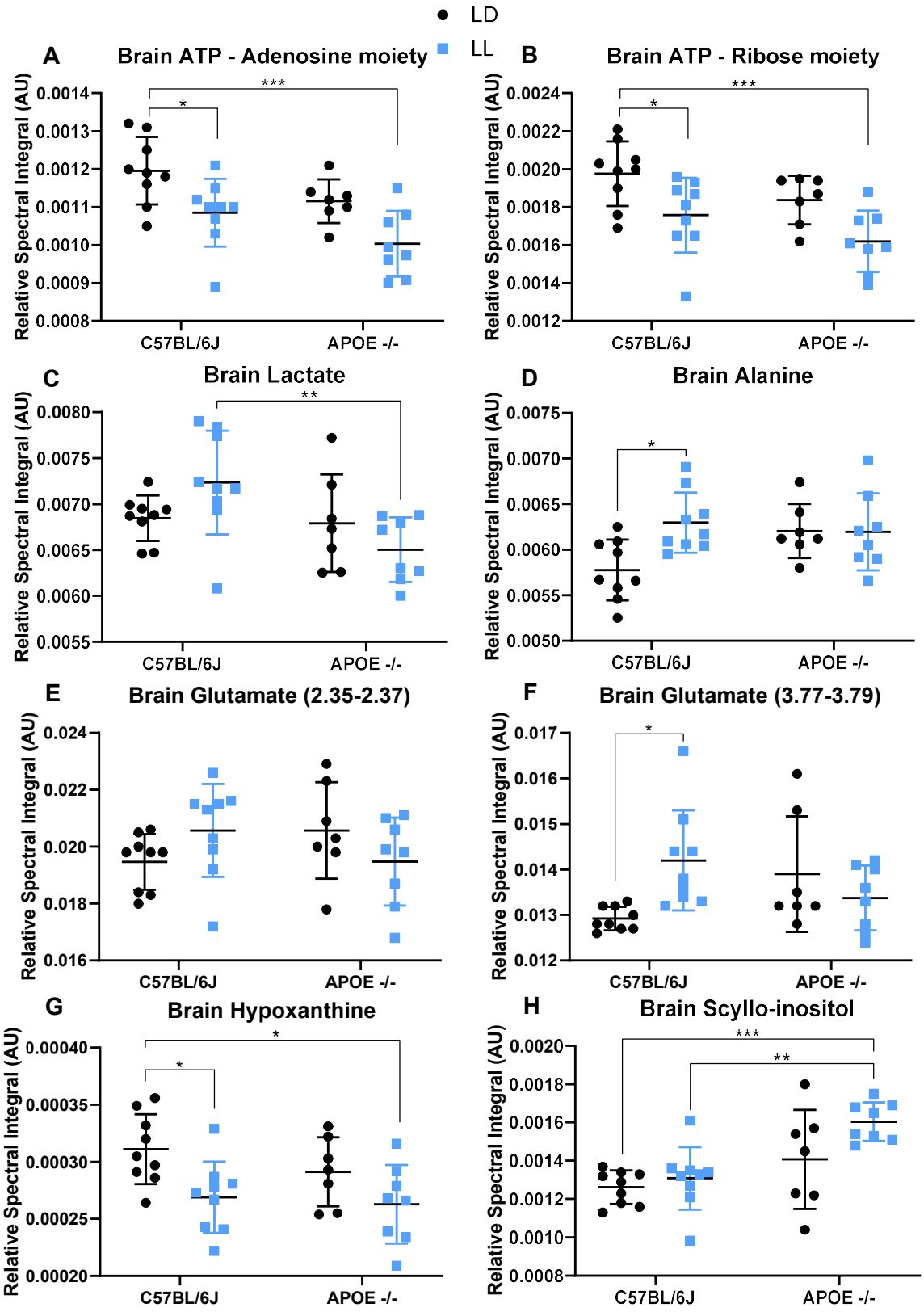

LD
LL
A
Brain ATP - Adenosine moiety
B
Brain ATP - Ribose moiety
C
Brain Lactate
D
Brain Alanine
E
Brain Glutamate (2.35-2.37)
F
Brain Glutamate (3.77-3.79)
G
Brain Hypoxanthine
H
Brain Scyllo-inositol
Relative Spectral Integral (AU)
C57BL/6J
APOE -/-

Figure 5.4: Brain metabolites involved in energy metabolism are significantly altered by genotype, light or the interaction between the two.
Both the APOE-/- genotype and L:L exposure decreased the levels of ATP **A)** Adenosine moiety and the **B)** Ribose moiety**. C)** The interaction between genotype and L:L exposure had a significant impact on lactate levels, and genotype significantly decreased lactate levels**. D)** Alanine levels were significantly altered by the interaction between genotype and light, and light significantly increased alanine levels. The interaction between genotype and L:L exposure had a significant impact on glutamate levels **E)** and **F). G)** Hypoxanthine levels were reduced by L:L exposure. **H)** Scyllo-inositol levels were significantly increased by both genotype and L:L exposure. 2-way ANOVA; data presented as mean ± SD of 7-9 mice per group. Statistically significant differences between groups are shown as *, p ≤ 0.05, **, p ≤ 0.01; *** and p ≤ 0.001.

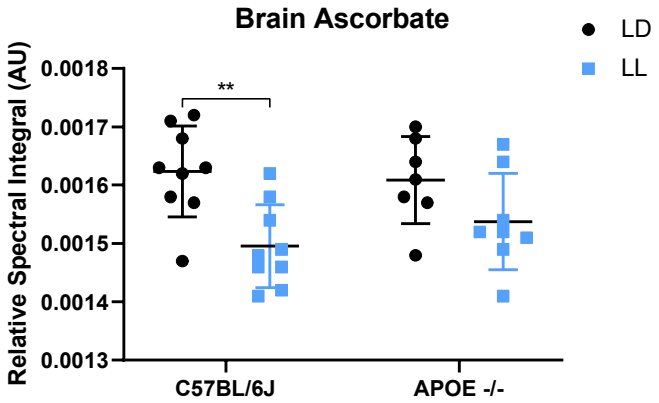


Figure 5.5: Brain metabolites involved in antioxidant decreased by light exposure.
Ascorbate levels were decreased by L:L exposure. 2-way ANOVA; data presented as mean ± SD of 7-9 mice per group. Statistically significant differences between groups are shown as *, p ≤ 0.05 and **, p ≤ 0.01.

alanine levels by 4% (p=0.0459, F(1,29)=4.349). Post hoc testing revealed that the C57BL/6J:LL group had a significantly higher level of alanine than the control group (p=0.0181). The interaction between the APOE-/- genotype and L:L exposure had a significant effect on glutamate (2.35-2.37 ppm) levels (p=0.0426, F(1,29)=4.548; Figure 5.4E). However, post hoc testing did not reveal further differences between groups. Glutamate (3.77-3.79 ppm) levels were affected by a significant interaction between genotype and L:L (p=0.0076, F(1,29)=8.243; Figure 5.4F). Post hoc tests revealed that the C57BL/6J:LL group had a significant higher glutamate level than the control group (p=0.0253). Hypoxanthine was significantly decreased by 4.5% by L:L (p=0.0035, F(1,29)=10.13; Figure 5.4G). Post hoc testing revealed that the control group had higher hypoxanthine levels than the C57BL/6J:LL group (p=0.0401) and the APOE-/-:LL group (p=0.0193). The APOE-/- genotype significantly increased scyllo-inositol levels by 17%

(p=0.0005, F(1,29)=15.43; Figure 5.4H). Additionally, L:L exposure significantly increased scyllo-inositol levels by 9% (p=0.0386, F(1,29)=4.695). Post hoc testing revealed that the APOE-/-:LL group had significantly higher scyllo-inositol levels than the control group (p=0.0008) and the C57BL/6J:LL group (p=0.0037). Ascorbate levels were significantly decreased by 6% by L:L exposure (p=0.0009, F(1,29)=13.76; Figure 5.5). Post hoc testing revealed that the C57BL/6J:LL group had significantly lower ascorbate levels than the control group (p=0.0071).

5.2.3 Liver metabolites levels

In the liver, the PLS-DA scores plot showed differences in clustering due to L:L exposure, and due to genotype (Figure 5.2C). Cumulative R2X was 0.349, cumulative R2Y was 0.3, and cumulative Q2 was 0.041. Two-way ANOVA was used to investigate differences between groups for each metabolite. Results are summarised in Table S*3*

The top VIP scores generated by the PLS-DA corresponded with multiple bins on the spectra assigned to different parts of the glutathione molecule. Glutathione Glu-αCH levels were significantly increased by 16.5% by L:L exposure. (p<0.0001, F(1,29)=51.27; Figure 5.6A). Post hoc testing revealed that the C57BL/6J:LL group had significantly higher Glutathione Glu-αCH levels compared to the control group (p<0.0001). Additionally, the APOE-/-:LL group had significantly higher Glutathione Glu-αCH levels compared to the control group (p=0.0002) and the APOE-/-:LD group (p=0.001). L:L exposure significantly increased Glutathione Glu-βCH2 levels by 39.1% (p<0.0001, F(1,29)=26.31; Figure 5.6B). Post hoc testing revealed that the C57BL/6J:LL group had significantly higher Glutathione Glu-βCH2 levels compared to the control group (p=0.0003). L:L significantly increased Glutathione Glu-γCH2 (2.57-2.59 ppm) levels by 43.6% (p<0.0001, F(1,29)=34.25; Figure 5.6C). There was also a trend towards the APOE-/- genotype reducing levels but this did not reach significance (p=0.069, F(1,29)=3.565). Post hoc testing revealed that the C57BL/6J:LL group had significantly higher Glutathione Glu-γCH2 levels compared to the control group (p<0.0001).

Additionally, the APOE-/-:LL group had significantly higher Glutathione Glu-αCH levels compared to the control group (p=0.0382) and the APOE-/-:LD group (p=0.0267). Glutathione Glu-γCH2 (2.55-2.57 ppm) levels were significantly increased by 45.7% by L:L exposure (p<0.0001, F(1,29)=30.89; Figure 5.6D). There were also trends that did not reach significance towards the interaction between genotype and L:L exposure effecting levels (p=0.0871, F(1,29)=3.136), and towards genotype increasing levels (p=0.0899, F(1,29)=3.078). Post hoc testing showed that the APOE-/-:LL group had higher Glutathione Glu-γCH2 levels compared to the CONTROL group (p<0.0001) and the APOE-/-:LD group (p=0.0001). Glutathione Cys-βCH2 (2.93-2.95 ppm) levels were significantly increased by 54.3% by L:L (p<0.0001, F(1,29)=24.33; Figure 5.6E). There was also a trend towards genotype decreasing levels (p=0.0802, F(1,29)=3.286). Post hoc testing revealed that the C57BL/6J:LL group had significantly higher Glutathione Cys-βCH2 levels compared to the control group (p=0.0003). L:L exposure significantly increased Glutathione Cys-βCH2 (2.95-2.97 ppm) levels by 43.45% (p<0.0001, F(1,29)=22.12; Figure 5.6F). Post hoc testing revealed that the C57BL/6J:LL group had significantly higher Glutathione Cys-βCH2 levels than the control group (p=0.0012). L:L significantly increased Glutathione Glu-Cys-αCH levels by 63.5% (p<0.0001, F(1,29)=25.74; Figure 5.6G). Post hoc testing revealed that the C57BL/6J:LL group had significantly higher Glutathione Glu-Cys-αCH levels compared to the control group (p=0.0004). L:L exposure significantly reduced Choline levels by 22.3% (p=0.0007, F(1,29)=14.33; Figure 5.7). Post hoc testing revealed that the C57BL/6J:LL group had significantly lower choline levels than the control group (p=0.0026).

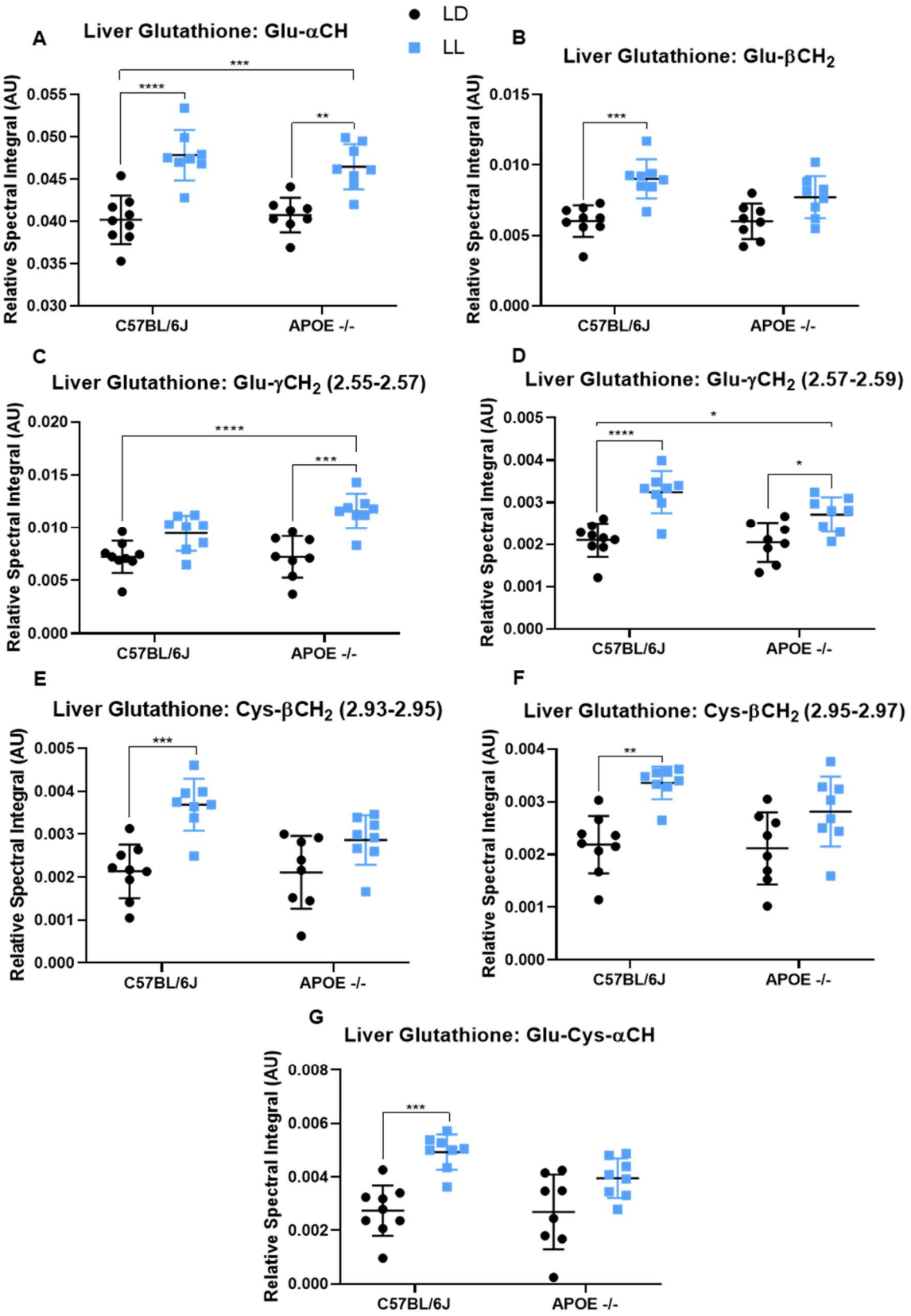

LD
LL
A
Liver Glutathione: Glu-αCH
Relative Spectral Integral (AU)
0.055
0.050
0.045
0.040
0.035
0.030
****
***
**
C57BL/6J
APOE -/-
B
Liver Glutathione: Glu-βCH2
0.015
0.010
0.005
0.000
***
C
Liver Glutathione: Glu-γCH2 (2.55-2.57)
0.020
0.015
0.010
0.005
0.000
****
***
D
Liver Glutathione: Glu-γCH2 (2.57-2.59)
0.005
0.004
0.003
0.002
0.001
0.000
*
****
E
Liver Glutathione: Cys-βCH2 (2.93-2.95)
F
Liver Glutathione: Cys-βCH2 (2.95-2.97)
G
Liver Glutathione: Glu-Cys-αCH
0.008
0.006
0.004
0.002
0.000

Figure 5.6: Liver metabolites involved in antioxidant activity are significantly altered by 3 weeks of constant light exposure.
Levels of various glutathione groups at different points on the ^{1}H NMR spectrum were all significantly increased by L:L**. A) - G).** 2-way ANOVA; data presented as mean ± SD of 7-9 mice per group. Statistically significant differences between groups are shown as *; p<0.05; **, p ≤ 0.01; ***, p ≤ 0.001 and ****, p ≤ 0.0001

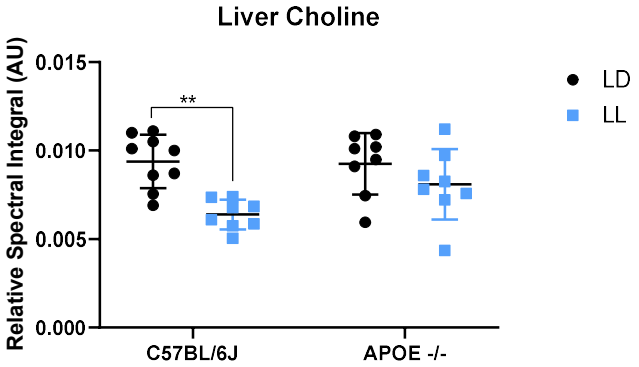


Figure 5.7.: Liver levels of essential nutrient choline reduced by L:L exposure.
Choline levels were significantly decreased by L:L exposure. 2-way ANOVA; data presented as mean ± SD of 7-9 mice per group. Statistically significant differences between groups are shown as **, p ≤ 0.01.

5.2.4 Correlations of metabolites with behavioural outcomes

The correlations between key metabolites from the three tissues of interest, gene expression in the brain and liver (from Chapter 4.3) and significant behavioural outcomes (from Chapter 4.3) were investigated. Correlations were performed between metabolites with the highest-ranking VIP scores from plasma, brain and liver with behavioural results found to be significantly altered by genotype or L:L exposure. Results were then adjusted using the BH method to control for multiple comparisons. There were 7-9 animals per group (n = 33-34 per correlation). Results discussed here are only strong positive correlations, where r≥0.6. All of the correlations are detailed in tables S4-S12 in the Supplementary.

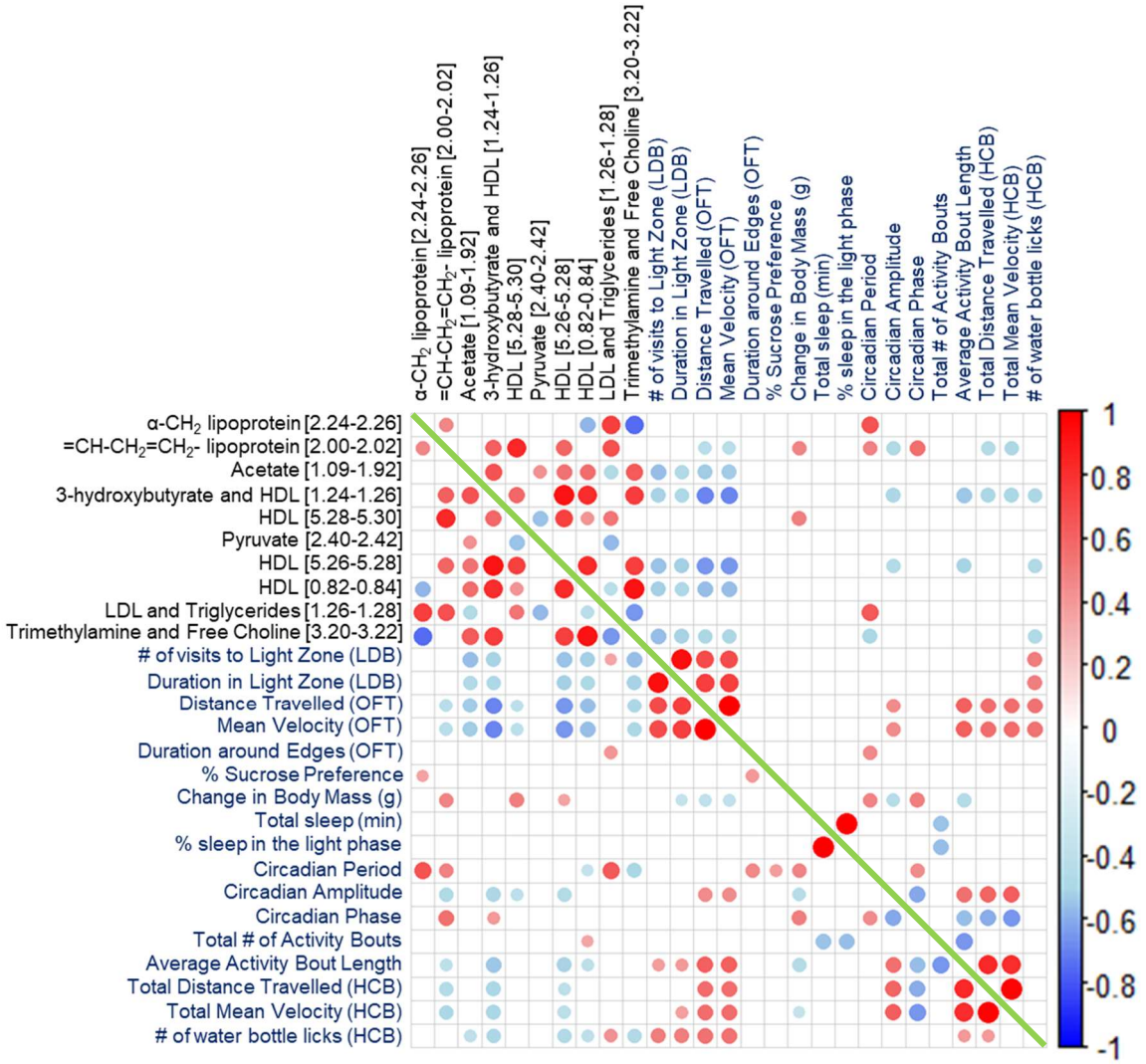


Figure 5.8: Plasma metabolites correlate with circadian and locomotor parameters. Correlations are colour-coded for both correlation direction and strength (bar on right hand side). Red is a strong positive correlation, white is no correlation, and blue is a strong negative correlation. The intensity of the colour corresponds to the value of the correlation coefficient. The size of circles corresponds to the significance of the correlation, where $p<0.05$, and non-significant points are removed. Points above the diagonal have been corrected for multiple testing, points below the diagonal have not.

In the plasma (Figure 5.8; Table S4), αCH2 lipoprotein had a strong positive correlation with circadian period (r=0.66, p=0.00027). β-hydroxybutyrate and HDL had strong negative correlations with Distance Travelled (OFT) (r=-0.68, p=0.00014) and Mean velocity (OFT) (r=-0.68, p=0.00014). HDL [5.26-5.28] had strong negative correlations with Distance Travelled (OFT) (r=-0.65, p=0.00042), and Mean velocity (OFT) (r=-0.65, p=0.00042). LDL and triglycerides had a strong positive correlation with circadian period

(r=0.64, p=0.00049).

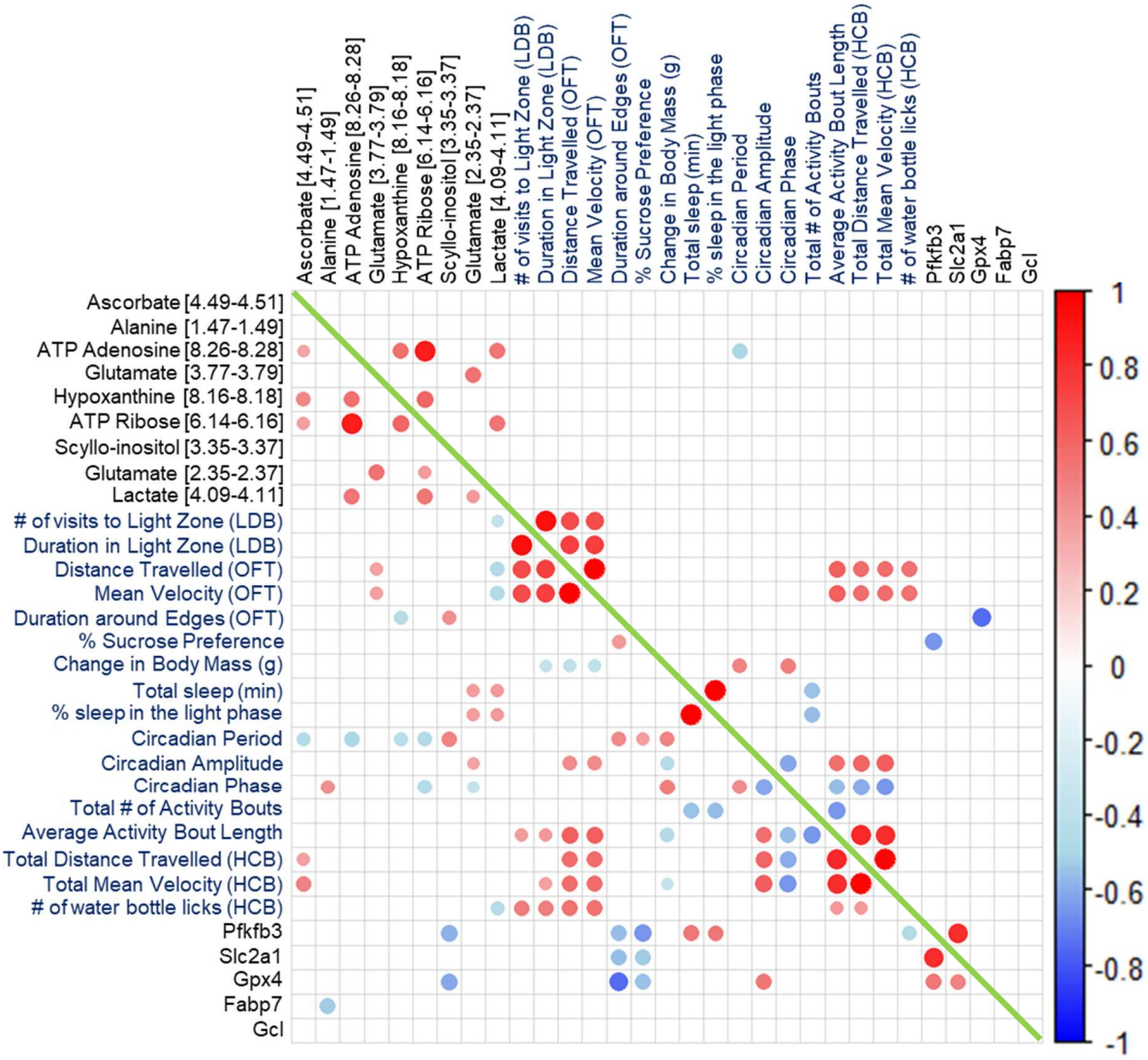


Figure 5.9: Behavioural outcomes correlate with gene expression but not metabolites. Correlations are colour-coded for both correlation direction and strength (bar on right hand side). Red is a strong positive correlation, white is no correlation, and blue is a strong negative correlation. The intensity of the colour corresponds to the value of the correlation coefficient. The size of circles corresponds to the significance of the correlation, where p<0.05, and non-significant points are removed. Points above the diagonal have been corrected for multiple testing, points below the diagonal have not.

In the brain (Figure 5.9; Table S5), there were strong negative correlations between Pfkfb3 and % Sucrose preference (r=-0.64, p=0.023), and between Gpx4 and Duration around edges (OFT) (r=-0.74, p=0.0058).

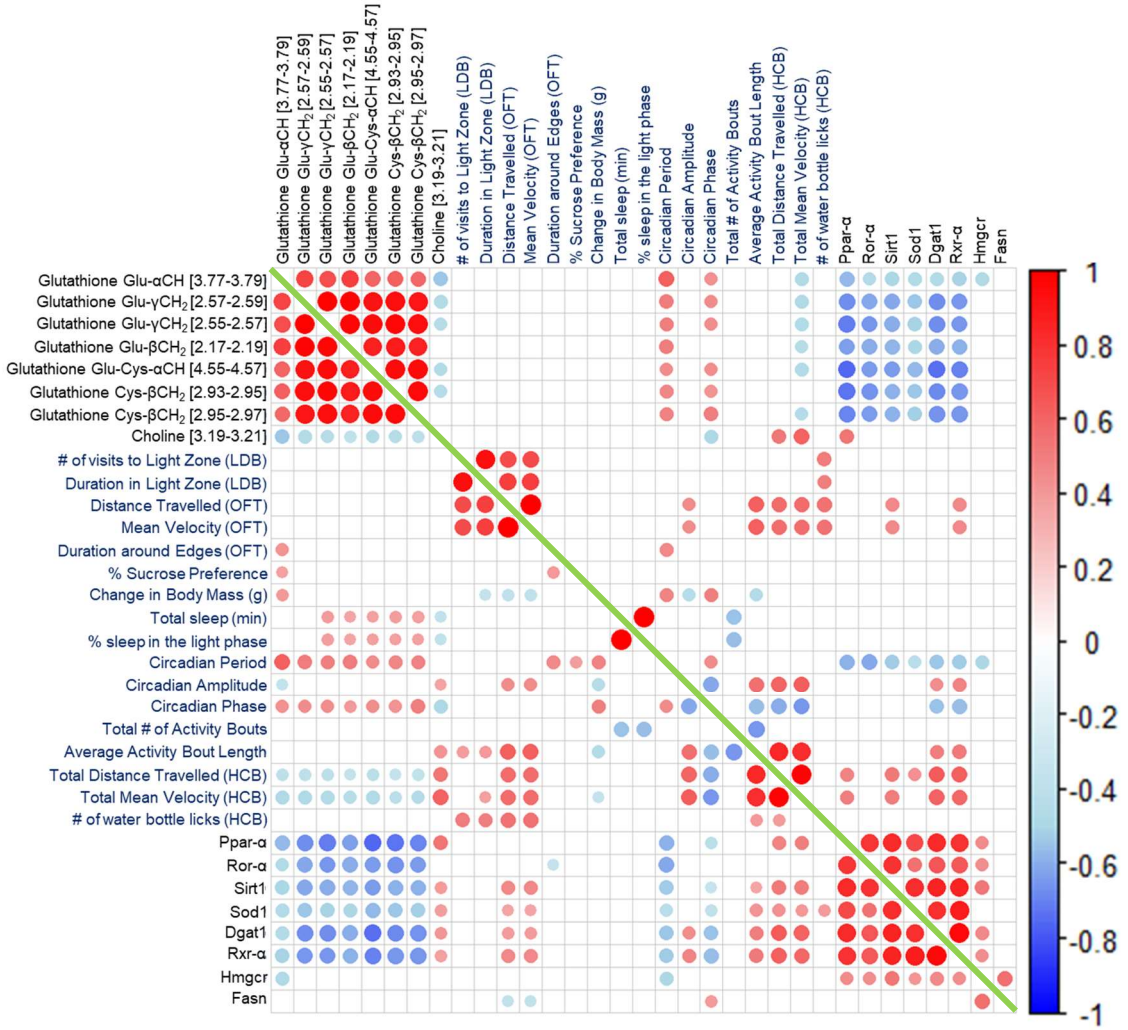


Figure 5.10: Locomotor and circadian behaviour correlate with liver metabolites and genes Correlations are colour-coded for both correlation direction and strength (bar on right hand side). Red is a strong positive correlation, white is no correlation, and blue is a strong negative correlation. The intensity of the colour corresponds to the value of the correlation coefficient. The size of circles corresponds to the significance of the correlation, where $p<0.05$, and non-significant points are removed. Points above the diagonal have been corrected for multiple testing, points below the diagonal have not.

In the liver (Figure 5.10; Table S8), circadian period had a strong positive correlation with Glutathione Glu-αCH [3.77-3.79] (r=0.62, p=0.0001. Additionally, circadian period had a strong negative correlation with *Ror-α* (r=-0.60, p=0.0011). Total Distance Travelled in home cage behaviour (HCB) had strong positive correlations with *Dgat1* (r=0.64, p=0.00074) and *Rxr-α* (r=0.61, p=0.0011). Total Mean Velocity (HCB) had strong positive correlations with Choline (r=0.61, p=0.0012) and *Dgat1* (r=0.60, p=0.0017).

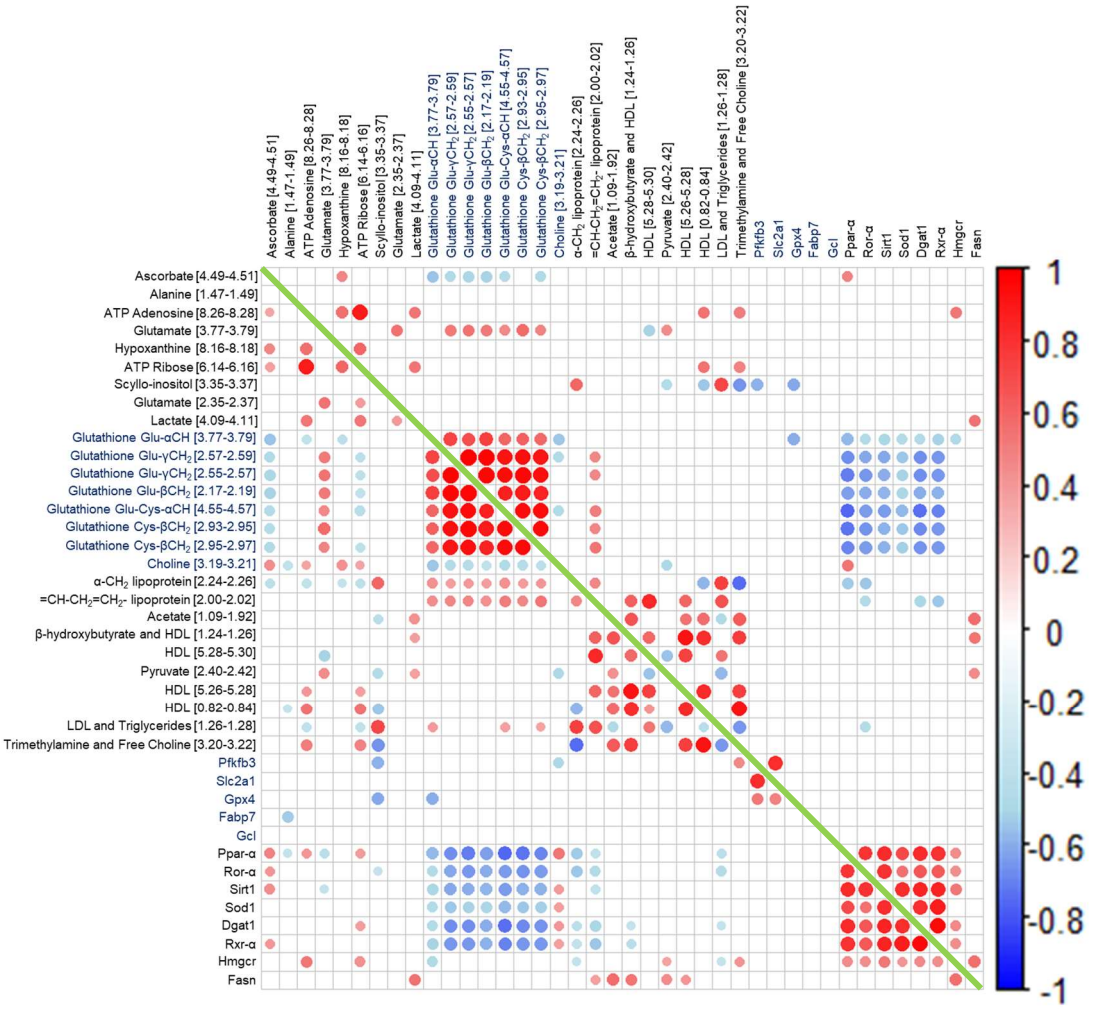
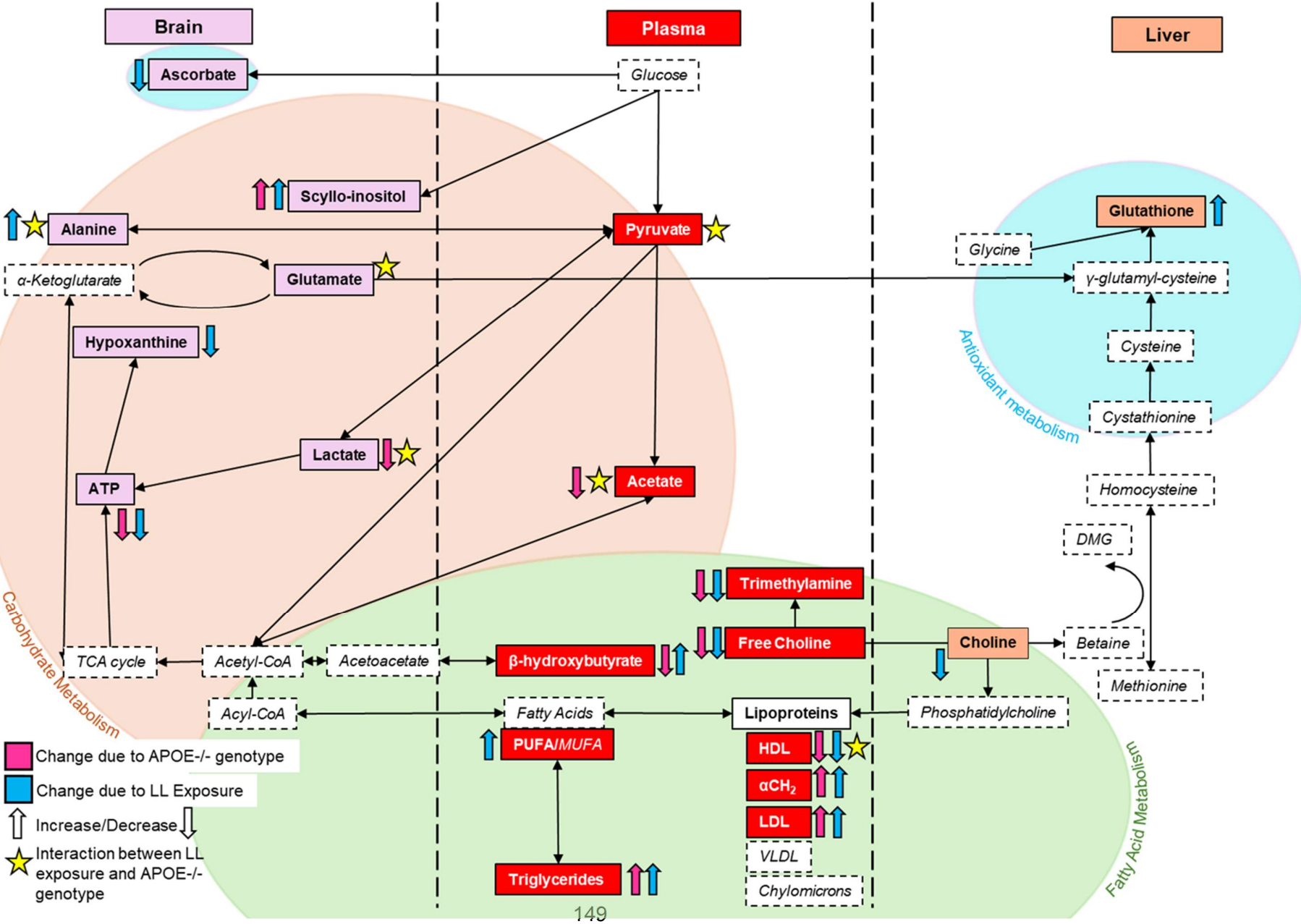


Figure 5.11: Correlations of brain, liver and plasma metabolites with gene expression in the brain and liver.
Correlations are colour-coded for both correlation direction and strength (bar on right hand side). Red is a strong positive correlation, white is no correlation, and blue is a strong negative correlation. The intensity of the colour corresponds to the value of the correlation coefficient. The size of circles corresponds to the significance of the correlation, where p<0.05, and non-significant points are removed. Points above the diagonal have been corrected for multiple testing, points below the diagonal have not.

Looking at correlations between brain and liver and plasma metabolites and gene expression (Figure 5.11; Table S9), Scyllo-inositol had a strong positive correlation with LDL and triglycerides (r=0.72, p<0.0001), and had strong negative correlations with Trimethylamine and free choline (r=-0.66, p=0.00044) and *Gpx4* (r=-0.61, p=0.032). *Ppar-α* had strong negative correlations with Glutathione Glu-γCH$_2$ [2.57-2.59] (r=-0.67, p=0.00031) and other glutathione groups (See Table S9). *Ror-α* had strong negative correlations with Glutathione Glu-γCH$_2$ [2.57-2.59] (r=-0.61, p=0.0018) and other

glutathione groups (See Table S9). *Sirt1* had strong negative correlations with Glutathione Glu-γCH_2 [2.57-2.59] (r=-0.60, p=0.0021) and other glutathione groups (See Table S9)., *Dgat1* had strong negative correlations with Glutathione Glu-γCH_2 [2.57-2.59] (r=-0.66, p=0.00065) and the other glutathione groups (See Table S9). *Rxr-α* had strong negative correlations with Glutathione Glu-γCH_2 [2.57-2.59] (r=-0.64, p=0.00090) and the other glutathione groups (See Table S9).

Figure 5.12: Multi-organ metabolomics reveals changes in carbohydrate and lipid metabolism, and alterations in redox homeostasis.
A map showing the connection of significant metabolites from PLS-DA analysis across the three tissues. Tissue compartments are separated by black dashes. Metabolites in purple are significant brain metabolites (n=7-9 per group), metabolites in red are significant plasma metabolites (n=8-9 per group), and metabolites in orange are significant liver metabolites (n=7-9 per group). Metabolites in white dashed boxes were not found to be significant by PLS-DA. Pink arrows show changes due to genotype, blue arrows show changes due to L:L. Stars show that there is an interaction between genotype and L:L.


Brain
Plasma
Liver
Ascorbate
Glucose
Scyllo-inositol
Alanine
Pyruvate
Glutathione
Glycine
α-Ketoglutarate
Glutamate
γ-glutamyl-cysteine
Hypoxanthine
Cysteine
Antioxidant metabolism
Cystathionine
Lactate
ATP
Acetate
Homocysteine
DMG
Trimethylamine
Free Choline
Choline
Betaine
Carbohydrate Metabolism
TCA cycle
Acetyl-CoA
Acetoacetate
β-hydroxybutyrate
Methionine
Acyl-CoA
Fatty Acids
Lipoproteins
Phosphatidylcholine
PUFA/MUFA
HDL
αCH2
LDL
VLDL
Chylomicrons
Triglycerides
Fatty Acid Metabolism
Change due to APOE-/- genotype
Change due to LL Exposure
Increase/Decrease
Interaction between LL exposure and APOE-/- genotype

5.3 Discussion

The aims of this chapter were to investigate the gene-environment interaction between circadian disruption and CVD, using the APOE-/- model of atherosclerosis and L:L exposure. It was found that there were disturbances in carbohydrate metabolism, lipid metabolism and redox homeostasis across plasma, brain and liver (**Error! Reference source not found.**).

Carbohydrate metabolism was disrupted by the interaction between the APOE-/- genotype and L:L exposure, the APOE-/- genotype and L:L exposure, as seen by changes in pyruvate, lactate, alanine, glutamate, acetate, scyllo-inositol and ATP levels.

Plasma pyruvate levels were affected by the interaction between the APOE-/- genotype and L:L exposure, driven by the APOE-/-:LL group having significantly lower plasma pyruvate than the C57BL/6J:LL group. This is the first time it has been shown that pyruvate is affected by this interaction. Pyruvate is the product of glycolysis, where two pyruvate molecules are generated from one glucose molecule, producing 2 ATP molecules in the process. However, it can also be produced from other sources, such as alanine; through the alanine aminotransferase reaction using alanine aminotransferase (ALT), lactate; from the oxidation of lactate using lactate dehydrogenase (LDH), and possibly acetate. Previous studies in the APOE-/- model have shown reduced serum pyruvate levels after 2 weeks of a HFD compared to APOE-/- mice on a standard chow diet, but levels normalise by 4 weeks HFD and remain normal at 8 weeks HFD [356]. However, in a study that compared APOE-/- mice to C57BL/6J mice on a regular chow diet, serum pyruvate was significantly increased in the APOE-/- mice, and remained increased when the mice were given a HFD for 4 and 8 weeks [357]. In a hamster model of diet-induced atherosclerosis, plasma pyruvate was increased in the high fat and high cholesterol (HFHC) diet group at 24 and increased further at 48 days [365]. In humans, patients with atherosclerosis had reduced plasma pyruvate compared to healthy subjects

[355]. Constant light exposure seems to reduce pyruvate levels, C57BL/6J mice exposed to L:L for 12 weeks had reduced plasma pyruvate, and the pyruvate was also reduced in fruit flies exposed to constant blue light for 14 days [364, 366]. In this study it seems that the exposure to LL has a higher effect on pyruvate levels in APOE-/- mice compared to the control group.

Brain lactate levels were reduced in the APOE-/- genotype and were also affected by the interaction between the APOE-/- genotype and L:L exposure, similarly driven by the APOE-/-:LL group having significantly lower brain lactate than the C57BL/6J:LL group. This interaction has not been shown before. Lactate is produced by the reduction of pyruvate in anaerobic conditions, catalysed by LDH, when ATP is required but there isn't sufficient oxygen to undergo aerobic respiration. Lactate is the main source of circulating carbohydrates and is thought to circulate to where there is energetic need, becomes oxidised to pyruvate and enters the TCA cycle [367]. This allows preservation of glucose for vital systems, such as the brain. A reduction in lactate levels is seen consistently over 8 weeks of a HFD in serum of APOE-/- mice compared to APOE-/- mice on regular diet [356]. Consistent with this, reduced hepatic lactate levels were seen in a hamster model of diet-induced atherosclerosis [365]. However, hepatic lactate levels were increased in APOE-/- mice on HFD compared to C57BL/6J mice on normal diet [368]. This effect may be due to the HFD, or the interaction between diet and genotype rather than solely the APOE-/- genotype. In humans, patients with stable carotid atherosclerosis had reduced plasma lactate compared to healthy subjects [355]. Additionally, lactate was shown to have a positive association with carotid intima-media thickness (IMT) in a study using cohort data from the Multi-Ethnic Study of Atherosclerosis (MESA), the Rotterdam study and the London Life Sciences Prospective Population Study (LOLIPOP) [354]. Therefore, the reduction in lactate due to genotype as seen in this chapter is in concordance with the existing literature. The effect of light exposure on lactate has not been well characterised. However, it has been shown in several studies that L:L exposure increases blood glucose

levels and decreases insulin sensitivity, showing that carbohydrate metabolism and energy balance are negatively affected by abnormal light exposure [262, 285].

Brain alanine levels were altered by the interaction between genotype and light, and light significantly increased alanine. This is driven by the C57BL/6J:LL group having significantly higher alanine levels than the control group. This is the first time these results have been reported. Alanine is a non-essential amino acid which plays a key role in the glucose-alanine cycle, as it is a major source of pyruvate. As mentioned above, alanine can produce pyruvate through the alanine aminotransferase reaction, where the amino group from alanine is transferred to α-ketoglutarate, using alanine aminotransferase (ALT). This reductive amination of α-ketoglutarate produces pyruvate and glutamate. Pyruvate can also generate alanine, using the glutamate dehydrogenase (GDH) enzyme to deaminate glutamate to α-ketoglutarate in the process known as oxidative deamination. Alanine and lactate also play a key role in hepatic gluconeogenesis. They are transported to the liver and converted to pyruvate, which is then used to synthesize glucose via the gluconeogenesis pathway [369]. In models of atherosclerosis using the APOE-/- mouse model, a HFD for 8 weeks increased serum alanine levels compared to APOE-/- mice on regular diet [356]. Additionally faecal and hepatic alanine levels were increased in APOE-/- mice on a HFD compared to C57BL/6J mice on a normal diet [368, 370]. However, in a hamster model of diet-induced atherosclerosis, plasma and hepatic alanine levels decreased at 24 weeks of a HFD and remain decreased at 42 weeks [365]. Reduced alanine levels were also seen in the plasma of patients with stable carotid atherosclerosis compared to healthy subjects [355]. However, alanine was found to have a direct association with coronary artery calcium (CAC) in study using cohort data from MESA, the Rotterdam study and LOLIPOP [354]. There aren't relevant studies looking at changes in alanine levels with L:L exposure. However, L:L is known to cause oxidative stress, and alanine has been shown to exhibit protection against damage induced by free radicals by stimulating the expression and enzymatic activity of the antioxidant defence protein heme

oxygenase-1 in human endothelial cells [371]. Therefore, the increase of alanine levels in light may be a compensation to maintain redox balance in the presence of oxidative stress induced by L:L. Alternatively, the change in alanine levels may be in response, or to compensate for, the altered pyruvate levels.

For the first time it was shown that brain glutamate levels were altered by the interaction between genotype and light, driven by the difference between the C57BL/6J:LL group and the control group at 3.77-3.79ppm. Glutamate is an amino acid and is the is the primary excitatory neurotransmitter in vertebrates. It takes part in multiple metabolic pathways, including aminotransferase reactions for amino acid metabolism and undergoing oxidative deamination to form α-ketoglutarate to replenish TCA cycle intermediaries in carbohydrate metabolism [372]. Additionally, in the brain, glutamate is part of the glutamine-glutamate cycle, where glutamate released by glutamatergic neurones is taken up by astrocytes and converted to glutamine, catalysed by astrocytic glutamine synthetase (GS) [373]. Glutamine is transported to neurons and is hydrolysed to glutamate by phosphate-activated glutaminase (PAG). Glutamate is also involved in the production of the antioxidant molecule glutathione, catalysed by glutamate-cysteine ligase (GCL), it couples with cysteine to form γ-glutamylcysteine, which, with the addition of glycine forms glutathione [335]. High glutamate concentrations cause excitotoxicity and result in neuronal cell death. Oxidative stress may be involved, as application of SOD reduced the toxicity of a glutamate agonist in cultured cells [374]. Previous studies in the APOE-/- model have shown reduced hepatic and faecal glutamate levels in APOE-/- mice on a HFD compared to C57BL/6J mice on normal diet [368, 370]. However, in a hamster model of diet-induced atherosclerosis, hepatic glutamate was elevated at 24 weeks through to 42 weeks on the HFD [365]. In humans, a cross sectional study found that plasma glutamate levels were elevated in individuals with higher IMT, after adjustment for body fat mass, visceral fat mass, liver fat content and insulin sensitivity [375]. However, glutamate was found to have an inverse association with CAC and IMT in study using

cohort data from the MESA, the Rotterdam study and LOLIPOP [354]. Additionally, in patients with suspected coronary artery disease (CAD), high levels of glutamate and a low glutamine to glutamate ratio were independently associated with high risk of CAD, and the severity of CAD [376]. There was little evidence available on the effect of L:L, in drosophila it was found that constant light exposure, exposure to blue light for 14 days reduced glutamate levels [366]. This is different to what is seen in this chapter, but changes seen in flies may not correspond to changes in mice given how different the species are biologically. In Chapter 4.3.12, astrocyte morphology was shown to be affected by the interaction between L:L and genotype. Those changes in morphology could have a knock-on effect on glutamate synthesis, and cause the changes seen here. Additionally, glutamate seems to be affected by the L:L-genotype interaction in a similar manner to alanine, and so their levels may both be affected by the change in pyruvate levels.

Plasma acetate levels were affected by the interaction between light and genotype, and genotype significantly decreased acetate levels. The interaction has not been reported before. Acetate is a short-chain fatty acid (SCFA) and can arise from several sources. The most well-known source of acetate is the gut microbiota, which ferment dietary fibre and other products and produce acetate, as well as other SCFAs propionate and butyrate [377]. Additionally, acetate can be produced by pyruvate, as shown by ^{13}C NMR, and by the deacetylation of histones [378, 379]. Production of acetate from pyruvate seems to occur through two pathways, the coupling of pyruvate with ROS, which indicates that pyruvate has antioxidant activity, and through keto acid dehydrogenases acting as keto acid decarboxylases [380]. Acetate is converted to Acetyl-CoA, which can enter the TCA cycle and produce ATP, and it is also a major substrate for FA synthesis [381-383]. Additionally, acetate can be used by the liver as a substrate for gluconeogenesis when pyruvate availability is low [384]. In the literature, serum acetate was significantly decreased in APOE-/- mice compared to controls on a regular diet, and it remained

decreased when given a HFD for 4 and 8 weeks [357]. Additionally, hepatic acetate levels were reduced in APOE-/- mice on HFD compared to C57BL/6J mice on normal diet, and reduced acetate seen in a hamster model of diet-induced atherosclerosis [365, 368]. Therefore, the reduced acetate in the APOE-/- mice in this chapter agrees with the existing literature. There does not seem to be existing literature on the effect of L:L on acetate levels. However, acetate is impacted by the interaction between L:L and genotype like its precursor pyruvate. Therefore, the interaction between L:L and genotype seems to have an impact on carbohydrate metabolism and FA metabolism. Additionally, acetate levels have moderate negative correlations with behaviour in the LDB and the OFT. This could be through the role of acetate in the TCA cycle, or in FA synthesis.

For the first time it was shown that scyllo-inositol levels were significantly increased by both genotype and L:L. Scyllo-inositol is one of eight naturally occurring stereoisomers of inositol, and the second most abundant form found in the brain after myo-inositol, accounting for around 10% of brain inositol content [385]. Inositols are cyclic sugar-like alcohols that are produced from glucose 6-phosphate [386]. They can cross the BBB and have a diverse array of functions, including acting as second messengers of the insulin-signalling pathway and as antioxidants [387-389]. Myo-inositol has been a focus of research as a treatment for insulin resistance [388, 390, 391]. In humans with atherosclerosis, myo-inositol was found to be directly associated with coronary artery calcium (CAC) in a study using cohort data from MESA, the Rotterdam study and LOLIPOP [354]. In APOE-/- mice on a HFD, serum levels of myo-inositol were elevated at 2, 4 and 8 weeks compared to control APOE-/- mice on regular chow [356]. Looking at the brain in humans using *in vivo* ^{1}H-magnetic resonance spectroscopy, Voila et al., found elevated levels of scyllo-inositol in the brains of non-detoxified chronic alcoholics [392]. The authors hypothesised that there was a defect in the glycolysis pathway in the brain, leading to an accumulation of glucose which was channelled to the pathway of scyllo-inositol synthesis [392]. Significantly elevated scyllo-inositol levels were also reported in the brains of patients with Alzheimer's

disease, but not in patients with mild cognitive impairment, indicating that there are distinct metabolic differences between the two conditions [393]. There is a lack of literature that has examined the effect of circadian disruption on inositol levels, and in the limited studies available investigating constant light exposure and its effect on the metabolome, inositols have not been identified. However, as L:L exposure causes oxidative stress, and scyllo-inositol has antioxidant activity, scyllo-inositol levels may increase as a compensatory mechanism to maintain oxidative stress. Additionally, as metabolites related to glycolysis are altered by L:L and genotype, it may be that the glucose-inositol pathway is upregulated to compensate.

ATP levels (both adenosine and ribose moieties) were decreased by both genotype and light, driven by the two L:L groups having lower ATP levels than the control group. ATP is the energy currency of the cell, produced by glucose metabolism via four metabolic processes – glycolysis, tricarboxylic acid cycle (TCA), OXPHOS, and in anaerobic conditions, lactic fermentation [394]. Glycolysis and lactic fermentation occur independently of mitochondria, whilst the TCA and OXPHOS, where the majority of ATP is generated, are mitochondria dependent [394]. ATP is in an area of the NMR spectra that isn't often investigated. Alterations in ATP levels have not been reported or investigated in the APOE-/- model or in atherosclerosis, however, altered pyruvate, lactate, acetate and scyllo-inositol levels as mentioned above indicate a disturbance in carbohydrate metabolism, which would impact ATP production, as substrates for mitochondrial OXPHOS are reduced. Again, there are limited studies looking at the impact of L:L, but Yang et al., report that ATP levels were significantly reduced in flies exposed to constant blue light for 14 days compared to controls in normal light [366]. Looking at circadian disruption, as L:L is a circadian disruptor, C57BL/6J mice that were exposed to a jetlag protocol had lower cellular ATP levels than the control mice on a normal L:D regimen [395]. As the substrates for the TCA cycle are affected by L:L and genotype, this likely has a knock-on effect on OXPHOS and so likely cause the reduced

ATP levels. Additionally, L:L causes oxidative stress, which has an effect on mitochondrial function and could be the cause of reduced ATP levels in L:L. ATP levels show circadian rhythmicity, driven by mitochondrial OXPHOS, and a loss of rhythmicity in OXPHOS or mitochondria may reduce ATP levels [396, 397]. Interestingly, ATP has a moderate negative correlation with circadian period, indicating that altered energy metabolism underlies the changes in period seen in L:L and the APOE-/- genotype.

Given the changes seen in the metabolome across tissues due to the APOE-/- genotype, and the existing literature, it can be concluded that glycolysis, both aerobic and anaerobic, is downregulated or defective in the APOE-/- model, leading to downregulation of the TCA cycle, OXPHOS and reduction in ATP production. This is supported by the positive correlation between lactate and ATP. Additionally, other pyruvate pathways are also impacted and downregulated. The accumulation of glucose is then channelled into scyllo-inositol production. Tzoulaki et al concluded that glycolysis was a central pathway associated with atherosclerosis [354]. Additionally, Teul et al concluded that in patients with atherosclerosis, glucose transport to the cytosol, pyruvate production from glycolysis and glycogenolysis was decreased, and glycogenogenesis and gluconeogenesis was increased [355]. Yang et al., also concluded that glycolysis was downregulated in atherosclerosis, based on the reduction in levels of lactate and pyruvate [356]. Additionally, the negative correlation between pyruvate and scyllo-inositol supports this theory. The interaction of L:L with the APOE-/- genotype also downregulates glycolysis and impacts pyruvate generation. L:L seems to increase the levels of metabolites with antioxidant activity, potentially as a compensatory mechanism to maintain redox homeostasis.

Redox homeostasis, the balance between pro- and antioxidants, was altered by L:L exposure, as seen by changes in glutathione, ascorbate and hypoxanthine levels. Prooxidants include ROS, which are naturally generated in tissues with high metabolic activity. ROS include free radicals, highly reactive molecules with an unpaired electron

such as hydroxyl (OH•), and non-radical oxidants, such as hydrogen peroxide (H_2O_2). ROS react with biological macromolecules by donating an unpaired electron, or removing an electron from the macromolecule, leading to chain reactions of radical generation and significant damage. Antioxidants are both enzymatic, i.e. free radical scavenging enzymes such as superoxide dismutases (SODs), and non-enzymatic, i.e. radical-scavenging chemicals such as Vitamin E and C (ascorbic acid). [155]. Antioxidant enzymes catalyse multiple reactions to convert ROS to stable molecules such as water and oxygen [398]. Non-enzymatic antioxidants can directly inactivate ROS. When there is homeostasis between prooxidants and antioxidants, free-radical chain reactions are usually prevented.

Glutathione levels were increased by L:L. Glutathione is a potent non enzymatic antioxidant, synthesized primarily in the liver from three constituent amino acids, glutamate, cysteine and glycine [399]. It has many essential roles, including protecting mitochondria against prooxidants generated by the electron transport chain [399]. It can react directly as an antioxidant and act as a co-factor for other enzymatic antioxidants. Elevation of glutathione levels would not necessarily be expected in the presence of ROS. Indeed, exposure to unpredictable varied L:D cycles for 40 days reduced glutathione levels [400]. However, drosophila exposed to blue light for 14 days showed elevated glutathione levels [366]. It may be that there is a time-dependent change in glutathione levels, where they are first elevated and then as the stressor becomes more chronic, glutathione is unable to be produced at the same rate, resulting in reduced levels. The changes in glutathione levels may be due to GCL activity, it was shown that incubation with a substance that induces ROS increased glutathione levels by increasing GCL activity, potentially through post-translational oxidative modifications to GCL [401]. This could be part of a feedback mechanism to try and maintain redox homeostasis. Interestingly, glutathione correlated with behavioural outcomes. There was a strong positive correlation with circadian period and a moderate positive correlation with circadian phase. This indicates that the L:L induced changes in period and phase are

associated with oxidative stress. Additionally, total mean velocity in the home cage behaviour had a moderate negative correlation with glutathione, again indicating that the L:L induced reduction in velocity is associated with oxidative stress.

Here, it was shown for the first time that ascorbate levels were significantly decreased by L:L. Ascorbate is a non-enzymatic antioxidant and free radical scavenger [402]. It can donate an electron to stabilise ROS, and once oxidised, can be reduced by glutathione [399]. Ascorbate has been shown to ameliorate oxidative stress caused by hypoxanthine and correlation analyses showed a moderate positive correlation between ascorbate and hypoxanthine [403]. L:L exposure may increase the breakdown of ATP to hypoxanthine, leading to increased oxidation of hypoxanthine to xanthine and uric acid, leading to both reduced hypoxanthine levels and the production of hydrogen peroxide and superoxide. Ascorbate levels may then decrease in compensation, due to non-enzymatic reduction of these free radicals into water, itself becoming oxidised to monodehydroascorbate [404]. Alternatively, light may reduce ascorbate levels, leading to increased activity of xanthine oxidase and oxidative stress.

Hypoxanthine was significantly decreased by L:L, which has not been shown before. Hypoxanthine is a purine derivative, and a breakdown product of adenosine and therefore of ATP, which is seen with a moderate positive correlation [405]. It can act as a substrate for xanthine oxidase, which catalyses the oxidation of hypoxanthine to xanthine and uric acid, generating reactive oxygen species (ROS) [406]. Hypoxanthine has been shown to accumulate in ischaemic tissues and is thought to convert to xanthine upon oxygen returning to the tissue, leading to hydrogen peroxide and superoxide generation [407-409]. Generation of these free radicals is modified by the antioxidant action of ascorbate [410]. Increased levels of hypoxanthine are associated with cardiac ischaemia, diabetes, and other metabolic disturbances [411, 412]. However, here hypoxanthine levels are decreased. Circadian disruption with light at night increases the activity of xanthine oxidase [413]. Increased xanthine oxidase activity explains the reduced hypoxanthine

levels seen here.

Abnormal exposure to visible light has been shown to significantly increase ROS generation and lipid peroxidation and dysregulate mitochondria [414-417]. Here, it seems that oxidative stress increases the rate of glutathione synthesis, possibly as a regulatory mechanism. Additionally, ascorbate levels are decreased, likely in response to L:L-induced oxidative stress. Glutathione and ascorbate have a compensatory relationship, and are negatively correlated, indicating that increased glutathione levels may also be compensatory for reduced ascorbate levels [418]. ROS generation is increased in L:L, as seen in reduced hypoxanthine levels which are likely due to increased activity of xanthine oxidase.

Lipid metabolism is affected by the interaction between L:L and the APOE-/- genotype, L:L and the APOE-/- genotype, as seen by changes in lipoproteins, triglycerides, choline, trimethylamine and β-hydroxybutyrate. Additionally, metabolites involved in lipid metabolism have strong correlates with behavioural outcomes, including circadian period, amplitude, the LDB and the OFT, indicating that altered lipid transport may lead to behavioural abnormalities.

In the APOE-/- model, there is a very high plasma lipid content which affects the resulting ^{1}H NMR spectra. The lipid content induces broad peaks, an unstable baseline and overlaps with resonances of low mw metabolites. Data from Soininen et al., and in-house correlation data was used to assign lipoproteins in the ^{1}H NMR plasma spectra [419].

Levels of LDL and triglycerides were increased in both APOE-/- model and L:L. α-CH_2 has a strong correlation with LDL and triglycerides, and is likely to be a part of LDL, or other pro-atherogenic lipoproteins like VLDL and IDL. Increased LDL and non-HDL cholesterol is a risk factor for atherosclerosis and therefore CVD, especially when HDL cholesterol is also decreased [420]. Additionally, triglycerides are an independent risk factor for CVD [421]. They are a neutral storage form of FA and are primarily transported in triglyceride-

rich lipoproteins (VLDL and chylomicrons) [422]. APOE-/- mice are known to exhibit hypercholesterolaemia on a regular chow diet, exhibiting increased total plasma cholesterol levels with lower HDL levels and higher VLDL, IDL and LDL levels compared to controls [423-426]. They also exhibit increased triglyceride levels [424, 426]. This is because ApoB (which is the main apolipoprotein in LDL) has two isoforms, B-100 and B-48, a truncated form of B-100 which doesn't contain the LDL-receptor binding region [426, 427]. In wildtype mice, the ration of APOB-48 to APOB-100 is 1:1. However, in APOE-/- mice, the ratio is altered, changing the ratio of ApoB-48 to ApoB-100 to 20:1 [424]. In wildtype mice, VLDL and IDL contain mostly B48 and clearance relies almost entirely on APOE, and only LDL clearance relies on APOB [426]. In APOE-/- mice, APOB is the main method of clearance of VLDL, IDL and LDL, and given that most APOB in APOE-/- mice is APOB-48, lipoprotein clearance by the liver is severely impaired [428]. Therefore, the result in this chapter was expected, due to the absence of APOE, and the alteration in APOB-48 to APOB-100 ratio. Looking in the literature at the impact of L:L on cholesterol and lipoproteins, it was shown that APOE−/− mice exposed to L:L for days had increased total serum cholesterol, caused by increased VLDL/LDL particles, compared to control male APOE−/− mice in LD [209]. However, L:L did not alter the total serum triglycerides concentration in that study [209]. Additionally, in the APOE*3-Leiden.CETP mouse model, which is used a model of human-like lipid metabolism and atherosclerosis, mice in L:L showed significantly higher plasma cholesterol over the period of the 14 week study compared to mice in LD, with both groups being fed a western-type diet (WTD) [283]. Furthermore, non-HDL cholesterol was also increased by L:L exposure in this model [283]. In 6-week-old C57BL/6J mice exposed to L:L for 90 days, there was a significant increase in total cholesterol and triglycerides in the serum compared to the control group in normal LD [429]. Similar results were seen in Wistar rats, 3-month-old rats were exposed to L:L for 7 days, and exhibited significantly higher LDL cholesterol levels and significantly lower HDL cholesterol levels compared to control rats in LD [430]. The LDL identified on the ^{1}H NMR spectra is likely a mix of native LDL and Ox-LDL. Ox-LDL has

been shown to be a valid marker of oxidative stress, and therefore increased LDL may be due to the oxidative stress induced by L:L [431]. LDL and triglycerides and α-CH_2 showed strong positive correlations with circadian period, indicating that abnormalities in lipid transport and homeostasis may lengthen circadian period, or occur as a consequence of lengthened circadian period.

HDL levels were affected by the interaction between genotype and L:L across the three spectral bins identified by PLS-DA. This has not been reported before. Genotype also reduced HDL levels at 5.26-5.28ppm and 0.82-0.84ppm, and L:L reduced HDL levels at 0.82-0.84ppm. Reduced HDL cholesterol is a risk factor for CVD [432, 433]. APOE-/- mice have lower HDL cholesterol levels than wildtype mice and have significantly altered, lipid poor, HDL particles [434, 435]. In mice, APOE plays a significant role in the metabolism of APOA-I containing HDL particles [435, 436]. In the absence of APOE, HDL particles are poorly lipidated, which is thought to impact their function. HDL cholesterol has antioxidant properties and can inhibit lipid peroxidation [437]. However, it can also undergo oxidative modifications which impact function, including reverse cholesterol transport, and is associated with increased lipid peroxidation [438, 439]. As mentioned above, L:L exposure increases non-HDL cholesterol in rodents, altering the ratio with HDL, and can decrease HDL levels. This could be because L:L induces oxidation of HDL, changing its structure and impacting function. This may explain the interaction between L:L and genotype seen, and the decrease in HDL induced by L:L at 0.82-0.84ppm. HDL had strong negative correlations with locomotor activity in the open field, and moderate negative correlations with circadian period, activity bout length, frequency of visits into the light (LDB) and the duration spent in the light (LDB). This lends further support to the hypothesis that aberrant lipid transport in the CNS underlies the alterations seen in locomotor behaviour and circadian behaviour. Interestingly, HDL also correlated with the measurement of drinking.

=CH-CH_2=CH_2- levels were reduced with L:L exposure. This has not been reported

before. =CH-CH_2=CH_2- is likely a PUFA. PUFAs are abundant in phospholipid bilayers and are therefore important structural components of cellular and intracellular membranes. They are also components of cholesterol particles. They are susceptible to lipid peroxidation because hydrogen is easily abstracted from the double bonds in the FA chains by free radicals [440]. L:L can induce lipid peroxidation of PUFAs, leading to free radical mediated chain reactions and ultimately apoptosis [441]. This can explain why =CH-CH_2=CH_2- levels are reduced by L:L. Additionally, =CH-CH_2=CH_2- levels had moderate negative correlations with locomotor activity in the OFT and home cage behaviour and circadian amplitude, as well as moderate positive correlations with change in body mass, circadian period and phase. This again supports the hypothesis that L:L exerts its effects by induction of oxidative stress.

Choline in the liver was reduced by L:L exposure. This is the first time that this result has been reported. Choline is an essential nutrient and has multiple biological roles, including acetylcholine synthesis, phospholipid formation for cell and mitochondrial membranes, lipoprotein formation and synthesis of S-adenosylmethionine, a source of methyl groups [442]. Reduced choline levels impact mitochondrial structure and function, and FA β-oxidation [443]. Mitochondria in choline deficient hepatocytes generate increased ROS, as their membranes are choline deficient and so are hyperpermeable, leading to increased oxidative stress and further damage to the mitochondria [443]. L:L likely reduces hepatic choline levels by inducing lipid peroxidation, which damages the phospholipid membranes which contain choline. Choline has moderate and strong positive correlations with locomotor activity in the home cage environment, and a moderate negative correlation with circadian phase. Additionally, a strong negative correlation with *Rxr-a* indicates that choline is associated with the L:L induced suppression of FA β-oxidation. This indicates that mitochondrial function is likely impaired and is connected to behavioural alterations.

Trimethylamine and free choline in the plasma were reduced by both the APOE-/-

genotype and L:L. Trimethylamine is a microbial breakdown product of carnitine, betaine and choline, which are sourced from diets rich in animal proteins [444]. Trimethylamine is absorbed and metabolised into trimethylamine N-oxide (TMAO). This metabolic pathway has been identified to contribute to the pathogenesis of CVD and atherosclerosis [444]. TMAO is shown to promote foam cell formation and reduce reverse cholesterol formation at the site of atherosclerotic plaques [445]. In APOE-/- mice, choline levels began to decrease at 4 weeks on a HFD, compared to APOE-/- mice on a regular diet, indicating altered phospholipid metabolism in HFD-induced atherosclerosis development [356]. There have been no previous reports of alterations in trimethylamine and free choline levels due to L:L. TMAO is also associated with vascular oxidative stress and has been shown to induce oxidative stress [446]. Reduced trimethylamine and free choline seen here could indicate increased production of the atherogenic and prooxidant TMAO in both the APOE-/- model and L:L-induced oxidative stress. Additionally, trimethylamine and free choline levels have moderate negative correlations with multiple behavioural outcomes: locomotor activity in the OFT, behaviour in the LDB, circadian period and drinking behaviour in the home cage environment. This indicates that choline and choline breakdown, and therefore mitochondrial function is linked to the behavioural changes reported here

β-hydroxybutyrate was significantly decreased by genotype and significantly increased by L:L. The effect of L:L on β-hydroxybutyrate levels has not been shown before. β-hydroxybutyrate is the most abundant mammalian ketone body, produced in the liver from Acetyl-CoA via FA β-oxidation during fasting or intense exercise [447]. It can be an alternate energy source in place of glucose in the brain, heart and skeletal muscle [448]. It is distributed to metabolically active tissues and metabolised to Acetyl-CoA to enter the TCA and produce ATP [449]. When given exogenously to APOE-/- mice, 100 mg $kg^{-1}d^{-1}$ of β-hydroxybutyrate reduced atherogenesis compared to controls, measured by looking at lesion areas, intraplaque macrophage infiltration, and lipid deposition in the plaque of

the aortic roots, indicating that β-hydroxybutyrate is protective against atherosclerosis [447]. In humans with atherosclerosis, β-hydroxybutyrate is directly associated with CAC and intracranial internal carotid artery calcification (ICAC), and indirectly associated with IMT [354, 355]. Therefore, a decrease in β-hydroxybutyrate may be part of the mechanism of atherosclerosis progression, a consequence of reduced Acetyl-CoA production due to reduced pyruvate metabolism as discussed above, or due to reduced FA β-oxidation. In Chapter 4.3, alterations in genes involved in lipid metabolism were seen in APOE-/- mice and it was hypothesised that lipid accumulation in the hepatocytes overloaded the mitochondria and led to altered FA β-oxidation and oxidative stress. β-hydroxybutyrate is also a histone deacetylase inhibitor. Application has been shown to protect mitochondria against oxidative stress damage, improve mitochondrial function and induce expression of antioxidant genes in rat myocardial cells [450]. β-hydroxybutyrate has also been shown to be protective against lipid peroxidation [451]. Therefore, its increase in L:L may be a compensatory response to ameliorate oxidative stress and maintain redox homeostasis, or a way to compensate for oxidative stress-induced lipid accumulation. Additionally, β-hydroxybutyrate and HDL showed strong negative correlations with locomotor activity in the OFT, and moderate negative correlations with behaviour in the LDB, locomotor activity in the home cage environment, drinking behaviour in the home cage environment, activity bout length and circadian amplitude, again implying that alterations in lipid transport and homeostasis may underlie the behavioural changes seen here.

Both L:L and the APOE-/- genotype induce an atherogenic lipoprotein profile. L:L induces oxidative stress, which is key for the development of atherosclerosis. Additionally, APOE-/- mice have impaired lipoprotein clearance, leading to lipid accumulation and the development of atherosclerosis. L:L also causes lipid peroxidation, increasing ROS and leading to mitochondrial dysfunction. In the APOE-/- mice, correlation analyses indicate that the alterations in lipid metabolism underlie the behavioural changes seen in Chapter

3.3. Diets high in saturated fat have been shown to increase anxiety- and depressive- like behaviour [452]. Knockout of the lipolysis-stimulated lipoprotein receptor (LSR) led to altered behaviour, including hyperactivity, as well as dysregulated cholesterol metabolism [453]. Additionally, it has been shown that administration of LDL, but not HDL ameliorates sickness behaviour induced by LPS [454].

5.4 Conclusions

This has been the first time the interaction between L:L and the APOE-/- genotype has been investigated using multi-organ metabolomics. This gene-environment interaction altered the levels of plasma HDL, acetate and pyruvate; as well as brain lactate, alanine and glutamate. These results indicate that there is an alteration in carbohydrate metabolism and reverse cholesterol transport. Additionally, L:L altered plasma levels of αCH_2 lipoprotein, =CH-CH2=CH2- lipoprotein, β-hydroxybutyrate and HDL, HDL, LDL and triglyceride and trimethylamine and free choline; as well as brain levels of ATP adenosine, ATP ribose, alanine, hypoxanthine, scyllo-inositol, ascorbate and levels of liver glutathione and choline. In addition, the APOE-/- genotype affected the levels of plasma αCH_2 lipoprotein, β-hydroxybutyrate and HDL, HDL, LDL and triglyceride, acetate and trimethylamine and free choline; as well as levels of brain ATP adenosine, ATP ribose, lactate and scyllo-inositol. Collectively, these results indicate that both L:L and the APOE-/- genotype and their interaction cause alterations in energy metabolism through the pathways of carbohydrate and lipid metabolism, and L:L also alters redox homeostasis. These changes in energy metabolism indicate altered mitochondrial function. There are reduced substrates for OXPHOS, there is reduced FA β-oxidation, lipid and cholesterol accumulation and increased ROS and lipid peroxidation. Behavioural hyperactivity is connected to lipid metabolism and is likely due to abnormal lipid transport in the CNS.

.

.

6 General Discussion

The overarching aim of this thesis was to investigate the gene-environment interaction between circadian disruption and CVD, using the APOE-/- mouse model and L:L, employing behavioural, molecular, histological, and metabolomic methods.

In the first aim, differences in behaviour and molecular biology were assessed in the APOE-/- model compared to controls. APOE-/- mice consistently exhibited heightened locomotor activity, with alterations in behavioural rhythms and circadian period. Distinct changes in sleep patterns were observed along with variations in energy metabolism, characterized by increased food intake without a corresponding change in weight. Furthermore, the mice demonstrated increased anxiety-like behaviour. It was concluded that impaired CNS cholesterol transport underlies the hyperactivity seen in the APOE-/- model.

The second aim focused on investigating how L:L exposure differentially effects behaviour, molecular biology, and the glial cell response in APOE-/- mouse model. Results showed that L:L exposure induced an altered metabolic state, affected glial cell response, and led to changes in behavioural circadian rhythms and sleep. It was concluded that these effects were likely mediated through lipid accumulation, oxidative stress, and the loss of the anti-inflammatory actions of APOE.

For the third aim, the effect of the gene-environment interaction between L:L and the APOE-/- model on the metabolome of the plasma, brain and liver was investigated to identify metabolic pathways underlying the changes seen in Chapters 3 and 4. The gene-environment interaction led to altered carbohydrate metabolism and reverse cholesterol transport. Additionally, both L:L and the APOE-/- caused alterations in energy metabolism through the pathways of carbohydrate and lipid metabolism, and L:L also altered redox homeostasis. Correlation analyses highlighted the connection between abnormal lipid

metabolism and behaviour. Mitochondrial function was implicated as an underlying connecting pathway.

Mitochondria have a significant role energy metabolism, as they are the site of the TCA cycle and OXPHOS, as well as the site of lipid degradation through fatty acid β-oxidation and ketogenesis [455, 456]. Carbohydrate metabolism, including glycolysis, the TCA cycle and OXPHOS was downregulated by the gene-environment interaction between L:L and the APOE-/- model as well as the APOE-/- model, indicating reduced mitochondrial energy substrate availability, and reduced mitochondria energy generation.

Fatty acid β-oxidation, and the synthesis of lipids, TGs and cholesterol were shown to be suppressed by L:L, APOE-/- and the interaction between the two. Additionally, both L:L exposure and the APOE-/- genotype showed alterations in lipid metabolism to a pro-atherogenic state. Abnormal lipid metabolism can result in mitochondrial overload and lead to mitochondrial dysfunction, further supporting a role for mitochondrial dysfunction in the gene-environment interaction [457].

Furthermore, L:L is known to induce oxidative stress, and oxidative stress is involved in atherosclerosis development [17, 156, 157]. Oxidative stress markers were altered at the metabolite and mRNA level, and it was hypothesised that astrocyte morphology was altered by L:L through oxidative stress. Mitochondria are known to be vulnerable to oxidative stress as they constantly generate ROS during respiratory oxidative phosphorylation (OXPHOS). When redox homeostasis is lost, ROS can cause damage to mitochondrial DNA (mtDNA) which leads to mitochondrial dysfunction, increased oxidative stress, lipid peroxidation of the mitochondrial inner membrane, mitochondrial calcium overload and cell death [458].

Behavioural changes caused by the absence of APOE were hypothesised to be caused by abnormal cholesterol transport in the CNS, and correlation analyses showed strong correlations between lipid metabolism and behaviour. Cholesterol accumulation has a

negative impact on mitochondrial function, and mitochondrial function is associated with behavioural differences in mice [459, 460]. Additionally, APOE-/- mice show differences in mitochondrial proteins [461]. Therefore, it is likely that mitochondrial alterations are involved in the innate behavioural differences shown in the APOE-/- mice.

Future research is needed to understand the mechanisms and pathophysiology of mitochondrial dysfunction and how it connects to CVD and circadian disruption, and whether targeting mitochondrial dysfunction can ameliorate the risk of CVD.

Future work and limitations

It would be interesting to do further home cage behaviour analysis in L:D, D:D and L:L to assess interaction of the endogenous rhythms of APOE-/- mice with their behaviour, such as the timing of drinking and eating, to further investigate the changes in body mass and drinking behaviour. Additionally, performing an electrophysiological assessment of sleep to investigate the changes in sleep seen in Chapters 3 and 4 would be really fascinating, as this has not been done in the APOE-/- model, and it would shed light on mechanisms by which altered CNS lipid transport affects sleep. Furthermore, it would be useful to investigate mitochondrial structure and activity to understand how the gene-environment interaction between L:L and the APOE-/- model might alter mitochondrial function. This could be done using immunohistochemistry and metabolomic analyses, as well as the Seahorse assay. It would also be interesting to use a brain-specific conditional APOE knockout model to assess the contribution of lipid accumulation in the periphery to the brain and behavioural changes seen here.

The gene expression results in L:L were only at one time point, rather than examining the circadian rhythm of expression. This means that it is difficult to draw conclusions about circadian changes in these genes. However, the n number would have needed to be significantly higher in order to have a high experimental power for using multiple time

points, which went against principles of the 3Rs in animal research and wasn't feasible with the timescale of the experiment.

The metabolomics analysis had limitations, as the NMR spectra was split into automatic bins, which often split the peaks of metabolites. However, automatic binning ensures that results are repeatable and reliable, as manually binning the spectra is less reproducible. A targeted analysis to investigate the changes in one or several metabolic pathways would shed light on where the changes reported in Chapter 5 are occurring, for example in a particular enzymatic reaction. Additionally, it would be interesting to use ^{13}C tracking to follow exactly how the carbohydrate metabolism pathway is changed in the APOE-/- model and with L:L, and to confirm whether glucose is funnelled down the inositol production pathway [462].

Another limitation of this study was that only male mice were used, as Chalfant et al., demonstrated that L:L only exacerbated atherosclerosis in male mice [209], and the study would have required significantly more mice to increase the power for assessing sex differences. This would have gone against the principles of the 3Rs in animal research as well as being very expensive. However, investigating sex differences would be valuable, as the literature indicates that there are sex differences in behaviour in APOE-/- mice [209, 225, 233, 238].

Final remarks

This thesis investigated the gene-environment interaction between circadian disruption and cardiovascular disease (CVD) using the APOE-/- mouse model. Results suggest that this interaction leads to increased dyslipidaemia, which correlates strongly with behavioural changes; reduced lipid and glucose metabolism, leading to lipid overload in cells and increased oxidative stress, indicating dysfunctional mitochondria. Future work is necessary to understand whether mitochondrial function is affected by this gene-

environment interaction, and whether this can lead to advances in treatment and diagnostics.

References

[1] L. Lundberg, "Effect of exposure to electromagnetic fields on brain function and behaviour in mice," University of Oxford, 2017.

[2] J. C. Ong and M. Park, "Chronic headaches and insomnia: Working toward a biobehavioral model," *Cephalalgia,* vol. 32, no. 14, pp. 1059-1070, 2012, doi: 10.1177/0333102412455709.

[3] R. Grippo and A. Guler, "Dopamine Signaling in Circadian Photoentrainment: Consequences of Desynchrony," *The Yale journal of biology and medicine,* vol. 92, pp. 271-281, 06/27 2019.

[4] G. A. Roth *et al.*, "Global, Regional, and National Burden of Cardiovascular Diseases for 10 Causes, 1990 to 2015," *Journal of the American College of Cardiology,* vol. 70, no. 1, pp. 1-25, 2017/07/04/ 2017, doi: https://doi.org/10.1016/j.jacc.2017.04.052.

[5] B. H. Foundation, "BHF UK CVD Factsheet [Fact sheet]," 2023. [Online]. Available: https://www.bhf.org.uk/-/media/files/for-professionals/research/heart-statistics/bhf-cvd-statistics-uk-factsheet.pdf

[6] W. Herrington, B. Lacey, P. Sherliker, J. Armitage, and S. Lewington, "Epidemiology of Atherosclerosis and the Potential to Reduce the Global Burden of Atherothrombotic Disease," *Circulation Research,* vol. 118, no. 4, pp. 535-546, 2016, doi: doi:10.1161/CIRCRESAHA.115.307611.

[7] Joseph L. Goldstein and Michael S. Brown, "A Century of Cholesterol and Coronaries: From Plaques to Genes to Statins," *Cell,* vol. 161, no. 1, pp. 161-172, 2015, doi: 10.1016/j.cell.2015.01.036.

[8] J. E. Muller *et al.*, "Circadian Variation in the Frequency of Onset of Acute Myocardial Infarction," *New England Journal of Medicine,* vol. 313, no. 21, pp. 1315-1322, 1985, doi: 10.1056/nejm198511213132103.

[9] M. Millar-Craig, C. Bishop, and E. B. Raftery, "CIRCADIAN VARIATION OF BLOOD-PRESSURE," *The Lancet,* vol. 311, no. 8068, pp. 795-797, 1978/04/15/ 1978, doi: https://doi.org/10.1016/S0140-6736(78)92998-7.

[10] G. H. Tofler *et al.*, "Concurrent Morning Increase in Platelet Aggregability and the Risk of Myocardial Infarction and Sudden Cardiac Death," *New England Journal of Medicine,* vol. 316, no. 24, pp. 1514-1518, 1987, doi: 10.1056/nejm198706113162405.

[11] M. F. Hilton, M. U. Umali, C. A. Czeisler, J. K. Wyatt, and S. A. Shea, "Endogenous circadian control of the human autonomic nervous system," (in eng), *Comput Cardiol,* vol. 27, pp. 197-200, 2000.

[12] R. Manfredini *et al.*, "Daylight Saving Time and Acute Myocardial Infarction: A Meta-Analysis," *Journal of Clinical Medicine,* vol. 8, no. 3, p. 404, 2019. [Online]. Available: https://www.mdpi.com/2077-0383/8/3/404.

[13] P. M. Wong, B. P. Hasler, T. W. Kamarck, M. F. Muldoon, and S. B. Manuck, "Social Jetlag, Chronotype, and Cardiometabolic Risk," *The Journal of Clinical Endocrinology & Metabolism,* vol. 100, no. 12, pp. 4612-4620, 2015, doi: 10.1210/jc.2015-2923.

[14] B. Karlsson, A. Knutsson, and B. Lindahl, "Is there an association between shift work and having a metabolic syndrome? Results from a population based study of 27 485 people," *Occupational and Environmental Medicine,* vol. 58, no. 11, pp. 747-752, 2001, doi: 10.1136/oem.58.11.747.

[15] S. Puttonen, M. Härmä, and C. Hublin, "Shift work and cardiovascular disease - pathways from circadian stress to morbidity," (in eng), *Scand J Work Environ Health,* vol. 36, no. 2, pp. 96-108, Mar 2010, doi: 10.5271/sjweh.2894.

[16] E. Falk, "Pathogenesis of Atherosclerosis," *Journal of the American College of Cardiology,* vol. 47, no. 8, Supplement, pp. C7-C12, 2006/04/18/ 2006, doi: https://doi.org/10.1016/j.jacc.2005.09.068.

[17] C. Khatana *et al.*, "Mechanistic Insights into the Oxidized Low-Density Lipoprotein-Induced Atherosclerosis," *Oxidative Medicine and Cellular Longevity,* vol. 2020, p. 5245308, 2020/09/15 2020, doi: 10.1155/2020/5245308.

[18] P. Libby, Andrew H. Lichtman, and Göran K. Hansson, "Immune Effector Mechanisms Implicated in Atherosclerosis: From Mice to Humans," *Immunity,* vol. 38, no. 6, pp. 1092-1104, 2013, doi: 10.1016/j.immuni.2013.06.009.

[19] C. K. Glass and J. L. Witztum, "Atherosclerosis: The Road Ahead," *Cell,* vol. 104, no. 4, pp. 503-516, 2001, doi: 10.1016/S0092-8674(01)00238-0.

[20] D. A. Chistiakov, I. A. Sobenin, and A. N. Orekhov, "Vascular Extracellular Matrix in Atherosclerosis," *Cardiology in Review,* vol. 21, no. 6, pp. 270-288, 2013, doi: 10.1097/CRD.0b013e31828c5ced.

[21] A. J. Kattoor, N. V. K. Pothineni, D. Palagiri, and J. L. Mehta, "Oxidative Stress in Atherosclerosis," *Current Atherosclerosis Reports,* vol. 19, no. 11, p. 42, 2017/09/18 2017, doi: 10.1007/s11883-017-0678-6.

[22] Z. S. Galis *et al.*, "Cytokine-stimulated human vascular smooth muscle cells synthesize a complement of enzymes required for extracellular matrix digestion," *Circulation Research,* vol. 75, no. 1, pp. 181-189, 1994, doi: doi:10.1161/01.RES.75.1.181.

[23] T. Huff, B. Boyd, and I. Jialal, "Physiology, Cholesterol," in *StatPearls*. Treasure Island (FL) ineligible companies. Disclosure: Brandon Boyd declares no relevant financial relationships with ineligible companies. Disclosure: Ishwarlal Jialal declares no relevant financial relationships with ineligible companies.: StatPearls Publishing
Copyright © 2023, StatPearls Publishing LLC., 2023.

[24] R. W. Mahley, T. L. Innerarity, S. C. Rall, Jr., and K. H. Weisgraber, "Plasma lipoproteins: apolipoprotein structure and function," (in eng), *J Lipid Res,* vol. 25, no. 12, pp. 1277-94, Dec 1 1984.

[25] L. S. Ang, Cruz, Rani P., Hendel, Alon., Granville, David J. , "Apolipoprotein E, an important player in longevity and age-related diseases," *Experimental Gerontology,* vol. 43, no. 7, pp. 615-622, 2008, doi: https://doi.org/10.1016/j.exger.2008.03.010.

[26] L. Zhou *et al.*, "Degeneration and energy shortage in the suprachiasmatic nucleus underlies the circadian rhythm disturbance in ApoE−/− mice: implications for Alzheimer's disease," *Scientific Reports,* vol. 6, no. 1, p. 36335, 2016/11/08 2016, doi: 10.1038/srep36335.

[27] D. Bhatnagar, J. Schofield, and H. Soran, "Chapter 14 - Genetic disorders of lipoprotein metabolism," in *Clinical Molecular Medicine*, D. Kumar Ed.: Academic Press, 2020, pp. 245-265.

[28] M. H. Dominiczak and M. J. Caslake, "Apolipoproteins: metabolic role and clinical biochemistry applications," *Annals of Clinical Biochemistry,* vol. 48, no. 6, pp. 498-515, 2011, doi: 10.1258/acb.2011.011111.

[29] H. N. Ginsberg, "Lipoprotein metabolism and its relationship to atherosclerosis," *Medical Clinics of North America,* vol. 78, no. 1, pp. 1-20, 1994/01/01/ 1994, doi: https://doi.org/10.1016/S0025-7125(16)30174-2.

[30] K. R. Feingold, "Introduction to Lipids and Lipoproteins," in *Endotext*, K. R. Feingold *et al.* Eds. South Dartmouth (MA): MDText.com, Inc.
Copyright © 2000-2023, MDText.com, Inc., 2000.

[31] A. M. Gotto, H. J. Pownall, and R. J. Havel, "[1] Introduction to the plasma lipoproteins," in *Methods in Enzymology*, vol. 128: Academic Press, 1986, pp. 3-41.

[32] P. Srisawasdi *et al.*, "Heterogeneous properties of intermediate- and low-density lipoprotein subpopulations," *Clinical Biochemistry,* vol. 46, no. 15, pp. 1509-1515, 2013/10/01/ 2013, doi: https://doi.org/10.1016/j.clinbiochem.2013.06.021.

[33] R. W. Mahley, "Apolipoprotein E: from cardiovascular disease to neurodegenerative disorders," *Journal of Molecular Medicine,* vol. 94, no. 7, pp. 739-746, 2016/07/01 2016, doi: 10.1007/s00109-016-1427-y.

[34] A. Mehta and M. D. Shapiro, "Apolipoproteins in vascular biology and atherosclerotic disease," *Nature Reviews Cardiology,* vol. 19, no. 3, pp. 168-179, 2022/03/01 2022, doi: 10.1038/s41569-021-00613-5.

[35] O. Gursky, "Apolipoprotein structure and dynamics," *Current Opinion in Lipidology,* vol. 16, no. 3, pp. 287-294, 2005, doi: 10.1097/01.mol.0000169348.61191.ac.

[36] J. Borén, M.-R. Taskinen, and M. Adiels, "Kinetic studies to investigate lipoprotein metabolism," *Journal of Internal Medicine,* vol. 271, no. 2, pp. 166-173, 2012, doi: https://doi.org/10.1111/j.1365-2796.2011.02497.x.

[37] A. D. Marais, "Apolipoprotein E in lipoprotein metabolism, health and cardiovascular disease," *Pathology,* vol. 51, no. 2, pp. 165-176, 2019/02/01/ 2019, doi: https://doi.org/10.1016/j.pathol.2018.11.002.

[38] M. C. Phillips, "Apolipoprotein E isoforms and lipoprotein metabolism," *IUBMB Life,* vol. 66, no. 9, pp. 616-623, 2014, doi: https://doi.org/10.1002/iub.1314.

[39] M. H. Moghadasian *et al.*, "Pathophysiology of apolipoprotein E deficiency in mice: relevance to apo E-related disorders in humans," *The FASEB Journal,* vol. 15, no. 14, pp. 2623-2630, 2001, doi: https://doi.org/10.1096/fj.01-0463com.

[40] J. A. Piedrahita, S. H. Zhang, J. R. Hagaman, P. M. Oliver, and N. Maeda, "Generation of mice carrying a mutant apolipoprotein E gene inactivated by gene targeting in embryonic stem cells," (in eng), *Proc Natl Acad Sci U S A,* vol. 89, no. 10, pp. 4471-4475, 1992/05// 1992, doi: 10.1073/pnas.89.10.4471.

[41] T. Yamamoto, H. W. Choi, and R. O. Ryan, "Apolipoprotein E isoform-specific binding to the low-density lipoprotein receptor," (in eng), *Anal Biochem,* vol. 372, no. 2, pp. 222-6, Jan 15 2008, doi: 10.1016/j.ab.2007.09.005.

[42] N. Zhao, C.-C. Liu, W. Qiao, and G. Bu, "Apolipoprotein E, Receptors, and Modulation of Alzheimer's Disease," *Biological Psychiatry,* vol. 83, no. 4, pp. 347-357, 2018/02/15/ 2018, doi: https://doi.org/10.1016/j.biopsych.2017.03.003.

[43] M. L. Blue, D. L. Williams, S. Zucker, S. A. Khan, and C. B. Blum, "Apolipoprotein E synthesis in human kidney, adrenal gland, and liver," (in eng), *Proc Natl Acad Sci U S A,* vol. 80, no. 1, pp. 283-287, 1983/01// 1983, doi: 10.1073/pnas.80.1.283.

[44] N. A. Elshourbagy, W. S. Liao, R. W. Mahley, and J. M. Taylor, "Apolipoprotein E mRNA is abundant in the brain and adrenals, as well as in the liver, and is present in other peripheral tissues of rats and marmosets," *Proceedings of the National Academy of Sciences,* vol. 82, no. 1, pp. 203-207, 1985, doi: doi:10.1073/pnas.82.1.203.

[45] R. W. Mahley, "Central Nervous System Lipoproteins," *Arteriosclerosis, Thrombosis, and Vascular Biology,* vol. 36, no. 7, pp. 1305-1315, 2016, doi: doi:10.1161/ATVBAHA.116.307023.

[46] R. E. Pitas, J. K. Boyles, S. H. Lee, D. Foss, and R. W. Mahley, "Astrocytes synthesize apolipoprotein E and metabolize apolipoprotein E-containing lipoproteins," *Biochimica et Biophysica Acta (BBA) - Lipids and Lipid Metabolism,* vol. 917, no. 1, pp. 148-161, 1987/01/13/ 1987, doi: https://doi.org/10.1016/0005-2760(87)90295-5.

[47] M. Liu, D. G. Kuhel, L. Shen, D. Y. Hui, and S. C. Woods, "Apolipoprotein E does not cross the blood-cerebrospinal fluid barrier, as revealed by an improved technique for sampling CSF from mice," (in eng), *Am J Physiol Regul Integr Comp Physiol,* vol. 303, no. 9, pp. R903-8, Nov 1 2012, doi: 10.1152/ajpregu.00219.2012.

[48] M. F. Linton *et al.*, "Phenotypes of apolipoprotein B and apolipoprotein E after liver transplantation," *The Journal of Clinical Investigation,* vol. 88, no. 1, pp. 270-281, 07/01/ 1991, doi: 10.1172/JCI115288.

[49] J. K. Boyles, R. E. Pitas, E. Wilson, R. W. Mahley, and J. M. Taylor, "Apolipoprotein E associated with astrocytic glia of the central nervous system and with nonmyelinating glia of the peripheral nervous system," *The Journal of Clinical Investigation,* vol. 76, no. 4, pp. 1501-1513, 10/01/ 1985, doi: 10.1172/JCI112130.

[50] Q. Xu, A. Bernardo, D. Walker, T. Kanegawa, R. W. Mahley, and Y. Huang, "Profile and Regulation of Apolipoprotein E (ApoE) Expression in the CNS in Mice with Targeting of Green Fluorescent Protein Gene to the ApoE Locus," *The Journal of Neuroscience,* vol. 26, no. 19, pp. 4985-4994, 2006, doi: 10.1523/jneurosci.5476-05.2006.

[51] R. E. Pitas, J. K. Boyles, S. H. Lee, D. Hui, and K. H. Weisgraber, "Lipoproteins and their receptors in the central nervous system. Characterization of the lipoproteins in cerebrospinal fluid and identification of apolipoprotein B,E(LDL) receptors in the brain," (in eng), *J Biol Chem,* vol. 262, no. 29, pp. 14352-60, Oct 15 1987.

[52] S. E. Wahrle *et al.*, "ABCA1 Is Required for Normal Central Nervous System ApoE Levels and for Lipidation of Astrocyte-secreted apoE*," *Journal of Biological Chemistry,* vol. 279, no. 39, pp. 40987-40993, 2004/09/24/ 2004, doi: https://doi.org/10.1074/jbc.M407963200.

[53] G. J. Snipes, C. B. McGuire, J. J. Norden, and J. A. Freeman, "Nerve injury stimulates the secretion of apolipoprotein E by nonneuronal cells," *Proceedings of the National Academy of Sciences,* vol. 83, no. 4, pp. 1130-1134, 1986, doi: doi:10.1073/pnas.83.4.1130.

[54] M. J. Ignatius *et al.*, "Expression of apolipoprotein E during nerve degeneration and regeneration," *Proceedings of the National Academy of Sciences,* vol. 83, no. 4, pp. 1125-1129, 1986, doi: doi:10.1073/pnas.83.4.1125.

[55] H. Hayashi, R. B. Campenot, D. E. Vance, and J. E. Vance, "Glial Lipoproteins Stimulate Axon Growth of Central Nervous System Neurons in Compartmented Cultures*," *Journal of Biological Chemistry,* vol. 279, no. 14, pp. 14009-14015, 2004/04/02/ 2004, doi: https://doi.org/10.1074/jbc.M313828200.

[56] D. H. Mauch *et al.*, "CNS Synaptogenesis Promoted by Glia-Derived Cholesterol," *Science,* vol. 294, no. 5545, pp. 1354-1357, 2001, doi: doi:10.1126/science.294.5545.1354.

[57] X. Li *et al.*, "Astrocytic ApoE reprograms neuronal cholesterol metabolism and histone-acetylation-mediated memory," *Neuron,* vol. 109, no. 6, pp. 957-970.e8, 2021, doi: 10.1016/j.neuron.2021.01.005.
[58] K. Nieweg, H. Schaller, and F. W. Pfrieger, "Marked differences in cholesterol synthesis between neurons and glial cells from postnatal rats," *Journal of Neurochemistry,* vol. 109, no. 1, pp. 125-134, 2009, doi: https://doi.org/10.1111/j.1471-4159.2009.05917.x.
[59] C. G. Fernandez, M. E. Hamby, M. L. McReynolds, and W. J. Ray, "The Role of APOE4 in Disrupting the Homeostatic Functions of Astrocytes and Microglia in Aging and Alzheimer's Disease," (in English), *Frontiers in Aging Neuroscience,* Review vol. 11, 2019-February-11 2019, doi: 10.3389/fnagi.2019.00014.
[60] P. Abondio *et al.*, "The Genetic Variability of APOE in Different Human Populations and Its Implications for Longevity," *Genes,* vol. 10, no. 3, p. 222, 2019. [Online]. Available: https://www.mdpi.com/2073-4425/10/3/222.
[61] L. A. Farrer *et al.*, "Effects of Age, Sex, and Ethnicity on the Association Between Apolipoprotein E Genotype and Alzheimer Disease: A Meta-analysis," *JAMA,* vol. 278, no. 16, pp. 1349-1356, 1997, doi: 10.1001/jama.1997.03550160069041.
[62] F. J. Wolters *et al.*, "The impact of APOE genotype on survival: Results of 38,537 participants from six population-based cohorts (E2-CHARGE)," *PLOS ONE,* vol. 14, no. 7, p. e0219668, 2019, doi: 10.1371/journal.pone.0219668.
[63] T. A. Khan *et al.*, "Apolipoprotein E genotype, cardiovascular biomarkers and risk of stroke: Systematic review and meta-analysis of 14 015 stroke cases and pooled analysis of primary biomarker data from up to 60 883 individuals," *International Journal of Epidemiology,* vol. 42, no. 2, pp. 475-492, 2013, doi: 10.1093/ije/dyt034.
[64] J. L. Breslow, V. I. Zannis, T. R. SanGiacomo, J. L. Third, T. Tracy, and C. J. Glueck, "Studies of familial type III hyperlipoproteinemia using as a genetic marker the apoE phenotype E2/2," (in eng), *J Lipid Res,* vol. 23, no. 8, pp. 1224-35, Nov 1982.
[65] R. W. Mahley, Y. Huang, and S. C. Rall, Jr., "Pathogenesis of type III hyperlipoproteinemia (dysbetalipoproteinemia): questions, quandaries, and paradoxes," *Journal of Lipid Research,* vol. 40, no. 11, pp. 1933-1949, 1999, doi: 10.1016/S0022-2275(20)32417-2.
[66] M. de Andrade, I. Thandi, S. Brown, A. Gotto, Jr., W. Patsch, and E. Boerwinkle, "Relationship of the apolipoprotein E polymorphism with carotid artery atherosclerosis," (in eng), *Am J Hum Genet,* vol. 56, no. 6, pp. 1379-90, Jun 1995.
[67] D. Marais, "Dysbetalipoproteinemia: an extreme disorder of remnant metabolism," *Current Opinion in Lipidology,* vol. 26, no. 4, pp. 292-297, 2015, doi: 10.1097/mol.0000000000000192.
[68] A. M. Saunders *et al.*, "Association of apolipoprotein E allele ϵ4 with late-onset familial and sporadic Alzheimer's disease," *Neurology,* vol. 43, no. 8, pp. 1467-1467, 1993, doi: 10.1212/wnl.43.8.1467.
[69] E. H. Corder *et al.*, "Gene Dose of Apolipoprotein E Type 4 Allele and the Risk of Alzheimer's Disease in Late Onset Families," *Science,* vol. 261, no. 5123, pp. 921-923, 1993, doi: doi:10.1126/science.8346443.
[70] L. Wu and L. Zhao, "ApoE2 and Alzheimer's disease: time to take a closer look," *Neural Regeneration Research,* vol. 11, no. 3, pp. 412-413, 2016, doi: 10.4103/1673-5374.179044.
[71] E. Kok *et al.*, "Apolipoprotein E–dependent accumulation of Alzheimer disease–related lesions begins in middle age," *Annals of Neurology,* vol. 65, no. 6, pp. 650-657, 2009, doi: https://doi.org/10.1002/ana.21696.
[72] P. Tiraboschi, L. A. Hansen, E. Masliah, M. Alford, L. J. Thal, and J. Corey-Bloom, "Impact of APOE genotype on neuropathologic and neurochemical markers of Alzheimer disease," *Neurology,* vol. 62, no. 11, pp. 1977-1983, 2004, doi: 10.1212/01.Wnl.0000128091.92139.0f.
[73] A. S. Plump, C. J. Scott, and J. L. Breslow, "Human apolipoprotein A-I gene expression increases high density lipoprotein and suppresses atherosclerosis in the apolipoprotein E-deficient mouse," (in eng), *Proc Natl Acad Sci U S A,* vol. 91, no. 20, pp. 9607-11, Sep 27 1994, doi: 10.1073/pnas.91.20.9607.
[74] A. S. Plump and J. L. Breslow, "Apolipoprotein E and the Apolipoprotein E-Deficient Mouse," *Annual Review of Nutrition,* vol. 15, no. 1, pp. 495-518, 1995, doi: 10.1146/annurev.nu.15.070195.002431.
[75] G. Lo Sasso, W. K. Schlage, S. Boué, E. Veljkovic, M. C. Peitsch, and J. Hoeng, "The Apoe−/− mouse model: a suitable model to study cardiovascular and respiratory diseases

in the context of cigarette smoke exposure and harm reduction," *Journal of Translational Medicine,* vol. 14, no. 1, p. 146, 2016/05/20 2016, doi: 10.1186/s12967-016-0901-1.

[76] J. L. Breslow, "Mouse Models of Atherosclerosis," *Science,* vol. 272, no. 5262, pp. 685-688, 1996, doi: 10.1126/science.272.5262.685.

[77] M. A. Said, N. Verweij, and P. van der Harst, "Associations of Combined Genetic and Lifestyle Risks With Incident Cardiovascular Disease and Diabetes in the UK Biobank Study," *JAMA Cardiology,* vol. 3, no. 8, pp. 693-702, 2018, doi: 10.1001/jamacardio.2018.1717.

[78] A. Bhatnagar, "Environmental Determinants of Cardiovascular Disease," *Circulation Research,* vol. 121, no. 2, pp. 162-180, 2017, doi: doi:10.1161/CIRCRESAHA.117.306458.

[79] J. A. Hartiala, J. R. Hilser, S. Biswas, A. J. Lusis, and H. Allayee, "Gene-Environment Interactions for Cardiovascular Disease," *Current Atherosclerosis Reports,* vol. 23, no. 12, p. 75, 2021/10/14 2021, doi: 10.1007/s11883-021-00974-9.

[80] R. M. Voigt, Forsyth, C. B., Green, S. J., Engen, P. A., Keshavarzian, A., "Circadian Rhythm and the Gut Microbiome,," in *Gut Microbiome and Behaviour*, vol. 131, G. C. J.F. Cryan Ed. International Review of Neurobiology, Academic Press, 2016, ch. Nine, pp. 193-205.

[81] D.-J. Dijk and M. von Schantz, "Timing and Consolidation of Human Sleep, Wakefulness, and Performance by a Symphony of Oscillators," *Journal of Biological Rhythms,* vol. 20, no. 4, pp. 279-290, 2005, doi: 10.1177/0748730405278292.

[82] R. E. Mistlberger, "Neurobiology of food anticipatory circadian rhythms," *Physiology & Behavior,* vol. 104, no. 4, pp. 535-545, 2011/09/26/ 2011, doi: https://doi.org/10.1016/j.physbeh.2011.04.015.

[83] K. L. Gamble, R. Berry, S. J. Frank, and M. E. Young, "Circadian clock control of endocrine factors," *Nature Reviews Endocrinology,* vol. 10, no. 8, pp. 466-475, 2014/08/01 2014, doi: 10.1038/nrendo.2014.78.

[84] D. Weinert, "Circadian temperature variation and ageing," *Ageing Research Reviews,* vol. 9, no. 1, pp. 51-60, 2010/01/01/ 2010, doi: https://doi.org/10.1016/j.arr.2009.07.003.

[85] Y. H. Kim and M. A. Lazar, "Transcriptional Control of Circadian Rhythms and Metabolism: A Matter of Time and Space," *Endocrine Reviews,* vol. 41, no. 5, pp. 707-732, 2020, doi: 10.1210/endrev/bnaa014.

[86] C. Scheiermann, Y. Kunisaki, and P. S. Frenette, "Circadian control of the immune system," *Nature Reviews Immunology,* vol. 13, no. 3, pp. 190-198, 2013/03/01 2013, doi: 10.1038/nri3386.

[87] J. Aschoff, "Exogenous and endogenous components in circadian rhythms," (in eng), *Cold Spring Harb Symp Quant Biol,* vol. 25, pp. 11-28, 1960, doi: 10.1101/sqb.1960.025.01.004.

[88] M. U. Gillette, "SCN Electrophysiology In Vitro; Rhythmic Activity and Endogenous Clock Properties," in *Suprachiasmatic Nucleus: The Mind's Clock*, R. Y. M. a. S. M. R. D.C. Klein Ed. New York, NY: Oxford University Press, 1991, ch. 6, pp. pp. 125-143.

[89] S.-H. Yoo *et al.*, "PERIOD2::LUCIFERASE real-time reporting of circadian dynamics reveals persistent circadian oscillations in mouse peripheral tissues," *Proceedings of the National Academy of Sciences,* vol. 101, no. 15, pp. 5339-5346, 2004, doi: doi:10.1073/pnas.0308709101.

[90] E. D. Buhr and J. S. Takahashi, "Molecular Components of the Mammalian Circadian Clock," in *Circadian Clocks*, A. Kramer and M. Merrow Eds. Berlin, Heidelberg: Springer Berlin Heidelberg, 2013, pp. 3-27.

[91] C. L. Partch, C. B. Green, and J. S. Takahashi, "Molecular architecture of the mammalian circadian clock," *Trends in Cell Biology,* vol. 24, no. 2, pp. 90-99, 2014, doi: 10.1016/j.tcb.2013.07.002.

[92] R. Zhang, N. F. Lahens, H. I. Ballance, M. E. Hughes, and J. B. Hogenesch, "A circadian gene expression atlas in mammals: Implications for biology and medicine," *Proceedings of the National Academy of Sciences,* vol. 111, no. 45, pp. 16219-16224, 2014, doi: doi:10.1073/pnas.1408886111.

[93] G. E. Duffield, "DNA Microarray Analyses of Circadian Timing: The Genomic Basis of Biological Time," *Journal of Neuroendocrinology,* vol. 15, no. 10, pp. 991-1002, 2003, doi: https://doi.org/10.1046/j.1365-2826.2003.01082.x.

[94] I. K. Sundar, H. Yao, M. T. Sellix, and I. Rahman, "Circadian molecular clock in lung pathophysiology," *American Journal of Physiology-Lung Cellular and Molecular Physiology,* vol. 309, no. 10, pp. L1056-L1075, 2015, doi: 10.1152/ajplung.00152.2015.

[95] E. Maury, "Off the Clock: From Circadian Disruption to Metabolic Disease," *Int. J. Mol. Sci.,* vol. 20, no. 7, 2019.
[96] A. M. Schroeder and C. S. Colwell, "How to fix a broken clock," *Trends in Pharmacological Sciences,* vol. 34, no. 11, pp. 605-619, 2013, doi: 10.1016/j.tips.2013.09.002.
[97] D. A. Golombek and R. E. Rosenstein, "Physiology of Circadian Entrainment," *Physiological Reviews,* vol. 90, no. 3, pp. 1063-1102, 2010, doi: 10.1152/physrev.00009.2009.
[98] B. M. Gabriel and J. R. Zierath, "Circadian rhythms and exercise — re-setting the clock in metabolic disease," *Nature Reviews Endocrinology,* vol. 15, no. 4, pp. 197-206, 2019/04/01 2019, doi: 10.1038/s41574-018-0150-x.
[99] J. J. Bennie, J. P. Duffy, R. Inger, and K. J. Gaston, "Biogeography of time partitioning in mammals," *Proceedings of the National Academy of Sciences,* vol. 111, no. 38, pp. 13727-13732, 2014, doi: doi:10.1073/pnas.1216063110.
[100] W.-J. A. Remé CE, Terman M., " The Visual Input Stage of the Mammalian Circadian Pacemaking System: I. Is There a Clock in the Mammalian Eye?," *Journal of Biological Rhythms,* vol. 6, no. 1, pp. 5-29, 1991, doi: 10.1177/074873049100600104.
[101] J. A. Mohawk, C. B. Green, and J. S. Takahashi, "Central and Peripheral Circadian Clocks in Mammals," *Annual Review of Neuroscience,* vol. 35, no. 1, pp. 445-462, 2012, doi: 10.1146/annurev-neuro-060909-153128.
[102] R. Y. Moore and N. J. Lenn, "A retinohypothalamic projection in the rat," *Journal of Comparative Neurology,* vol. 146, no. 1, pp. 1-14, 1972, doi: https://doi.org/10.1002/cne.901460102.
[103] D. M. Berson, F. A. Dunn, and M. Takao, "Phototransduction by Retinal Ganglion Cells That Set the Circadian Clock," *Science,* vol. 295, no. 5557, pp. 1070-1073, 2002, doi: doi:10.1126/science.1067262.
[104] S. Hattar, H.-W. Liao, M. Takao, D. M. Berson, and K.-W. Yau, "Melanopsin-Containing Retinal Ganglion Cells: Architecture, Projections, and Intrinsic Photosensitivity," *Science,* vol. 295, no. 5557, pp. 1065-1070, 2002, doi: doi:10.1126/science.1069609.
[105] M. T. H. Do and K.-W. Yau, "Intrinsically Photosensitive Retinal Ganglion Cells," *Physiological Reviews,* vol. 90, no. 4, pp. 1547-1581, 2010, doi: 10.1152/physrev.00013.2010.
[106] F. J. P. Ebling, "The role of glutamate in the photic regulation of the suprachiasmatic nucleus," *Progress in Neurobiology,* vol. 50, no. 2, pp. 109-132, 1996/10/01/ 1996, doi: https://doi.org/10.1016/S0301-0082(96)00032-9.
[107] A. Ramkisoensing and J. H. Meijer, "Synchronization of Biological Clock Neurons by Light and Peripheral Feedback Systems Promotes Circadian Rhythms and Health," (in English), *Frontiers in Neurology,* Review vol. 6, no. 128, 2015-June-05 2015, doi: 10.3389/fneur.2015.00128.
[108] S. B. Khalsa, M. E. Jewett, C. Cajochen, and C. A. Czeisler, "A phase response curve to single bright light pulses in human subjects," (in eng), *J Physiol,* vol. 549, no. Pt 3, pp. 945-52, Jun 15 2003, doi: 10.1113/jphysiol.2003.040477.
[109] P. J. De Coursey, "Daily Light Sensitivity Rhythm in a Rodent," *Science,* vol. 131, no. 3392, pp. 33-35, 1960, doi: 10.1126/science.131.3392.33.
[110] A. M. Rosenwasser and S. M. Dwyer, "Circadian phase shifting: Relationships between photic and nonphotic phase–response curves," *Physiology & Behavior,* vol. 73, no. 1, pp. 175-183, 2001/05/01/ 2001, doi: https://doi.org/10.1016/S0031-9384(01)00466-8.
[111] J. H. Meijer and W. J. Schwartz, "In Search of the Pathways for Light-Induced Pacemaker Resetting in the Suprachiasmatic Nucleus," *Journal of Biological Rhythms,* vol. 18, no. 3, pp. 235-249, 2003, doi: 10.1177/0748730403018003006.
[112] J. D. Plautz, M. Kaneko, J. C. Hall, and S. A. Kay, "Independent Photoreceptive Circadian Clocks Throughout Drosophila," *Science,* vol. 278, no. 5343, pp. 1632-1635, 1997, doi: doi:10.1126/science.278.5343.1632.
[113] E. D. Buhr, S.-H. Yoo, and J. S. Takahashi, "Temperature as a Universal Resetting Cue for Mammalian Circadian Oscillators," *Science,* vol. 330, no. 6002, pp. 379-385, 2010, doi: doi:10.1126/science.1195262.
[114] S. Amir and J. Stewart, "Resetting of the circadian clock by a conditioned stimulus," *Nature,* vol. 379, no. 6565, pp. 542-545, 1996/02/01 1996, doi: 10.1038/379542a0.
[115] R. Mistlberger and M. Antle, "Entrainment of circadian clocks in mammals by arousal and food," *Essays in biochemistry,* vol. 49, pp. 119-36, 06/30 2011, doi: 10.1042/bse0490119.

[116] L. P. Morin, "The circadian visual system," *Brain Research Reviews,* vol. 19, no. 1, pp. 102-127, 1994/01/01/ 1994, doi: https://doi.org/10.1016/0165-0173(94)90005-1.
[117] E. Meyer-Bernstein and L. Morin, "Differential serotonergic innervation of the suprachiasmatic nucleus and the intergeniculate leaflet and its role in circadian rhythm modulation," *The Journal of Neuroscience,* vol. 16, no. 6, pp. 2097-2111, 1996, doi: 10.1523/jneurosci.16-06-02097.1996.
[118] A. C. West and D. A. Bechtold, "The cost of circadian desynchrony: Evidence, insights and open questions," (in eng), *Bioessays,* vol. 37, no. 7, pp. 777-88, Jul 2015, doi: 10.1002/bies.201400173.
[119] K. Begemann, A.-M. Neumann, and H. Oster, "Regulation and function of extra-SCN circadian oscillators in the brain," *Acta Physiologica,* vol. 229, no. 1, p. e13446, 2020, doi: https://doi.org/10.1111/apha.13446.
[120] L. P. Morin, "Neuroanatomy of the extended circadian rhythm system," *Experimental Neurology,* vol. 243, pp. 4-20, 2013/05/01/ 2013, doi: https://doi.org/10.1016/j.expneurol.2012.06.026.
[121] A. Patke, M. W. Young, and S. Axelrod, "Molecular mechanisms and physiological importance of circadian rhythms," *Nature Reviews Molecular Cell Biology,* vol. 21, no. 2, pp. 67-84, 2020/02/01 2020, doi: 10.1038/s41580-019-0179-2.
[122] C. Cailotto *et al.*, "The suprachiasmatic nucleus controls the daily variation of plasma glucose via the autonomic output to the liver: are the clock genes involved?," *European Journal of Neuroscience,* vol. 22, no. 10, pp. 2531-2540, 2005, doi: https://doi.org/10.1111/j.1460-9568.2005.04439.x.
[123] A. Balsalobre, F. Damiola, and U. Schibler, "A Serum Shock Induces Circadian Gene Expression in Mammalian Tissue Culture Cells," *Cell,* vol. 93, no. 6, pp. 929-937, 1998, doi: 10.1016/S0092-8674(00)81199-X.
[124] U. Schibler and P. Sassone-Corsi, "A Web of Circadian Pacemakers," *Cell,* vol. 111, no. 7, pp. 919-922, 2002, doi: 10.1016/S0092-8674(02)01225-4.
[125] F. K. Stephan, J. M. Swann, and C. L. Sisk, "Entrainment of circadian rhythms by feeding schedules in rats with suprachiasmatic lesions," *Behavioral and Neural Biology,* vol. 25, no. 4, pp. 545-554, 1979/04/01/ 1979, doi: https://doi.org/10.1016/S0163-1047(79)90332-7.
[126] F. K. Stephan, "The “Other” Circadian System: Food as a Zeitgeber," *Journal of Biological Rhythms,* vol. 17, no. 4, pp. 284-292, 2002, doi: 10.1177/074873040201700402.
[127] K.-A. Stokkan, S. Yamazaki, H. Tei, Y. Sakaki, and M. Menaker, "Entrainment of the Circadian Clock in the Liver by Feeding," *Science,* vol. 291, no. 5503, pp. 490-493, 2001, doi: doi:10.1126/science.291.5503.490.
[128] F. Damiola, N. Le Minh, N. Preitner, B. Kornmann, F. Fleury-Olela, and U. Schibler, "Restricted feeding uncouples circadian oscillators in peripheral tissues from the central pacemaker in the suprachiasmatic nucleus," (in eng), *Genes Dev,* vol. 14, no. 23, pp. 2950-61, Dec 1 2000, doi: 10.1101/gad.183500.
[129] I. Kolbe, B. Leinweber, M. Brandenburger, and H. Oster, "Circadian clock network desynchrony promotes weight gain and alters glucose homeostasis in mice," (in eng), *Mol Metab,* vol. 30, pp. 140-151, Dec 2019, doi: 10.1016/j.molmet.2019.09.012.
[130] S. Yamazaki *et al.*, "Resetting Central and Peripheral Circadian Oscillators in Transgenic Rats," *Science,* vol. 288, no. 5466, pp. 682-685, 2000, doi: doi:10.1126/science.288.5466.682.
[131] B. Rasch and J. Born, "About sleep's role in memory," (in eng), *Physiol Rev,* vol. 93, no. 2, pp. 681-766, Apr 2013, doi: 10.1152/physrev.00032.2012.
[132] N. Niethard, M. Hasegawa, T. Itokazu, Carlos N. Oyanedel, J. Born, and Takashi R. Sato, "Sleep-Stage-Specific Regulation of Cortical Excitation and Inhibition," *Current Biology,* vol. 26, no. 20, pp. 2739-2749, 2016, doi: 10.1016/j.cub.2016.08.035.
[133] J. E. Zimmerman, N. Naidoo, D. M. Raizen, and A. I. Pack, "Conservation of sleep: insights from non-mammalian model systems," (in eng), *Trends Neurosci,* vol. 31, no. 7, pp. 371-6, Jul 2008, doi: 10.1016/j.tins.2008.05.001.
[134] S. Soltani *et al.*, "Sleep–Wake Cycle in Young and Older Mice," (in English), *Frontiers in Systems Neuroscience,* Original Research vol. 13, 2019-September-24 2019, doi: 10.3389/fnsys.2019.00051.
[135] L. D. Lewis, "The interconnected causes and consequences of sleep in the brain," *Science,* vol. 374, no. 6567, pp. 564-568, 2021, doi: doi:10.1126/science.abi8375.

[136] W. J. Schwartz and E. B. Klerman, "Circadian Neurobiology and the Physiologic Regulation of Sleep and Wakefulness," (in eng), *Neurol Clin,* vol. 37, no. 3, pp. 475-486, Aug 2019, doi: 10.1016/j.ncl.2019.03.001.
[137] A. A. Borbély, S. Daan, A. Wirz-Justice, and T. Deboer, "The two-process model of sleep regulation: a reappraisal," *Journal of Sleep Research,* vol. 25, no. 2, pp. 131-143, 2016, doi: 10.1111/jsr.12371.
[138] J. Aschoff, "Freerunning and Entrained Circadian Rhythms," in *Biological Rhythms*, J. Aschoff Ed. Boston, MA: Springer US, 1981, pp. 81-93.
[139] C. A. Czeisler *et al.*, "Stability, precision, and near-24-hour period of the human circadian pacemaker," (in eng), *Science,* vol. 284, no. 5423, pp. 2177-81, Jun 25 1999, doi: 10.1126/science.284.5423.2177.
[140] P. Sollars, D. Kimble, and G. Pickard, "Restoration of circadian behavior by anterior hypothalamic heterografts," *The Journal of Neuroscience,* vol. 15, no. 3, pp. 2109-2122, 1995, doi: 10.1523/jneurosci.15-03-02109.1995.
[141] J. Aschoff, "Circadian Rhythms: Influences of Internal and External Factors on the Period Measured in Constant Conditions1," *Zeitschrift für Tierpsychologie,* vol. 49, no. 3, pp. 225-249, 1979, doi: https://doi.org/10.1111/j.1439-0310.1979.tb00290.x.
[142] H. Ohta, S. Yamazaki, and D. G. McMahon, "Constant light desynchronizes mammalian clock neurons," (in eng), *Nat Neurosci,* vol. 8, no. 3, pp. 267-9, Mar 2005, doi: 10.1038/nn1395.
[143] C. Eastman and A. Rechtschaffen, "Circadian temperature and wake rhythms of rats exposed to prolonged continuous illumination," *Physiology & Behavior,* vol. 31, no. 4, pp. 417-427, 1983/10/01/ 1983, doi: https://doi.org/10.1016/0031-9384(83)90061-6.
[144] A. Báez-Ruiz *et al.*, "Food in synchrony with melatonin and corticosterone relieves constant light disturbed metabolism," (in English), *Journal of Endocrinology,* vol. 235, no. 3, pp. 167-178, 01 Dec. 2017 2017, doi: 10.1530/joe-17-0370.
[145] C. S. Pittendrigh and S. Daan, "A functional analysis of circadian pacemakers in nocturnal rodents," *Journal of comparative physiology,* vol. 106, no. 3, pp. 333-355, 1976/10/01 1976, doi: 10.1007/BF01417860.
[146] L. K. Fonken *et al.*, "Influence of light at night on murine anxiety- and depressive-like responses," (in eng), *Behav Brain Res,* vol. 205, no. 2, pp. 349-54, Dec 28 2009, doi: 10.1016/j.bbr.2009.07.001.
[147] J. Tchekalarova, L. Kortenska, N. Ivanova, M. Atanasova, and P. Marinov, "Agomelatine treatment corrects impaired sleep-wake cycle and sleep architecture and increases MT(1) receptor as well as BDNF expression in the hippocampus during the subjective light phase of rats exposed to chronic constant light," (in eng), *Psychopharmacology (Berl),* vol. 237, no. 2, pp. 503-518, Feb 2020, doi: 10.1007/s00213-019-05385-y.
[148] F. Hölker, T. Moss, B. Griefahn, W. Kloas, C. C. Voigt, D. Henckel, A. Hänel, P. M. Kappeler, S. Völker, A. Schwope, S. Franke, D. Uhrlandt, J. Fischer, R. Klenke, C. Wolter, and K. Tockner., "The dark side of light: a transdisciplinary research agenda for light pollution policy.," *Ecology and Society [online],* vol. 15, no. 13, 4, 2010. [Online]. Available: http://www.ecologyandsociety.org/vol15/iss4/art13/.
[149] A.-M. Chang, D. Aeschbach, J. F. Duffy, and C. A. Czeisler, "Evening use of light-emitting eReaders negatively affects sleep, circadian timing, and next-morning alertness," *Proceedings of the National Academy of Sciences,* vol. 112, no. 4, pp. 1232-1237, 2015, doi: 10.1073/pnas.1418490112.
[150] F. A. J. L. Scheer, M. F. Hilton, C. S. Mantzoros, and S. A. Shea, "Adverse metabolic and cardiovascular consequences of circadian misalignment," *Proceedings of the National Academy of Sciences,* vol. 106, no. 11, pp. 4453-4458, 2009, doi: doi:10.1073/pnas.0808180106.
[151] A. J. Davidson, M. T. Sellix, J. Daniel, S. Yamazaki, M. Menaker, and G. D. Block, "Chronic jet-lag increases mortality in aged mice," (in eng), *Curr Biol,* vol. 16, no. 21, pp. R914-6, Nov 7 2006, doi: 10.1016/j.cub.2006.09.058.
[152] G. Costa, "Shift work and occupational medicine: an overview," *Occupational Medicine,* vol. 53, no. 2, pp. 83-88, 2003, doi: 10.1093/occmed/kqg045.
[153] V. Rafnsson, H. Tulinius, J. G. Jónasson, and J. Hrafnkelsson, "Risk of breast cancer in female flight attendants: a population-based study (Iceland)," *Cancer Causes & Control,* vol. 12, no. 2, pp. 95-101, 2001/02/01 2001, doi: 10.1023/A:1008983416836.

[154] Y. Nakashima, S. Ohta, and A. M. Wolf, "Blue light-induced oxidative stress in live skin," (in eng), *Free Radic Biol Med,* vol. 108, pp. 300-310, Jul 2017, doi: 10.1016/j.freeradbiomed.2017.03.010.
[155] D. P. Jones, "Radical-free biology of oxidative stress," *American Journal of Physiology-Cell Physiology,* vol. 295, no. 4, pp. C849-C868, 2008, doi: 10.1152/ajpcell.00283.2008.
[156] S. G. Jarrett and M. E. Boulton, "Consequences of oxidative stress in age-related macular degeneration," *Molecular Aspects of Medicine,* vol. 33, no. 4, pp. 399-417, 2012/08/01/ 2012, doi: https://doi.org/10.1016/j.mam.2012.03.009.
[157] P. Pospíšil, A. Prasad, and M. Rác, "Role of reactive oxygen species in ultra-weak photon emission in biological systems," *Journal of Photochemistry and Photobiology B: Biology,* vol. 139, pp. 11-23, 2014/10/05/ 2014, doi: https://doi.org/10.1016/j.jphotobiol.2014.02.008.
[158] S. Steven *et al.*, "Vascular Inflammation and Oxidative Stress: Major Triggers for Cardiovascular Disease," *Oxidative Medicine and Cellular Longevity,* vol. 2019, p. 7092151, 2019/06/23 2019, doi: 10.1155/2019/7092151.
[159] A. van der Pol, W. H. van Gilst, A. A. Voors, and P. van der Meer, "Treating oxidative stress in heart failure: past, present and future," *European Journal of Heart Failure,* vol. 21, no. 4, pp. 425-435, 2019, doi: https://doi.org/10.1002/ejhf.1320.
[160] R. A. Cairns, I. S. Harris, and T. W. Mak, "Regulation of cancer cell metabolism," (in eng), *Nat Rev Cancer,* vol. 11, no. 2, pp. 85-95, Feb 2011, doi: 10.1038/nrc2981.
[161] D. M. Teleanu *et al.*, "An Overview of Oxidative Stress, Neuroinflammation, and Neurodegenerative Diseases," *International Journal of Molecular Sciences,* vol. 23, no. 11, p. 5938, 2022. [Online]. Available: https://www.mdpi.com/1422-0067/23/11/5938.
[162] M. N. Melissa Wilking, Hasan Mukhtar and Nihal Ahmad, "Circadian Rhythm Connections to Oxidative Stress: Implications for Human Health," *Antioxidants & Redox Signaling,* vol. 19, no. 2, pp. 192-208, 2013, doi: 10.1089/ars.2012.4889.
[163] C. S. McAlpine and F. K. Swirski, "Circadian Influence on Metabolism and Inflammation in Atherosclerosis," *Circulation Research,* vol. 119, no. 1, pp. 131-141, 2016, doi: doi:10.1161/CIRCRESAHA.116.308034.
[164] E. C.-P. Chua *et al.*, "Extensive diversity in circadian regulation of plasma lipids and evidence for different circadian metabolic phenotypes in humans," *Proceedings of the National Academy of Sciences,* vol. 110, no. 35, pp. 14468-14473, 2013, doi: doi:10.1073/pnas.1222647110.
[165] X. Pan, X.-C. Jiang, and M. M. Hussain, "Impaired Cholesterol Metabolism and Enhanced Atherosclerosis in Clock Mutant Mice," *Circulation,* vol. 128, no. 16, pp. 1758-1769, 2013, doi: doi:10.1161/CIRCULATIONAHA.113.002885.
[166] N. Covassin and P. Singh, "Sleep Duration and Cardiovascular Disease Risk: Epidemiologic and Experimental Evidence," (in eng), *Sleep Med Clin,* vol. 11, no. 1, pp. 81-9, Mar 2016, doi: 10.1016/j.jsmc.2015.10.007.
[167] M. R. Sands *et al.*, "Short Sleep Duration Is Associated With Carotid Intima-Media Thickness Among Men in the Coronary Artery Risk Development in Young Adults (CARDIA) Study," *Stroke,* vol. 43, no. 11, pp. 2858-2864, 2012, doi: doi:10.1161/STROKEAHA.112.660332.
[168] M. Fan *et al.*, "Sleep patterns, genetic susceptibility, and incident cardiovascular disease: a prospective study of 385 292 UK biobank participants," *European Heart Journal,* vol. 41, no. 11, pp. 1182-1189, 2019, doi: 10.1093/eurheartj/ehz849.
[169] J. Yin *et al.*, "Relationship of Sleep Duration With All-Cause Mortality and Cardiovascular Events: A Systematic Review and Dose-Response Meta-Analysis of Prospective Cohort Studies," (in eng), *J Am Heart Assoc,* vol. 6, no. 9, Sep 9 2017, doi: 10.1161/jaha.117.005947.
[170] L. A. F. Brown, A.S.; Pothecary, C.A.; Peirson, S.N., "Telling the Time with a Broken Clock: Quantifying Circadian Disruption in Animal Models.," *Biology,* vol. 8, no. 18, 2019.
[171] H. S. Brown LA, Foster RG and Peirson SN, "COMPASS: Continuous Open Mouse Phenotyping of Activity and Sleep Status," *Wellcome Open Res,* vol. 1, 2, 2017.
[172] A. I. Pack *et al.*, "Novel method for high-throughput phenotyping of sleep in mice," (in eng), *Physiological genomics,* vol. 28, no. 2, pp. 232-8, Jan 17 2007, doi: 10.1152/physiolgenomics.00139.2006.
[173] G. S. Fisher SP., Pothecary CA., Hankins MW., Foster RG., Peirson SN., "Rapid assessment of sleep-wake behavior in mice.," *J Biol Rhythms,* vol. 27, pp. 48-58, 2012.
[174] M. Haahr. "RANDOM.ORG: True Random Number Service." https://www.random.org (accessed June 27 2024).

[175] T. D. Gould, D. T. Dao, and C. E. Kovacsics, "The Open Field Test," in *Mood and Anxiety Related Phenotypes in Mice: Characterization Using Behavioral Tests*, T. D. Gould Ed. Totowa, NJ: Humana Press, 2009, pp. 1-20.
[176] M. Hascoët and M. Bourin, "The Mouse Light–Dark Box Test," in *Mood and Anxiety Related Phenotypes in Mice: Characterization Using Behavioral Tests*, T. D. Gould Ed. Totowa, NJ: Humana Press, 2009, pp. 197-223.
[177] T. Strekalova and H. Steinbusch, "Factors of Reproducibility of Anhedonia Induction in a Chronic Stress Depression Model in Mice," in *Mood and Anxiety Related Phenotypes in Mice: Characterization Using Behavioral Tests*, T. D. Gould Ed. Totowa, NJ: Humana Press, 2009, pp. 153-176.
[178] P. Willner, A. Towell, D. Sampson, S. Sophokleous, and R. Muscat, "Reduction of sucrose preference by chronic unpredictable mild stress, and its restoration by a tricyclic antidepressant," *Psychopharmacology,* vol. 93, no. 3, pp. 358-364, 1987/11/01 1987, doi: 10.1007/BF00187257.
[179] A. G. Yates, C. M. Weglinski, Y. Ying, I. K. Dunstan, T. Strekalova, and D. C. Anthony, "Nafamostat reduces systemic inflammation in TLR7-mediated virus-like illness," *Journal of Neuroinflammation,* vol. 19, no. 1, p. 8, 2022/01/06 2022, doi: 10.1186/s12974-021-02357-y.
[180] J. Ye, G. Coulouris, I. Zaretskaya, I. Cutcutache, S. Rozen, and T. L. Madden, "Primer-BLAST: A tool to design target-specific primers for polymerase chain reaction," *BMC Bioinformatics,* vol. 13, no. 1, p. 134, 2012/06/18 2012, doi: 10.1186/1471-2105-13-134.
[181] N. A. O'Leary *et al.*, "Reference sequence (RefSeq) database at NCBI: current status, taxonomic expansion, and functional annotation," (in eng), *Nucleic Acids Res,* vol. 44, no. D1, pp. D733-45, Jan 4 2016, doi: 10.1093/nar/gkv1189.
[182] W. A. Kibbe, "OligoCalc: an online oligonucleotide properties calculator," (in eng), *Nucleic Acids Res,* vol. 35, no. Web Server issue, pp. W43-6, Jul 2007, doi: 10.1093/nar/gkm234.
[183] J. Ji, S.-L. Hu, Z.-W. Cui, and W.-F. Li, "Probiotic Bacillus amyloliquefaciens mediate M1 macrophage polarization in mouse bone marrow-derived macrophages," *Archives of Microbiology,* vol. 195, no. 5, pp. 349-356, 2013/05/01 2013, doi: 10.1007/s00203-013-0877-7.
[184] D. H. Loh, C. Abad, C. S. Colwell, and J. A. Waschek, "Vasoactive intestinal peptide is critical for circadian regulation of glucocorticoids," (in eng), *Neuroendocrinology,* vol. 88, no. 4, pp. 246-55, 2008, doi: 10.1159/000140676.
[185] Z. Zhu *et al.*, "Altered Clock and Lipid Metabolism-Related Genes in Atherosclerotic Mice Kept with Abnormal Lighting Condition," *BioMed Research International,* vol. 2016, p. 5438589, 2016/08/18 2016, doi: 10.1155/2016/5438589.
[186] J.-K. Long, W. Dai, Y.-W. Zheng, and S.-P. Zhao, "miR-122 promotes hepatic lipogenesis via inhibiting the LKB1/AMPK pathway by targeting Sirt1 in non-alcoholic fatty liver disease," *Molecular Medicine,* vol. 25, no. 1, p. 26, 2019/06/13 2019, doi: 10.1186/s10020-019-0085-2.
[187] A. Dettlaff-Pokora, T. Sledzinski, and J. Swierczynski, "Up-Regulation Mttp and Apob Gene Expression in Rat Liver is Related to Post-Lipectomy Hypertriglyceridemia," (in eng), *Cell Physiol Biochem,* vol. 36, no. 5, pp. 1767-77, 2015, doi: 10.1159/000430149.
[188] N. Garay-Lugo *et al.*, "n-3 Fatty acids modulate the mRNA expression of the Nlrp3 inflammasome and Mtor in the liver of rats fed with high-fat or high-fat/fructose diets," *Immunopharmacology and Immunotoxicology,* vol. 38, no. 5, pp. 353-363, 2016/09/02 2016, doi: 10.1080/08923973.2016.1208221.
[189] E. Seo, H. Kang, H. Choi, W. Choi, and H.-S. Jun, "Reactive oxygen species-induced changes in glucose and lipid metabolism contribute to the accumulation of cholesterol in the liver during aging," *Aging Cell,* vol. 18, no. 2, p. e12895, 2019, doi: https://doi.org/10.1111/acel.12895.
[190] N. Nasiri-Ansari *et al.*, "Empagliflozin Attenuates Non-Alcoholic Fatty Liver Disease (NAFLD) in High Fat Diet Fed ApoE(-/-) Mice by Activating Autophagy and Reducing ER Stress and Apoptosis," *International Journal of Molecular Sciences,* vol. 22, no. 2, p. 818, 2021. [Online]. Available: https://www.mdpi.com/1422-0067/22/2/818.
[191] C. Vicente-Gutierrez *et al.*, "Astrocytic mitochondrial ROS modulate brain metabolism and mouse behaviour," *Nature Metabolism,* vol. 1, no. 2, pp. 201-211, 2019/02/01 2019, doi: 10.1038/s42255-018-0031-6.

[192] D. S. Wishart, "Emerging applications of metabolomics in drug discovery and precision medicine," *Nature Reviews Drug Discovery,* vol. 15, no. 7, pp. 473-484, 2016/07/01 2016, doi: 10.1038/nrd.2016.32.
[193] J. A. Aguilar *et al.*, "Reliable, high-quality suppression of NMR signals arising from water and macromolecules: application to bio-fluid analysis," (in eng), *Analyst,* vol. 144, no. 24, pp. 7270-7277, Dec 2 2019, doi: 10.1039/c9an01005j.
[194] *R: A language and environment for statistical computing.* (2021). R Foundation for Statistical Computing, Vienna, Austria. [Online]. Available: https://www.R-project.org/
[195] D. S. Wishart *et al.*, "HMDB 5.0: the Human Metabolome Database for 2022," (in eng), *Nucleic Acids Res,* vol. 50, no. D1, pp. D622-d631, Jan 7 2022, doi: 10.1093/nar/gkab1062.
[196] *R package "corrplot": Visualization of a Correlation Matrix*. (2017). [Online]. Available: https://github.com/taiyun/corrplot
[197] T. G. Brooks *et al.*, "Nitecap: An Exploratory Circadian Analysis Web Application," (in eng), *J Biol Rhythms,* vol. 37, no. 1, pp. 43-52, Feb 2022, doi: 10.1177/07487304211054408.
[198] P. F. Thaben and P. O. Westermark, "Detecting rhythms in time series with RAIN," (in eng), *J Biol Rhythms,* vol. 29, no. 6, pp. 391-400, Dec 2014, doi: 10.1177/0748730414553029.
[199] E. A. Thévenot, A. Roux, Y. Xu, E. Ezan, and C. Junot, "Analysis of the Human Adult Urinary Metabolome Variations with Age, Body Mass Index, and Gender by Implementing a Comprehensive Workflow for Univariate and OPLS Statistical Analyses," *Journal of Proteome Research,* vol. 14, no. 8, pp. 3322-3335, 2015/08/07 2015, doi: 10.1021/acs.jproteome.5b00354.
[200] M. Cortes-Canteli *et al.*, "Subclinical Atherosclerosis and Brain Metabolism in Middle-Aged Individuals: The PESA Study," *Journal of the American College of Cardiology,* vol. 77, no. 7, pp. 888-898, 2021/02/23/ 2021, doi: https://doi.org/10.1016/j.jacc.2020.12.027.
[201] A. E. Roher *et al.*, "Circle of Willis Atherosclerosis Is a Risk Factor for Sporadic Alzheimer's Disease," *Arteriosclerosis, Thrombosis, and Vascular Biology,* vol. 23, no. 11, pp. 2055-2062, 2003, doi: doi:10.1161/01.ATV.0000095973.42032.44.
[202] B. K. Marebwa *et al.*, "Cardiovascular Risk Factors and Brain Health: Impact on Long-Range Cortical Connections and Cognitive Performance," *Journal of the American Heart Association,* vol. 7, no. 23, p. e010054, 2018, doi: doi:10.1161/JAHA.118.010054.
[203] J. N. Crawley, "Behavioral Phenotyping Strategies for Mutant Mice," *Neuron,* vol. 57, no. 6, pp. 809-818, 2008, doi: 10.1016/j.neuron.2008.03.001.
[204] G. W. Rebeck, "The role of APOE on lipid homeostasis and inflammation in normal brains: Thematic Review Series: ApoE and Lipid Homeostasis in Alzheimer's Disease," *Journal of Lipid Research,* vol. 58, no. 8, pp. 1493-1499, 2017, doi: 10.1194/jlr.R075408.
[205] L. Chen and G. Yang, "Recent advances in circadian rhythms in cardiovascular system," (in eng), *Front Pharmacol,* vol. 6, p. 71, 2015, doi: 10.3389/fphar.2015.00071.
[206] K. J. Reid, "Assessment of Circadian Rhythms," (in eng), *Neurol Clin,* vol. 37, no. 3, pp. 505-526, Aug 2019, doi: 10.1016/j.ncl.2019.05.001.
[207] A. Mukherji, S. M. Bailey, B. Staels, and T. F. Baumert, "The circadian clock and liver function in health and disease," *Journal of Hepatology,* vol. 71, no. 1, pp. 200-211, 2019, doi: 10.1016/j.jhep.2019.03.020.
[208] R. Parsons, R. Parsons, N. Garner, H. Oster, and O. Rawashdeh, "CircaCompare: a method to estimate and statistically support differences in mesor, amplitude and phase, between circadian rhythms," *Bioinformatics,* vol. 36, no. 4, pp. 1208-1212, 2019, doi: 10.1093/bioinformatics/btz730.
[209] J. M. Chalfant, D. A. Howatt, L. R. Tannock, A. Daugherty, and J. S. Pendergast, "Circadian disruption with constant light exposure exacerbates atherosclerosis in male ApolipoproteinE-deficient mice," *Scientific Reports,* vol. 10, no. 1, p. 9920, 2020/06/18 2020, doi: 10.1038/s41598-020-66834-9.
[210] J. Aschoff, uuml, and rgen, "Masking and Parametric Effects of High-Frequency Light-Dark Cycles," *The Japanese Journal of Physiology,* vol. 49, no. 1, pp. 11-18, 1999, doi: 10.2170/jjphysiol.49.11.
[211] V. S. Valentinuzzi, K. Scarbrough, J. S. Takahashi, and F. W. Turek, "Effects of aging on the circadian rhythm of wheel-running activity in C57BL/6 mice," (in eng), *Am J Physiol,* vol. 273, no. 6, pp. R1957-64, Dec 1997, doi: 10.1152/ajpregu.1997.273.6.R1957.

[212] I. Griesauer *et al.*, "Circadian abnormalities in a mouse model of high trait anxiety and depression," *Annals of Medicine,* vol. 46, no. 3, pp. 148-154, 2014/05/01 2014, doi: 10.3109/07853890.2013.866440.
[213] J. W. S. Timothy *et al.*, "Circadian Disruptions in the Myshkin Mouse Model of Mania Are Independent of Deficits in Suprachiasmatic Molecular Clock Function," *Biological Psychiatry,* vol. 84, no. 11, pp. 827-837, 2018, doi: 10.1016/j.biopsych.2017.04.018.
[214] J. J. Graybeal *et al.*, "Human ApoE ε4 Alters Circadian Rhythm Activity, IL-1β, and GFAP in CRND8 Mice," *Journal of Alzheimer's Disease,* vol. 43, pp. 823-834, 2015, doi: 10.3233/JAD-132009.
[215] K. M. Full *et al.*, "Sleep Irregularity and Subclinical Markers of Cardiovascular Disease: The Multi-Ethnic Study of Atherosclerosis," *Journal of the American Heart Association,* vol. 12, no. 4, p. e027361, 2023, doi: doi:10.1161/JAHA.122.027361.
[216] F. Domínguez *et al.*, "Association of Sleep Duration and Quality With Subclinical Atherosclerosis," *Journal of the American College of Cardiology,* vol. 73, no. 2, pp. 134-144, 2019/01/22/ 2019, doi: https://doi.org/10.1016/j.jacc.2018.10.060.
[217] C. S. McAlpine *et al.*, "Sleep modulates haematopoiesis and protects against atherosclerosis," *Nature,* vol. 566, no. 7744, pp. 383-387, 2019/02/01 2019, doi: 10.1038/s41586-019-0948-2.
[218] B. Yang, H. Zhang, T. Jiang, and S. Yu, "Natural brain state change with E/I balance shifting toward inhibition is associated with vigilance impairment," *iScience,* vol. 26, no. 10, p. 107963, 2023/10/20/ 2023, doi: https://doi.org/10.1016/j.isci.2023.107963.
[219] G.-Z. Sun *et al.*, "Hippocampal synaptic and neural network deficits in young mice carrying the human APOE4 gene," *CNS Neuroscience & Therapeutics,* vol. 23, no. 9, pp. 748-758, 2017, doi: https://doi.org/10.1111/cns.12720.
[220] J. Lin *et al.*, "Defects in Adaptive Energy Metabolism with CNS-Linked Hyperactivity in PGC-1α Null Mice," *Cell,* vol. 119, no. 1, pp. 121-135, 2004, doi: 10.1016/j.cell.2004.09.013.
[221] L. Shen *et al.*, "Brain Apolipoprotein E: an Important Regulator of Food Intake in Rats," *Diabetes,* vol. 57, no. 8, pp. 2092-2098, 2008, doi: 10.2337/db08-0291.
[222] C. I. F. Janssen *et al.*, "The Effect of a High-Fat Diet on Brain Plasticity, Inflammation and Cognition in Female ApoE4-Knockin and ApoE-Knockout Mice," *PLOS ONE,* vol. 11, no. 5, p. e0155307, 2016, doi: 10.1371/journal.pone.0155307.
[223] D. Jansen *et al.*, "Impact of a multi-nutrient diet on cognition, brain metabolism, hemodynamics, and plasticity in apoE4 carrier and apoE knockout mice," *Brain Structure and Function,* vol. 219, no. 5, pp. 1841-1868, 2014/09/01 2014, doi: 10.1007/s00429-013-0606-7.
[224] J. Grootendorst, E. R. de Kloet, S. Dalm, and M. S. Oitzl, "Reversal of cognitive deficit of apolipoprotein E knockout mice after repeated exposure to a common environmental experience," *Neuroscience,* vol. 108, no. 2, pp. 237-247, 2001/12/10/ 2001, doi: https://doi.org/10.1016/S0306-4522(01)00412-2.
[225] J. Raber *et al.*, "Isoform-specific effects of human apolipoprotein E on brain function revealed in ApoE knockout mice: Increased susceptibility of females," *Proceedings of the National Academy of Sciences,* vol. 95, no. 18, pp. 10914-10919, 1998, doi: doi:10.1073/pnas.95.18.10914.
[226] K. Hu *et al.*, "Effects of the Lipid Metabolites and the Gut Microbiota in ApoE−/− Mice on Atherosclerosis Co-Depression From the Microbiota-Gut-Brain Axis," (in English), *Frontiers in Molecular Biosciences,* Original Research vol. 9, 2022-April-26 2022, doi: 10.3389/fmolb.2022.786492.
[227] L. Li *et al.*, "Chaihu-Shugan-San and absorbed meranzin hydrate induce anti-atherosclerosis and behavioral improvements in high-fat diet ApoE-/- mice via anti-inflammatory and BDNF-TrkB pathway," *Biomedicine & Pharmacotherapy,* vol. 115, p. 108893, 2019/07/01/ 2019, doi: https://doi.org/10.1016/j.biopha.2019.108893.
[228] J. Grootendorst, E. R. de Kloet, C. Vossen, S. Dalm, and M. S. Oitzl, "Repeated exposure to rats has persistent genotype-dependent effects on learning and locomotor activity of apolipoprotein E knockout and C57Bl/6 mice," *Behavioural Brain Research,* vol. 125, no. 1, pp. 249-259, 2001/11/08/ 2001, doi: https://doi.org/10.1016/S0166-4328(01)00294-7.
[229] G. A. Elder *et al.*, "Increased locomotor activity in mice lacking the low-density lipoprotein receptor," (in eng), *Behav Brain Res,* vol. 191, no. 2, pp. 256-65, Aug 22 2008, doi: 10.1016/j.bbr.2008.03.036.

[230] G. S. Getz and C. A. Reardon, "Do the Apoe-/- and Ldlr-/- Mice Yield the Same Insight on Atherogenesis?," (in eng), *Arterioscler Thromb Vasc Biol,* vol. 36, no. 9, pp. 1734-41, Sep 2016, doi: 10.1161/atvbaha.116.306874.
[231] P. Simon, R. Dupuis, and J. Costentin, "Thigmotaxis as an index of anxiety in mice. Influence of dopaminergic transmissions," *Behavioural Brain Research,* vol. 61, no. 1, pp. 59-64, 1994/03/31/ 1994, doi: https://doi.org/10.1016/0166-4328(94)90008-6.
[232] Y. Li *et al.*, "High fat diet-induced obesity leads to depressive and anxiety-like behaviors in mice via AMPK/mTOR-mediated autophagy," *Experimental Neurology,* vol. 348, p. 113949, 2022/02/01/ 2022, doi: https://doi.org/10.1016/j.expneurol.2021.113949.
[233] C. S. McLachlan and C. Yi Xing Soh, "Differences in anxiety-related behavior between apolipoprotein E-deficient C57BL/6 and wild type C57BL/6 mice," (in eng), *Physiol Res,* vol. 54, no. 6, pp. 701-4, 2005.
[234] J. Robertson, J. Curley, J. Kaye, J. Quinn, T. Pfankuch, and J. Raber, "apoE isoforms and measures of anxiety in probable AD patients and Apoe−/− mice," *Neurobiology of Aging,* vol. 26, no. 5, pp. 637-643, 2005/05/01/ 2005, doi: https://doi.org/10.1016/j.neurobiolaging.2004.06.003.
[235] P. Lestaevel *et al.*, "Influence of Environmental Enrichment and Depleted Uranium on Behaviour, Cholesterol and Acetylcholine in Apolipoprotein E-Deficient Mice," *Journal of Molecular Neuroscience,* vol. 53, no. 3, pp. 469-479, 2014/07/01 2014, doi: 10.1007/s12031-013-0038-0.
[236] Y. Kurhe and R. Mahesh, "Pioglitazone, a PPARγ agonist rescues depression associated with obesity using chronic unpredictable mild stress model in experimental mice," *Neurobiology of Stress,* vol. 3, pp. 114-121, 2016/06/01/ 2016, doi: https://doi.org/10.1016/j.ynstr.2016.05.001.
[237] S. Dutheil, K. T. Ota, E. S. Wohleb, K. Rasmussen, and R. S. Duman, "High-Fat Diet Induced Anxiety and Anhedonia: Impact on Brain Homeostasis and Inflammation," *Neuropsychopharmacology,* vol. 41, no. 7, pp. 1874-1887, 2016/06/01 2016, doi: 10.1038/npp.2015.357.
[238] E. Dere *et al.*, "Cognitive, emotional and social phenotyping of mice in an observer-independent setting," *Neurobiology of Learning and Memory,* vol. 150, pp. 136-150, 2018/04/01/ 2018, doi: https://doi.org/10.1016/j.nlm.2018.02.023.
[239] C. Pitzer, B. Kurpiers, and A. Eltokhi, "Sex Differences in Depression-Like Behaviors in Adult Mice Depend on Endophenotype and Strain," (in English), *Frontiers in Behavioral Neuroscience,* Brief Research Report vol. 16, 2022-March-17 2022, doi: 10.3389/fnbeh.2022.838122.
[240] J. H. van Ree *et al.*, "Diet-induced hypercholesterolemia and atherosclerosis in heterozygous apolipoprotein E-deficient mice," *Atherosclerosis,* vol. 111, no. 1, pp. 25-37, 1994/11/01/ 1994, doi: https://doi.org/10.1016/0021-9150(94)90188-0.
[241] A. Cerbone and A. G. Sadile, "Behavioral habituation to spatial novelty: Interference and noninterference studies," *Neuroscience & Biobehavioral Reviews,* vol. 18, no. 4, pp. 497-518, 1994/12/01/ 1994, doi: https://doi.org/10.1016/0149-7634(94)90004-3.
[242] L. Hou, C. Lu, Y. Huang, S. Chen, L. Hua, and R. Qian, "Effect of hyperlipidemia on the expression of circadian genes in apolipoprotein E knock-out atherosclerotic mice," *Lipids in Health and Disease,* vol. 8, no. 1, p. 60, 2009/12/30 2009, doi: 10.1186/1476-511X-8-60.
[243] Y. Yang *et al.*, "Regulation of SIRT1 and Its Roles in Inflammation," (in English), *Frontiers in Immunology,* Review vol. 13, 2022-March-11 2022, doi: 10.3389/fimmu.2022.831168.
[244] Y. Nakahata *et al.*, "The NAD+-Dependent Deacetylase SIRT1 Modulates CLOCK-Mediated Chromatin Remodeling and Circadian Control," *Cell,* vol. 134, no. 2, pp. 329-340, 2008/07/25/ 2008, doi: https://doi.org/10.1016/j.cell.2008.07.002.
[245] R. C. Ribeiro, P. J. Kushner, and J. D. Baxter, "The nuclear hormone receptor gene superfamily," (in eng), *Annu Rev Med,* vol. 46, pp. 443-53, 1995, doi: 10.1146/annurev.med.46.1.443.
[246] T. H. Bugge, J. Pohl, O. Lonnoy, and H. G. Stunnenberg, "RXR alpha, a promiscuous partner of retinoic acid and thyroid hormone receptors," *The EMBO Journal,* vol. 11, no. 4, pp. 1409-1418, 1992, doi: https://doi.org/10.1002/j.1460-2075.1992.tb05186.x.
[247] P. Lefebvre, Y. Benomar, and B. Staels, "Retinoid X receptors: common heterodimerization partners with distinct functions," *Trends in Endocrinology & Metabolism,* vol. 21, no. 11, pp. 676-683, 2010/11/01/ 2010, doi: https://doi.org/10.1016/j.tem.2010.06.009.

[248] P. McNamara, S.-b. Seo, R. D. Rudic, A. Sehgal, D. Chakravarti, and G. A. FitzGerald, "Regulation of CLOCK and MOP4 by Nuclear Hormone Receptors in the Vasculature: A Humoral Mechanism to Reset a Peripheral Clock," *Cell,* vol. 105, no. 7, pp. 877-889, 2001, doi: 10.1016/S0092-8674(01)00401-9.

[249] J. L. Goldstein and M. S. Brown, "Regulation of the mevalonate pathway," *Nature,* vol. 343, no. 6257, pp. 425-430, 1990/02/01 1990, doi: 10.1038/343425a0.

[250] M. M. Schumacher and R. A. DeBose-Boyd, "Posttranslational Regulation of HMG CoA Reductase, the Rate-Limiting Enzyme in Synthesis of Cholesterol," (in eng), *Annu Rev Biochem,* vol. 90, pp. 659-679, Jun 20 2021, doi: 10.1146/annurev-biochem-081820-101010.

[251] C. He *et al.*, "Circadian Rhythm Disruption Influenced Hepatic Lipid Metabolism, Gut Microbiota and Promoted Cholesterol Gallstone Formation in Mice," (in English), *Frontiers in Endocrinology,* Original Research vol. 12, 2021-October-21 2021, doi: 10.3389/fendo.2021.723918.

[252] S. L. Chellappa, N. Vujovic, J. S. Williams, and F. A. J. L. Scheer, "Impact of Circadian Disruption on Cardiovascular Function and Disease," *Trends in Endocrinology & Metabolism,* vol. 30, no. 10, pp. 767-779, 2019/10/01/ 2019, doi: https://doi.org/10.1016/j.tem.2019.07.008.

[253] Y. Zhao *et al.*, "Disruption of Circadian Rhythms by Shift Work Exacerbates Reperfusion Injury in Myocardial Infarction," *Journal of the American College of Cardiology,* vol. 79, no. 21, pp. 2097-2115, 2022/05/31/ 2022, doi: https://doi.org/10.1016/j.jacc.2022.03.370.

[254] N. Wang *et al.*, "Long-term night shift work is associated with the risk of atrial fibrillation and coronary heart disease," *European Heart Journal,* vol. 42, no. 40, pp. 4180-4188, 2021, doi: 10.1093/eurheartj/ehab505.

[255] A. Tapia-Osorio, R. Salgado-Delgado, M. Angeles-Castellanos, and C. Escobar, "Disruption of circadian rhythms due to chronic constant light leads to depressive and anxiety-like behaviors in the rat," *Behavioural Brain Research,* vol. 252, pp. 1-9, 2013/09/01/ 2013, doi: https://doi.org/10.1016/j.bbr.2013.05.028.

[256] L. Polidarová, M. Sládek, M. Soták, J. Pácha, and A. Sumová, "Hepatic, Duodenal, and Colonic Circadian Clocks Differ in their Persistence under Conditions of Constant Light and in their Entrainment by Restricted Feeding," *Chronobiology International,* vol. 28, no. 3, pp. 204-215, 2011/04/01 2011, doi: 10.3109/07420528.2010.548615.

[257] L. c. L. Lobo, B. Claustrat, G. Debilly, L. Paut-Pagano, M. Jouvet, and J.-L. Valatx, "Hypoprolactinemic rats under conditions of constant darkness or constant light. Effects on the sleep–wake cycle, cerebral temperature and sulfatoxymelatonin levels," *Brain Research,* vol. 835, no. 2, pp. 282-289, 1999/07/24/ 1999, doi: https://doi.org/10.1016/S0006-8993(99)01608-X.

[258] K. M. Capri *et al.*, "Male C57BL6/N and C57BL6/J Mice Respond Differently to Constant Light and Running-Wheel Access," (in English), *Frontiers in Behavioral Neuroscience,* Brief Research Report vol. 13, 2019-December-10 2019, doi: 10.3389/fnbeh.2019.00268.

[259] M. Okuliarova, N. Mazgutova, M. Majzunova, V. S. Rumanova, and M. Zeman, "Dim Light at Night Impairs Daily Variation of Circulating Immune Cells and Renal Immune Homeostasis," (in English), *Frontiers in Immunology,* Original Research vol. 11, 2021-January-22 2021, doi: 10.3389/fimmu.2020.614960.

[260] H. Mizutani, R. Tamagawa-Mineoka, R. Yasuike, Y. Minami, K. Yagita, and N. Katoh, "Effects of constant light exposure on allergic and irritant contact dermatitis in mice reared under constant light conditions," *Experimental Dermatology,* vol. 30, no. 5, pp. 739-744, 2021, doi: https://doi.org/10.1111/exd.14308.

[261] P. Ketelauri, K. Scharov, C. von Gall, and S. Johann, "Acute Circadian Disruption Due to Constant Light Promotes Caspase 1 Activation in the Mouse Hippocampus," *Cells,* vol. 12, no. 14, p. 1836, 2023. [Online]. Available: https://www.mdpi.com/2073-4409/12/14/1836.

[262] C. P. Coomans *et al.*, "Detrimental effects of constant light exposure and high-fat diet on circadian energy metabolism and insulin sensitivity," (in eng), *Faseb j,* vol. 27, no. 4, pp. 1721-32, Apr 2013, doi: 10.1096/fj.12-210898.

[263] E. P. de Chaves and V. Narayanaswami, "Apolipoprotein E and cholesterol in aging and disease in the brain," (in eng), *Future Lipidol,* vol. 3, no. 5, pp. 505-530, Oct 2008, doi: 10.2217/17460875.3.5.505.

[264] G. W. Rebeck *et al.*, "Structure and Functions of Human Cerebrospinal Fluid Lipoproteins from Individuals of Different APOE Genotypes," *Experimental Neurology,* vol. 149, no. 1, pp. 175-182, 1998/01/01/ 1998, doi: https://doi.org/10.1006/exnr.1997.6710.

[265] A. M. Fagan *et al.*, "Evidence for Normal Aging of the Septo-Hippocampal Cholinergic System in apoE (−/−) Mice but Impaired Clearance of Axonal Degeneration Products Following Injury," *Experimental Neurology,* vol. 151, no. 2, pp. 314-325, 1998/06/01/ 1998, doi: https://doi.org/10.1006/exnr.1998.6818.

[266] C. S. von Bartheld, J. Bahney, and S. Herculano-Houzel, "The search for true numbers of neurons and glial cells in the human brain: A review of 150 years of cell counting," (in eng), *J Comp Neurol,* vol. 524, no. 18, pp. 3865-3895, Dec 15 2016, doi: 10.1002/cne.24040.

[267] D. Giulian, "Ameboid microglia as effectors of inflammation in the central nervous system," *Journal of Neuroscience Research,* vol. 18, no. 1, pp. 155-171, 1987, doi: https://doi.org/10.1002/jnr.490180123.

[268] M. B. Graeber and W. J. Stre'rt, "Microglia: Immune Network in the CNS," *Brain Pathology,* vol. 1, no. 1, pp. 2-5, 1990, doi: https://doi.org/10.1111/j.1750-3639.1990.tb00630.x.

[269] A. Nimmerjahn, F. Kirchhoff, and F. Helmchen, "Resting Microglial Cells Are Highly Dynamic Surveillants of Brain Parenchyma in Vivo," *Science,* vol. 308, no. 5726, pp. 1314-1318, 2005, doi: doi:10.1126/science.1110647.

[270] N. Stence, M. Waite, and M. E. Dailey, "Dynamics of microglial activation: A confocal time-lapse analysis in hippocampal slices," *Glia,* vol. 33, no. 3, pp. 256-266, 2001, doi: https://doi.org/10.1002/1098-1136(200103)33:3<256::AID-GLIA1024>3.0.CO;2-J.

[271] I. Mori, Y. Imai, S. Kohsaka, and Y. Kimura, "Upregulated Expression of Iba1 Molecules in the Central Nervous System of Mice in Response to Neurovirulent Influenza A Virus Infection," *Microbiology and Immunology,* vol. 44, no. 8, pp. 729-735, 2000, doi: https://doi.org/10.1111/j.1348-0421.2000.tb02556.x.

[272] K. Ohsawa, Y. Imai, Y. Sasaki, and S. Kohsaka, "Microglia/macrophage-specific protein Iba1 binds to fimbrin and enhances its actin-bundling activity," (in eng), *J Neurochem,* vol. 88, no. 4, pp. 844-56, Feb 2004, doi: 10.1046/j.1471-4159.2003.02213.x.

[273] U.-K. Hanisch, "Microglia as a source and target of cytokines," *Glia,* vol. 40, no. 2, pp. 140-155, 2002, doi: https://doi.org/10.1002/glia.10161.

[274] R. B. Rock *et al.*, "Role of Microglia in Central Nervous System Infections," *Clinical Microbiology Reviews,* vol. 17, no. 4, pp. 942-964, 2004, doi: doi:10.1128/cmr.17.4.942-964.2004.

[275] S. A. Liddelow *et al.*, "Neurotoxic reactive astrocytes are induced by activated microglia," *Nature,* vol. 541, no. 7638, pp. 481-487, 2017/01/01 2017, doi: 10.1038/nature21029.

[276] G. A. Banker, "Trophic Interactions Between Astroglial Cells and Hippocampal Neurons in Culture," *Science,* vol. 209, no. 4458, pp. 809-810, 1980, doi: doi:10.1126/science.7403847.

[277] E. Beard, S. Lengacher, S. Dias, P. J. Magistretti, and C. Finsterwald, "Astrocytes as Key Regulators of Brain Energy Metabolism: New Therapeutic Perspectives," (in eng), *Front Physiol,* vol. 12, p. 825816, 2021, doi: 10.3389/fphys.2021.825816.

[278] M. Kreft, L. K. Bak, H. S. Waagepetersen, and A. Schousboe, "Aspects of Astrocyte Energy Metabolism, Amino Acid Neurotransmitter Homoeostasis and Metabolic Compartmentation," *ASN Neuro,* vol. 4, no. 3, p. AN20120007, 2012, doi: 10.1042/an20120007.

[279] A. Bignami, L. F. Eng, D. Dahl, and C. T. Uyeda, "Localization of the glial fibrillary acidic protein in astrocytes by immunofluorescence," *Brain Research,* vol. 43, no. 2, pp. 429-435, 1972/08/25/ 1972, doi: https://doi.org/10.1016/0006-8993(72)90398-8.

[280] U. Wilhelmsson *et al.*, "Redefining the concept of reactive astrocytes as cells that remain within their unique domains upon reaction to injury," (in eng), *Proc Natl Acad Sci U S A,* vol. 103, no. 46, pp. 17513-8, Nov 14 2006, doi: 10.1073/pnas.0602841103.

[281] P. J. Sollars, M. D. Ogilvie, M. A. Rea, and G. E. Pickard, "5-HT1B Receptor Knockout Mice Exhibit an Enhanced Response to Constant Light," *Journal of Biological Rhythms,* vol. 17, no. 5, pp. 428-437, 2002, doi: 10.1177/074873002237137.

[282] C. Beaulé, L. M. Houle, and S. Amir, "Expression profiles of PER2 immunoreactivity within the shell and core regions of the rat suprachiasmatic nucleus," *Journal of Molecular Neuroscience,* vol. 21, no. 2, pp. 133-147, 2003/10/01 2003, doi: 10.1385/JMN:21:2:133.

[283] M. Schilperoort *et al.*, "Continuous Light Does Not Affect Atherosclerosis in APOE*3-Leiden.CETP Mice," *Journal of Biological Rhythms,* vol. 35, no. 6, pp. 598-611, 2020, doi: 10.1177/0748730420951320.

[284] S. K. E. Tam *et al.*, "Dim light in the evening causes coordinated realignment of circadian rhythms, sleep, and short-term memory," *Proceedings of the National Academy of Sciences,* vol. 118, no. 39, p. e2101591118, 2021, doi: doi:10.1073/pnas.2101591118.

[285] L. Wei *et al.*, "Constant Light Exposure Alters Gut Microbiota and Promotes the Progression of Steatohepatitis in High Fat Diet Rats," (in English), *Frontiers in Microbiology,* Original Research vol. 11, 2020-August-21 2020, doi: 10.3389/fmicb.2020.01975.
[286] F. Yue *et al.*, "Effects of constant light exposure on sphingolipidomics and progression of NASH in high-fat-fed rats," *Journal of Gastroenterology and Hepatology,* vol. 35, no. 11, pp. 1978-1989, 2020, doi: https://doi.org/10.1111/jgh.15005.
[287] D. Yamamuro *et al.*, "Peripheral circadian rhythms in the liver and white adipose tissue of mice are attenuated by constant light and restored by time-restricted feeding," (in eng), *PLoS One,* vol. 15, no. 6, p. e0234439, 2020, doi: 10.1371/journal.pone.0234439.
[288] A. Sharma and R. Goyal, "Long-term exposure to constant light induces dementia, oxidative stress and promotes aggregation of sub-pathological Aβ42 in Wistar rats," *Pharmacology Biochemistry and Behavior,* vol. 192, p. 172892, 2020/05/01/ 2020, doi: https://doi.org/10.1016/j.pbb.2020.172892.
[289] K. Matthews, N. Forbes, and I. C. Reid, "Sucrose consumption as an hedonic measure following chronic unpredictable mild stress," (in eng), *Physiol Behav,* vol. 57, no. 2, pp. 241-8, Feb 1995, doi: 10.1016/0031-9384(94)00286-e.
[290] C. Bainier, M. Mateo, M.-P. Felder-Schmittbuhl, and J. Mendoza, "Circadian rhythms of hedonic drinking behavior in mice," *Neuroscience,* vol. 349, pp. 229-238, 2017/05/04/ 2017, doi: https://doi.org/10.1016/j.neuroscience.2017.03.002.
[291] K. Roybal *et al.*, "Mania-like behavior induced by disruption of CLOCK," (in eng), *Proc Natl Acad Sci U S A,* vol. 104, no. 15, pp. 6406-11, Apr 10 2007, doi: 10.1073/pnas.0609625104.
[292] N. S. Chandel, "Lipid Metabolism," (in eng), *Cold Spring Harb Perspect Biol,* vol. 13, no. 9, Sep 1 2021, doi: 10.1101/cshperspect.a040576.
[293] V. S. Rumanova, M. Okuliarova, E. Foppen, A. Kalsbeek, and M. Zeman, "Exposure to dim light at night alters daily rhythms of glucose and lipid metabolism in rats," (in English), *Frontiers in Physiology,* Original Research vol. 13, 2022-August-29 2022, doi: 10.3389/fphys.2022.973461.
[294] K. OISHI, H. SHIRAI, and N. ISHIDA, "CLOCK is involved in the circadian transactivation of peroxisome-proliferator-activated receptor α (PPARα) in mice," *Biochemical Journal,* vol. 386, no. 3, pp. 575-581, 2005, doi: 10.1042/bj20041150.
[295] L. Canaple *et al.*, "Reciprocal Regulation of Brain and Muscle Arnt-Like Protein 1 and Peroxisome Proliferator-Activated Receptor α Defines a Novel Positive Feedback Loop in the Rodent Liver Circadian Clock," *Molecular Endocrinology,* vol. 20, no. 8, pp. 1715-1727, 2006, doi: 10.1210/me.2006-0052.
[296] A. Purushotham, T. T. Schug, Q. Xu, S. Surapureddi, X. Guo, and X. Li, "Hepatocyte-specific deletion of SIRT1 alters fatty acid metabolism and results in hepatic steatosis and inflammation," (in eng), *Cell Metab,* vol. 9, no. 4, pp. 327-38, Apr 2009, doi: 10.1016/j.cmet.2009.02.006.
[297] J. Tzeng *et al.*, "An Ideal PPAR Response Element Bound to and Activated by PPARα," (in eng), *PLoS One,* vol. 10, no. 8, p. e0134996, 2015, doi: 10.1371/journal.pone.0134996.
[298] T. Gulick, S. Cresci, T. Caira, D. D. Moore, and D. P. Kelly, "The peroxisome proliferator-activated receptor regulates mitochondrial fatty acid oxidative enzyme gene expression," (in eng), *Proc Natl Acad Sci U S A,* vol. 91, no. 23, pp. 11012-6, Nov 8 1994, doi: 10.1073/pnas.91.23.11012.
[299] K. Schoonjans, B. Staels, and J. Auwerx, "Role of the peroxisome proliferator-activated receptor (PPAR) in mediating the effects of fibrates and fatty acids on gene expression," (in eng), *J Lipid Res,* vol. 37, no. 5, pp. 907-25, May 1996.
[300] A. Sharma, A. Mohammad, A. K. Saini, and R. Goyal, "Neuroprotective Effects of Fluoxetine on Molecular Markers of Circadian Rhythm, Cognitive Deficits, Oxidative Damage, and Biomarkers of Alzheimer's Disease-Like Pathology Induced under Chronic Constant Light Regime in Wistar Rats," *ACS Chemical Neuroscience,* vol. 12, no. 12, pp. 2233-2246, 2021/06/16 2021, doi: 10.1021/acschemneuro.1c00238.
[301] M. Yamakuchi, M. Ferlito, and C. J. Lowenstein, "miR-34a repression of SIRT1 regulates apoptosis," *Proceedings of the National Academy of Sciences,* vol. 105, no. 36, pp. 13421-13426, 2008, doi: doi:10.1073/pnas.0801613105.
[302] D. Chai, B. Wang, L. Shen, J. Pu, X.-k. Zhang, and B. He, "RXR agonists inhibit high-glucose-induced oxidative stress by repressing PKC activity in human endothelial cells,"

Free Radical Biology and Medicine, vol. 44, no. 7, pp. 1334-1347, 2008/04/01/ 2008, doi: https://doi.org/10.1016/j.freeradbiomed.2007.12.022.

[303] R. S. Guleria, R. Choudhary, T. Tanaka, K. M. Baker, and J. Pan, "Retinoic acid receptor-mediated signaling protects cardiomyocytes from hyperglycemia induced apoptosis: Role of the renin-angiotensin system," *Journal of Cellular Physiology,* vol. 226, no. 5, pp. 1292-1307, 2011, doi: https://doi.org/10.1002/jcp.22457.

[304] D. Töbelmann and M. Dittmar, "Diurnal relationship between core clock gene BMAL1, antioxidant SOD1 and oxidative RNA/DNA damage in young and older healthy women," *Experimental Gerontology,* vol. 151, p. 111422, 2021/08/01/ 2021, doi: https://doi.org/10.1016/j.exger.2021.111422.

[305] V. Martín, R. María Sainz, J. Carlos Mayo, I. Antolín, F. Herrera, and C. Rodríguez, "Daily Rhythm of Gene Expression in Rat Superoxide Dismutases," *Endocrine Research,* vol. 29, no. 1, pp. 83-95, 2003/01/01 2003, doi: 10.1081/ERC-120018679.

[306] J. Hwang *et al.*, "SOD1 suppresses pro-inflammatory immune responses by protecting against oxidative stress in colitis," (in eng), *Redox Biol,* vol. 37, p. 101760, Oct 2020, doi: 10.1016/j.redox.2020.101760.

[307] M. M. Shuey *et al.*, "Systems Approach to Integrating Preclinical Apolipoprotein E-Knockout Investigations Reveals Novel Etiologic Pathways and Master Atherosclerosis Network in Humans," *Arteriosclerosis, Thrombosis, and Vascular Biology,* vol. 42, no. 1, pp. 35-48, 2022, doi: doi:10.1161/ATVBAHA.121.317071.

[308] T. Claudel *et al.*, "Reduction of atherosclerosis in apolipoprotein E knockout mice by activation of the retinoid X receptor," *Proceedings of the National Academy of Sciences,* vol. 98, no. 5, pp. 2610-2615, 2001, doi: doi:10.1073/pnas.041609298.

[309] L. Shen *et al.*, "Sulindac-derived retinoid X receptor-α modulator attenuates atherosclerotic plaque progression and destabilization in ApoE(-/-) mice," (in eng), *Br J Pharmacol,* vol. 176, no. 14, pp. 2559-2572, Jul 2019, doi: 10.1111/bph.14682.

[310] S. S. Chirala and S. J. Wakil, "Structure and function of animal fatty acid synthase," *Lipids,* vol. 39, no. 11, pp. 1045-1053, 2004/11/01 2004, doi: 10.1007/s11745-004-1329-9.

[311] L. A. Rowland *et al.*, "De novo lipogenesis fuels adipocyte autophagosome and lysosome membrane dynamics," *Nature Communications,* vol. 14, no. 1, p. 1362, 2023/03/13 2023, doi: 10.1038/s41467-023-37016-8.

[312] M. Wallace and C. M. Metallo, "Tracing insights into de novo lipogenesis in liver and adipose tissues," *Seminars in Cell & Developmental Biology,* vol. 108, pp. 65-71, 2020/12/01/ 2020, doi: https://doi.org/10.1016/j.semcdb.2020.02.012.

[313] M. Alves-Bezerra and D. E. Cohen, "Triglyceride Metabolism in the Liver," in *Comprehensive Physiology*, 2017, pp. 1-22.

[314] I. Sazaki *et al.*, "Oxidized Low-Density Lipoproteins Trigger Hepatocellular Oxidative Stress with the Formation of Cholesteryl Ester Hydroperoxide-Enriched Lipid Droplets," *International Journal of Molecular Sciences,* vol. 24, no. 5, p. 4281, 2023. [Online]. Available: https://www.mdpi.com/1422-0067/24/5/4281.

[315] G. C. Ness and K. R. Gertz, "Hepatic HMG-CoA reductase expression and resistance to dietary cholesterol," (in eng), *Exp Biol Med (Maywood),* vol. 229, no. 5, pp. 412-6, May 2004, doi: 10.1177/153537020422900509.

[316] F. E. Thorngate, P. A. Strockbine, S. K. Erickson, and D. L. Williams, "Altered adrenal gland cholesterol metabolism in the apoE-deficient mouse," *Journal of Lipid Research,* vol. 43, no. 11, pp. 1920-1926, 2002, doi: 10.1194/jlr.M200205-JLR200.

[317] J. Xu *et al.*, "Effects of DHA dietary intervention on hepatic lipid metabolism in apolipoprotein E-deficient and C57BL/6J wild-type mice," *Biomedicine & Pharmacotherapy,* vol. 144, p. 112329, 2021/12/01/ 2021, doi: https://doi.org/10.1016/j.biopha.2021.112329.

[318] M. S. Brown and J. L. Goldstein, "Multivalent feedback regulation of HMG CoA reductase, a control mechanism coordinating isoprenoid synthesis and cell growth," (in eng), *J Lipid Res,* vol. 21, no. 5, pp. 505-17, Jul 1980.

[319] R. A. DeBose-Boyd, "Feedback regulation of cholesterol synthesis: sterol-accelerated ubiquitination and degradation of HMG CoA reductase," *Cell Research,* vol. 18, no. 6, pp. 609-621, 2008/06/01 2008, doi: 10.1038/cr.2008.61.

[320] C.-L. E. Yen, S. J. Stone, S. Koliwad, C. Harris, and R. V. Farese, Jr., "Thematic Review Series: Glycerolipids. DGAT enzymes and triacylglycerol biosynthesis," *Journal of Lipid Research,* vol. 49, no. 11, pp. 2283-2301, 2008, doi: 10.1194/jlr.R800018-JLR200.

[321] X. Cheng *et al.*, "Targeting DGAT1 Ameliorates Glioblastoma by Increasing Fat Catabolism and Oxidative Stress," *Cell Metabolism,* vol. 32, no. 2, pp. 229-242.e8, 2020, doi: 10.1016/j.cmet.2020.06.002.
[322] L. Liu *et al.*, "DGAT1 deficiency decreases PPAR expression and does not lead to lipotoxicity in cardiac and skeletal muscle [S]," *Journal of Lipid Research,* vol. 52, no. 4, pp. 732-744, 2011, doi: 10.1194/jlr.M011395.
[323] E. Hams *et al.*, "Role for Retinoic Acid-Related Orphan Receptor Alpha (RORα) Expressing Macrophages in Diet-Induced Obesity," (in English), *Frontiers in Immunology,* Original Research vol. 11, 2020-August-27 2020, doi: 10.3389/fimmu.2020.01966.
[324] H. S. Kang *et al.*, "Gene expression profiling reveals a regulatory role for RORα and RORγ in phase I and phase II metabolism," *Physiological genomics,* vol. 31, no. 2, pp. 281-294, 2007, doi: 10.1152/physiolgenomics.00098.2007.
[325] A. A. Dannerfjord, L. A. Brown, R. G. Foster, and S. N. Peirson, "Light Input to the Mammalian Circadian Clock," in *Circadian Clocks: Methods and Protocols*, S. A. Brown Ed. New York, NY: Springer US, 2021, pp. 233-247.
[326] A. K. Verma, S. Singh, and S. I. Rizvi, "Age-dependent effect of continuous 'artificial light at night' on circadian rhythm in male rats: neuroprotective role of melatonin," *Biogerontology,* vol. 22, no. 5, pp. 531-545, 2021/10/01 2021, doi: 10.1007/s10522-021-09933-y.
[327] D. Gao *et al.*, "The Effects of Palmitate on Hepatic Insulin Resistance Are Mediated by NADPH Oxidase 3-derived Reactive Oxygen Species through JNK and p38^{MAPK} Pathways *," *Journal of Biological Chemistry,* vol. 285, no. 39, pp. 29965-29973, 2010, doi: 10.1074/jbc.M110.128694.
[328] L. Ding *et al.*, "Peroxisomal β-oxidation acts as a sensor for intracellular fatty acids and regulates lipolysis," *Nature Metabolism,* vol. 3, no. 12, pp. 1648-1661, 2021/12/01 2021, doi: 10.1038/s42255-021-00489-2.
[329] P. J. Magistretti and I. Allaman, "Lactate in the brain: from metabolic end-product to signalling molecule," *Nature Reviews Neuroscience,* vol. 19, no. 4, pp. 235-249, 2018/04/01 2018, doi: 10.1038/nrn.2018.19.
[330] Y. Xu *et al.*, "Endothelial PFKFB3 Plays a Critical Role in Angiogenesis," *Arteriosclerosis, Thrombosis, and Vascular Biology,* vol. 34, no. 6, pp. 1231-1239, 2014, doi: doi:10.1161/ATVBAHA.113.303041.
[331] K. Tanegashima, Y. Sato-Miyata, M. Funakoshi, Y. Nishito, T. Aigaki, and T. Hara, "Epigenetic regulation of the glucose transporter gene Slc2a1 by β-hydroxybutyrate underlies preferential glucose supply to the brain of fasted mice," *Genes to Cells,* vol. 22, no. 1, pp. 71-83, 2017, doi: https://doi.org/10.1111/gtc.12456.
[332] W. M. Pardridge, R. J. Boado, and C. R. Farrell, "Brain-type glucose transporter (GLUT-1) is selectively localized to the blood-brain barrier. Studies with quantitative western blotting and in situ hybridization," *Journal of Biological Chemistry,* vol. 265, no. 29, pp. 18035-18040, 1990/10/15/ 1990, doi: https://doi.org/10.1016/S0021-9258(18)38267-X.
[333] G. C. Forcina and S. J. Dixon, "GPX4 at the Crossroads of Lipid Homeostasis and Ferroptosis," *PROTEOMICS,* vol. 19, no. 18, p. 1800311, 2019, doi: https://doi.org/10.1002/pmic.201800311.
[334] Q. Xue *et al.*, "Copper-dependent autophagic degradation of GPX4 drives ferroptosis," *Autophagy,* vol. 19, no. 7, pp. 1982-1996, 2023/07/03 2023, doi: 10.1080/15548627.2023.2165323.
[335] S. C. Lu, "Glutathione synthesis," *Biochimica et Biophysica Acta (BBA) - General Subjects,* vol. 1830, no. 5, pp. 3143-3153, 2013/05/01/ 2013, doi: https://doi.org/10.1016/j.bbagen.2012.09.008.
[336] A. Kurtz, A. Zimmer, F. Schnütgen, G. Brüning, F. Spener, and T. Müller, "The expression pattern of a novel gene encoding brain-fatty acid binding protein correlates with neuronal and glial cell development," *Development,* vol. 120, no. 9, pp. 2637-2649, 1994, doi: 10.1242/dev.120.9.2637.
[337] J. R. Gerstner, Q. Z. Bremer, W. M. Vander Heyden, T. M. LaVaute, J. C. Yin, and C. F. Landry, "Brain Fatty Acid Binding Protein (Fabp7) Is Diurnally Regulated in Astrocytes and Hippocampal Granule Cell Precursors in Adult Rodent Brain," *PLOS ONE,* vol. 3, no. 2, p. e1631, 2008, doi: 10.1371/journal.pone.0001631.
[338] T. M. Driessen, C. Zhao, M. Saenz, S. A. Stevenson, Y. Owada, and S. C. Gammie, "Down-regulation of fatty acid binding protein 7 (Fabp7) is a hallmark of the postpartum

brain," *Journal of Chemical Neuroanatomy,* vol. 92, pp. 92-101, 2018/10/01/ 2018, doi: https://doi.org/10.1016/j.jchemneu.2018.07.003.

[339] Y. Wu *et al.*, "Apolipoprotein E Deficiency Aggravates Neuronal Injury by Enhancing Neuroinflammation via the JNK/c-Jun Pathway in the Early Phase of Experimental Subarachnoid Hemorrhage in Mice," *Oxidative Medicine and Cellular Longevity,* vol. 2019, p. 3832648, 2019/12/26 2019, doi: 10.1155/2019/3832648.

[340] M. J. LaDu *et al.*, "Apolipoprotein E and apolipoprotein E receptors modulate Aβ-induced glial neuroinflammatory responses," *Neurochemistry International,* vol. 39, no. 5, pp. 427-434, 2001/11/01/ 2001, doi: https://doi.org/10.1016/S0197-0186(01)00050-X.

[341] Y. Zhu *et al.*, "APOE genotype alters glial activation and loss of synaptic markers in mice," *Glia,* vol. 60, no. 4, pp. 559-569, 2012, doi: https://doi.org/10.1002/glia.22289.

[342] G. J. Harry, C. Lefebvre d'Hellencourt, A. Bruccoleri, and D. Schmechel, "Age-Dependent Cytokine Responses: Trimethyltin Hippocampal Injury in Wild-Type, APOE Knockout, and APOE4 Mice," *Brain, Behavior, and Immunity,* vol. 14, no. 4, pp. 288-304, 2000/12/01/ 2000, doi: https://doi.org/10.1006/brbi.2000.0606.

[343] A. Pocivavsek, M. P. Burns, and G. W. Rebeck, "Low-density lipoprotein receptors regulate microglial inflammation through c-Jun N-terminal kinase," (in eng), *Glia,* vol. 57, no. 4, pp. 444-53, Mar 2009, doi: 10.1002/glia.20772.

[344] A. Pocivavsek, I. Mikhailenko, D. K. Strickland, and G. W. Rebeck, "Microglial low-density lipoprotein receptor-related protein 1 modulates c-Jun N-terminal kinase activation," *Journal of Neuroimmunology,* vol. 214, no. 1, pp. 25-32, 2009/09/29/ 2009, doi: https://doi.org/10.1016/j.jneuroim.2009.06.010.

[345] D. Champagne, J. Rochford, and J. Poirier, "Effect of apolipoprotein E deficiency on reactive sprouting in the dentate gyrus of the hippocampus following entorhinal cortex lesion: role of the astroglial response," *Experimental Neurology,* vol. 194, no. 1, pp. 31-42, 2005/07/01/ 2005, doi: https://doi.org/10.1016/j.expneurol.2005.01.016.

[346] H. Buchanan, C. Hull, M. Cacho Barraza, M. Delibegovic, and B. Platt, "Apolipoprotein E loss of function: Influence on murine brain markers of physiology and pathology," *Aging Brain,* vol. 2, p. 100055, 2022/01/01/ 2022, doi: https://doi.org/10.1016/j.nbas.2022.100055.

[347] D. Atanasova, N. Lazarov, D. S. Stoyanov, R. H. Spassov, A. B. Tonchev, and J. Tchekalarova, "Reduced neuroinflammation and enhanced neurogenesis following chronic agomelatine treatment in rats undergoing chronic constant light," *Neuropharmacology,* vol. 197, p. 108706, 2021/10/01/ 2021, doi: https://doi.org/10.1016/j.neuropharm.2021.108706.

[348] T. Moriya *et al.*, "Involvement of glial fibrillary acidic protein (GFAP) expressed in astroglial cells in circadian rhythm under constant lighting conditions in mice," (in eng), *J Neurosci Res,* vol. 60, no. 2, pp. 212-8, Apr 15 2000, doi: 10.1002/(sici)1097-4547(20000415)60:2<212::Aid-jnr10>3.0.Co;2-p.

[349] M. M. Benedetto, M. G. Bruera, M. A. Contin, A. L. Degano, and M. E. Guido, "Glial cell response to constant low light exposure in rat retina," *Visual Neuroscience,* vol. 39, p. E005, 2022, Art no. E005, doi: 10.1017/S0952523822000049.

[350] G. Baydas, R. J. Reiter, V. S. Nedzvetskii, P. A. Nerush, and S. V. Kirichenko, "Altered glial fibrillary acidic protein content and its degradation in the hippocampus, cortex and cerebellum of rats exposed to constant light: reversal by melatonin," *Journal of Pineal Research,* vol. 33, no. 3, pp. 134-139, 2002, doi: https://doi.org/10.1034/j.1600-079X.2002.02110.x.

[351] J. R. Larkin *et al.*, "Metabolomic Biomarkers in Blood Samples Identify Cancers in a Mixed Population of Patients with Nonspecific Symptoms," (in eng), *Clin Cancer Res,* vol. 28, no. 8, pp. 1651-1661, Apr 14 2022, doi: 10.1158/1078-0432.Ccr-21-2855.

[352] F. Probert *et al.*, "NMR analysis reveals significant differences in the plasma metabolic profiles of Niemann Pick C1 patients, heterozygous carriers, and healthy controls," (in eng), *Sci Rep,* vol. 7, no. 1, p. 6320, Jul 24 2017, doi: 10.1038/s41598-017-06264-2.

[353] T. Yeo *et al.*, "Metabolomics detects clinically silent neuroinflammatory lesions earlier than neurofilament-light chain in a focal multiple sclerosis animal model," (in eng), *J Neuroinflammation,* vol. 19, no. 1, p. 252, Oct 9 2022, doi: 10.1186/s12974-022-02614-8.

[354] I. Tzoulaki *et al.*, "Serum metabolic signatures of coronary and carotid atherosclerosis and subsequent cardiovascular disease," *European Heart Journal,* vol. 40, no. 34, pp. 2883-2896, 2019, doi: 10.1093/eurheartj/ehz235.

[355] J. Teul *et al.*, "Improving Metabolite Knowledge in Stable Atherosclerosis Patients by Association and Correlation of GC-MS and 1H NMR Fingerprints," *Journal of Proteome Research,* vol. 8, no. 12, pp. 5580-5589, 2009/12/04 2009, doi: 10.1021/pr900668v.
[356] Y. Yang *et al.*, "Serum metabonomic analysis of apoE−/− mice reveals progression axes for atherosclerosis based on NMR spectroscopy," *Molecular BioSystems,* 10.1039/C4MB00334A vol. 10, no. 12, pp. 3170-3178, 2014, doi: 10.1039/C4MB00334A.
[357] Q. Li *et al.*, "1H-NMR-Based Metabonomics Study to Reveal the Progressive Metabolism Regulation of SAP Deficiency on ApoE−/− Mice," *Metabolites,* vol. 12, no. 12, p. 1278, 2022. [Online]. Available: https://www.mdpi.com/2218-1989/12/12/1278.
[358] N. M. Kettner *et al.*, "Circadian Homeostasis of Liver Metabolism Suppresses Hepatocarcinogenesis," *Cancer Cell,* vol. 30, no. 6, pp. 909-924, 2016/12/12/ 2016, doi: https://doi.org/10.1016/j.ccell.2016.10.007.
[359] J. Padilla *et al.*, "Circadian dysfunction induces NAFLD-related human liver cancer in a mouse model," *Journal of Hepatology,* 2023/10/27/ 2023, doi: https://doi.org/10.1016/j.jhep.2023.10.018.
[360] K. L. Russell, H. R. Rodman, and V. M. Pak, "Sleep insufficiency, circadian rhythms, and metabolomics: the connection between metabolic and sleep disorders," (in eng), *Sleep Breath,* vol. 27, no. 6, pp. 2139-2153, Dec 2023, doi: 10.1007/s11325-023-02828-x.
[361] S. K. Davies *et al.*, "Effect of sleep deprivation on the human metabolome," *Proceedings of the National Academy of Sciences,* vol. 111, no. 29, pp. 10761-10766, 2014, doi: doi:10.1073/pnas.1402663111.
[362] D. Guan *et al.*, "The hepatocyte clock and feeding control chronophysiology of multiple liver cell types," *Science,* vol. 369, no. 6509, pp. 1388-1394, 2020, doi: doi:10.1126/science.aba8984.
[363] A. H. Emwas, "The strengths and weaknesses of NMR spectroscopy and mass spectrometry with particular focus on metabolomics research," (in eng), *Methods Mol Biol,* vol. 1277, pp. 161-93, 2015, doi: 10.1007/978-1-4939-2377-9_13.
[364] Y.-M. Kim *et al.*, "Light-Stress Influences the Composition of the Murine Gut Microbiome, Memory Function, and Plasma Metabolome," (in English), *Frontiers in Molecular Biosciences,* Original Research vol. 6, 2019-October-18 2019, doi: 10.3389/fmolb.2019.00108.
[365] W. Guo *et al.*, "Quantitative Metabolomic Profiling of Plasma, Urine, and Liver Extracts by 1H NMR Spectroscopy Characterizes Different Stages of Atherosclerosis in Hamsters," *Journal of Proteome Research,* vol. 15, no. 10, pp. 3500-3510, 2016/10/07 2016, doi: 10.1021/acs.jproteome.6b00179.
[366] J. Yang *et al.*, "Chronic blue light leads to accelerated aging in Drosophila by impairing energy metabolism and neurotransmitter levels," (in English), *Frontiers in Aging,* Original Research vol. 3, 2022-August-31 2022, doi: 10.3389/fragi.2022.983373.
[367] J. D. Rabinowitz and S. Enerbäck, "Lactate: the ugly duckling of energy metabolism," (in eng), *Nat Metab,* vol. 2, no. 7, pp. 566-571, Jul 2020, doi: 10.1038/s42255-020-0243-4.
[368] T. Song *et al.*, "Salidroside simultaneously reduces de novo lipogenesis and cholesterol biosynthesis to attenuate atherosclerosis in mice," *Biomedicine & Pharmacotherapy,* vol. 134, p. 111137, 2021/02/01/ 2021, doi: https://doi.org/10.1016/j.biopha.2020.111137.
[369] María M. Adeva-Andany, N. Pérez-Felpete, C. Fernández-Fernández, C. Donapetry-García, and C. Pazos-García, "Liver glucose metabolism in humans," *Bioscience Reports,* vol. 36, no. 6, 2016, doi: 10.1042/bsr20160385.
[370] Y. Zhang *et al.*, "Dingxin Recipe IV attenuates atherosclerosis by regulating lipid metabolism through LXR-α/SREBP1 pathway and modulating the gut microbiota in ApoE-/- mice fed with HFD," *Journal of Ethnopharmacology,* vol. 266, p. 113436, 2021/02/10/ 2021, doi: https://doi.org/10.1016/j.jep.2020.113436.
[371] N. Grosser, S. Oberle, G. Berndt, K. Erdmann, A. Hemmerle, and H. Schröder, "Antioxidant action of l-alanine: heme oxygenase-1 and ferritin as possible mediators," *Biochemical and Biophysical Research Communications,* vol. 314, no. 2, pp. 351-355, 2004/02/06/ 2004, doi: https://doi.org/10.1016/j.bbrc.2003.12.089.
[372] J. V. Andersen *et al.*, "Glutamate metabolism and recycling at the excitatory synapse in health and neurodegeneration," *Neuropharmacology,* vol. 196, p. 108719, 2021/09/15/ 2021, doi: https://doi.org/10.1016/j.neuropharm.2021.108719.
[373] M. D. Norenberg and A. Martinez-Hernandez, "Fine structural localization of glutamine synthetase in astrocytes of rat brain," *Brain Research,* vol. 161, no. 2, pp. 303-310, 1979/02/02/ 1979, doi: https://doi.org/10.1016/0006-8993(79)90071-4.

[374] J. A. Dykens, A. Stern, and E. Trenkner, "Mechanism of Kainate Toxicity to Cerebellar Neurons In Vitro Is Analogous to Reperfusion Tissue Injury," *Journal of Neurochemistry,* vol. 49, no. 4, pp. 1222-1228, 1987, doi: https://doi.org/10.1111/j.1471-4159.1987.tb10014.x.

[375] A. Lehn-Stefan *et al.*, "Elevated Circulating Glutamate Is Associated With Subclinical Atherosclerosis Independently of Established Risk Markers: A Cross-Sectional Study," *The Journal of Clinical Endocrinology & Metabolism,* vol. 106, no. 2, pp. e982-e989, 2020, doi: 10.1210/clinem/dgaa898.

[376] X. Wang *et al.*, "Serum glutamate and glutamine-to-glutamate ratio are associated with coronary angiography defined coronary artery disease," *Nutrition, Metabolism and Cardiovascular Diseases,* vol. 32, no. 1, pp. 186-194, 2022/01/01/ 2022, doi: https://doi.org/10.1016/j.numecd.2021.09.021.

[377] S. Bose, V. Ramesh, and J. W. Locasale, "Acetate Metabolism in Physiology, Cancer, and Beyond," *Trends in Cell Biology,* vol. 29, no. 9, pp. 695-703, 2019/09/01/ 2019, doi: https://doi.org/10.1016/j.tcb.2019.05.005.

[378] A. Vysochan, A. Sengupta, A. M. Weljie, J. C. Alwine, and Y. Yu, "ACSS2-mediated acetyl-CoA synthesis from acetate is necessary for human cytomegalovirus infection," *Proceedings of the National Academy of Sciences,* vol. 114, no. 8, pp. E1528-E1535, 2017, doi: doi:10.1073/pnas.1614268114.

[379] C. Ye and B. P. Tu, "Sink into the Epigenome: Histones as Repositories That Influence Cellular Metabolism," *Trends in Endocrinology & Metabolism,* vol. 29, no. 9, pp. 626-637, 2018/09/01/ 2018, doi: https://doi.org/10.1016/j.tem.2018.06.002.

[380] X. Liu *et al.*, "Acetate Production from Glucose and Coupling to Mitochondrial Metabolism in Mammals," *Cell,* vol. 175, no. 2, pp. 502-513.e13, 2018, doi: 10.1016/j.cell.2018.08.040.

[381] E. V. Prochownik and H. Wang, "The Metabolic Fates of Pyruvate in Normal and Neoplastic Cells," *Cells,* vol. 10, no. 4, p. 762, 2021. [Online]. Available: https://www.mdpi.com/2073-4409/10/4/762.

[382] K. L. Zambell, M. D. Fitch, and S. E. Fleming, "Acetate and Butyrate Are the Major Substrates for De Novo Lipogenesis in Rat Colonic Epithelial Cells," *The Journal of Nutrition,* vol. 133, no. 11, pp. 3509-3515, 2003/11/01/ 2003, doi: https://doi.org/10.1093/jn/133.11.3509.

[383] P. Nguyen *et al.*, "Liver lipid metabolism," *Journal of Animal Physiology and Animal Nutrition,* vol. 92, no. 3, pp. 272-283, 2008, doi: https://doi.org/10.1111/j.1439-0396.2007.00752.x.

[384] T. B. Patel, L. L. Barron, and M. S. Olson, "The stimulation of hepatic gluconeogenesis by acetoacetate precursors. A role for the monocarboxylate translocator," *Journal of Biological Chemistry,* vol. 259, no. 12, pp. 7525-7531, 1984/06/25/ 1984, doi: https://doi.org/10.1016/S0021-9258(17)42822-5.

[385] S. K. Fisher, J. E. Novak, and B. W. Agranoff, "Inositol and higher inositol phosphates in neural tissues: homeostasis, metabolism and functional significance," *Journal of Neurochemistry,* vol. 82, no. 4, pp. 736-754, 2002, doi: https://doi.org/10.1046/j.1471-4159.2002.01041.x.

[386] F. Eisenberg, "d-Myoinositol 1-Phosphate as Product of Cyclization of Glucose 6-Phosphate and Substrate for a Specific Phosphatase in Rat Testis," *Journal of Biological Chemistry,* vol. 242, no. 7, pp. 1375-1382, 1967/04/10/ 1967, doi: https://doi.org/10.1016/S0021-9258(18)96102-8.

[387] R. Spector, "Myo-inositol transport through the blood-brain barrier," *Neurochemical Research,* vol. 13, no. 8, pp. 785-787, 1988/08/01 1988, doi: 10.1007/BF00971603.

[388] M. A. Sortino, S. Salomone, M. O. Carruba, and F. Drago, "Polycystic Ovary Syndrome: Insights into the Therapeutic Approach with Inositols," (in English), *Frontiers in Pharmacology,* Review vol. 8, 2017-June-08 2017, doi: 10.3389/fphar.2017.00341.

[389] A. J. López-Gambero, C. Sanjuan, P. J. Serrano-Castro, J. Suárez, and F. Rodríguez de Fonseca, "The Biomedical Uses of Inositols: A Nutraceutical Approach to Metabolic Dysfunction in Aging and Neurodegenerative Diseases," *Biomedicines,* vol. 8, no. 9, p. 295, 2020. [Online]. Available: https://www.mdpi.com/2227-9059/8/9/295.

[390] P. P. Hipps, W. H. Holland, and W. R. Sherman, "Interconversion of myo- and scyllo-inositol with simultaneous formation of neo-inositol by an NADP+ dependent epimerase from bovine brain," *Biochemical and Biophysical Research Communications,* vol. 77, no. 1, pp. 340-346, 1977/07/11/ 1977, doi: https://doi.org/10.1016/S0006-291X(77)80202-7.

[391] W. R. Sherman, M. A. Stewart, M. M. Kurien, and S. L. Goodwin, "The measurement of myo-inositol, myo-inosose-2 and scyllo-inositol in mammalian tissues," *Biochimica et Biophysica Acta (BBA) - General Subjects,* vol. 158, no. 2, pp. 197-205, 1968/05/14/ 1968, doi: https://doi.org/10.1016/0304-4165(68)90131-1.
[392] A. Viola *et al.*, "High cerebral scyllo-inositol: a new marker of brain metabolism disturbances induced by chronic alcoholism," *Magnetic Resonance Materials in Physics, Biology and Medicine,* vol. 17, no. 1, pp. 47-61, 2004/09/01 2004, doi: 10.1007/s10334-004-0044-x.
[393] H. R. Griffith *et al.*, "Elevated brain scyllo-inositol concentrations in patients with Alzheimer's disease," (in eng), *NMR Biomed,* vol. 20, no. 8, pp. 709-16, Dec 2007, doi: 10.1002/nbm.1132.
[394] M. Bonora *et al.*, "ATP synthesis and storage," *Purinergic Signalling,* vol. 8, no. 3, pp. 343-357, 2012/09/01 2012, doi: 10.1007/s11302-012-9305-8.
[395] Y.-D. Chen *et al.*, "The association between disruption of the circadian rhythm and aggravation of colitis in mice," *Gastroenterology Report,* vol. 10, 2022, doi: 10.1093/gastro/goac028.
[396] K. Schmitt *et al.*, "Circadian Control of DRP1 Activity Regulates Mitochondrial Dynamics and Bioenergetics," *Cell Metabolism,* vol. 27, no. 3, pp. 657-666.e5, 2018, doi: 10.1016/j.cmet.2018.01.011.
[397] L. Marpegan *et al.*, "Circadian Regulation of ATP Release in Astrocytes," *The Journal of Neuroscience,* vol. 31, no. 23, pp. 8342-8350, 2011, doi: 10.1523/jneurosci.6537-10.2011.
[398] A. Rahal *et al.*, "Oxidative Stress, Prooxidants, and Antioxidants: The Interplay," *BioMed Research International,* vol. 2014, p. 761264, 2014/01/23 2014, doi: 10.1155/2014/761264.
[399] D. A. Averill-Bates, "Chapter Five - The antioxidant glutathione," in *Vitamins and Hormones*, vol. 121, G. Litwack Ed.: Academic Press, 2023, pp. 109-141.
[400] O. S. Faborode, I. O. Yusuf, P. O. Okpe, A. O. Okudaje, and S. A. Onasanwo, "Exposure to prolonged unpredictable light impairs spatial memory via induction of oxidative stress and tumor necrosis factor-alpha in rats," (in eng), *J Basic Clin Physiol Pharmacol,* vol. 33, no. 3, pp. 355-362, Apr 20 2021, doi: 10.1515/jbcpp-2020-0160.
[401] T. Ochi, "Menadione causes increases in the level of glutathione and in the activity of γ-glutamylcysteine synthetase in cultured Chinese hamster V79 cells," *Toxicology,* vol. 112, no. 1, pp. 45-55, 1996/08/01/ 1996, doi: https://doi.org/10.1016/0300-483X(96)03348-3.
[402] F. E. Harrison and J. M. May, "Vitamin C function in the brain: vital role of the ascorbate transporter SVCT2," *Free Radical Biology and Medicine,* vol. 46, no. 6, pp. 719-730, 2009/03/15/ 2009, doi: https://doi.org/10.1016/j.freeradbiomed.2008.12.018.
[403] D. A. Mickle *et al.*, "Myocardial salvage with trolox and ascorbic acid for an acute evolving infarction," (in eng), *Ann Thorac Surg,* vol. 47, no. 4, pp. 553-7, Apr 1989, doi: 10.1016/0003-4975(89)90431-1.
[404] D. Njus, P. M. Kelley, Y.-J. Tu, and H. B. Schlegel, "Ascorbic acid: The chemistry underlying its antioxidant properties," *Free Radical Biology and Medicine,* vol. 159, pp. 37-43, 2020/11/01/ 2020, doi: https://doi.org/10.1016/j.freeradbiomed.2020.07.013.
[405] Á. Sánchez-Illana, J. D. Piñeiro-Ramos, V. Ramos-Garcia, I. Ten-Doménech, M. Vento, and J. Kuligowski, "Chapter Three - Oxidative stress biomarkers in the preterm infant," in *Advances in Clinical Chemistry*, vol. 102, G. S. Makowski Ed.: Elsevier, 2021, pp. 127-189.
[406] Y. Y. Sautin and R. J. Johnson, "Uric Acid: The Oxidant-Antioxidant Paradox," *Nucleosides, Nucleotides & Nucleic Acids,* vol. 27, no. 6-7, pp. 608-619, 2008/07/23 2008, doi: 10.1080/15257770802138558.
[407] E. T. Chouchani *et al.*, "Ischaemic accumulation of succinate controls reperfusion injury through mitochondrial ROS," *Nature,* vol. 515, no. 7527, pp. 431-435, 2014/11/01 2014, doi: 10.1038/nature13909.
[408] H. Hagberg, P. Andersson, J. Lacarewicz, I. Jacobson, S. Butcher, and M. Sandberg, "Extracellular Adenosine, Inosine, Hypoxanthine, and Xanthine in Relation to Tissue Nucleotides and Purines in Rat Striatum During Transient Ischemia," *Journal of Neurochemistry,* vol. 49, no. 1, pp. 227-231, 1987, doi: https://doi.org/10.1111/j.1471-4159.1987.tb03419.x.
[409] D. N. Granger and P. R. Kvietys, "Reperfusion injury and reactive oxygen species: The evolution of a concept," *Redox Biology,* vol. 6, pp. 524-551, 2015/12/01/ 2015, doi: https://doi.org/10.1016/j.redox.2015.08.020.
[410] A. Gęgotek and E. Skrzydlewska, "Chapter Nine - Ascorbic acid as antioxidant," in *Vitamins and Hormones*, vol. 121, G. Litwack Ed.: Academic Press, 2023, pp. 247-270.

[411] Y. G. C. Varadaiah, S. Sivanesan, S. B. Nayak, and K. R. Thirumalarao, "Purine metabolites can indicate diabetes progression," *Archives of Physiology and Biochemistry,* vol. 128, no. 1, pp. 87-91, 2022/01/02 2022, doi: 10.1080/13813455.2019.1663219.
[412] D. E. Farthing, C. A. Farthing, and L. Xi, "Inosine and hypoxanthine as novel biomarkers for cardiac ischemia: From bench to point-of-care," *Experimental Biology and Medicine,* vol. 240, no. 6, pp. 821-831, 2015, doi: 10.1177/1535370215584931.
[413] M. G. Varadinova, M. L. Valcheva-Traykova, and N. I. Boyadjieva, "Effect of Circadian Rhythm Disruption and Alcohol on the Oxidative Stress Level in Rat Brain," *American Journal of Therapeutics,* vol. 23, no. 6, pp. e1801-e1805, 2016, doi: 10.1097/mjt.0000000000000363.
[414] T. Nakanishi-Ueda *et al.*, "Blue LED light exposure develops intracellular reactive oxygen species, lipid peroxidation, and subsequent cellular injuries in cultured bovine retinal pigment epithelial cells," *Free Radical Research,* vol. 47, no. 10, pp. 774-780, 2013/10/01 2013, doi: 10.3109/10715762.2013.829570.
[415] F. Liebel, S. Kaur, E. Ruvolo, N. Kollias, and M. D. Southall, "Irradiation of Skin with Visible Light Induces Reactive Oxygen Species and Matrix-Degrading Enzymes," *Journal of Investigative Dermatology,* vol. 132, no. 7, pp. 1901-1907, 2012/07/01/ 2012, doi: https://doi.org/10.1038/jid.2011.476.
[416] G. Lascaratos, D. Ji, J. P. Wood, and N. N. Osborne, "Visible light affects mitochondrial function and induces neuronal death in retinal cell cultures," (in eng), *Vision Res,* vol. 47, no. 9, pp. 1191-201, Apr 2007, doi: 10.1016/j.visres.2006.12.014.
[417] P. Rajput, D. Kumar, and S. Krishnamurthy, "Chronic exposure to dim artificial light disrupts the daily rhythm in mitochondrial respiration in mouse suprachiasmatic nucleus," (in eng), *Chronobiol Int,* pp. 1-14, Jul 24 2023, doi: 10.1080/07420528.2023.2236708.
[418] A. Meister, "Glutathione-ascorbic acid antioxidant system in animals," *Journal of Biological Chemistry,* vol. 269, no. 13, pp. 9397-9400, 1994/04/01/ 1994, doi: https://doi.org/10.1016/S0021-9258(17)36891-6.
[419] P. Soininen *et al.*, "High-throughput serum NMR metabonomics for cost-effective holistic studies on systemic metabolism," *Analyst,* 10.1039/B910205A vol. 134, no. 9, pp. 1781-1785, 2009, doi: 10.1039/B910205A.
[420] M. S. Duncan, R. S. Vasan, and V. Xanthakis, "Trajectories of Blood Lipid Concentrations Over the Adult Life Course and Risk of Cardiovascular Disease and All-Cause Mortality: Observations From the Framingham Study Over 35 Years," *Journal of the American Heart Association,* vol. 8, no. 11, p. e011433, 2019, doi: doi:10.1161/JAHA.118.011433.
[421] N. Sarwar *et al.*, "Triglycerides and the Risk of Coronary Heart Disease," *Circulation,* vol. 115, no. 4, pp. 450-458, 2007, doi: doi:10.1161/CIRCULATIONAHA.106.637793.
[422] M. Alves-Bezerra and D. E. Cohen, "Triglyceride Metabolism in the Liver," in *Comprehensive Physiology*, pp. 1-22.
[423] Y. Nakashima, A. S. Plump, E. W. Raines, J. L. Breslow, and R. Ross, "ApoE-deficient mice develop lesions of all phases of atherosclerosis throughout the arterial tree," *Arteriosclerosis and Thrombosis: A Journal of Vascular Biology,* vol. 14, no. 1, pp. 133-140, 1994, doi: doi:10.1161/01.ATV.14.1.133.
[424] S. H. Zhang, R. L. Reddick, J. A. Piedrahita, and N. Maeda, "Spontaneous Hypercholesterolemia and Arterial Lesions in Mice Lacking Apolipoprotein E," *Science,* vol. 258, no. 5081, pp. 468-471, 1992, doi: doi:10.1126/science.1411543.
[425] R. L. Reddick, S. H. Zhang, and N. Maeda, "Atherosclerosis in mice lacking apo E. Evaluation of lesional development and progression," *Arteriosclerosis and Thrombosis: A Journal of Vascular Biology,* vol. 14, no. 1, pp. 141-147, 1994, doi: doi:10.1161/01.ATV.14.1.141.
[426] A. S. Plump *et al.*, "Severe hypercholesterolemia and atherosclerosis in apolipoprotein E-deficient mice created by homologous recombination in ES cells," *Cell,* vol. 71, no. 2, pp. 343-353, 1992/10/16/ 1992, doi: https://doi.org/10.1016/0092-8674(92)90362-G.
[427] S.-H. Chen *et al.*, "Apolipoprotein B-48 Is the Product of a Messenger RNA with an Organ-Specific In-Frame Stop Codon," *Science,* vol. 238, no. 4825, pp. 363-366, 1987, doi: doi:10.1126/science.3659919.
[428] R. V. Farese, Jr. *et al.*, "Phenotypic analysis of mice expressing exclusively apolipoprotein B48 or apolipoprotein B100," (in eng), *Proc Natl Acad Sci U S A,* vol. 93, no. 13, pp. 6393-8, Jun 25 1996, doi: 10.1073/pnas.93.13.6393.

[429] Z. Sun *et al.*, "Circadian rhythm disorders elevate macrophages cytokines release and promote multiple tissues/organs dysfunction in mice," *Physiology & Behavior,* vol. 249, p. 113772, 2022/05/15/ 2022, doi: https://doi.org/10.1016/j.physbeh.2022.113772.
[430] I. Túnez, M. C. Muñoz, M. Feijoo-López, E. Valdelvira, I. Bujalance-Arenas, and P. Montilla, "Effect of melatonin on hyperlipidemic nephropathy under constant light exposure," *Journal of Physiology and Biochemistry,* vol. 58, no. 2, pp. 109-114, 2002/06/01 2002, doi: 10.1007/BF03179846.
[431] J. Frijhoff *et al.*, "Clinical Relevance of Biomarkers of Oxidative Stress," (in eng), *Antioxid Redox Signal,* vol. 23, no. 14, pp. 1144-70, Nov 10 2015, doi: 10.1089/ars.2015.6317.
[432] T. E. R. F. Collaboration*, "Major Lipids, Apolipoproteins, and Risk of Vascular Disease," *JAMA,* vol. 302, no. 18, pp. 1993-2000, 2009, doi: 10.1001/jama.2009.1619.
[433] D. J. Gordon *et al.*, "High-density lipoprotein cholesterol and cardiovascular disease. Four prospective American studies," *Circulation,* vol. 79, no. 1, pp. 8-15, 1989, doi: doi:10.1161/01.CIR.79.1.8.
[434] L. M. Hinder, A. M. Vincent, J. M. Hayes, L. L. McLean, and E. L. Feldman, "Apolipoprotein E knockout as the basis for mouse models of dyslipidemia-induced neuropathy," *Experimental Neurology,* vol. 239, pp. 102-110, 2013/01/01/ 2013, doi: https://doi.org/10.1016/j.expneurol.2012.10.002.
[435] M. Tani, R. Matera, K. V. Horvath, T. S. Hasan, E. J. Schaefer, and B. F. Asztalos, "The influence of apoE-deficiency and LDL-receptor-deficiency on the HDL subpopulation profile in mice and in humans," *Atherosclerosis,* vol. 233, no. 1, pp. 39-44, 2014, doi: 10.1016/j.atherosclerosis.2013.11.080.
[436] S. H. Zhang, R. L. Reddick, B. Burkey, and N. Maeda, "Diet-induced atherosclerosis in mice heterozygous and homozygous for apolipoprotein E gene disruption," (in eng), *J Clin Invest,* vol. 94, no. 3, pp. 937-45, Sep 1994, doi: 10.1172/jci117460.
[437] M. I. Mackness, S. Arrol, and P. N. Durrington, "Paraoxonase prevents accumulation of lipoperoxides in low-density lipoprotein," (in eng), *FEBS Lett,* vol. 286, no. 1-2, pp. 152-4, Jul 29 1991, doi: 10.1016/0014-5793(91)80962-3.
[438] G. Ferretti, T. Bacchetti, A. Nègre-Salvayre, R. Salvayre, N. Dousset, and G. Curatola, "Structural modifications of HDL and functional consequences," *Atherosclerosis,* vol. 184, no. 1, pp. 1-7, 2006/01/01/ 2006, doi: https://doi.org/10.1016/j.atherosclerosis.2005.08.008.
[439] D. W. Morel, "Reduced Cholesterol Efflux to Mildly Oxidized High Density Lipoprotein," *Biochemical and Biophysical Research Communications,* vol. 200, no. 1, pp. 408-416, 1994/04/15/ 1994, doi: https://doi.org/10.1006/bbrc.1994.1464.
[440] B. A. Wagner, G. R. Buettner, and C. P. Burns, "Free Radical-Mediated Lipid Peroxidation in Cells: Oxidizability Is a Function of Cell Lipid bis-Allylic Hydrogen Content," *Biochemistry,* vol. 33, no. 15, pp. 4449-4453, 1994/04/19 1994, doi: 10.1021/bi00181a003.
[441] A. W. Girotti and T. Kriska, "Role of lipid hydroperoxides in photo-oxidative stress signaling," (in eng), *Antioxid Redox Signal,* vol. 6, no. 2, pp. 301-10, Apr 2004, doi: 10.1089/152308604322899369.
[442] S. H. Zeisel and K. A. da Costa, "Choline: an essential nutrient for public health," (in eng), *Nutr Rev,* vol. 67, no. 11, pp. 615-23, Nov 2009, doi: 10.1111/j.1753-4887.2009.00246.x.
[443] K. D. Corbin and S. H. Zeisel, "Choline metabolism provides novel insights into nonalcoholic fatty liver disease and its progression," *Current Opinion in Gastroenterology,* vol. 28, no. 2, pp. 159-165, 2012, doi: 10.1097/MOG.0b013e32834e7b4b.
[444] Z. Wang *et al.*, "Gut flora metabolism of phosphatidylcholine promotes cardiovascular disease," *Nature,* vol. 472, no. 7341, pp. 57-63, 2011/04/01 2011, doi: 10.1038/nature09922.
[445] S. Rath, B. Heidrich, D. H. Pieper, and M. Vital, "Uncovering the trimethylamine-producing bacteria of the human gut microbiota," *Microbiome,* vol. 5, no. 1, p. 54, 2017/05/15 2017, doi: 10.1186/s40168-017-0271-9.
[446] V. E. Brunt *et al.*, "Trimethylamine-N-Oxide Promotes Age-Related Vascular Oxidative Stress and Endothelial Dysfunction in Mice and Healthy Humans," *Hypertension,* vol. 76, no. 1, pp. 101-112, 2020, doi: doi:10.1161/HYPERTENSIONAHA.120.14759.
[447] S. J. Zhang *et al.*, "Ketone Body 3-Hydroxybutyrate Ameliorates Atherosclerosis via Receptor Gpr109a-Mediated Calcium Influx," (in eng), *Adv Sci (Weinh),* vol. 8, no. 9, p. 2003410, May 2021, doi: 10.1002/advs.202003410.

[448] L. Wang, P. Chen, and W. Xiao, "β-hydroxybutyrate as an Anti-Aging Metabolite," *Nutrients,* vol. 13, no. 10, p. 3420, 2021. [Online]. Available: https://www.mdpi.com/2072-6643/13/10/3420.

[449] J. C. Newman and E. Verdin, "β-Hydroxybutyrate: A Signaling Metabolite," (in eng), *Annu Rev Nutr,* vol. 37, pp. 51-76, Aug 21 2017, doi: 10.1146/annurev-nutr-071816-064916.

[450] L. Ji *et al.*, "Ketone Body β-Hydroxybutyrate Prevents Myocardial Oxidative Stress in Septic Cardiomyopathy," *Oxidative Medicine and Cellular Longevity,* vol. 2022, p. 2513837, 2022/03/18 2022, doi: 10.1155/2022/2513837.

[451] T. Shimazu *et al.*, "Suppression of oxidative stress by β-hydroxybutyrate, an endogenous histone deacetylase inhibitor," (in eng), *Science,* vol. 339, no. 6116, pp. 211-4, Jan 11 2013, doi: 10.1126/science.1227166.

[452] H.-C. Lee, Y.-C. Lo, S.-C. Yu, T.-H. Tung, I. H. Lin, and S.-Y. Huang, "Degree of lipid saturation affects depressive-like behaviour and gut microbiota in mice," *International Journal of Food Sciences and Nutrition,* vol. 71, no. 4, pp. 440-452, 2020/05/18 2020, doi: 10.1080/09637486.2019.1681380.

[453] A. El Hajj *et al.*, "Targeted Suppression of Lipoprotein Receptor LSR in Astrocytes Leads to Olfactory and Memory Deficits in Mice," *International Journal of Molecular Sciences,* vol. 23, no. 4, p. 2049, 2022. [Online]. Available: https://www.mdpi.com/1422-0067/23/4/2049.

[454] D. E. Radford-Smith, A. G. Yates, L. Rizvi, D. C. Anthony, and F. Probert, "HDL and LDL have distinct, opposing effects on LPS-induced brain inflammation," *Lipids in Health and Disease,* vol. 22, no. 1, p. 54, 2023/04/24 2023, doi: 10.1186/s12944-023-01817-z.

[455] S. M. Houten, S. Violante, F. V. Ventura, and R. J. Wanders, "The Biochemistry and Physiology of Mitochondrial Fatty Acid β-Oxidation and Its Genetic Disorders," (in eng), *Annu Rev Physiol,* vol. 78, pp. 23-44, 2016, doi: 10.1146/annurev-physiol-021115-105045.

[456] A. S. Monzel, J. A. Enríquez, and M. Picard, "Multifaceted mitochondria: moving mitochondrial science beyond function and dysfunction," *Nature Metabolism,* vol. 5, no. 4, pp. 546-562, 2023/04/01 2023, doi: 10.1038/s42255-023-00783-1.

[457] J.-a. Kim, Y. Wei, and J. R. Sowers, "Role of Mitochondrial Dysfunction in Insulin Resistance," *Circulation Research,* vol. 102, no. 4, pp. 401-414, 2008, doi: doi:10.1161/CIRCRESAHA.107.165472.

[458] C. Guo, L. Sun, X. Chen, and D. Zhang, "Oxidative stress, mitochondrial damage and neurodegenerative diseases," (in eng), *Neural Regen Res,* vol. 8, no. 21, pp. 2003-14, Jul 25 2013, doi: 10.3969/j.issn.1673-5374.2013.21.009.

[459] L. Goicoechea, L. Conde de la Rosa, S. Torres, C. García-Ruiz, and J. C. Fernández-Checa, "Mitochondrial cholesterol: Metabolism and impact on redox biology and disease," (in eng), *Redox Biol,* vol. 61, p. 102643, May 2023, doi: 10.1016/j.redox.2023.102643.

[460] U. Gimsa, E. Kanitz, W. Otten, and S. M. Ibrahim, "Behavior and Stress Reactivity in Mouse Strains with Mitochondrial DNA Variations," *Annals of the New York Academy of Sciences,* vol. 1153, no. 1, pp. 131-138, 2009, doi: https://doi.org/10.1111/j.1749-6632.2008.03960.x.

[461] M. Suski *et al.*, "Proteomic analysis of changes in protein expression in liver mitochondria in apoE knockout mice," *Journal of Proteomics,* vol. 74, no. 6, pp. 887-893, 2011/05/16/ 2011, doi: https://doi.org/10.1016/j.jprot.2011.03.003.

[462] R. A. de Graaf, D. L. Rothman, and K. L. Behar, "State of the art direct 13C and indirect 1H-[13C] NMR spectroscopy in vivo. A practical guide," (in eng), *NMR Biomed,* vol. 24, no. 8, pp. 958-72, Oct 2011, doi: 10.1002/nbm.1761.

Supplementary

Table S1: Plasma metabolite statistics

		ANOVA main effects			Post hoc analysis							
Tissue	Metabolite	APOE-/- vs C57BL/6J	L:L vs L:D	Int.	C57BL/6J:LL vs. C57BL/6J:LD	APOE-/-:LD vs. C57BL/6J:LD	APOE -/-:LL vs. C57BL/6J:LD	APOE -/-:LD vs. C57BL/6J:LL	APOE -/-:LL vs C57BL/6J:LL	APOE -/-:LL vs. APOE -/-:LD	VIP score	NMR ppm
Plasma	αCH_2 lipoprotein	↑***	↑****	ns	↑***	↑**	↑****	ns	ns	↑*	1.88	2.24-2.26
	$=CH-CH_2=CH_2$ PUFA	ns	↑****	ns	ns	ns	ns	↓***	ns	↑***	1.86	2.00-2.02
	Acetate	↓****	ns	*	ns	↓****	↓**	↓**	↓****	ns	1.67	1.90-1.92
	β-hydroxybutyrate and HDL	↓****	↑**	ns	ns	↓****	↓****	↓****	↓****	↑**	1.56	1.24-1.26
	HDL	ns	ns	**	ns	↓**	ns	ns	ns	↑*	1.51	5.28-5.30
	Pyruvate	ns	ns	**	ns	ns	ns	ns	↓**	ns	1.42	2.40-2.42
	HDL	↓****	ns	*	ns	↓***	↓**	↓****	↓****	ns	1.36	5.26-5.28
	HDL	↓****	↓**	*	↓**	↓****	↓****	↓***	↓****	ns	1.35	0.82-0.84
	LDL and triglycerides	↑****	↑****	ns	ns	ns	↑****	ns	↑***	↑***	1.32	1.26-1.28
	Trimethylamine and free choline	↓****	↓****	ns	↓**	↓****	↓****	↓****	↓****	ns	1.29	3.20-3.22

Table S2: Brain metabolite statistics

		ANOVA main effects			Post hoc analysis							
Tissue	Metabolite	APOE-/- vs C57BL/6J	L:L vs L:D	Int.	C57BL/6J:LL vs. C57BL/6J:LD	APOE-/-:LD vs. C57BL/6J:LD	APOE -/-:LL vs. C57BL/6J:LD	APOE -/-:LD vs. C57BL/6J:LL	APOE -/-:LL vs C57BL/6J:LL	APOE -/-:LL vs. APOE -/-:LD	VIP score	NMR ppm
Brain	Ascorbate	ns	↓***	ns	↓**	ns	ns	↑*	ns	ns	1.96	4.49-4.51
	Alanine	ns	↑*	*	↑*	ns	ns	ns	ns	ns	1.89	1.47-1.49
	ATP Adenosine moiety	↓**	↓***	ns	↓*	ns	↓***	ns	ns	ns	1.85	8.26-8.28
	Glutamate	ns	ns	**	↑*	ns	ns	ns	ns	ns	1.73	3.77-3.79
	Hypoxanthine	ns	↓**	ns	↓*	ns	↓*	ns	ns	ns	1.63	8.16-8.18
	ATP Ribose moiety	↓*	↓***	ns	↓*	ns	↓***	ns	ns	ns	1.63	6.14-6.16
	Scyllo-inositol	↑***	↑*	ns	ns	ns	↑***	ns	↑**	ns	1.58	3.35-3.37
	Glutamate	ns	ns	*	ns	ns	ns	ns	ns	ns	1.58	2.35-2.37
	Lactate	↓*	ns	*	ns	ns	ns	ns	↓**	ns	1.49	4.09-4.11

Table S3: Liver Metabolite Statistics

		ANOVA main effects			Post hoc analysis							
Tissue	Metabolite	APOE-/- vs C57BL/6J	L:L vs L:D	Int.	C57BL/6J:LL vs. C57BL/6J:LD	APOE-/-:LD vs. C57BL/6J:LD	APOE -/-:LL vs. C57BL/6J:LD	APOE -/-:LD vs. C57BL/6J:LL	APOE -/-:LL vs C57BL/6J:LL	APOE -/-:LL vs. APOE -/-:LD	VIP score	NMR ppm
Liver	Glutathione Glu-αCH	ns	↑****	ns	↑****	ns	↑***	↓****	ns	↑**	2.19	3.77-3.79
	Glutathione Glu-γCH2	ns	↑****	ns	↑****	ns	↑*	↓****	ns	↑*	2.08	2.57-2.59
	Glutathione Glu-γCH2	ns	↑****	ns	ns	ns	↑****	ns	ns	↑***	2.04	2.55-2.57
	Glutathione Glu-βCH2	ns	↑****	ns	↑***	ns	ns	↓***	ns	ns	1.96	2.17-2.19
	Glutathione Glu-Cys-αCH	ns	↑****	ns	↑***	ns	ns	↓***	ns	ns	1.95	4.55-4.57
	Glutathione Cys-βCH2	ns	↑****	ns	↑***	ns	ns	↓***	ns	ns	1.94	2.93-2.95
	Glutathione Cys-βCH2	ns	↑****	ns	↑**	ns	ns	↓***	ns	ns	1.87	2.95-2.97
	Choline	ns	↓***	ns	↓**	ns	ns	↑**	ns	ns	1.69	3.19-3.21

Table S4: Correlations between plasma metabolites and behavioural results

	Plasma Metabolites									
Behavioural results	αCH2 [2.24-2.26]	=CH-CH_2=CH_2- [2.00-2.02]	Acetate [1.90-1.92]	β-hydroxybutyrate and HDL [1.24-1.26]	HDL [5.28-5.30]	Pyruvate [2.40-2.42]	HDL [5.26-5.28]	HDL [0.82-0.84]	LDL and triglycerides [1.26-1.28]	Trimethylamine and free choline [3.20-3.22]
Frequency to light (LDB)	r=0.24 p=ns	r=-0.16 p=ns	**r=-0.55** **p=0.0047**	**r=-0.50** **p=0.013**	r=-0.21 p=ns	r=-0.28 p=ns	**r=-0.55** **p=0.0049**	**r=-0.51** **p=0.0099**	r=0.35 p=ns	**r=-0.56** **p=0.0043**
Duration in light (LDB)	r=0.24 p=ns	r=-0.18 p=ns	**r=-0.46** **p=0.023**	**r=-0.48** **p=0.019**	r=-0.21 p=ns	r=-0.27 p=ns	**r=-0.51** **p=0.011**	**r=-0.48** **p=0.019**	r=0.28 p=ns	**r=-0.50** **p=0.012**
Distance travelled (OFT)	r=0.15 p=ns	**r=-0.41** **p=0.049**	**r=-0.52** **p=0.0089**	**r=-0.68** **p=0.00014**	r=-0.40 p=ns	r=-0.032 p=ns	**r=-0.65** **p=0.00042**	**r=-0.56** **p=0.0044**	r=0.13 p=ns	**r=-0.48** **p=0.017**
Mean velocity (OFT)	r=0.15 p=ns	**r=-0.41** **p=0.049**	**r=-0.52** **p=0.0089**	**r=-0.68** **p=0.00014**	r=-0.40 p=ns	r=-0.032 p=ns	**r=-0.65** **p=0.00042**	**r=-0.56** **p=0.0044**	r=0.13 p=ns	**r=-0.48** **p=0.017**
Duration around edges (OFT)	r=0.30 p=ns	r=0.29 p=ns	r=-0.058 p=ns	r=0.012 p=ns	r=0.24 p=ns	r=-0.15 p=ns	r=0.44 p=ns	r=-0.13 p=ns	r=0.41 p=ns	r=-0.17 p=ns
% Sucrose preference	r=0.35 p=ns	r=0.20 p=ns	r=0.21 p=ns	r=0.051 p=ns	r=0.037 p=ns	r=0.071 p=ns	r=-0.079 p=ns	r=-0.13 p=ns	r=0.27 p=ns	r=-0.19 p=ns
Change in body mass (g)	r=0.11 p=ns	**r=0.47** **p=0.019**	r=-0.022 p=ns	r=0.30 p=ns	**r=0.50** **p=0.013**	r=-0.21 p=ns	r=0.35 p=ns	r=0.037 p=ns	r=0.31 p=ns	r=-0.0087 p=ns
Total sleep (min)	r=0.25 p=ns	r=0.067 p=ns	r=-00.011 p=ns	r=-0.081 p=ns	r=-0.12 p=ns	r=0.26 p=ns	r=-0.060 p=ns	r=-0.15 p=ns	r=0.042 p=ns	r=-0.098 p=ns
% Sleep in light phase	r=0.24 p=ns	r=0.064 p=ns	r=-0.011 p=ns	r=-0.083 p=ns	r=-0.12 p=ns	r=0.26 p=ns	r=-0.060 p=ns	r=-0.15 p=ns	r=0.039 p=ns	r=-0.095 p=ns

Table S4: Continued

	Plasma Metabolites									
Behavioural results	αCH2 [2.24-2.26]	=CH-CH_2=CH_2- [2.00-2.02]	Acetate [1.90-1.92]	β-hydroxybutyrate and HDL [1.24-1.26]	HDL [5.28-5.30]	Pyruvate [2.40-2.42]	HDL [5.26-5.28]	HDL [0.82-0.84]	LDL and triglycerides [1.26-1.28]	Trimethylamine and free choline [3.20-3.22]
Circadian period	**r=0.66 p=0.00027**	**r=0.48 p=0.017**	r=-0.19 p=ns	r=-0.045 p=ns	r=0.23 p=ns	r=-0.22 p=ns	r=-0.093 p=ns	r=-0.35 p=ns	**r=0.64 p=0.00049**	**r=-0.49 p=0.015**
Circadian Amplitude	r=-0.11 p=ns	**r=-0.47 p=0.022**	r=-0.26 p=ns	**r=-0.49 p=0.016**	r=-0.40 p=ns	r=0.027 p=ns	**r=-0.46 p=0.025**	r=-0.21 p=ns	r=-0.19 p=ns	r=-0.17 p=ns
Circadian phase	r=0.28 p=ns	**r=0.55 p=0.0046**	r=0.11 p=ns	r=0.40 p=ns	r=0.29 p=ns	r=0.12 p=ns	r=0.29 p=ns	r=-0.066 p=ns	r=0.30 p=ns	r=-0.048 p=ns
Total activity bouts	r=-0.33 p=ns	r=-0.026 p=ns	r=0.15 p=ns	r=0.25 p=ns	r=0.17 p=ns	r=-0.075 p=ns	r=0.31 p=ns	r=0.35 p=ns	r=0.22 p=ns	r=0.30 p=ns
Average activity bout length	r=0.030 p=ns	r=-0.38 p=ns	r=-0.30 p=ns	**r=-0.54 p=0.0062**	r=-0.28 p=ns	r=-0.083 p=ns	**r=-0.51 p=0.011**	r=-0.39 p=ns	r=0.041 p=ns	r=-0.32 p=ns
Total Distance Travelled (HCB)	r=-0.13 p=ns	**r=-0.45 p=0.028**	r=-0.31 p=ns	**r=-0.50 p=0.013**	r=-0.22 p=ns	r=-0.064 p=ns	r=-0.39 p=ns	r=-0.24 p=ns	r=-0.091 p=ns	r=-0.17 p=ns
Total Mean Velocity (HCB)	r=-0.18 p=ns	r=-0.48 p=ns	r=-0.31 p=ns	**r=-0.50 p=0.013**	r=-0.23 p=ns	r=-0.13 p=ns	r=-0.40 p=ns	r=-0.20 p=ns	r=-0.11 p=ns	r=-0.16 p=ns
Total # water bottle licks (HCB)	r=0.30 p=ns	r=-0.071 p=ns	r=-0.39 p=ns	**r=-0.48 p=0.027**	r=-0.12 p=ns	r=-0.22 p=ns	**r=-0.46 p=0.033**	r=-0.38 p=ns	r=0.43 p=ns	**r=-0.47 p=0.032**

	Plasma Metabolites									
Behavioural results	αCH2 [2.24-2.26]	=CH-CH_2=CH_2- [2.00-2.02]	Acetate [1.90-1.92]	β-hydroxybutyrate and HDL [1.24-1.26]	HDL [5.28-5.30]	Pyruvate [2.40-2.42]	HDL [5.26-5.28]	HDL [0.82-0.84]	LDL and triglycerides [1.26-1.28]	Trimethylamine and free choline [3.20-3.22]
Frequency to light (LDB)	r=0.24 p=ns	r=-0.16 p=ns	**r=-0.55** **p=0.0047**	**r=-0.50** **p=0.013**	r=-0.21 p=ns	r=-0.28 p=ns	**r=-0.55** **p=0.0049**	**r=-0.51** **p=0.0099**	r=0.35 p=ns	**r=-0.56** **p=0.0043**
Duration in light (LDB)	r=0.24 p=ns	r=-0.18 p=ns	**r=-0.46** **p=0.023**	**r=-0.48** **p=0.019**	r=-0.21 p=ns	r=-0.27 p=ns	**r=-0.51** **p=0.011**	**r=-0.48** **p=0.019**	r=0.28 p=ns	**r=-0.50** **p=0.012**
Distance travelled (OFT)	r=0.15 p=ns	**r=-0.41** **p=0.049**	**r=-0.52** **p=0.0089**	**r=-0.68** **p=0.00014**	r=-0.40 p=ns	r=-0.032 p=ns	**r=-0.65** **p=0.00042**	**r=-0.56** **p=0.0044**	r=0.13 p=ns	**r=-0.48** **p=0.017**
Mean velocity (OFT)	r=0.15 p=ns	**r=-0.41** **p=0.049**	**r=-0.52** **p=0.0089**	**r=-0.68** **p=0.00014**	r=-0.40 p=ns	r=-0.032 p=ns	**r=-0.65** **p=0.00042**	**r=-0.56** **p=0.0044**	r=0.13 p=ns	**r=-0.48** **p=0.017**
Duration around edges (OFT)	r=0.30 p=ns	r=0.29 p=ns	r=-0.058 p=ns	r=0.012 p=ns	r=0.24 p=ns	r=-0.15 p=ns	r=0.44 p=ns	r=-0.13 p=ns	r=0.41 p=ns	r=-0.17 p=ns
% Sucrose preference	r=0.35 p=ns	r=0.20 p=ns	r=0.21 p=ns	r=0.051 p=ns	r=0.037 p=ns	r=0.071 p=ns	r=-0.079 p=ns	r=-0.13 p=ns	r=0.27 p=ns	r=-0.19 p=ns
Change in body mass (g)	r=0.11 p=ns	**r=0.47** **p=0.019**	r=-0.022 p=ns	r=0.30 p=ns	**r=0.50** **p=0.013**	r=-0.21 p=ns	r=0.35 p=ns	r=0.037 p=ns	r=0.31 p=ns	r=-0.0087 p=ns
Total sleep (min)	r=0.25 p=ns	r=0.067 p=ns	r=-00.011 p=ns	r=-0.081 p=ns	r=-0.12 p=ns	r=0.26 p=ns	r=-0.060 p=ns	r=-0.15 p=ns	r=0.042 p=ns	r=-0.098 p=ns
% Sleep in light phase	r=0.24 p=ns	r=0.064 p=ns	r=-0.011 p=ns	r=-0.083 p=ns	r=-0.12 p=ns	r=0.26 p=ns	r=-0.060 p=ns	r=-0.15 p=ns	r=0.039 p=ns	r=-0.095 p=ns

Table S5: Correlations between brain metabolites and behavioural results

	Brain Metabolites								
Behavioural results	Ascorbate [4.49-4.51]	Alanine [1.47-1.49]	ATP Adenosine moiety [8.26-8.28]	Glutamate [3.77-3.79]	Hypoxanthine [8.16-8.18]	ATP Ribose moiety [6.14-6.16]	Scyllo-inositol [3.35-3.37]	Glutamate [2.35-2.37]	Lactate [4.09-4.11]
Frequency to light (LDB)	r=0.15 p=ns	r=0.096 p=ns	r=-0.24 p=ns	r=0.16 p=ns	r=0.045 p=ns	r=-0.31 p=ns	r=0.34 p=ns	r=0.041 p=ns	r=-0.35 p=ns
Duration in light (LDB)	r=0.17 p=ns	r=0.062 p=ns	r=-0.18 p=ns	r=0.20 p=ns	r=-0.039 p=ns	r=-0.33 p=ns	r=0.32 p=ns	r=-0.039 p=ns	r=-0.34 p=ns
Distance travelled (OFT)	r=0.25 p=ns	r=0.065 p=ns	r=-0.30 p=ns	r=0.36 p=ns	r=-0.11 p=ns	r=-0.34 p=ns	r=0.21 p=ns	r=0.028 p=ns	r=-0.46 p=ns
Mean velocity (OFT)	r=0.25 p=ns	r=0.065 p=ns	r=-0.30 p=ns	r=0.36 p=ns	r=-0.11 p=ns	r=-0.34 p=ns	r=0.21 p=ns	r=0.028 p=ns	r=-0.46 p=ns
Duration around edges (OFT)	r=-0.13 p=ns	r=0.17 p=ns	r=-0.26 p=ns	r=-0.10 p=ns	r=-0.42 p=ns	r=-0.24 p=ns	r=0.44 p=ns	r=-0.23 p=ns	r=-0.099 p=ns
% Sucrose preference	r=0.060 p=ns	r=-0.10 p=ns	r=-0.23 p=ns	r=0.177 p=ns	r=-0.13 p=ns	r=-0.20 p=ns	r=0.32 p=ns	r=0.23 p=ns	r=-0.069 p=ns
Change in body mass (g)	r=-0.20 p=ns	r=0.045 p=ns	r=-0.026 p=ns	r=-0.29 p=ns	r=-0.024 p=ns	r=-0.049 p=ns	r=0.073 p=ns	r=-0.31 p=ns	r=0.046 p=ns
Total sleep (min)	r=-0.34 p=ns	r=0.21 p=ns	r=-0.050 p=ns	r=0.33 p=ns	r=-0.19 p=ns	r=0.021 p=ns	r=-0.055 p=ns	r=0.37 p=ns	r=0.39 p=ns
% Sleep in light phase	r=-0.34 p=ns	r=0.21 p=ns	r=-0.046 p=ns	r=0.33 p=ns	r=-0.19 p=ns	r=0.026 p=ns	r=-0.055 p=ns	r=0.38 p=ns	r=0.39 p=ns
Circadian period	r=-0.44 p=ns	r=0.25 p=ns	**r=-0.49** **p=0.043**	r=0.16 p=ns	r=-0.41 p=ns	r=-0.44 p=ns	r=0.48 p=ns	r=0.026 p=ns	r=-0.070 p=ns

Table S5: Continued

	Brain Metabolites								
Behavioural results	Ascorbate [4.49-4.51]	Alanine [1.47-1.49]	ATP Adenosine moiety [8.26-8.28]	Glutamate [3.77-3.79]	Hypoxanthine [8.16-8.18]	ATP Ribose moiety [6.14-6.16]	Scyllo-inositol [3.35-3.37]	Glutamate [2.35-2.37]	Lactate [4.09-4.11]
Circadian Amplitude	r=0.21 p=ns	r=-0.077 p=ns	r=0.15 p=ns	r=0.23 p=ns	r=0.28 p=ns	r=0.22 p=ns	r=-0.096 p=ns	r=0.35 p=ns	r=-0.034 p=ns
Circadian phase	r=-0.27 p=ns	r=0.44 p=ns	r=-0.30 p=ns	r=-0.015 p=ns	r=-0.30 p=ns	r=-0.45 p=ns	r=0.096 p=ns	r=-0.36 p=ns	r=0.065 p=ns
Total activity bouts	r=0.13 p=ns	r=-0.041 p=ns	r=0.24 p=ns	r=-0.32 p=ns	r=0.25 p=ns	r=0.27 p=ns	r=-0.22 p=ns	r=-0.095 p=ns	r=-0.051 p=ns
Average activity bout length	r=0.29 p=ns	r=-0.19 p=ns	r=-0.027 p=ns	r=0.23 p=ns	r=0.11 p=ns	r=-0.053 p=ns	r=0.29 p=ns	r=0.11 p=ns	r=-0.26 p=ns
Total Distance Travelled (HCB)	r=0.37 p=ns	r=-0.29 p=ns	r=0.15 p=ns	r=0.070 p=ns	r=0.20 p=ns	r=0.15 p=ns	r=0.14 p=ns	r=0.093 p=ns	r=-0.30 p=ns
Total Mean Velocity (HCB)	r=0.48 p=ns	r=-0.34 p=ns	r=0.19 p=ns	r=0.039 p=ns	r=0.32 p=ns	r=0.22 p=ns	r=0.15 p=ns	r=0.19 p=ns	r=-0.33 p=ns
Total # water bottle licks (HCB)	r=-0.13 p=ns	r=0.12 p=ns	r=-0.27 p=ns	r=0.18 p=ns	r=-0.21 p=ns	r=-0.28 p=ns	r=0.30 p=ns	r=0.013 p=ns	r=-0.43 p=ns

Table S6: Correlations between brain gene expression and behavioural results

	Brain Gene Expression										
Behavioural results	Pfkfb3	Slc2a1	Gpx4	Fabp7	Gcl	Behavioural results	Pfkfb3	Slc2a1	Gpx4	Fabp7	Gcl
Frequency to light (LDB)	r=-0.20 p=ns	r=-0.18 p=ns	r=-0.025 p=ns	r=-0.19 p=ns	r=0.064 p=ns	Circadian period	r=-0.42 p=ns	r=-0.38 p=ns	r=-0.39 p=ns	r=0.00064 p=ns	r=0.30 p=ns
Duration in light (LDB)	r=-0.24 p=ns	r=-0.19 p=ns	r=-0.057 p=ns	r=-0.10 p=ns	r=0.080 p=ns	Circadian Amplitude	r=0.14 p=ns	r=-0.015 p=ns	r=0.53 p=ns	r=-0.17 p=ns	r=-0.12 p=ns
Distance travelled (OFT)	r=-0.21 p=ns	r=-0.27 p=ns	r=0.051 p=ns	r=-0.20 p=ns	r=-0.028 p=ns	Circadian phase	r=-0.014 p=ns	r=0.11 p=ns	r=-0.23 p=ns	r=-0.035 p=ns	r=0.19 p=ns
Mean velocity (OFT)	r=-0.21 p=ns	r=-0.27 p=ns	r=0.052 p=ns	r=-0.20 p=ns	r=-0.028 p=ns	Total activity bouts	r=0.0039 p=ns	r=0.35 p=ns	r=0.066 p=ns	r=0.098 p=ns	r=-0.18 p=ns
Duration around edges (OFT)	r=-0.56 p=ns	r=-0.55 p=ns	**r=-0.74 p=0.0058**	r=-0.29 p=ns	r=0.0039 p=ns	Average activity bout length	r=-0.27 p=ns	r=-0.29 p=ns	r=-0.020 p=ns	r=-0.15 p=ns	r=0.031 p=ns
% Sucrose preference	**r=-0.64 p=0.023**	r=-0.53 p=ns	r=-0.55 p=ns	r=-0.22 p=ns	r=0.23 p=ns	Total Distance Travelled (HCB)	r=-0.32 p=ns	r=-0.24 p=ns	r=-0.037 p=ns	r=-0.21 p=ns	r=0.057 p=ns
Change in body mass (g)	r=-0.099 p=ns	r=0.066 p=ns	r=-0.025 p=ns	r=0.28 p=ns	r=0.12 p=ns	Total Mean Velocity (HCB)	r=-0.35 p=ns	r=-0.24 p=ns	r=0.036 p=ns	r=-0.090 p=ns	r=0.064 p=ns
Total sleep (min)	r=0.52 p=ns	r=0.12 p=ns	r=0.16 p=ns	r=-0.39 p=ns	r=-0.26 p=ns	Total # water bottle licks (HCB)	r=-0.46 p=ns	r=-0.33 p=ns	r=-0.25 p=ns	r=-0.078 p=ns	r=-0.11 p=ns
% Sleep in light phase	r=0.52 p=ns	r=0.12 p=ns	r=0.16 p=ns	r=-0.39 p=ns	r=-0.26 p=ns						

Table S7: Correlations between liver metabolites and behavioural results

	Liver Metabolites							
Behavioural results	Glutathione [3.77-3.79]	Glutathione [2.57-2.59]	Glutathione [2.55-2.57]	Glutathione [2.17-2.19]	Glutathione [4.55-4.57]	Glutathione [2.93-2.95]	Glutathione [2.95-2.97]	Choline [3.19-3.21]
Frequency to light (LDB)	r=-0.063 p=ns	r=-0.045 p=ns	r=-0.19 p=ns	r=-0.053 p=ns	r=0.11 p=ns	r=0.031 p=ns	r=0.018 p=ns	r=0.15 p=ns
Duration in light (LDB)	r=-0.074 p=ns	r=-0.017 p=ns	r=0.0011 p=ns	r=-0.030 p=ns	r=0.11 p=ns	r=0.045 p=ns	r=0.025 p=ns	r=0.20 p=ns
Distance travelled (OFT)	r=-0.10 p=ns	r=-0.083 p=ns	r=-0.077 p=ns	r=-0.092 p=ns	r=-0.071 p=ns	r=-0.044 p=ns	r=-0.082 p=ns	r=0.16 p=ns
Mean velocity (OFT)	r=-0.10 p=ns	r=-0.083 p=ns	r=-0.077 p=ns	r=-0.092 p=ns	r=-0.071 p=ns	r=-0.044 p=ns	r=-0.083 p=ns	r=0.16 p=ns
Duration around edges (OFT)	r=0.41 p=ns	r=0.098 p=ns	r=0.068 p=ns	r=0.074 p=ns	r=0.05 p=ns	r=0.051 p=ns	r=0.080 p=ns	r=-0.14 p=ns
% Sucrose preference	r=0.36 p=ns	r=0.34 p=ns	r=0.30 p=ns	r=0.31 p=ns	r=0.28 p=ns	r=0.30 p=ns	r=0.23 p=ns	r=0.067 p=ns
Change in body mass (g)	r=0.39 p=ns	r=0.16 p=ns	r=0.11 p=ns	r=0.18 p=ns	r=0.064 p=ns	r=0.063 p=ns	r=0.14 p=ns	r=-0.15 p=ns
Total sleep (min)	r=0.26 p=ns	r=0.34 p=ns	r=0.38 p=ns	r=0.35 p=ns	r=0.37 p=ns	r=0.37 p=ns	r=0.37 p=ns	r=-0.36 p=ns
% Sleep in light phase	r=0.25 p=ns	r=0.34 p=ns	r=0.38 p=ns	r=0.34 p=ns	r=0.36 p=ns	r=0.37 p=ns	r=0.36 p=ns	r=-0.36 p=ns
Circadian period	**r=0.62** **p=0.00010**	**r=0.50** **p=0.013**	**r=0.50** **p=0.014**	**r=0.51** **p=0.011**	**r=0.44** **p=0.032**	**r=0.46** **p=0.025**	**r=0.49** **p=0.016**	r=-0.22 p=ns

Table S7: Continued

	Liver Metabolites							
Behavioural results	Glutathione [3.77-3.79]	Glutathione [2.57-2.59]	Glutathione [2.55-2.57]	Glutathione [2.17-2.19]	Glutathione [4.55-4.57]	Glutathione [2.93-2.95]	Glutathione [2.95-2.97]	Choline [3.19-3.21]
Circadian Amplitude	r=-0.36 p=ns	r=-0.24 p=ns	r=-0.21 p=ns	r=-0.18 p=ns	r=-0.22 p=ns	r=-0.19 p=ns	r=-0.28 p=ns	r=0.36 p=ns
Circadian phase	**r=0.43 p=0.042**	**r=0.44 p=0.032**	**r=0.43 p=0.038**	r=0.39 p=ns	**r=0.44 p=0.035**	**r=0.41 p=0.050 (0.0498)**	**r=0.50 p=0.013**	**r=-0.48 p=0.019**
Total activity bouts	r=-0.15 p=ns	r=-0.21 p=ns	r=-0.21 p=ns	r=-0.19 p=ns	r=-0.19 p=ns	r=-0.18 p=ns	r=-0.18 p=ns	r=0.060 p=ns
Average activity bout length	r=-0.30 p=ns	r=-0.24 p=ns	r=-0.23 p=ns	r=-0.23 p=ns	r=-0.19 p=ns	r=-0.20 p=ns	r=-0.21 p=ns	r=0.41 p=ns
Total Distance Travelled (HCB)	r=-0.39 p=ns	r=-0.39 p=ns	r=-0.39 p=ns	r=-0.35 p=ns	r=-0.41 p=ns	r=-0.35 p=ns	r=-0.37 p=ns	**r=0.53 p=0.0075**
Total Mean Velocity (HCB)	**r=-0.46 p=0.025**	**r=-0.46 p=0.025**	**r=-0.46 p=0.026**	**r=-0.43 p=0.041**	**r=-0.46 p=0.027**	r=-0.40 p=ns	**r=-0.44 p=0.035**	**r=0.61 p=0.0012**
Total # water bottle licks (HCB)	r=-0.0051 p=ns	r=0.0052 p=ns	r=0.034 p=ns	r=0.013 p=ns	r=0.012 p=ns	r=0.072 p=ns	r=0.036 p=ns	r=0.026 p=ns

Table S8: Correlations between liver gene expression and behavioural results

	Liver Genes							
Behavioural results	Ppar-α	Ror-α	Sirt1	Sod1	Dgat1	Rxr-α	Hmgcr	Fasn
Frequency to light (LDB)	r=-0.67 p=ns	r=0.11 p=ns	r=0.21 p=ns	r=0.039 p=ns	r=0.051 p=ns	r=0.10 p=ns	r=0.059 p=ns	r=-0.28 p=ns
Duration in light (LDB)	r=-0.031 p=ns	r=0.076 p=ns	r=0.24 p=ns	r=0.041 p=ns	r=0.078 p=ns	r=0.10 p=ns	r=0.12 p=ns	r=-0.23 p=ns
Distance travelled (OFT)	r=0.18 p=ns	r=0.22 p=ns	**r=0.46** **p=0.025**	r=0.34 p=ns	r=0.38 p=ns	**r=0.46** **p=0.027**	r=0.11 p=ns	r=-0.36 p=ns
Mean velocity (OFT)	r=0.18 p=ns	r=0.22 p=ns	**r=0.46** **p=0.025**	r=0.34 p=ns	r=0.38 p=ns	**r=0.46** **p=0.027**	r=0.11 p=ns	r=-0.36 p=ns
Duration around edges (OFT)	r=-0.28 p=ns	r=-0.35 p=ns	r=-0.21 p=ns	r=-0.23 p=ns	r=-0.18 p=ns	r=-0.25 p=ns	r=-0.076 p=ns	r=0.024 p=ns
% Sucrose preference	r=-0.19 p=ns	r=-0.29 p=ns	r=-0.20 p=ns	r=-0.23 p=ns	r=-0.32 p=ns	r=-0.26 p=ns	r=-0.070 p=ns	r=0.14 p=ns
Change in body mass (g)	r=-0.0042 p=ns	r=-0.024 p=ns	r=-0.215 p=ns	r=-0.25 p=ns	r=-0.23 p=ns	r=-0.28 p=ns	r=-0.25 p=ns	r=-0.037 p=ns
Total sleep (min)	r=-0.32 p=ns	r=-0.29 p=ns	r=-0.17 p=ns	r=0.037 p=ns	r=-0.0080 p=ns	r=0.061 p=ns	r=-0.20 p=ns	r=0.0039 p=ns
% Sleep in light phase	r=-0.32 p=ns	r=-0.29 p=ns	r=-0.17 p=ns	r=0.040 p=ns	r=-0.0024 p=ns	r=0.066 p=ns	r=-0.20 p=ns	r=0.0034 p=ns
Circadian period	**r=-0.59** **p=0.0016**	**r=-0.60** **p=0.0011**	**r=-0.52** **p=0.0075**	**r=-0.42** **p=0.047**	**r=-0.53** **p=0.0081**	**r=-0.52** **p=0.0086**	**r=-0.48** **p=0.016**	r=-0.062 p=ns

Table S8: Continued

	Liver Genes continued							
Behavioural results	Ppar-α	Ror-α	Sirt1	Sod1	Dgat1	Rxr-α	Hmgcr	Fasn
Circadian Amplitude	r=0.20 p=ns	r=0.19 p=ns	r=0.34 p=ns	r=0.27 p=ns	**r=0.43** **p=0.039**	**r=0.48** **p=0.019**	r=0.17 p=ns	r=-0.24 p=ns
Circadian phase	**r=-0.40** p=ns	r=-0.18 p=ns	r=-0.34 p=ns	r=-0.38 p=ns	**r=-0.54** **p=0.0071**	**r=-0.56** **p=0.0040**	r=0.00033 p=ns	r=0.39 p=ns
Total activity bouts	r=0.17 p=ns	r=0.23 p=ns	r=0.064 p=ns	r=-0.15 p=ns	r=-0.16 p=ns	r=-0.15 p=ns	r=0.18 p=ns	r=0.013 p=ns
Average activity bout length	r=0.28 p=ns	r=0.15 p=ns	r=0.35 p=ns	**r=0.41** p=ns	**r=0.49** **p=0.016**	**r=0.52** **p=0.0092**	r=0.091 p=ns	r=-0.21 p=ns
Total Distance Travelled (HCB)	**r=0.48** **p=0.016**	r=0.27 p=ns	**r=0.51** **p=0.0088**	**r=0.43** **p=0.039**	**r=0.64** **p=0.00074**	**r=0.61** **p=0.0011**	r=0.28 p=ns	r=-0.24 p=ns
Total Mean Velocity (HCB)	**r=0.49** **p=0.013**	r=0.29 p=ns	**r=0.50** **p=0.011**	r=0.39 p=ns	**r=0.60** **p=0.0017**	**r=0.59** **p=0.0019**	r=0.28 p=ns	r=-0.26 p=ns
Total # water bottle licks (HCB)	r=-0.040 p=ns	r=-0.12 p=ns	r=0.17 p=ns	r=0.38 p=ns	r=0.13 p=ns	r=0.14 p=ns	r=0.012 p=ns	r=-0.24 p=ns

Table S9: Correlations between gene expression and metabolites across tissues

Metabolites vs gene expression	αCH_2 [2.24-2.26]	$=CH-CH_2=CH_2$ - [2.00-2.02]	Acetate [1.90-1.92]	β-hydroxybutyrate and HDL [1.24-1.26]	HDL [5.28-5.30]	Pyruvate [2.40-2.42]	HDL [5.26-5.28]	HDL [0.82-0.84]	LDL and triglycerides [1.26-1.28]	Trimethylamine and free choline [3.20-3.22]	Ascorbate [4.49-4.51]	Alanine [1.47-1.49]
Pfkfb3	r=-0.41 p=ns	r=-0.074 p=ns	r=0.050 p=ns	r=0.27 p=ns	r=-0.062 p=ns	r=0.17 p=ns	r=0.26 p=ns	r=0.35 p=ns	r=-0.38 p=ns	r=0.46 p=ns	r=--0.012 p=ns	r=0.13 p=ns
Slc2a1	r=-0.41 p=ns	r=-0.070 p=ns	r=0.027 p=ns	r=0.27 p=ns	r=-0.033 p=ns	r=0.059 p=ns	r=0.23 p=ns	r=0.31 p=ns	r=-0.37 p=ns	r=0.43 p=ns	r=0.24 p=ns	r=-0.052 p=ns
Gpx4	r=-0.39 p=ns	r=-0.36 p=ns	r=-0.079 p=ns	r=-0.096 p=ns	r=-0.37 p=ns	r=0.12 p=ns	r=-0.24 p=ns	r=0.15 p=ns	r=-0.44 p=ns	r=0.22 p=ns	r=0.16 p=ns	r=-0.20 p=ns
Fabp7	r=-0.17 p=ns	r=0.035 p=ns	r=-0.092 p=ns	r=0.18 p=ns	r=0.091 p=ns	r=-0.37 p=ns	r=0.065 p=ns	r=0.26 p=ns	r=-0.054 p=ns	r=0.12 p=ns	r=0.073 p=ns	**r=-0.53** p=ns
Gcl	r=0.30 p=ns	r=0.20 p=ns	r=-0.36 p=ns	r=-0.012 p=ns	r=0.11 p=ns	r=-0.079 p=ns	r=-0.074 p=ns	r=-0.062 p=ns	r=0.28 p=ns	r=-0.20 p=ns	r=0.014 p=ns	r=-0.10 p=ns
Ppar-α	**r=-0.53 p=0.0092**	r=-0.37 p=ns	r=-0.0086 p=ns	r=-0.10 p=ns	r=0.0015 p=ns	r=0.0040 p=ns	r=0.039 p=ns	r=0.24 p=ns	r=-0.41 p=ns	r=0.30 p=ns	**r=0.48 p=0.027**	r=-0.35 p=ns
Ror-α	**r=-0.54 p=0.0081**	**r=-0.46 p=0.035**	r=-0.076 p=ns	r=-0.14 p=ns	r=-0.21 p=ns	r=0.18 p=ns	r=-0.086 p=ns	r=0.099 p=ns	**r=-0.44 p=0.047**	r=0.24 p=ns	**r=0.40** p=ns	r=-0.096 p=ns
Sirt1	r=-0.32 p=ns	r=-0.37 p=ns	r=-0.17 p=ns	r=-0.28 p=ns	r=-0.14 p=ns	r=0.061 p=ns	r=-0.17 p=ns	r=-0.0017 p=ns	r=-0.24 p=ns	r=0.067 p=ns	**r=0.43** p=ns	r=-0.047 p=ns
Sod1	r=-0.23 p=ns	r=-0.31 p=ns	r=-0.11 p=ns	r=-0.29 p=ns	r=-0.15 p=ns	r=0.13 p=ns	r=-0.20 p=ns	r=-0.060 p=ns	r=-0.18 p=ns	r=0.025 p=ns	r=0.24 p=ns	r=0.11 p=ns
Dgat1	r=-0.40 p=ns	**r=-0.50 p=0.022**	r=-0.19 p=ns	r=-0.35 p=ns	r=-0.23 p=ns	r=0.074 p=ns	r=-0.22 p=ns	r=0.031 p=ns	r=-0.35 p=ns	r=0.11 p=ns	r=0.33 p=ns	r=-0.26 p=ns

Table S9: Continued

Metabolites vs gene expression	αCH$_2$ [2.24-2.26]	=CH-CH$_2$=CH$_2$- [2.00-2.02]	Acetate [1.90-1.92]	β-hydroxybutyrate and HDL [1.24-1.26]	HDL [5.28-5.30]	Pyruvate [2.40-2.42]	HDL [5.26-5.28]	HDL [0.82-0.84]	LDL and triglycerides [1.26-1.28]	Trimethylamine and free choline [3.20-3.22]	Ascorbate [4.49-4.51]	Alanine [1.47-1.49]
Rxr-α	r=-0.36 p=ns	**r=-0.53 p=0.010**	r=-0.21 p=ns	r=-0.42 p=ns	r=-0.31 p=ns	r=0.13 p=ns	r=-0.33 p=ns	r=-0.072 p=ns	r=-0.34 p=ns	r=0.043 p=ns	r=0.40 p=ns	r=-0.16 p=ns
Hmgcr	r=-0.35 p=ns	r=-0.059 p=ns	r=0.21 p=ns	r=0.24 p=ns	r=0.029 p=ns	r=0.36 p=ns	r=0.22 p=ns	r=0.31 p=ns	r=-0.35 p=ns	r=0.41 p=ns	r=0.30 p=ns	r=-0.013 p=ns
Fasn	r=0.15 p=ns	r=0.37 p=ns	**r=0.57 p=0.0041**	**r=0.54 p=0.0080**	r=0.14 p=ns	**r=0.44 p=0.042**	**r=0.40** p=ns	r=0.31 p=ns	r=-0.13 p=ns	r=0.32 p=ns	r=-0.089 p=ns	r=0.12 p=ns

Table S9: Continued

Metabolites vs gene expression	ATP Adenosine moiety [8.26-8.28]	Glutamate [3.77-3.79]	Hypoxanthine [8.16-8.18]	ATP Ribose moiety [6.14-6.16]	Scyllo-inositol [3.35-3.37]	Glutamate [2.35-2.37]	Lactate [4.09-4.11]	Glutathione [3.77-3.79]	Glutathione [2.57-2.59]	Glutathione [2.55-2.57]	Glutathione [2.17-2.19]	Glutathione [4.55-4.57]	Glutathione [2.93-2.95]
Pfkfb3	r=0.38 p=ns	r=0.046 p=ns	r=0.19 p=ns	r=0.20 p=ns	**r=-0.59** **p=0.029**	r=-0.081 p=ns	r=0.35 p=ns	r=-0.15 p=ns	r=0.18 p=ns	r=0.23 p=ns	r=0.15 p=ns	r=0.26 p=ns	r=0.29 p=ns
Slc2a1	r=0.36 p=ns	r=-0.17 p=ns	r=0.29 p=ns	r=0.17 p=ns	r=-0.39 p=ns	r=-0.28 p=ns	r=0.079 p=ns	r=-0.30 p=ns	r=-0.022 p=ns	r=0.044 p=ns	r=-0.027 p=ns	r=0.092 p=ns	r=0.13 p=ns
Gpx4	r=0.20 p=ns	r=0.049 p=ns	r=0.31 p=ns	r=0.079 p=ns	**r=-0.61** **p=0.032**	r=0.056 p=ns	r=-0.085 p=ns	**r=-0.60** **p=0.037**	r=-0.21 p=ns	r=-0.17 p=ns	r=-0.23 p=ns	r=-0.14 p=ns	r=-0.082 p=ns
Fabp7	r=-0.076 p=ns	r=-0.20 p=ns	r=0.26 p=ns	r=-0.11 p=ns	r=-0.24 p=ns	r=-0.25 p=ns	r=-0.26 p=ns	r=-0.30 p=ns	r=-0.066 p=ns	r=-0.10 p=ns	r=-0.081 p=ns	r=-0.12 p=ns	r=-0.15 p=ns
Gcl	r=-0.037 p=ns	r=0.11 p=ns	r=0.21 p=ns	r=-0.11 p=ns	r=0.0069 p=ns	r=0.0064 p=ns	r=0.0066 p=ns	r=0.16 p=ns	r=0.28 p=ns	r=0.22 p=ns	r=0.28 p=ns	r=0.15 p=ns	r=0.18 p=ns
Ppar-α	r=0.41 p=ns	r=-0.41 p=ns	r=0.30 p=ns	r=0.39 p=ns	r=-0.25 p=ns	r=-0.24 p=ns	r=-0.068 p=ns	**r=-0.56** **p=0.0054**	**r=-0.67** **p=0.00031**	**r=-0.70** **p<0.0001**	**r=-0.63** **p=0.00096**	**r=-0.75** **p<0.0001**	**r=-0.72** **p<0.0001**
Ror-α	r=0.31 p=ns	r=-0.30 p=ns	r=0.32 p=ns	r=0.23 p=ns	r=-0.35 p=ns	r=-0.32 p=ns	r=-0.068 p=ns	**r=-0.45** **p=0.042**	**r=-0.61** **p=0.0018**	**r=-0.64** **p=0.00075**	**r=-0.59** **p=0.0027**	**r=-0.64** **p=0.00076**	**r=-0.65** **p=0.00056**
Sirt1	r=0.32 p=ns	r=-0.36 p=ns	r=0.17 p=ns	r=0.26 p=ns	r=-0.16 p=ns	r=-0.25 p=ns	r=-0.012 p=ns	**r=-0.50** **p=0.019**	**r=-0.60** **p=0.0021**	**r=-0.60** **p=0.0023**	**r=-0.57** **p=0.0042**	**r=-0.63** **p=0.00090**	**r=-0.59** **p=0.0028**
Sod1	r=0.14 p=ns	r=-0.16 p=ns	r=-0.042 p=ns	r=0.19 p=ns	r=0.054 p=ns	r=-0.19 p=ns	r=0.049 p=ns	**r=-0.45** **p=0.044**	**r=-0.53** **p=0.011**	**r=-0.51** **p=0.018**	**r=-0.49** **p=0.027**	**r=-0.57** **p=0.0056**	**r=-0.53** **p=0.011**
Dgat1	r=0.34 p=ns	r=-0.22 p=ns	r=0.095 p=ns	r=0.37 p=ns	r=-0.17 p=ns	r=-0.13 p=ns	r=-0.0070 p=ns	**r=-0.46** **p=0.045**	**r=-0.66** **p=0.00065**	**r=-0.67** **p=0.00053**	**r=-0.60** **p=0.0034**	**r=-0.74** **p<0.0001**	**r=-0.68** **p=0.00044**

Table S9: Continued

Metabolites vs gene expression continued	ATP Adenosine moiety [8.26-8.28]	Glutamate [3.77-3.79]	Hypoxanthine [8.16-8.18]	ATP Ribose moiety [6.14-6.16]	Scyllo-inositol [3.35-3.37]	Glutamate [2.35-2.37]	Lactate [4.09-4.11]	Glutathione [3.77-3.79]	Glutathione [2.57-2.59]	Glutathione [2.55-2.57]	Glutathione [2.17-2.19]	Glutathione [4.55-4.57]	Glutathione [2.93-2.95]
Rxr-α	r=0.25 p=ns	r=-0.15 p=ns	r=0.095 p=ns	r=0.32 p=ns	r=-0.060 p=ns	r=-0.089 p=ns	r=-0.016 p=ns	**r=-0.50 p=0.021**	**r=-0.64 p=0.00090**	**r=-0.64 p=0.00090**	**r=-0.59 p=0.0035**	**r=-0.70 p=0.00015**	**r=-0.65 p=0.00077**
Hmgcr	**r=0.53 p=0.011**	r=-0.077 p=ns	r=0.33 p=ns	r=0.43 p=ns	r=-0.22 p=ns	r=-0.11 p=ns	r=0.24 p=ns	**r=-0.46 p=0.036**	r=-0.27 p=ns	r=-0.25 p=ns	r=-0.29 p=ns	r=-0.24 p=ns	r=-0.21 p=ns
Fasn	r=0.33 p=ns	r=0.096 p=ns	r=0.14 p=ns	r=0.24 p=ns	r=-0.080 p=ns	r=0.11 p=ns	**r=0.55 p=0.0073**	r=-0.027 p=ns	r=0.11 p=ns	r=0.13 p=ns	r=0.071 p=ns	r=0.12 p=ns	r=0.17 p=ns

Table S9: continued

Metabolites vs gene expression	Glutathione [2.95-2.97]	Choline [3.19-3.21]	Metabolites vs gene expression	Glutathione [2.95-2.97]	Choline [3.19-3.21]
Pfkfb3	r=0.27 p=ns	r=-0.47 p=ns	Rxr-α	**r=-0.64** **p=0.00082**	r=0.37 p=ns
Slc2a1	r=0.096 p=ns	r=-0.16 p=ns	Hmgcr	r=-0.19 p=ns	r=0.17 p=ns
Gpx4	r=-0.18 p=ns	r=-0.025 p=ns	Fasn	r=0.18 p=ns	r=-0.10 p=ns
Fabp7	r=-0.13 p=ns	r=0.32 p=ns			
Gcl	r=0.16 p=ns	r=0.18 p=ns			
Ppar-α	**r=-0.68** **p=0.00019**	**r=0.53** **p=0.010**			
Ror-α	**r=-0.63** **p=0.00090**	r=0.14 p=ns			
Sirt1	**r=-0.58** **p=0.0035**	r=0.38 p=ns			
Sod1	**r=-0.52** **p=0.015**	r=0.37 p=ns			
Dgat1	**r=-0.65** **p=0.00085**	r=0.41 p=ns			

Table S10: Correlations between all metabolites

Metabolites	=CH-CH_2=CH_2- [2.00-2.02]	Acetate [1.90-1.92]	β-hydroxybutyrate and HDL [1.24-1.26]	HDL [5.28-5.30]	Pyruvate [2.40-2.42]	HDL [5.26-5.28]	HDL [0.82-0.84]	LDL and triglycerides [1.26-1.28]	Trimethylamine and free choline [3.20-3.22]	Ascorbate [4.49-4.51]	Alanine [1.47-1.49]	ATP Adenosine moiety [8.26-8.28]
αCH_2 [2.24-2.26]	**r=0.46 p=0.033**	r=-0.29 p=ns	r=-0.26 p=ns	r=0.12 p=ns	r=-0.17 p=ns	r=-0.30 p=ns	**r=-0.57 p=0.0035**	**r=0.74 p<0.0001**	**r=-0.74 p<0.0001**	r=-0.39 p=ns	r=0.23 p=ns	r=-0.36 p=ns
	=CH-CH_2=CH_2- [2.00-2.02]	r=0.14 p=ns	**r=0.61 p=0.0012**	**r=0.84 p<0.0001**	r=-0.33 p=ns	**r=0.59 p=0.0022**	r=0.24 p=ns	**r=0.67 p=0.00020**	r=0.025 p=ns	r=-0.29 p=ns	r=0.15 p=ns	r=-0.023 p=ns
		Acetate [1.90-1.92]	**r=0.66 p=0.00030**	r=0.053 p=ns	r=0.42 p=ns	**r=0.54 p=0.00742**	**r=0.56 p=0.0045**	**r=-0.46 p=0.032**	**r=0.63 p=0.00076**	r=0.15 p=ns	r=-0.049 p=ns	r=0.26 p=ns
			β-hydroxybutyrate and HDL [1.24-1.26]	**r=0.58 p=0.0028**	r=0.078 p=ns	**r=0.92 p<0.0001**	**r=0.82 p<0.0001**	r=-0.12 p=ns	**r=0.75 p<0.0001**	r=-0.10 p=ns	r=-0.099 p=ns	r=0.30 p=ns
				HDL [5.28-5.30]	**r=-0.55 p=0.0068**	**r=0.73 p<0.0001**	r=0.42 p=ns	**r=0.53 p=0.0091**	r=0.20 p=ns	r=-0.023 p=ns	r=-0.053 p=ns	r=0.19 p=ns
					Pyruvate [2.40-2.42]	r=-0.059 p=ns	r=0.037 p=ns	**r=-0.56 p=0.0048**	r=0.30 p=ns	r=-0.071 p=ns	r=0.27 p=ns	r=0.090 p=ns
						HDL [5.26-5.28]	**r=0.82 p<0.0001**	r=-0.086 p=ns	**r=0.74 p<0.0001**	r=-0.050 p=ns	r=-0.12 p=ns	r=0.40 p=ns
							HDL [0.82-0.84]	r=-0.41 p=ns	**r=0.92 p<0.0001**	r=0.16 p=ns	r=-0.35 p=ns	**r=0.55 p=0.0077**
								LDL and triglycerides [1.26-1.28]	**r=-0.65 p=0.00053**	r=-0.23 p=ns	r=0.26 p=ns	r=-0.38 p=ns
									Trimethylamine and free choline [3.20-3.22]	r=0.17 p=ns	r=-0.25 p=ns	**r=0.51 p=0.016**
										Ascorbate [4.49-4.51]	r=-0.30 p=ns	r=0.35 p=ns
											Alanine [1.47-1.49]	r=-0.18 p=ns

Table S10: Continued

Metabolites continued	Glutamate [3.77-3.79]	Hypoxanthine [8.16-8.18]	ATP Ribose moiety [6.14-6.16]	Scyllo-inositol [3.35-3.37]	Glutamate [2.35-2.37]	Lactate [4.09-4.11]	Glutathione [3.77-3.79]	Glutathione [2.57-2.59]	Glutathione [2.55-2.57]	Glutathione [2.17-2.19]
αCH_2 [2.24-2.26]	r=0.15 p=ns	r=-0.35 p=ns	r=-0.38 p=ns	**r=0.59** **p=0.0029**	r=0.21 p=ns	r=0.087 p=ns	r=0.42 p=ns	r=0.37 p=ns	r=0.40 p=ns	r=0.37 p=ns
$=CH-CH_2=CH_2-$ [2.00-2.02]	r=-0.25 p=ns	r=-0.15 p=ns	r=-0.098 p=ns	r=0.32 p=ns	r=-0.14 p=ns	r=0.24 p=ns	r=0.43 p=ns	**r=0.46** **p=0.036**	**r=0.47** **p=0.034**	r=0.42 p=ns
Acetate [1.90-1.92]	r=0.061 p=ns	r=-0.053 p=ns	r=0.23 p=ns	r=-0.41 p=ns	r=0.14 p=ns	r=0.42 p=ns	r=0.093 p=ns	r=0.23 p=ns	r=0.22 p=ns	r=0.21 p=ns
β-hydroxybutyrate and HDL [1.24-1.26]	r=-0.15 p=ns	r=0.11 p=ns	r=0.25 p=ns	r=-0.33 p=ns	r=-0.095 p=ns	r=0.38 p=ns	r=0.19 p=ns	r=0.32 p=ns	r=0.30 p=ns	r=0.26 p=ns
HDL [5.28-5.30]	**r=-0.50** **p=0.017**	r=0.044 p=ns	r=0.15 p=ns	r=0.26 p=ns	r=-0.24 p=ns	r=0.095 p=ns	r=0.13 p=ns	r=0.090 p=ns	r=0.087 p=ns	r=0.062 p=ns
Pyruvate [2.40-2.42]	**r=0.45** **p=0.044**	r=-0.073 p=ns	r=0.13 p=ns	**r=-0.45** **p=0.044**	r=0.27 p=ns	r=0.36 p=ns	r=0.072 p=ns	r=0.16 p=ns	r=0.14 p=ns	r=0.13 p=ns
HDL [5.26-5.28]	r=-0.30 p=ns	r=0.13 p=ns	r=0.36 p=ns	r=-0.31 p=ns	r=-0.13 p=ns	r=0.33 p=ns	r=0.13 p=ns	r=0.16 p=ns	r=0.15 p=ns	r=0.13 p=ns
HDL [0.82-0.84]	r=-0.23 p=ns	r=0.33 p=ns	**r=0.55** **p=0.0077**	**r=-0.53** **p=0.010**	r=0.0050 p=ns	r=0.30 p=ns	r=-0.16 p=ns	r=-0.069 p=ns	r=-0.076 p=ns	r=-0.097 p=ns
LDL and triglycerides [1.26-1.28]	r=-0.14 p=ns	r=0.24 p=ns	r=-0.37 p=ns	**r=0.72** **p<0.0001**	r=-0.054 p=ns	r=-0.13 p=ns	r=0.40 p=ns	r=0.28 p=ns	r=0.30 p=ns	r=0.26 p=ns
Trimethylamine and free choline [3.20-3.22]	r=-0.12 p=ns	r=0.29 p=ns	**r=0.48** **p=0.025**	**r=-0.66** **p=0.00044**	r=-0.10 p=ns	r=0.28 p=ns	r=-0.18 p=ns	r=-0.067 p=ns	r=-0.085 p=ns	r=-0.095 p=ns
Ascorbate [4.49-4.51]	r=-0.27 p=ns	**r=0.46** **p=0.035**	r=0.37 p=ns	r=0.064 p=ns	r=-0.10 p=ns	r=-0.27 p=ns	**r=-0.54** **p=0.0092**	**r=-0.47** **p=0.037**	**r=-0.49** **p=0.026**	**r=-0.51** **p=0.018**
Alanine [1.47-1.49]	r=0.30 p=ns	r=-0.31 p=ns	r=-0.19 p=ns	r=0.16 p=ns	r=0.012 p=ns	r=0.34 p=ns	r=0.27 p=ns	r=0.26 p=ns	r=0.30 p=ns	r=0.27 p=ns

Table S10: Continued

Metabolites continued	Glutathione [4.55-4.57]	Glutathione [2.93-2.95]	Glutathione [2.95-2.97]	Choline [3.19-3.21]
αCH_2 [2.24-2.26]	r=0.42 p=ns	r=0.39 p=ns	r=0.41 p=ns	r=-0.11 p=ns
$=CH-CH_2=CH_2-$ [2.00-2.02]	**r=0.51** **p=0.017**	**r=0.46** **p=0.035**	**r=0.54** **p=0.0092**	r=-0.15 p=ns
Acetate [1.90-1.92]	r=0.16 p=ns	r=0.20 p=ns	r=0.16 p=ns	r=-0.091 p=ns
β-hydroxybutyrate and HDL [1.24-1.26]	r=0.29 p=ns	r=0.32 p=ns	r=0.33 p=ns	r=-0.21 p=ns
HDL [5.28-5.30]	r=0.15 p=ns	r=0.10 p=ns	r=0.22 p=ns	r=0.15 p=ns
Pyruvate [2.40-2.42]	r=0.021 p=ns	r=0.14 p=ns	r=0.039 p=ns	**r=-0.47** **p=0.031**
HDL [5.26-5.28]	r=0.14 p=ns	r=0.18 p=ns	r=0.24 p=ns	r=-0.073 p=ns
HDL [0.82-0.84]	r=-0.11 p=ns	r=-0.029 p=ns	r=-0.050 p=ns	r=0.083 p=ns
LDL and triglycerides [1.26-1.28]	r=0.37 p=ns	r=0.30 p=ns	r=0.35 p=ns	r=0.00027 p=ns
Trimethylamine and free choline [3.20-3.22]	r=-0.14 p=ns	r=-0.061 p=ns	r=-0.092 p=ns	r=-0.077 p=ns
Ascorbate [4.49-4.51]	**r=-0.45** **p=0.049**	r=-0.43 p=ns	**r=-0.46** **p=0.041**	r=0.44 p=ns
Alanine [1.47-1.49]	r=0.24 p=ns	r=0.27 p=ns	r=0.26 p=ns	r=-0.37 p=ns

Table S10: Continued

Metabolites	Glutamate [3.77-3.79]	Hypoxanthine [8.16-8.18]	ATP Ribose moiety [6.14-6.16]	Scyllo-inositol [3.35-3.37]	Glutamate [2.35-2.37]	Lactate [4.09-4.11]	Glutathione [3.77-3.79]	Glutathione [2.57-2.59]	Glutathione [2.55-2.57]	Glutathione [2.17-2.19]
ATP Adenosine moiety [8.26-8.28]	r=-0.19 p=ns	**r=0.56** **p=0.0060**	**r=0.88** **p=<0.0001**	r=-0.30 p=ns	r=0.16 p=ns	**r=0.54** **p=0.0092**	r=-0.36 p=ns	r=-0.32 p=ns	r=-0.30 p=ns	r=-0.27 p=ns
	Glutamate [3.77-3.79]	r=-0.047 p=ns	r=-0.15 p=ns	r=-0.15 p=ns	**r=0.55** **p=0.0076**	r=0.20 p=ns	r=0.33 p=ns	**r=0.52** **p=0.015**	**r=0.54** **p=0.0092**	**r=0.51** **p=0.017**
		Hypoxanthine [8.16-8.18]	**r=0.59** **p=0.0028**	r=-0.24 p=ns	r=0.20 p=ns	r=0.13 p=ns	r=-0.40 p=ns	r=-0.32 p=ns	r=-0.28 p=ns	r=-0.29 p=ns
			ATP Ribose moiety [6.14-6.16]	r=-0.20 p=ns	r=0.39 p=ns	**r=0.54** **p=0.0092**	r=-0.32 p=ns	r=-0.41 p=ns	r=-0.39 p=ns	r=-0.37 p=ns
				Scyllo-inositol [3.35-3.37]	r=-0.032 p=ns	r=-0.14 p=ns	r=0.10 p=ns	r=-0.074 p=ns	r=-0.046 p=ns	r=-0.081 p=ns
					Glutamate [2.35-2.37]	r=0.40 p=ns	r=0.10 p=ns	r=0.15 p=ns	r=0.20 p=ns	r=0.15 p=ns
						Lactate [4.09-4.11]	r=0.17 p=ns	r=0.15 p=ns	r=0.18 p=ns	r=0.19 p=ns
							Glutathione [3.77-3.79]	**r=0.72** **p<0.0001**	**r=0.69** **p=0.00016**	**r=0.74** **p<0.0001**
								Glutathione [2.57-2.59]	**r=0.99** **p<0.0001**	**r=0.98** **p<0.0001**
									Glutathione [2.55-2.57]	**r=0.97** **p<0.0001**

Table S10: Continued

Metabolites	Glutathione [4.55-4.57]	Glutathione [2.93-2.95]	Glutathione [2.95-2.97]	Choline [3.19-3.21]
ATP Adenosine moiety [8.26-8.28]	r=-0.32 p=ns	r=-0.27 p=ns	r=-0.26 p=ns	r=0.35 p=ns
Glutamate [3.77-3.79]	**r=0.46** **p=0.042**	**r=0.57** **p=0.0052**	**r=0.47** **p=0.034**	r=-0.26 p=ns
Hypoxanthine [8.16-8.18]	r=-0.27 p=ns	r=-0.22 p=ns	r=-0.25 p=ns	r=0.42 p=ns
ATP Ribose moiety [6.14-6.16]	r=-0.42 p=ns	r=-0.34 p=ns	r=-0.38 p=ns	r=0.35 p=ns
Scyllo-inositol [3.35-3.37]	r=0.085 p=ns	r=-0.052 p=ns	r=0.023 p=ns	r=0.17 p=ns
Glutamate [2.35-2.37]	r=0.18 p=ns	r=0.28 p=ns	r=0.16 p=ns	r=0.067 p=ns
Lactate [4.09-4.11	r=0.10 p=ns	r=0.16 p=ns	r=0.15 p=ns	r=-0.13 p=ns
Glutathione [3.77-3.79]	**r=0.59** **p=0.0027**	**r=0.61** **p=0.0017**	**r=0.59** **p=0.0029**	**r=-0.53** **p=0.010**
Glutathione [2.57-2.59]	**r=0.92** **p<0.0001**	**r=0.94** **p<0.0001**	**r=0.90** **p<0.0001**	**r=-0.45** **p=0.041**
Glutathione [2.55-2.57]	**r=0.94** **p<0.0001**	**r=0.97** **p<0.0001**	**r=0.94** **p<0.0001**	**r=-0.43** p=ns
Glutathione [2.17-2.19]	**r=0.86** **p<0.0001**	**r=0.89** **p<0.0001**	**r=0.85** **p<0.0001**	r=-0.37 p=ns

Metabolites	Glutathione [2.93-2.95]	Glutathione [2.95-2.97]	Choline [3.19-3.21]
Glutathione [4.55-4.57]	**r=0.95** **p<0.0001**	**r=0.95** **p<0.0001**	**r=-0.45** **p=0.042**
Glutathione [2.93-2.95]		**r=0.96** **p<0.0001**	r=-0.42 p=ns
		Glutathione [2.95-2.97]	r=-0.40 p=ns

Table S11: Correlations between gene expression in the brain and liver

Gene expression	Slc2a1	Gpx4	Fabp7	Gcl	Ppar-α	Ror-α	Sirt1	Sod1	Dgat1	Rxr-α	Hmgcr	Fasn
Pfkfb3	**r=0.81 p=0.00037**	**r=0.53** p=ns	r=-0.060 p=ns	r=-0.083 p=ns	r=-0.086 p=ns	r=0.16 p=ns	r=0.072 p=ns	r=-0.093 p=ns	r=0.064 p=ns	r=0.045 p=ns	r=0.13 p=ns	r=-0.032 p=ns
	Slc2a1	**r=0.48** p=ns	r=-0.048 p=ns	r=-0.18 p=ns	r=0.066 p=ns	r=0.17 p=ns	r=0.17 p=ns	r=0.051 p=ns	r=0.087 p=ns	r=0.099 p=ns	r=0.22 p=ns	r=0.090 p=ns
		Gpx4	**r=0.40** p=ns	r=-0.16 p=ns	r=0.17 p=ns	r=0.33 p=ns	r=0.24 p=ns	r=0.060 p=ns	r=0.19 p=ns	r=0.24 p=ns	r=0.048 p=ns	r=-0.23 p=ns
			Fabp7	r=0.33 p=ns	r=0.26 p=ns	r=0.054 p=ns	r=0.094 p=ns	r=-0.14 p=ns	r=-0.071 p=ns	r=-0.15 p=ns	r=-0.12 p=ns	r=-0.22 p=ns
				Gcl	r=0.0059 p=ns	r=0.016 p=ns	r=-0.15 p=ns	r=-0.36 p=ns	r=-0.19 p=ns	r=-0.31 p=ns	r=-0.050 p=ns	r=0.050 p=ns
					Ppar-α	**r=0.78 p<0.0001**	**r=0.82 p<0.0001**	**r=0.70 p<0.0001**	**r=0.82 p<0.0001**	**r=0.79 p<0.0001**	**r=0.45 p=0.042**	r=-0.094 p=ns
						Ror-α	**r=0.79 p<0.0001**	**r=0.54 p=0.0085**	**r=0.65 p=0.00069**	**r=0.65 p=0.00063**	**r=0.43 p=0.049**	r=-0.057 p=ns
							Sirt1	**r=0.82 p<0.0001**	**r=0.85 p<0.0001**	**r=0.86 p<0.0001**	**r=0.52 p=0.010**	r=-0.053 p=ns
								Sod1	**r=0.80 p<0.0001**	**r=0.87 p<0.0001**	**r=0.41** p=ns	r=-0.033 p=ns

Table S11: Continued

Gene expression	Rxr-α	Hmgcr	Fasn
Dgat1	**r=0.95 p<0.0001**	**r=0.46 p=0.042**	r=-0.15 p=ns
	Rxr-α	**r=0.44 p=0.049**	r=-0.17 p=ns
		Hmgcr	**r=0.56 p=0.0050**

Table S12: Correlations between behavioural results

Behavioural results	Duration in light (LDB)	Distance travelled (OFT)	Mean velocity (OFT)	Duration around edges (OFT)	% Sucrose preference	Change in body mass (g)	Total sleep (min)	% Sleep in light phase	Circadian period	Circadian Amplitude
Frequency to light (LDB)	**r=0.93 p<0.0001**	**r=0.69 p=0.00027**	**r=0.69 p=0.00027**	r=0.10 p=ns	r=0.16 p=ns	r=-0.34 p=ns	r=-0.15 p=ns	r=-0.15 p=ns	r=-0.066 p=ns	r=0.28 p=ns
	Duration in light (LDB)	**r=0.75 p<0.0001**	**r=0.75 p<0.0001**	r=0.21 p=ns	r=0.19 p=ns	r=-0.36 p=ns	r=-0.23 p=ns	r=-0.23 p=ns	r=-0.066 p=ns	r=0.26 p=ns
		Distance travelled	**r=1 p<0.0001**	r=0.11 p=ns	r=0.084 p=ns	r=-0.38 p=ns	r=0.024 p=ns	r=0.026 p=ns	r=-0.047 p=ns	**r=0.45** p=ns
			Mean velocity (OFT)	r=0.11 p=ns	r=0.084 p=ns	r=-0.38 p=ns	r=0.024 p=ns	r=0.026 p=ns	r=-0.047 p=ns	**r=0.45** p=ns
				Duration around edges (OFT)	r=0.40 p=ns	r=0.089 p=ns	r=-0.27 p=ns	r=-0.27 p=ns	**r=0.45** p=ns	r=-0.32 p=ns
					% Sucrose preference	r=-0.041 p=ns	r=-0.28 p=ns	r=-0.28 p=ns	r=0.38 p=ns	r=-0.14 p=ns
						Change in body mass (g)	r=-0.14 p=ns	r=-0.15 p=ns	**r=0.48 p=0.049**	**r=-0.42** p=ns
							Total sleep (min)	**r=0.999 p<0.0001**	r=0.018 p=ns	r=0.31 p=ns
								% Sleep in light phase	r=0.012 p=ns	r=0.31 p=ns
									Circadian period	r=-0.32 p=ns

Table S12: Continued

Behavioural results	Circadian phase	Total activity bouts	Average activity bout length	Total Distance Travelled (HCB)	Total Mean Velocity (HCB)	Total # water bottle licks (HCB)
Frequency to light (LDB)	r=-0.015 p=ns	r=-0.096 p=ns	r=0.37 p=ns	r=0.28 p=ns	r=0.32 p=ns	**r=0.50** p=ns
Duration in light (LDB)	r=-0.45 p=ns	r=-0.11 p=ns	r=0.39 p=ns	r=0.32 p=ns	r=0.36 p=ns	**r=0.49** p=ns
Distance travelled (OFT)	r=-0.31 p=ns	r=-0.32 p=ns	**r=0.62** **p=0.0029**	**r=0.57** **p=0.0088**	**r=0.56** **p=0.0090**	**r=0.55** **p=0.0023**
Mean velocity (OFT)	r=-0.31 p=ns	r=-0.32 p=ns	**r=0.62** **p=0.0029**	**r=0.57** **p=0.0088**	**r=0.56** **p=0.0090**	**r=0.55** **p=0.0023**
Duration around edges (OFT)	r=0.26 p=ns	r=-0.091 p=ns	r=-0.033 p=ns	r=0.044 p=ns	r=0.027 p=ns	r=0.26 p=ns
% Sucrose preference	r=0.13 p=ns	r=-0.0012 p=ns	r=0.12 p=ns	r=0.13 p=ns	r=0.13 p=ns	r=0.29 p=ns
Change in body mass (g)	**r=0.49** **p=0.040**	r=0.26 p=ns	**r=-0.44** **p=ns**	r=-0.32 p=ns	r=-0.34 p=ns	r=-0.31 p=ns
Total sleep (min)	r=-0.13 p=ns	**r=-0.55** **p=0.012**	r=0.082 p=ns	r=-0.15 p=ns	r=-0.24 p=ns	r=-0.28 p=ns
% Sleep in light phase	r=-0.13 p=ns	**r=-0.55** **p=0.012**	r=0.087 p=ns	r=-0.14 p=ns	r=-0.24 p=ns	r=-0.28 p=ns
Circadian period	**r=0.44** p=ns	r=-0.049 p=ns	r=-0.26 p=ns	r=-0.27 p=ns	r=-0.30 p=ns	r=0.20 p=ns
Circadian Amplitude	**r=-0.60** **p=0.0043**	r=-0.31 p=ns	**r=0.55** **p=0.012**	**r=0.60** **p=0.0044**	**r=0.63** **p=0.0024**	r=0.081 p=ns

Table S12: Continued

Behavioural results	Total activity bouts	Average activity bout length	Total Distance Travelled (HCB)	Total Mean Velocity (HCB)	Total # water bottle licks (HCB)
Circadian phase	r=0.15 p=ns	**r=-0.55** **p=0.012**	**r=-0.60** **p=0.0043**	**r=-0.64** **p=0.0015**	r=-0.19 p=ns
	Total activity bouts	**r=-0.65** **p=0.0012**	r=-0.29 p=ns	r=-0.21 p=ns	r=-0.086 p=ns
		Average activity bout length	**r=0.83** **p<0.0001**	**r=0.82** **p<0.0001**	r=0.39 p=ns
			Total Distance Travelled (HCB)	**r=0.98** **p<0.0001**	r=0.38 p=ns
				Total Mean Velocity (HCB)	r=0.35 p=ns
					Total # water bottle licks (HCB)